The Ontogeny of Osmoregulation in the Nile Tilapia (*Oreochromis niloticus* L.)

THESIS SUBMITTED FOR THE DEGREE OF DOCTOR OF PHILOSOPHY IN AQUACULTURE

By

Sophie Fridman

M.A., M.Sc.

February 2011

INSTITUTE OF AQUACULTURE

UNIVERSITY OF STIRLING

This thesis is dedicated to the memory of my father David Leeming and my father-in-

law David Fridman Sr., who would both have been very proud.

Declaration

The work and results presented in this thesis have been carried out by the candidate at the Institute of Aquaculture, University of Stirling, Scotland and have not been submitted for any other degree or qualification. All information from other sources has been acknowledged.

CANDIDATE: Name: Sophie Fridman

                     Signature:

                     Date: …………………………...

SUPERVISOR: Name: …………………………...

                     Signature:

                     Date: …………………………...

Acknowledgements

List of abbreviations

AC	accessory cell
AE	apical anion exchanger
ANOVA	analysis of variance
BSA	bovine serum albumin
CA	carbonic anhydrase
CFTR	cystic fibrosis transmembrane receptor
CSLM	confocal scanning laser microscope
DAPI	4',6-Diamidino-2-phenylindole
dph	days post-hatch
e.g.	for example
ENaC	epithelial sodium channel
g	gram
GLM	General Linear Model
h	hours
IgG	immunoglobin
i.e.	that is to say
kg	kilogram
L	litre
LM	light microscope
M	molar
MCC	multicellular complex
mg	milligram
min	minute
ml	millilitre
mm^{-2}	millimetres squared
mM	millimolar
mOsmol	milliosmoles
MRC	mitochondria-rich cell
mRNA	mitochondrial ribonucleic acid
MS222	tricaine methane sulphonate
Na^+/K^+-ATPase	sodium potassium adenotriphosphate

NCC	Na^+/Cl^- co-transporter
NGS	normal goat serum
NHE_3	Na^+/H^+ exchanger
NKCC	$Na^+/K^+/2Cl^-$ co-transporter
nm	nanometre
O_2	oxygen
PB	phosphate buffer
PBS	phosphate buffer saline
PVC	pavement cells
QO_2	$\mu l\ O_2$ mg dry weight $^{-1}$ h $^{-1}$
S.E.	standard error of means
SEM	scanning electron microscope
TEM	transmission electron microscope
U.K.	United Kingdom
U.S.	United States of America
$V-H^+-ATPase$	apical vacuolar or V-type proton ATPase
v/v	volume/volume
W	watt
w/v	weight/volume
YAE	yolk absorption efficiency
2-D	2-dimensional
3-D	3-dimensional
%	percentage
μg	microgram
μl	microlitre
μm	micrometre
μm^{-2}	micrometers squared

3-D glasses

Taxonomic classification

Throughout this thesis, the tilapia names are used according to the taxonomic classification of Trewavas (1983) rather than according to the author of the cited publication. *Tilapia nilotica* (Linnaeus), *Tilapia mossambica* (Peters) and *Tilapia aurea* (Steindachner) are referred to as *Oreochromis niloticus* (Linnaeus), *Oreochromis mossambicus* (Peters) and *Oreochromis aureus* (Steindachner) respectively. Rainbow trout (*Salmo gairdneri*, Richardson) are referred to as *Oncorhynchus mykiss* (Walbaum) according to recent classification.

Abstract

In recent times, diminishing freshwater resources, due to the rapidly increasing drain of urban, industrial and agricultural activities in combination with the impact of climate change, has led to an urgent need to manage marine and brackish water environments more efficiently. Therefore the diversification of aquacultural practices, either by the introduction of new candidate species or by the adaptation of culture methods for existing species, is vital at a time when innovation and adaptability of the aquaculture industry is fundamental in order to maintain its sustainability. The Nile tilapia (*Oreochromis niloticus*, Linnaeus, 1758), which has now been spread well beyond its natural range, dominates tilapia aquaculture because of its adaptability and fast growth rate. Although not considered to be amongst the most salt tolerant of the cultured tilapia species, the Nile tilapia still offers considerable potential for culture in low-salinity water. An increase in knowledge of the limits and basis of salinity tolerance of Nile tilapia during the sensitive early life stages and the ability to predict responses of critical life-history stages to environmental change could prove invaluable in improving larval rearing techniques and extend the scope of this globally important fish species.

The capability of early life stages of the Nile tilapia to withstand variations in salinity is due to their ability to osmoregulate, therefore the ontogeny of osmoregulation in the Nile tilapia was studied from spawning to yolk-sac absorption after exposure to different experimental conditions ranging from freshwater to 25 ppt. Eggs were able to withstand elevated rearing salinities up to 20 ppt, but transfer to 25 ppt induced 100% mortality by 48 h post-fertilisation. At all stages embryos and larvae hyper-regulated at lower salinities and hypo-regulated at higher salinities, relative to the salinity of the

external media. Osmoregulatory capacity increased during development and from 2 days post-hatch onwards remained constant until yolk-sac absorption. Adjustments to larval osmolality, following abrupt transfer from freshwater to experimental salinities (12.5 and 20 ppt), appeared to follow a pattern of crisis and regulation, with whole-body osmolality for larvae stabilising at $c.$ 48 h post-transfer for all treatments, regardless of age at time of transfer. Age at transfer to experimental salinities (7.5 – 20 ppt) had a significant positive effect on larval ability to osmoregulate; larvae transferred at 8 dph maintained a more constant range of whole body osmolality over the experimental salinities tested than larvae at hatch. Concomitantly, survival following transfer to experimental salinities increased with age. There was a significant effect (GLM; $p < 0.05$) of salinity of incubation and rearing media on the incidence of gross larval malformation that was seen to decline over the developmental period studied.

It is well established that salinity exerts a strong influence on development and growth in early life stages of fishes therefore the effects of varying low salinities (0 - 25 ppt) on hatchability, survival, growth and energetic parameters were examined in the Nile tilapia during early life stages. Salinity up to 20 ppt was tolerable, although reduced hatching rates at 15 and 20 ppt suggest that these salinites may be less than optimal. Optimum timing of transfer of eggs from freshwater to elevated salinities was 3-4 h post-fertilisation, following manual stripping and fertilisation of eggs, however increasing incubation salinity lengthened the time taken to hatch. Salinity was related to dry body weight, with larvae in salinities greater than 15 ppt displaying, at hatch, a significantly (GLM: $p < 0.05$) lower body weight but containing greater yolk reserves than those in freshwater or lower salinities. Survival at yolk-sac absorption displayed a significant (GLM; $p < 0.05$) inverse relationship with increasing salinity and mortalities

were particularly heavy in the higher salinities of 15, 20 and 25 ppt. Mortalities occurred primarily during early yolk-sac development yet stabilised from 5 dph onwards. Salinity had a negative effect on yolk absorption efficiency (YAE). Salinity-related differences in oxygen consumption rates were not detectable until 3 days post-hatch; oxygen consumption rates of larvae in freshwater between days $3 - 6$ post-hatch were always significantly higher (GLM $p < 0.05$) than those in 7.5, 15, 20 and 25 ppt, however, on day 9 post-hatch this pattern was reversed and freshwater larvae had a significantly lower QO_2 than those in elevated salinities. Salinity had a significant inverse effect on larval standard length, with elevated salinities producing shorter larvae from hatch until 6 dph, after which time there was no significant differences between treatments. Salinity had a significant effect on whole larval dry weight, with heavier larvae in elevated salinities throughout the yolk-sac period (GLM; $p < 0.05$).

The ability of the Nile tilapia to withstand elevated salinity during early life stages is due to morphological and ultrastructural modifications of extrabranchial mitochondria-rich cells (MRCs) that confer an osmoregulatory capacity before the development of the adult osmoregulatory system. A clearly defined temporal staging of the appearance of these adaptive mechanisms, conferring ability to cope with varying environmental conditions during early development, was evident. Ontogenetic changes in MRC location, 2-dimensional surface area, density and general morphological changes were investigated in larvae incubated and reared in freshwater and brackish water (15 ppt) from hatch until yolk-sac absorption using Na^+/K^+-ATPase immunohistochemistry with a combination of microscope techniques. The pattern of MRC distribution was seen to change during development under both treatments, with cell density decreasing significantly on the body from hatch to 7 days post-hatch, but appearing on the inner

opercular area at 3 days post-hatch and increasing significantly (GLM; $p < 0.05$) thereafter. Mitochondria-rich cells were always significantly (GLM; $p < 0.05$) denser in freshwater than in brackish water maintained larvae. In both freshwater and brackish water, MRCs located on the outer operculum and tail showed a marked increase in size with age, however, cells located on the abdominal epithelium of the yolk-sac and the inner operculum showed a significant decrease in size (GLM; $p < 0.05$) over time. Mitochondria-rich cells from brackish water maintained larvae from 1 day post-hatch onwards were always significantly larger (GLM; $p < 0.05$) than those maintained in freshwater. Preliminary scanning electron microscopy studies revealed structural differences in chloride cell morphology that varied according to environmental conditions.

Mitochondria-rich cell morphology and function are intricately related and the plasticity or adaptive response of this cell to environmental changes is vital in preserving physiological homeostasis and contributes to fishes' ability to inhabit diverse environments. Yolk-sac larvae were transferred from freshwater at 3 days post-hatch to 12.5 and 20 ppt and sampled at 24 and 48 h post-transfer. The use of scanning electron microscopy allowed a quantification of MRC, based on the appearance and surface area of their apical crypts, resulting in a reclassification of 'sub-types' *i.e.* Type I or absorptive, degenerating form (surface area range $5.2 - 19.6$ μm^2), Type II or active absorptive form (surface area range $1.1 - 15.7$ μm^2), Type III or differentiating form (surface area range $0.08 - 4.6$ μm^2) and Type IV or active secreting form (surface area range $4.1 - 11.7$ μm^2). In addition, the crypts of mucous cells were discriminated from those of MRCs based on the presence of globular extensions and similarly quantified. Density and frequency of MRCs and mucous cells varied significantly (GLM; $p < 0.05$)

according to the experimental salinity and according to time after transfer; in freshwater adapted larvae all types were present except Type IV but following transfer to elevated salinities, Type I and Type II crypts disappeared and appeared to be replaced by Type IV crypts. The density of Type III crypts remained constant following transfer. Immunogold labelling used in conjunction with transmission electron microscopy, using a novel, pre-fixation technique with anti-Na^+/K^+-ATPase and anti-CFTR, allowed complementary visualisation of specific localisation of the antibodies on active MRCs at an ultrastructural level, permitting a review of MRC apical morphology and related Na^+/K^+-ATPase binding sites.

Further in depth investigations using immunohistochemistry on whole-mount larvae using Fluoronanogold™ (Nanoprobes, U.S.) as a secondary immunoprobe allowed fluorescent labelling with the high resolution of confocal scanning laser miscroscopy, combined with the detection of immunolabelled target molecules at an ultrastructural level using transmission electron microscopy. Aspects of MRC ontogeny, differentiation and adaptation in Nile tilapia yolk-sac larvae following transfer from freshwater to 12.5 and 20 ppt were revealed. The development of a novel 3-D image analysis technique of confocal stacks, allowing visualisation of MRCs in relation to their spatial location, permitted assessment and classification of active and non-active MRCs based on the distance of the top of the immunopositive cell from the epithelial surface; mean active MRC volume was always significantly larger and displayed a greater staining intensity (GLM; $p < 0.05$) than non-active MRCs. Following transfer, the percentage of active MRCs was seen to increase as did MRC volume (GLM; $p < 0.05$). Immunogold labeling with anti-Na^+/K^+-ATpase allowed the identification of both active and non-active MRCs using transmission electron microscopy. The density of

immunogold particles appeared to increase following adaptation to 12.5 and 20 ppt and, similarly, the tubular system appeared denser in elevated salinities. Various developmental stages of MRCs were identified within the epithelium of the tail of yolk-sac larvae, thus contributing towards an understanding of the role of mitochondria-rich cells in the development of osmoregulatory capacity during the critical early hatchery stage, as well as providing valuable information concerning the functional plasticity of iono-regulatory cells.

The results of this study have increased our understanding of salinity tolerance of the Nile tilapia during the critical early life stages, which in turn could improve hatchery management practices and extend the scope of this species into brackish water environments. In addition, insights have been made into basic iono-regulatory processes that are fundamental to the understanding of osmoregulatory mechanisms during early life stages of teleosts.

Presentations and publications arising from this thesis

Conferences:

Fridman, S., Bron, J.E. and Rana, K.J. (2008). Salinity affects the distribution dynamics of chloride cells during early life stages of the Nile tilapia (*Oreochromis niloticus* (L.)). 8th International Symposium on Tilapia in Aquaculture, Cairo, Egypt. October 2008. **Poster presentation.**

Fridman, S., Bron, J.E. and Rana, K.J. (2011). The development of correlative microscopy techniques to define morphology and ultrastructure in chloride cells of Nile tilapia (*Oreochromis niloticus* (L.)) yolk-sac larvae. 9th International Symposium on Tilapia in Aquaculture, Shanghai, China. April 20th – 22nd 2011. **Poster presentation.**

Fridman, S., Bron, J.E. and Rana, K.J. (2011). Osmoregulatory capacity of the Nile tilapia (*Oreochromis niloticus* (L.)) during early life stages. 9th International Symposium on Tilapia in Aquaculture, Shanghai, China. April 20th – 22nd. **Oral presentation.**

Publications:

Fridman, S., Bron, J.E. and Rana, K.J. (2011). Ontogenetic changes in location and morphology of chloride cells during early life stages of the Nile tilapia (*Oreochromis niloticus* (L.)) adapted to freshwater and brackish water. *Journal of Fish Biology*. **In press.**

Fridman, S., Bron, J.E. and Rana, K.J. (2011). Influence of salinity on embryogenesis, survival, growth and oxygen consumption in embryos and yolk-sac larvae of the Nile tilapia (*Oreochromis niloticus (L.)*). **In preparation.**

Table of Contents

List of Figures

List of Tables

1 Chapter 1 General introduction

1.1 Brackish water aquaculture and tilapiine culture

1.1.1   Brackish water aquaculture

For many years it has been recognised that the culture of euryhaline fish species in brackish water or marine systems could potentially provide animal protein in areas where freshwater resources were limited (Loya and Fishelson, 1969). In recent times, the rapidly increasing drain of urban, industrial and agricultural activities on freshwater resources worldwide has limited the scope of freshwater aquaculture, especially in tropical and arid coastal areas (Suresh and Lin, 1992 a). There therefore exists an urgent need to manage marine and brackish water environments more efficiently and to diversify aquacultural practices either by the introduction of new candidate species or by the adaptation of culture methods for existing species. Whilst there are constraints limiting the expansion of brackish water aquaculture *e.g.* pollution, acidity or fluctuating salinity levels, there still exist specific areas where brackishwater aquaculture offers potential for expansion *e.g.* arid lands with brackish water ground water or areas without competition for alternative land use.

Worldwide brackish water aquaculture production of fish, crustaceans and mollusks has risen from 1,318,227 tonnes in 1990 or 3.4 % of total aquaculture production to 3,082,261 tonnes in 2008 or 7% of total aquaculture production (FAO; FishStat Plus,

2010) (Figure 1.1.). At the present time, shrimp and prawn culture dominates brackish water aquaculture and, in 2008, represented 55% of total brackish water culture at 2,362,859 tonnes. Worldwide brackish water culture of tilapia *spp.* stood at 414,821 tonnes in 2008, of which Egypt, which has shown a steady increase in production in recent years, produced 363,126 tonnes or 87% of total brackish water culture of tilapia *spp.*, at a value of $48,378,000 US (FAO; FishStat Plus, 2010).

- Mariculture
- Brackish water culture
- Freshwater culture
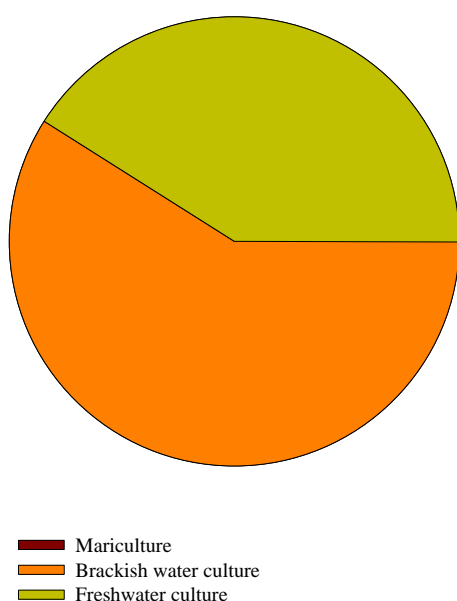
Figure 1. 1 Worldwide aquaculture production (%) by environment in 2008 (FAO; FishStat Plus 2010).

1.1.2   Tilapia; biology and distribution

Tilapia are endemic to Africa and the Levant, where more than 70 species have been identified (Philippart and Ruwet, 1982; Macintosh and Little, 1995; McAndrew, 2000) although few species are of aquacultural significance (Shelton and Popma, 2006). The

term 'tilapia' is used here to include the various fish species belonging to the family Cichlidae which were formerly grouped under the single genus Tilapia but are now separated, according to Trewavas (1982, 1983) into the three genera *Tilapia*, *Oreochromis* and *Sarotherodon.* These classifications were based on morphological, merististic and biogeographic traits as well as their specific reproductive characteristics *e.g. Tilapia* guard their developing eggs and fry in nests, *Oreochromis* females incubate their eggs and fry orally and *Sarotherodon* males and /or females incubate their eggs and fry orally.

Breeding is asynchronous for *Tilapia*, *Oreochromis* and *Sarotherodon spp.* and may take place year round with suitable temperatures. Breeding for *Oreochromis* and *Sarotherodon spp*. takes place in a 'lek' or arena system, where males prepare a nest and defend their territory within a spawning area. A ripe female will spawn in the nest, and, immediately after fertilization by the male, collects the eggs into her mouth and moves out of the territory. The male remains in his territory, guarding the nest, and is able to fertilize eggs from a succession of females. The female incubates the eggs in her mouth and broods the fry after hatching until the yolk-sac is absorbed (Figure 1.2.) however, even after fry are released, they may swim back into her mouth if danger threatens. Incubation and brooding is accomplished in 1 - 2 weeks, depending on water temperature, during which time the female will not eat. A notable feature of tilapia is the plasticity of initial sexual maturation relative to size and age, which, in unstable and restricted water bodies, may occur at less than half the time or half the size of those in more stable environments (Lowe-McConnell, 1982; Philippart and Ruwet, 1982).

Figure 1. 2 Female Nile tilapia (*Oreochromis niloticus*) with brood in mouth.

Tilapia are essentially tropical, lowland fish and display a general tolerance to poor environmental conditions *e.g.* high ammonia concentrations, low dissolved oxygen, turbidity, salinity and high temperatures. They do possess, however, a limiting tolerance to low temperatures. Adult tilapia are predominantly vegetarian but display ontogenic and species specific differences in their feeding habits (Bardach *et al.*, 1972; Balarin and Hatton, 1979; Bowen, 1982). Natural foods can range from macrophytes to phytoplankton, but tilapia will also eat aquatic invertebrates, plankton, benthic organisms, larval fish as well as decomposing organic matter. Larval stages and fry feed in shallower water than adults, mainly on detritus and neuston and juveniles feed on detritus and periphyton (Bruton and Boltt, 1975).

The suitability of tilapia for culture is, additionally, associated with their readiness to breed in captivity, their tolerance to handling and intensification of farming methods, their adaptability to various feedstuffs, their resistance to poor water quality and disease

as well as being perceived as a marketable and palatable product (Balarin and Haller, 1982). However, their intolerance to low temperatures has restricted their culture to warmer climates or to locations where warm water is available. The first documented presence of the tilapia outside their native range occurred as early as the beginning of the 20th century, however, it was only by the mid 20th century that tilapia species of biological and economic interest were extensively transplanted for fisheries or aquaculture. The Mozambique tilapia (*Oreochromis mossambicus*) was the first species to be distributed worldwide for culture (Balarin and Haller, 1982; Phillipart and Ruwet, 1982; Pullin *et al.,* 1997), followed, in the 1960s, by species that showed better culture characteristics such as faster growth *e.g.* the Nile tilapia (*Oreochromis niloticus*) and the Blue tilapia (*Oreochromis aureus*) (Pullin *et al.,* 1997). Now 98% of tilapia production occurs outside the species' native range. Worldwide distribution of the Mozambique tilapia and Nile tilapia are shown in Figure 1.3.
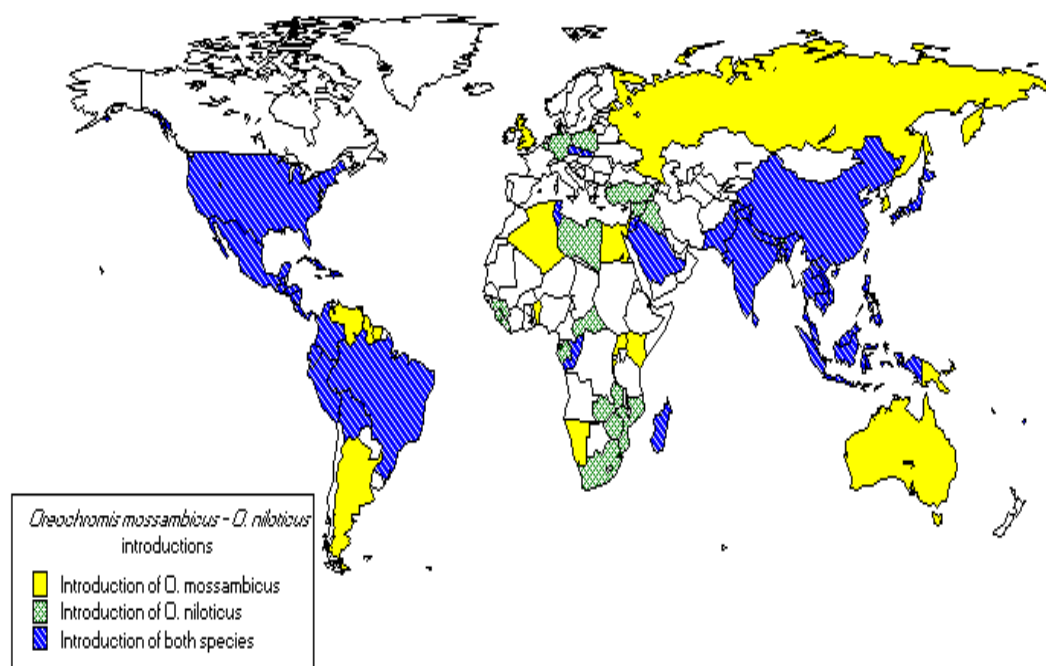
Figure 1. 3 Worldwide distribution of *O. mossambicus* and *O. niloticus* (FAO, 2010).

With the introduction of monosexing through hormonal sex-reversal techniques (Eckstein and Spira, 1965; Jalabert *et al.,* 1974) the problem of excessive recruitment, stunting and low percentage of market sized fish could be controlled, which, along with breakthroughs in research into nutrition and culture systems, led to a rapid expansion of the industry since the mid-1980s (Shelton and Popma, 2006). Tilapia and other cichlids are now the second most important cultured fish group in the world after carps, barbels and other cyprinids (FAO; FishStat Plus, 2010) and are also one of the fastest growing groups of cultured fish, with world aquaculture production of tilapias and other cichlids increasing from 379,184 tonnes in 1990 to 2,797,819 tonnes in 2008 (FAO; FishStat Plus, 2010).

1.1.3   The Nile tilapia (*Oreochromis niloticus*)

The Nile tilapia is endemic to shallow tropical and sub-tropical waters of Africa and is found widely distributed in river basins in West Africa, and throughout the Nile River basin, the Lake Chad basin and the Lakes Tanganyika, Albert, Edward and Kivu (Trewavas, 1983; Pullin and Lowe-McConnell, 1982). The lower and upper lethal temperatures for Nile tilapia are 11 - 12 °C and 42 °C, respectively. It is an omnivorous grazer that feeds on phytoplankton, periphyton, aquatic plants, small invertebrates, benthic fauna, detritus and bacterial films associated with detritus. Nile tilapia can live longer than 10 years and reach a weight exceeding 5 kg.

The Nile tilapia can be distinguished by a relatively strong vertical banding in the caudal fin of both sexes and by a gray-pink pigmentation in the gular regions. Males are larger than females after sexual maturation, and colouration becomes more pronounced

and widespread in breeding males (Figure 1.4.). Nile tilapia are maternal mouth-brooders (see Section 1.1.2. above). Their eggs are oval and orange-yellow in colour and egg size is, in general, influenced by age of female (Macintosh and Little, 1995). Nile tilapia (75 – 500 g body weight) can produce 50 – 2,000 eggs per spawning (Chimits, 1955). Optimal spawning temperature is between 25 to 30 °C.

Figure 1. 4 Adult male Nile tilapia (*Oreochromis niloticus*)

The Nile tilapia was exported from the 1960s onwards to around 46 countries outside Africa and to 11 countries within Africa (Pullin *et al.,* 1997). This species now dominates tilapia aquaculture because of its adaptability and fast growth rate (Macintosh and Little, 1995; Shelton, 2002) and global production of Nile tilapia has risen steadily over the years (Figure 1.5.A.). In 2008, production of Nile tilapia made up 83% of total tilapia production (FAO; Fishstat Plus, 2010). The main producers of Nile tilapia by country for 2008 are shown in Figure 1.5.B.
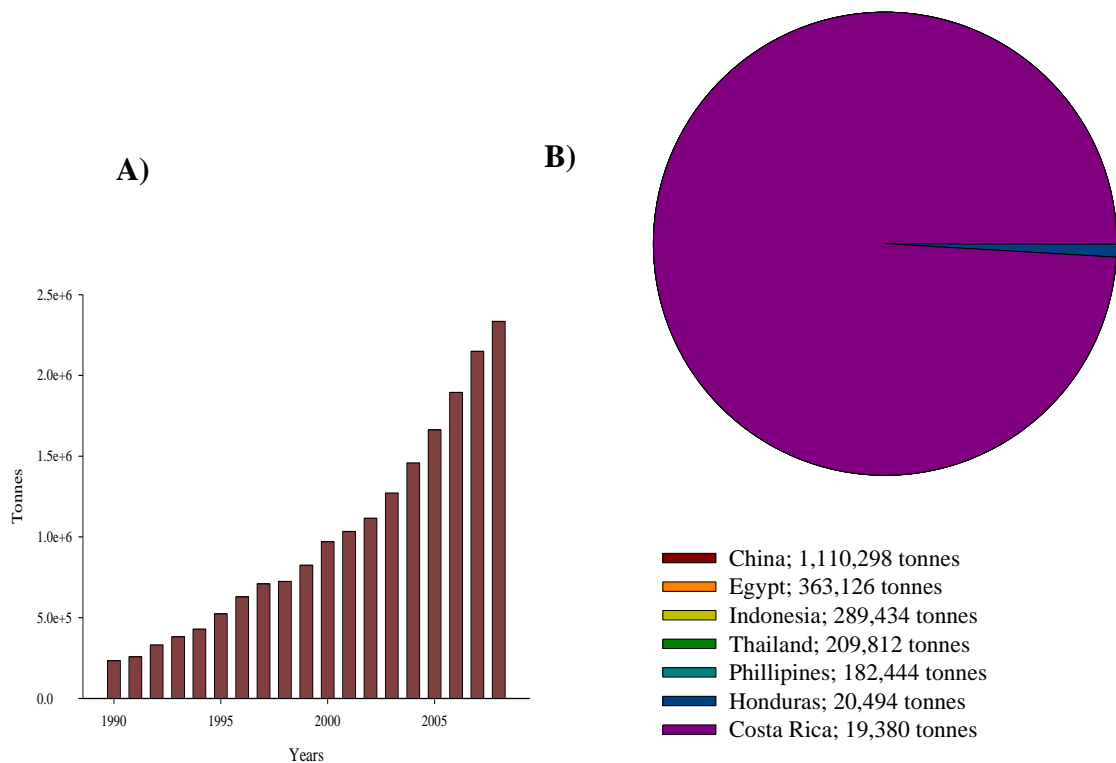
Figure 1. 5 A) Global aquaculture production (tonnes) of Nile tilapia from 1990 – 2008 (FAO; FishStat Plus, 2010) and **B)** Main producers of Nile tilapia in all environments *(i.e.* freshwater, brackish water and marine) by country in 2008 (FAO; FishStat Plus, 2010).

1.1.4   History of tilapia culture in saline waters

Tilapiine fishes, despite being predominantly freshwater species, display an ability to tolerate a broad range of naturally occurring variations in environmental salinities. Indeed, there have been reports of various species of tilapias occurring naturally in Africa and the Middle East in coastal or estuarine environments with salinities reaching or exceeding that of seawater (Stickney, 1986). Fitzsimmons (2006; p. 52) describes tilapia as 'adept pioneer fish' that show flexibility both in their utilisation of available resources and in their ability to colonise fluctuating ecosystems.   Although not specifically referring to the tilapia's salt tolerance, it could equally well describe their innate ability to exploit brackish water and marine systems in tropical and arid coastal

8

areas (Payne and Collinson, 1983; Hopkins *et al.,* 1989; Watanabe *et al.*, 1989 a and b; Watanabe, 1991; Suresh and Lin, 1992 a).

In the late 1950s, small-scale experiments in Hawaii to develop an intensive tank culture of the Mozambique tilapia at elevated salinities (10 − 15 ppt) to produce bait-fish for the skipjack tuna industry suggested that commercial production of the species in a brackish water system was feasible (Uchida and King, 1962). Around the same time in Israel, both small and larger-scale experiments were being carried out to study the adaptability of some commercial tilapia to varying salinities *e.g. O. aureus*, the hybrid *O. niloticus* x *O. aureus* and *Tilapia zillii* (Fishelson and Popper, 1968; Loya and Fishelson, 1969). Indeed, by this time, the potential of tilapia as candidate species for brackish water aquaculture through improved growth and inhibition of breeding had been noted (Hickling, 1963). However, it was only in the mid-1980s that the recognition of the possibility of culture of tilapia in waters of elevated salinity gathered momentum with the development of 'superior' strains or hybrids such as the Florida Red (see Section 1.1.5.5.) which presented the combined advantages of a lightened body colour, high growth and salinity tolerance. This offered a potential for culture and a wealth of research followed *e.g.* Hopkins (1983), Liao and Chen (1983), Payne and Collinson, (1983), Watanabe *et al.* (1984), Stickney (1986), Hopkins *et al.* (1989), Suresh and Lin (1992 a) and Watanabe *et al.* (1997).

During the 1990s, commercial saltwater culture in conjunction with marine shrimp production was initiated in the Caribbean (Head *et al*., 1996), Central America (Fitzsimmons, 2000) and Thailand. Semi-intensive culture of saline tolerant strains in

brackish water ponds and marine cages has developed in the Philippines (Romana-Eguia and Eguia, 1999) and interest in culture of the Florida Red strain in Egypt has emerged in recent years (Fitzsimmons, 2006).

1.1.5   Salinity tolerance of commercially important tilapia

Amongst the tilapia species of aquacultural interest, there is a clearly defined species specificity of salinity tolerance; many species are broadly euryhaline whilst others are restricted to fresh or low-salinity water. Numerous reviews of salinity tolerance of various cultured tilapias have been published *e.g.* Hickling (1963), Kirk (1972), Balarin and Hatton (1979), Chervinski (1982), Stickney (1986), Prunet and Bournancin (1989), Perschbacher (1992), Suresh and Lin (1992 a) and El-Sayed (2006).

The salinity tolerance ranges for the more commonly cultured species are briefly outlined below:

1.1.5.1   The Mozambique tilapia (*Oreochromis mossambicus*)

In its native range, the Mozambique tilapia is found in estuaries, and, following its introduction into culture systems around the world, has been found thriving naturally in marine and brackish water environments. It has been reported to withstand 27 ppt following direct acclimation (Al-Amoudi, 1987). It can grow normally and reproduce at a water salinity of 49 ppt (Popper and Lichatowich, 1975).

1.1.5.2   The Red-belly tilapia (*Tilapia zillii*)

The Red-belly tilapia similarly has a high salinity tolerance; they are found naturally occurring in highly saline environments (36 - 45 ppt) in many tropical and sub-tropical regions (Balarin and Hatton, 1979) and can also reproduce at 43 ppt (Bayoumi, 1969).

1.1.5.3   *Oreochromis spilurus*

This species offers potential for culture in seawater; it can be gradually acclimated to sea water from fry as small as 0.03 g (Jonassen *et al.*, 1997) and can be cultured in full strength sea water (Carmelo, 2002). Fecundity at 38 – 41 ppt is reported to be half of that of groundwater (3 – 4 ppt) (Al-Ahmad *et al.*, 1988). They also display a tolerance to lower temperatures (Hopkins *et al.*, 1989) but are not popular for culture due to their slow growth and over-reproduction (Chervinski and Zorn, 1974; Suresh and Lin, 1992 a).

1.1.5.4   The Blue tilapia (*Oreochromis aureus*)

The Blue tilapia is less tolerant to high salinities but can breed at salinities from 10 - 19 ppt (Wohlfarth and Hulata, 1983), produce fry equally well at freshwater and 4 ppt with fry production declining at 10 ppt (Perry and Avault, 1972).

1.1.5.5   Red hybrid tilapia

Hybridisation, in principal, offers the benefits of combining species that display a high growth capacity with species that display a high salinity tolerance. The red tilapia is generally thought to be attributed to crossbreeding of a mutant reddish-orange *O.*

mossambicus with other species *i.e. O. aureus*, *O. niloticus* and *Oreochromis hornorum* (Fitzgerald, 1979; Behrends *et al.,* 1982; Galman and Avtalion, 1983; Kuo and Tsay, 1984). Indeed the reddish or blond colouration proved more popular than the normal darker coloured species due to their similarity to marine species such as the red snapper (*Lutjanus campechanus*) and can command a premium price. Feasibility studies were first carried out with the Taiwanese red tilapia (*O. mossambicus* x *O. niloticus*) and good growth was reported at 17 and 37 ppt in Taiwan (Liao and Chen, 1983), at 11 to 17 ppt in Hawaii (Meriwether *et al.* 1984) and at 38 to 41 ppt in Kuwait (Hopkins *et al.,* 1989). The Florida red strain, descendants of an original cross between *O. hornorum* (female) and the mutant blond *O. mossambicus* (male) (Behrends *et al*., 1982) was actually found to exhibit better growth in brackish and sea water than in freshwater (Watanabe *et al.,* 1988), initiating detailed studies on culture methodology for this strain.

1.1.5.6   The Nile tilapia (*Oreochromis niloticus*)

The Nile tilapia is not considered to be amongst the more salt-tolerant of the tilapia species but still offers a great potential for low-salinity or brackish water culture (Stickney, 1986; Suresh and Lin, 1992 a). It has been reported to occur naturally in brackish water lakes in Egypt (Fryer and Iles, 1972; Kirk, 1972). The reported range of salinity tolerance of this species will be further discussed in the introduction to Chapter 4.

1.1.6 Potential for brackish water culture of tilapia

The availability of freshwater can be seen as a major bottleneck in the expansion of tilapia aquaculture, therefore the development of species that tolerate elevated salinities without a reduction in productivity is vital (Rengmark *et al*., 2007). Tilapia are suitable candidates for aquacultural diversification into coastal lagoons with brackish water and estuarine areas where culture of purely marine species is not suitable. The ease of both seed production and on-growing of tilapia as compared to marine species, that often have complicated and delicate early life stages, is obviously advantageous. The areas that offer potential for brackish water culture can be divided into 1.1.6.1. Sub-Saharan Africa, 1.1.6.2. Tilapia-shrimp polyculture, and 1.1.6.3. Arid-zone farming.

1.1.6.1 Sub-Saharan Africa

FAO's 2004 report on 'Current Economic Opportunities in sub-Saharan Africa' suggested that a diversification of both culture environments and cultured species could stimulate the development of the aquaculture sector in sub-Saharan Africa with a concomitant rise in economic opportunities. It reported that with freshwater aquaculture accounting for 87% of the 2002 total sub-Saharan Africa's aquaculture production (of which tilapia and catfish were the most popular cultivated species, accounting for 60% of freshwater aquaculture production), brackish water produced only 8% of total sub-Saharan Africa's aquaculture production or an estimated 6,522 tonnes (FAO; FishStat Plus, 2005). This draws attention to the enormous potential for the development of brackish water resources in coastal areas of sub-Saharan Africa where freshwater is limiting. Using the example of Egypt (see above Section 1.1.1.) and its steady growth in

brackish water production of Nile tilapia in recent years, sub-Saharan Africa could similarly benefit by utilising its brackish water resources.

1.1.6.2 Tilapia-shrimp polyculture

Flegal and Alday-Sanz (1998) observed that a better understanding of the shrimp pond environment was necessary in order to eliminate risks of widespread disease outbreaks that had devastated the shrimp industry. Polyculture of shrimp with tilapias may offer a sustainable and more economically viable alternative culture system (Fitzsimmons, 2001) and is being implemented in Thailand, the Philippines, Ecuador, Mexico and the U.S. (Yi and Fitzsimmons, 2004). Indeed, an increased yield of shrimp with tilapia has been reported (Akiyama and Anggawati, 1999; Garci-Perez *et al*., 2000; Yap, 2001). The presence of tilapia in ponds appears to reduce transmission of viruses and bacterial pathogens and, in addition, the foraging behaviour of the tilapia disturbs the sediment, releasing nutrients into the water column and interrupting the life cycle of shrimp pathogens (Yi and Fitzsimmons, 2004).

1.1.6.3 Arid-zone farming

Many arid regions are experiencing freshwater shortages, therefore euryhaline species such as tilapias, with known and economically viable culture practices, offer potential where seawater resources are abundant (Perschbacher, 1992). Also, the intensification of tilapia culture under controlled management systems *e.g.* closed culture systems especially in areas with limited freshwater or brackish water resources, is becoming more widespread in order to meet increasing demand (El-Sayed, 2006).

1.2 Adaptive mechanisms for salinity tolerance

1.2.1   Background

Fishes have evolved to occupy almost all types of natural waters, ranging from low-ionic strength fresh waters to those of salinities of 80 – 142 ppt (Kinne, 1964; Parry, 1966; Griffiths, 1974; Alderdice, 1988). Some fishes are restricted to living in a narrow range of salinity (stenohaline) while others are able to adapt to and tolerate broad ranges of salinity (euryhaline). Euryhalinity can range from either compulsory, migratory events in the life-cycle of a fish *e.g.* catadromous fishes which spend their pre-adult life in freshwater and return to spawn in the sea or, conversely, anadromous fishes which grow and mature in sea water but return to freshwater to spawn, to less clearly defined movements of fishes that occupy estuarine waters or coastal habitats and undergo regular and frequent variations in the salinity of the medium in which they inhabit. This ability to cope with salinity changes depends on their capacity to osmoregulate, and plays an important role in defining species and developmental stage-specific distribution (Schreiber, 2001).

It is generally accepted that the first vertebrates evolved in seawater (Holland and Chen, 2001), entered brackish and freshwater and then, in some cases, re-entered the marine environment (Carroll, 1988). The presence of functional glomerulii in the totally marine hagfish (Riegel, 1998), a modern member of the earliest fish lineage which has no freshwater ancestry, invalidates the early hypothesis that the presence of a renal glomerulus which is used to balance the osmotic uptake of water in freshwater fishes, is the result of a fresh water origin in vertebrates (Smith, 1932). Marine origin is further

supported by extant fossil records (Holland and Chen, 2001). The evolutionary sequence of movement of vertebrates from seawater to fresh water is represented in Figure 1.6.
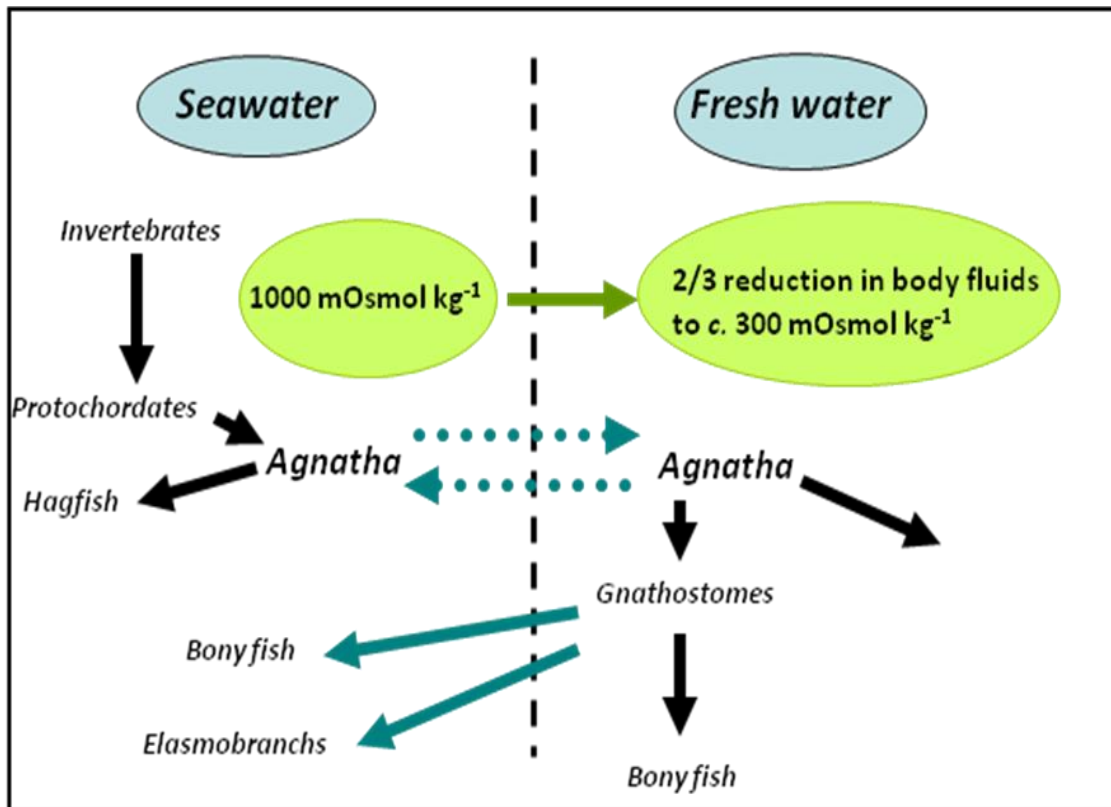
Figure 1. 6 Evolutionary sequence of movements of vertebrates from seawater to freshwater. Green arrow shows reduction in body fluid osmolality following movement to freshwater; blue arrows indicate movement between environments. Adapted from Evans, D.H. (1982).

1.2.2   Overview of osmoregulatory processes

Prunet and Bornancin (1989; p. 92) describe teleost fishes as 'an open system in dynamic equilibrium with aquatic surroundings'. As osmoregulators they are homeo-isosmotic *i.e.* are able to regulate the concentration of solutes within their cells or body

fluids therefore maintaining the total volume of water and solutes within their body at levels that are different to that of their surrounding environment. Hence their body fluids remain relatively constant in spite of alterations to their external medium. They are, therefore, able to maintain their blood osmolality in a 280 - 360 mOsm kg^{-1} range, at the equivalent of 10 – 12 ppt (Varsamos *et al.,* 2005). Hyper-osmotic regulators (most freshwater teleosts) maintain body fluid concentration above that of their external surroundings, and conversely, hypo-osmotic regulators (most marine teleosts) maintain body fluid concentration below that of their external medium (Figure 1.7.). Therefore, when faced with variations in external salinity, fishes must compensate for body fluid disturbances that result with an adaptive and regulative capacity to osmoregulate. The sites and mechanisms for the maintenance of fluid and electrolyte homeostasis across a range of salinities are described below.
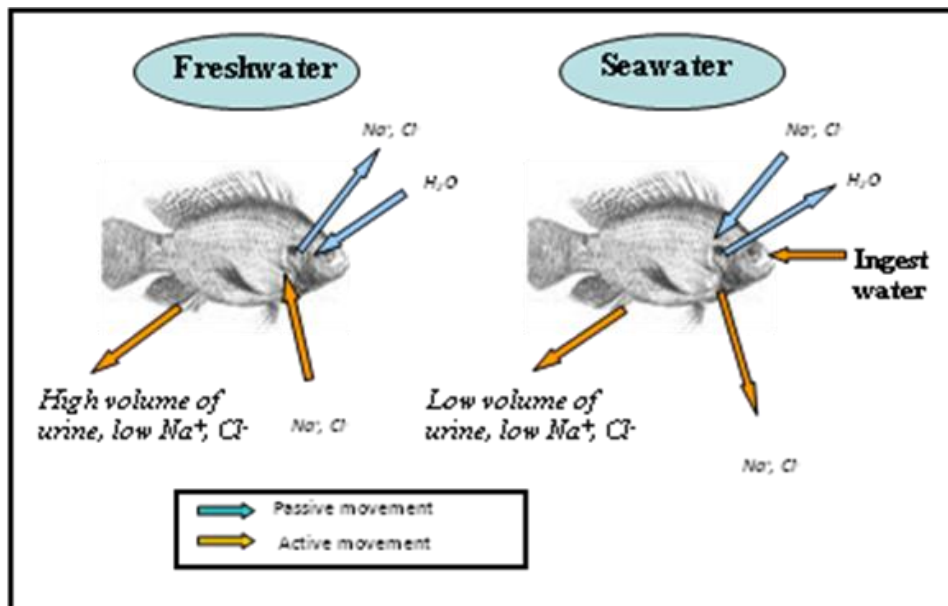
Figure 1. 7 Generalised schematic representation of movement of water and ions in adult teleost fishes.

1.2.3   Role of Na$^+$/K$^+$-ATPase in teleost osmoregulation

Ionic balance is maintained by Na$^+$/K$^+$-ATPase or the 'sodium-pump'. It is a universal membrane-bound enzyme that actively transports Na$^+$ out of and K$^+$ into animal cells (Hwang *et al.,* 1989). It not only maintains intracellular homeostasis but also provides the driving force for many transport systems in a variety of osmoregulatory epithelia, including fish gills (Evans *et al.,* 2005). Kamiya (1972) was the first to report that branchial mitochondria-rich cells in the Japanese eel (*Anguilla japonica*) contained high amounts of Na$^+$/K$^+$-ATPase located on the tubular system. Later, due to its ion-transporting function through direct movement of sodium and potassium across the plasma membrane or indirect generation of ionic and electrical gradients, it was postulated by Sardet *et al.* (1979) that the repeating units of transport-associated Na$^+$/K$^+$-ATPase, supplied with ATP from the numerous mitochondria, were directly involved in osmoregulation.

Na$^+$/K$^+$-ATPase is a P-type ATPase or heterodimeric, integral, membrane-spanning protein consisting of an ($\alpha\beta_2$) protein complex; the catalytic α-subunit has four isoforms (α1-α4) and has a molecular weight of approx. 100 kDa, whilst the glycosylated β-subunit has three isoforms (β1-β3) with a molecular weight of approx. 60 kDa (Scheiner-Bobis, 2002) (Figure 1.8.A.). The α-subunit contains binding sites for ions and is responsible for the transportation of three internal sodium ions outwards in exchange for two potassium ions. Each translocation of ions requiring the hydrolysis of ATP creating an electrogenic difference across the cell membrane (Figure 1.8.B.). It therefore contributes to ion transport either directly by movement of sodium and potassium across the plasma membrane or indirectly through generation of ionic and

electrical gradients (McCormick, 1995).
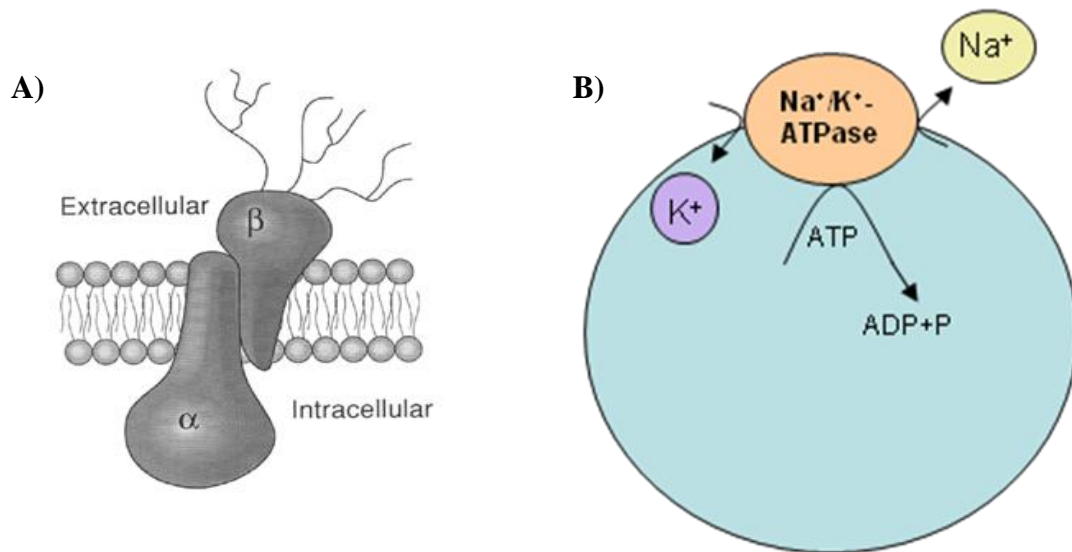
Figure 1. 8 A) $\alpha\beta_2$ protein complex of Na^+/K^+-ATPase and **B)** Schematic representation of Na^+/K^+-ATPase.

1.2.4   Branchial sites of osmoregulation in the adult teleost - the gills

It is widely accepted that the fish gill is a 'multi-functional organ' (Laurent and Perry, 1991; Evans *et al*., 2005) and plays a central role in the interaction between the internal environment of the fish and the external aquatic environment in which it lives. The gill comprises over half the body surface area and its functions include aquatic gas exchange, osmotic and ionic regulation, acid-base regulation and excretion of nitrogenous wastes (Evans *et al*., 2005).

1.2.4.1   Anatomy of the fish gill

The general anatomy of the gills varies among the three extant lineages of fishes; Agnatha (hagfish and lampreys), Chondrichthyes or Elasmobranchs (sharks, skates and rays) and Actinopterygii (bony fishes, with teleosts being the most prevalent). The gills of teleost fishes are located in the branchial chamber, near the head region, and are protected by a thin, bony flap called the operculum. Water enters the buccal cavity via the mouth, passes over the gills and exits via the openings of the operculii.

Hughes (1984; p.11) described the general organisation of the gills as one based on 'a system of progressive subdivision': the teleost fish has four gill arches, from whose internal base radiate laterally cartilaginous or bony support rods or gill rays which support the gill filaments or hemibranchs. These are a double row of filaments that taper at their distal ends and form the basic functional unit of gill tissue on both the cranial and the caudal side of the gill arch (Figure 1.9.A.). A pair of caudal and cranial filaments from the same arch is referred to as a holobranch. The connective tissue between these filaments form an inter-branchial septum (ibs) (Figure 1.9.B.), which is much reduced in teleosts as compared to elasmobranchs, usually only extending to the base of the filaments. Secondary lamellae on either side of the filament's surface are evenly distributed along a filament's length, connected by the inter-lamellar spaces (ils) (Figure 1.9.B.); lying perpendicular to the long axis they considerably increase the gill's functional surface area.
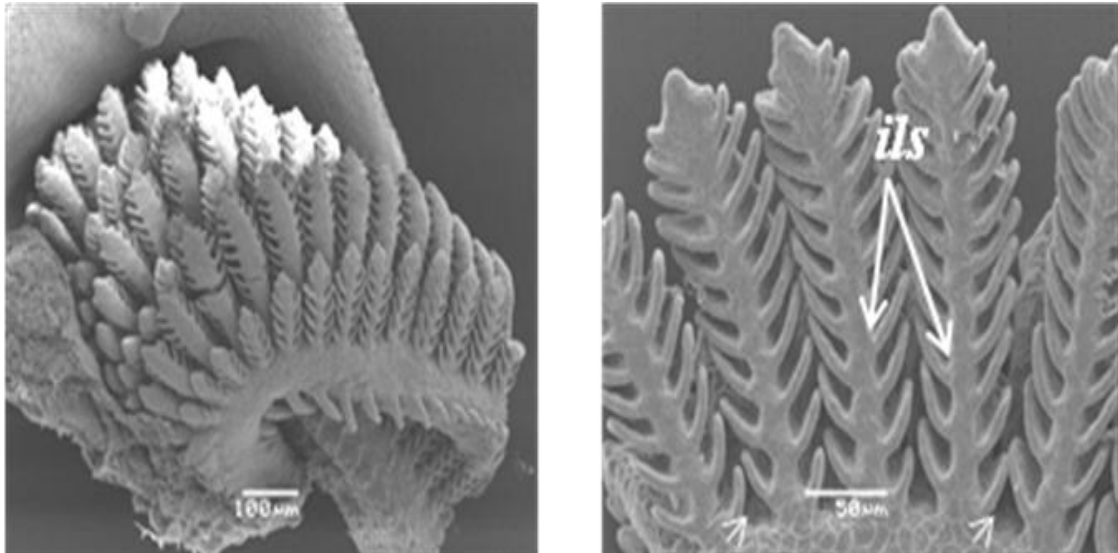
A)   **B)**

Figure 1. 9 Scanning electron micrographs of the gills of Nile tilapia larvae at yolk-sac absorption. **A)** Dissected gill arches [Bar = 100 μm] and **B)** Gill filaments or hemibranchs with secondary lamellae. Arrowheads indicate inter-branchial septa (ils; inter-lamellar spaces) [Bar = 50 μm].

1.2.4.2   Microcirculation and internal morphology of the vasculature of the gills

Blood flow has two distinct but interconnected circulatory systems: the arterioarterial vasculature and the arterio-venous vasculature:

- *Arterioarterial vasculature*

The arterioarterial vasculature (Laurent and Dunel, 1980) is also known as the respiratory pathway because it is responsible for the exchange of gas between the blood and its environment. Blood enters the gills via the afferent branchial arteries (A.B.A.) (Figure 1.10.), which receive the entire cardiac output from the ventral aorta, that lie alongside their respective branchial arches. This feeds the filaments on the hemibranchs

of an arch via afferent filamental arteries (A.F.A.), which travel along the length of a filament (Figure 1.10. and Figure 1.11.). Regularly spaced along these A.F.A.s are afferent lamellar arterioles (A.L.A.) that feed the lamellae (Figure 1.10. and Figure 1.11.). Lamellae are essentially two epithelial sheets held apart by a series of individual support cells called 'pillar cells' (P.C.) (Figure 1.11.) and the spaces between these pillar cells and the epithelial sheets are perfused or percolated with blood, flowing across the lamellae as a sheet.

Oxygenated blood is collected from the lamellae by the efferent lamellar arterioles (E.L.A.), short vessels that drain into the efferent filamental artery (E.F.A.) that travels along the length of the filament's efferent side, counter to the flow of that of the A.F.A. (Figure 1.11.). Blood also flows along a marginal channel (MC) which is free of pillar cells and which encircles the outer edge of the secondary lamellae (Figure 1.11.). The E.F.A. joins the efferent branchial artery (E.B.A.) at the site of a muscular sphincter, which may have a role in regulating lamellar blood flow, and this E.B.A. distributes it to the dorsal aorta for systemic circulation (Figure 1.10. and 1.11.).
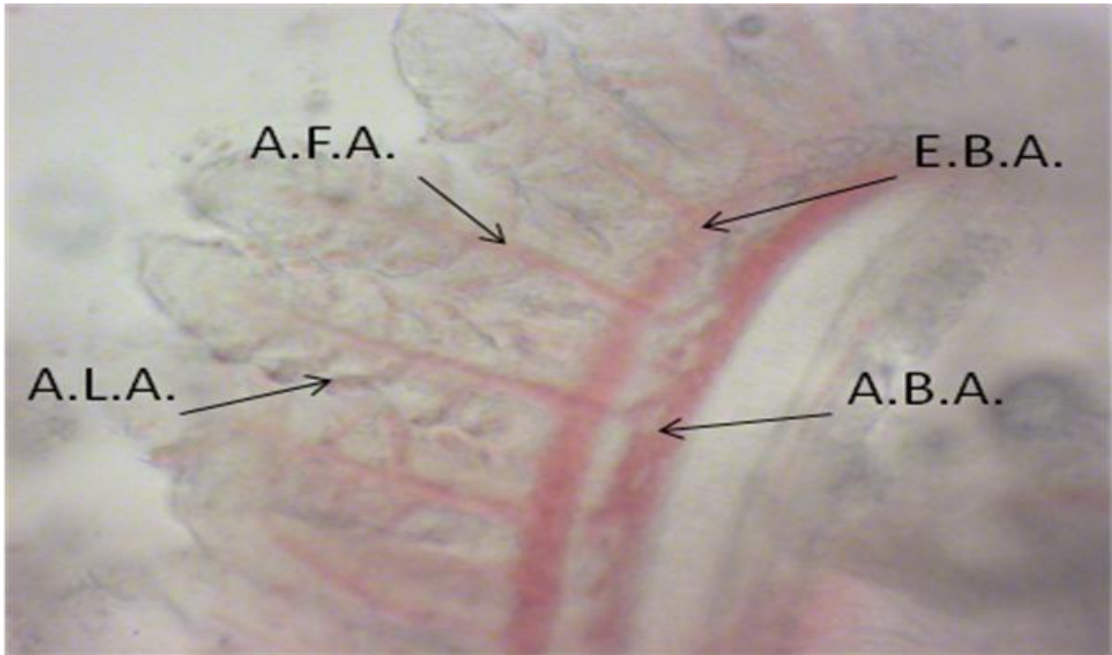
Figure 1. 10 Section of gill arch showing arterio-arterial vasculature. A.B.A.: afferent branchial artery; E.B.A.: efferent branchial artery; A.F.A.: afferent filamentary artery; A.L.A.: afferent lamellar arteriole (L.M.).
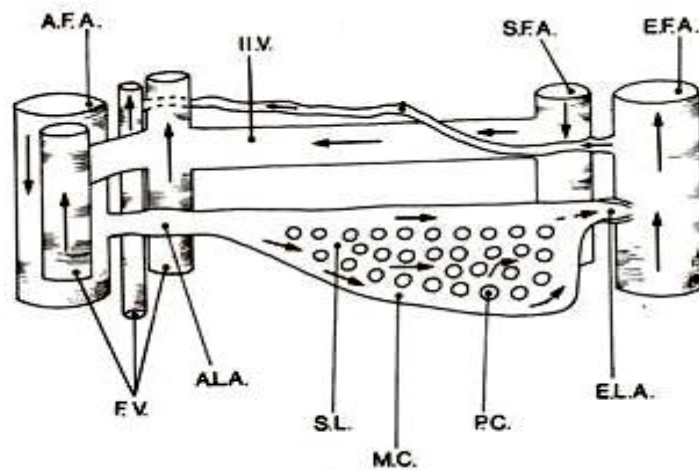
Figure 1. 11 The main vessels of the teleost gill showing arterioarterial and arteriovenous vasculature. A.F.A. afferent filamentary artery; A.L.A. afferent lamellae arteriole; E.F.A. efferent filamentary artery; E.L.A. efferent lamellar arteriole; P.C. pillar cell; S.L. secondary lamella; M.C. marginal channel; F.V. filamentary veins; Il.V. interlamellar vessel; S.F.A. subsidiary filamentary artery. Arrows indicate blood flow. From Satchell (1991).

23

- *Arteriovenous vasculature*

The arteriovenous vasculature (Olsen, 2000) is often referred to as the non-respiratory pathway. Its exact function is not entirely clear (Evans *et al.,* 2005) but is most likely involved with providing nutrients to the filament epithelium and underlying supportive tissues of the filaments, and may also provide a means for filamental blood to enter the venous circulation without crossing the lamellae.

The arterio-venous network is composed of a highly ordered series of very thin, sac-like vessels arranged like a ladder, often collectively known as the central venous sinus (CVS), the 'rungs' of which are called the inter-lamellar vessels (I.L.V.) and run parallel to the lamellae underneath the inter-lamellar epithelium. The 'legs' of the ladder of the I.L.V. run parallel to the length of the filament and connect to the afferent boundaries via filamentary veins (F.V.) and to efferent boundaries via the subsidiary filamentary artery (S.F.A.) (Figure 1.11.).

1.2.4.3   The branchial epithelium

The fish gill epithelia plays a critical role in the physiological function of the gill. The filament epithelium covers the filament and includes both the afferent and efferent edges as well as the spaces between the bases of the lamellae (interlamellar spaces or ILS) (Figure 1.9.B.). Within the filament and bordering much of the filament epithelium is the large central venous sinus (CVS), which forms part of the arterio-venous circulation (see above Section 1.2.4.2. and Figure 1.11.). The filament epithelium is thicker than the lamellar epithelium, and is usually composed of three or more cell

layers. Beneath the filament epithelium lie basal undifferentiated cells contacting the basal lamina and intermediate undifferentiated cells filling the intervening spaces.

The filamental epithelium is comprised of the following cells:

- Pavement cells (PVCs) make up the largest single fraction of the gill epithelium (*c.* 90 - 95%) and have been extensively studied (Hughes, 1979; Laurent and Dunel, 1980). Largely assumed to be important for gas exchange, they also provide mechanical support and protection (Dunel and Laurent, 1980). They are generally squamous (Evans *et al.,* 1999) and measure *c.* 3 - 10 μm in diameter (Laurent, 1984). They contain few mitochondria, but have other ultrastructural features suggesting metabolic activity including a well-developed Golgi apparatus, extensive rough endoplasmic reticulum, and numerous vesicles (Laurent and Dunel, 1980). External morphology has been found to vary from elaborate ridges like fingerprints to microvillus-like projections (Perry *et al.*, 1992) which are generally thought to play a role in mucus adhesion (Hughs, 1979).

- Mucous cells are not directly involved in ion or acid-base regulation, although they may have an indirect role in modulating ion transport by creating an ion-rich micro-environment (Handy, 1989). They are predominantly located on the leading and trailing edge of a filament, but can also be found in the inter-lamellar regions, close to the mitochondria-rich cells, but, as a general rule, the number and location is species specific and the density diminishes on transfer to seawater (Laurent, 1984).

- Serotonergic, neuroepithelial cells are also recorded on the gills but have no established, definitive role (Dunel-Erb *et al.,* 1982; Bailly *et al.,* 1992).

- Undifferentiated or stem cells are also present on the gill (Laurent, 1984).

- Mitochondria-rich cells (MRCs) (see Section 1.3. below).

- Accessory cells (ACs) (see Section 1.3.4. below).

1.2.4.4   Gas exchange

The gill evolved from the surface epithelium of the branchial basket of proto-vertebrates, probably appearing about 550 million years ago (Gilbert, 1997). Originally used in filter feeding, evolution appears to have modified the surface epithelium to facilitate gas exchange and provide the major pathway for oxygen and carbon dioxide transfer between environment and body tissues (Randall and Daxboeck, 1984). The fish gill is essentially composed of a highly complex vasculature surrounded by a high surface area epithelium, thus providing a thin barrier between a fish's blood and the aquatic environment. The lamellar epithelium overlays the arterio-arterial circulation (Olsen, 2000) and is typically one to three cell layers thick and composed of squamous pavements cells and basal and intermediate non-differentiated cells, supported by a strong basement membrane. Pillar cells are modified endothelial cells and support and define the lamellar blood spaces. The lamellar surface is likely to be the primary site for gas exchange; studies have shown a correlation between respiratory needs and lamellar surface *e.g.* benthic fishes have a much reduced surface area compared to more active pelagic fishes. Indeed the lamellar surface area can increase to $1.3m^2$ kg in the pelagic tuna or be as low as $< 0.1m^2$ kg in species that have alternative mechanisms for O_2 uptake (Perry and McDonald, 1993) *e.g.* the African catfish (*Clarias gariepinus*).

Gases move across membranes by simple diffusion down their partial pressure gradients, therefore specialised cell types are not required. Blood flow is counter-current to water flow and this counter-current system, combined with the increased surface area of the lamellae, makes the gills an ideal site for the uptake of oxygen and removal of carbon dioxide and ammonia. Haemoglobin, the respiratory pigment of fishes and other vertebrates, is contained in the red blood cells and provides an oxygen carrying device of high efficiency, enabling fish to take up in one unit volume of blood the oxygen contained in 15 – 25 times the same volume of water.

1.2.5   Extrabranchial sites of osmotic regulation in the adult teleost

1.2.5.1   Gastrointestinal tract

The digestive tract of adult teleosts is divided into oesophagus, stomach, anterior-middle–posterior intestine and rectum, and each display distinct morphological and osmoregulation-related functions and transport properties. Ambient salinity influences drinking rate such that marine teleosts, facing hyper-osmotic conditions, compensate for the loss of water by drinking large amounts of sea water. Available data for electrolyte transport and water flux across the digestive tract are limited to seawater or seawater-adapted species. Desalination begins in the oesophagus reducing the initially ingested water to half or less of initial salt concentration (Hirano and Mayer-Gostan, 1976; Nagashima and Ando, 1993), with salts absorbed through the epithelium by both active and passive processes. There is, however, a limited efflux of water due to low permeability of the oesophagus. The stomach has a minimal role in water or ion

processing (Hirano and Mayer-Gostan, 1976). Water transfer in the intestine occurs by a secondary active Na^+ K^+ Cl^- co-transporter driven pathway, that itself varies according to salinity (Musch *et al.,* 1982) and by passive osmotic water fluxes. The gut of marine teleosts also plays an essential part in compensating for the osmotic water loss. Seawater is processed along the gut in two steps: essentially ion diffusion with little net water uptake across the oesophagus (Hirano and Mayer-Gostan, 1976; Parmelee and Renfro, 1983) followed by active NaCl transport coupled to water absorption in the intestine (House and Green, 1965; Skadhauge, 1969; Field *et al.,* 1978; Frizzell *et al.*, 1984).

1.2.5.2   Urinary system

The urinary system *i.e.* the kidney and urinary bladder, plays an important role in fluid and ion balance in adult fish. Studies have shown that both structural and ultrastructural morphology can vary according to environmental salinity in relation to the different osmoregulatory functions of the kidney (Hickman and Trump, 1969; Elger and Hentschel, 1981; Nishimura and Imai, 1982; Hwang and Wu, 1988; Nishimura and Fan, 2003; Greenwell *et al*., 2003).

Freshwater-adapted teleost fish experience osmotic water gain through diffusive water gain across the gills and through ingestion with food (Kristiansen and Rankin, 2001)

and therefore have well-developed glomeruli that allow a high glomerular filtration rate (GFR) and a resulting high urine flow rate (UFR), producing urine that is hypotonic to the blood. Studies have detected an increase in kidney Na^+/K^+-ATPase activity during freshwater acclimation of some euryhaline teleosts *e.g.* sea bass (*D. labrax*) (Lasserre, 1971; Venturini *et al*., 1992), mullets (*Crenimugil labrosus*) (Lanserre, 1971), (*Chelon*

labrosus and *Liza ramada*) (Gallis and Bourdichon, 1976) implying the possible use of this enzyme in ion re-absorption from the glomerular filtrate. On the other hand, seawater-adapted teleosts face salt loading and dehydration, and, in order to compensate, there is a decrease in glomerular development and/or partial glomerular degeneration and corresponding decline in GFR and UFR *e.g.* tilapia (*O. mossambicus*) (Hwang and Wu, 1988) and salmonid *spp.* (*Oncorhynchus mykiss* and *Salmo irideus*) (Hickman and Trump, 1969). The kidney secretes divalent ions (mainly Mg^{2+} and SO_4^{2}) and produces small quantities of urine isotonic to blood.

It is established that the urinary bladder, as well as storing urine, also has a role in regulating re-absorption and secretion of ions and water. In freshwater teleosts, the urinary bladder actively reabsorbs Na^+ and Cl^- with a minimum of water in order to reduce excretory ion losses (Curtis and Wood, 1991). In seawater, teleosts must reabsorb water passively therefore increasing the concentration of divalent ions in the bladder.

1.3 The Mitochondria-rich Cell (MRC)

1.3.1   Introduction

In an aquatic environment, an organism that is not iso-osmotic to its environment will experience passive diffusional movements of solutes and water between the environment and the extra-cellular fluids. As opposed to movement of gases, specific compensatory ion movements require specific carriers and this 'metabolic machinery'

(Rombough, 2004) is found in a specific cell type *i.e.* the mitochondria-rich cell (MRC). Mitochondria-rich cells intersperse with pavements cells (PVCs) on the filamental epithelium and occupy a small fraction of the branchial epithelial surface area (< 10%). Numerous studies, dedicated to the study of their form and function, have established that these cells are the primary extra-renal site responsible for the trans-epithelial transport of ions in adults and juvenile teleosts (Laurent, 1984; Laurent and Dunel, 1980; Perry *et al.,* 1992; McCormick, 1995; Evans, 1999; Evans *et al.* 2005).

Large spherical cells with eosinophilic granules were first described by Keys and Willmer (1932) of the Physiological Laboratory, Cambridge (U.K.) as 'chloride-secreting cells', based on observations of the chloride secretory activity of gills of the adult eel (*Anguilla anguilla*) in seawater. The abbreviated name 'chloride cell' is probably attributable to Copeland (1948) and was later clarified by Foskett and Scheffey (1982), who confirmed active transport of chloride ions by these cells using vibrating probe experiments on the opercular epithelium of sea-water adapted tilapia *O. mossambicus*. The term 'ionocytes' was first intoduced by Watrin and Mayer-Gostan (1996) to describe ionoregulatory sites in the turbot (*Scophthalmus maximus*). The term 'mitochondria-rich cells' was first introduced by Lee *et al.* (1996) in order to emphasise the multifunctionality of the cells *i.e.* they do more than just excrete chloride ions in seawater adapted fish. Throughout this work, the term 'mitochondria-rich cells' or MRC will be used.

1.3.2   Location of mitochondria-rich cells in the adult teleost

Mitochondria-rich cells are mainly located on the filamental epithelium of the basal region of the lamellae of adult teleost gills (Wendelaar Bonga *et al.,* 1990), principally concentrated on the trailing or afferent edge of the filament of the adult teleost gill (Laurent, 1984; van der Heijden *et al.,* 1997). They have also been found on the lamellae of some freshwater species (Perry, 1997) and, after hypertonic shock, in the sea bass (*Dicentrachcus labrax*) (Varsamos *et al.,* 2002 b). They have also been reported on the inner surface of the operculum of the adult killifish (*Fundulus heteroclitus*) (Degnan *et al*., 1977) and tilapia (*O. mossambicus*) (Foskett *et al.,* 1981).

1.3.3   General structure of mitochondria-rich cells in the adult teleost

Mitochondria-rich cells are highly specialised, polarised cells which are characterised as being large and columnar/ovoid in shape in adult gills with distinct ultra-structural features characteristic of ion-transporting cells *i.e*. large numbers of mitochondria and a dense, tubular network that is continuous with the basolateral membrane causing extensive invagination (Doyle and Gorecki, 1961; Philpott, 1966). This tubular-vesicular system extends throughout most of the cytoplasm, and is closely associated with the mitochondria (Laurent, 1984; Philpott, 1980; Wilson *et al*., 2000 a and b) (Figure 1.12. and Figure 1.13. B.). It results in a large surface area for the placement of transport proteins, most importantly the ion-translocating enzyme Na^+/K^+-ATPase or 'sodium pump' (Garcia-Ayala *et al.* 1997) (see Section 1.2.3. above).
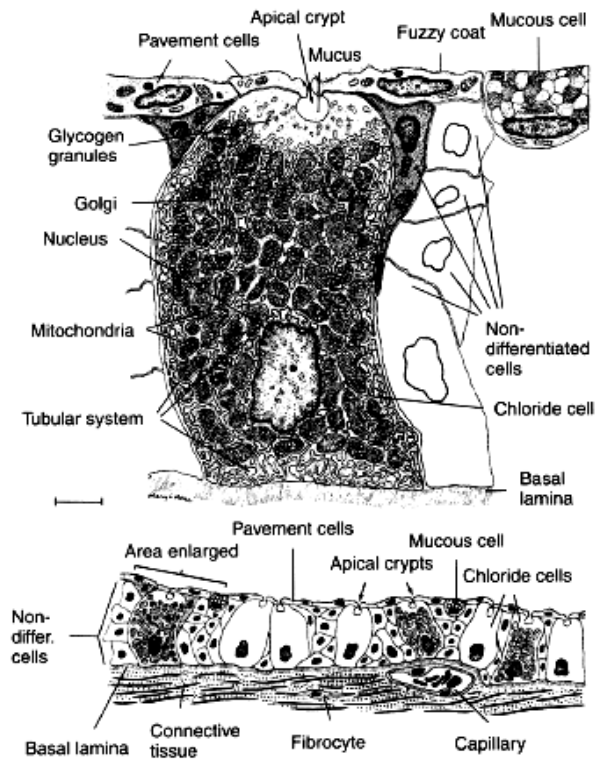
Figure 1. 12 Generalised drawing of mitochondria-rich cell and opercular epithelium based on multiple electronmicrographs. From Degnan *et al.* (1977).
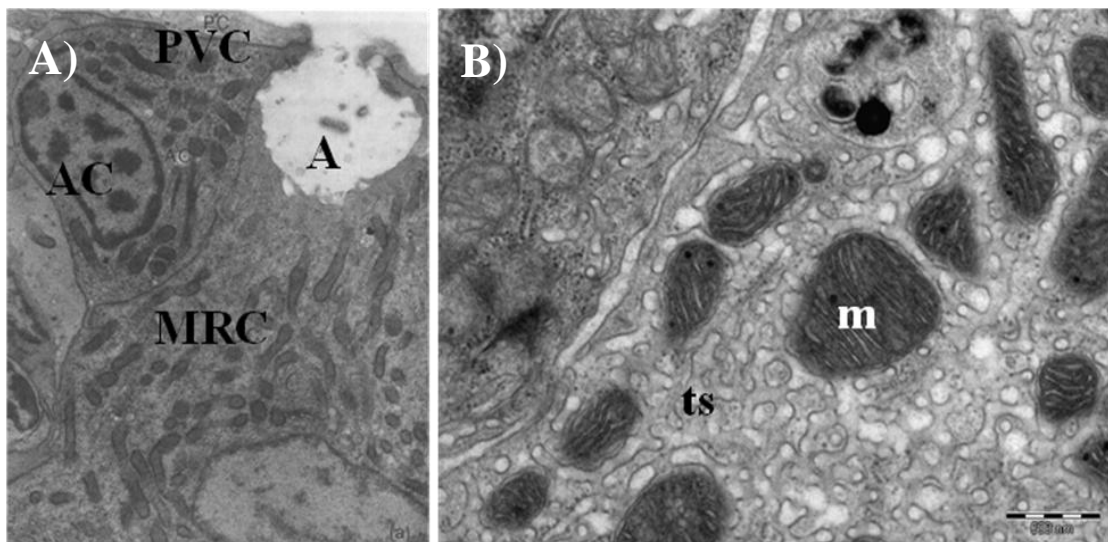
Figure 1. 13 Ultrastructure of mitochondria-rich cell in freshwater-adapted *Oreochromis niloticus.* **A)** A multicellular complex (MCC) formed by a mature mitochondria-rich cell (MRC) and an accessory cell (AC) sharing a single apical crypt (A) lying beneath a pavement cell (PVC). Reduced osmium staining; x 11,900. (From Cioni *et al.,* 1991) and **B)** Detail of mitochondria with tubular system (m; mitochondria, ts; tubular system) [Bar = 500 nm]

1.3.4 Accessory cells (ACs)

Hootman and Philpott (1980) first named the undifferentiated MRCs found beside mature MRCs in seawater flounder 'accessory cells' or ACs. They appeared to be structurally analogous to MRCs, in that they possessed large amounts of mitochondria and a labyrinthal tubular system, but were smaller and less developed than MRCs with a less developed tubular system and lower expression of Na^+/K^+-ATPase relative to mature MRCs. A single accessory cell (AC) or more than one AC cluster around a MRC forming a 'multi-cellular complex' (MCC) with a shared apical crypt. ACs are small, semi lunar or pear-shaped cells with lateral cytoplasmic processes that extend from the ACs to penetrate the apical portion of the adjacent MRC, sharing the apical cavity (Figure 1.13.A.). ACs share a single-stranded, shallow junction with a MRC, suggestive of a 'leaky' paracellular pathway thus giving additional paracellular pathways for the secretion of excess Na^+ from body fluids (Evans *et al*., 1999) (Figure 1.14.).

They are usually found in seawater-adapted fish but also found in some euryhaline species in freshwater *e.g.* killifish (*F. heteroclitus*) (Karnaky, 1986), ayu (*Plecoglossus altivelis*) (Hwang, 1988), rainbow trout (*Salmo gairdneri*) (Pisam *et al*., 1989) and the Mozambique tilapia (*O. mossambicus*) (Hwang, 1988; Wendelaar Bonga and van der Meij, 1989; Cioni *et al.,* 1991; Hiroi *et al*., 1999).

1.3.5   Mitochondria-rich cells in marine teleosts or euryhaline teleosts acclimated to seawater

Fishes in seawater are hypo-osmotic to their environment and therefore undergo an osmotic loss of water and a diffusional gain of Na^+ Cl^- (see Figure 1.7.). Therefore the major function of MRCs is osmoregulation, achieved through the secretion of excess chloride ions from the blood or basolateral side of the cell to the apical or environmental side, which is in turn accompanied by the passive paracellular flow of sodium ions to the external environment (Hirose *et al*., 2003).

1.3.5.1   Morphology

As a general rule, MRCs in seawater or seawater-adapted fishes have the following morphological characteristics; the apical membrane is recessed below the surface of the surrounding pavement cells to form a concave pore or 'crypt' that can be shared by accessory cells (ACs) (Karnaky, 1986), often forming 'multi-cellular complexes' (Section 1.3.4.) with cytoplasmic processes of accessory cells (ACs) extending into the apical cytoplasm of MRCs to form complex interdigitations (Laurent, 1984; Wilson and Laurent, 2002). These two types of cells share a single-stranded, 'shallow' junction, suggesting a 'leaky' pathway is present between the cells (Laurent, 1984; Hwang, 1988), thus providing a paracellular route for sodium extrusion (Sardet *et al*., 1979; Laurent, 1984) (Figure 1.14.).

1.3.5.2   Ion secretion

Early experiments confirmed labeled Na^+ and Cl^- efflux activity in live eels with the use of radioactive ouabain (a Na^+/K^+-ATPase inhibitor), thus inferring a basolateral location

34

for the transporter protein Na^+/K^+-ATPase in mitochondria-rich cells (Silva *et al*., 1977). Subsequent work established that fish gill epithelia expressed large quantities of Na^+/K^+-ATPase whose activity was usually proportional to the external salinity (de Rengis and Bornancin, 1984; McCormick, 1995) (see Section 1.2.3. above). This has been attributed to increased a-subunit mRNA abundance (Madsen *et al*. 1995; Singer *et al*., 2002) and protein amount (Tipsmark *et al.,* 2002; Lee *et al*., 2000; Lin *et al.,* 2003) or both (D'Cotta *et al*., 2000; Lin and Hwang 2004) and a model has been suggested for Na^+ Cl^- extrusion by the MRC (Marshall, 2002; Hirose *et al*., 2003; Evans *et al.,* 2005) (Figure 1.14.).

Briefly; basolateral Na^+/K^+-ATPase driven extrusion of three Na^+ from the cell to the plasma and entry of two K^+ into the cell (Figure 1.14.(3)) then generates an electrochemical gradient that drives Na^+, coupled with Cl^- and K^+, back from the plasma into the cell's cytoplasm, via the $Na^+/K^+/2Cl^-$ co-transporter or (NKCC) (Figure 1.14.(2)). NKCC therefore mediates the movements of Na^+, K^+ and Cl^- across the basolateral membrane of MRCs and has a key role in cell volume homeostasis, maintenance of the electrolyte content and transepithelial ion and water movement in polarized cells (Cutler and Cramb, 2002). K^+ therefore enters the cell basolaterally both via the Na^+/K^+-ATPase and the NKCC co-transporter, and is removed basolaterally from the cell via the potassium or K^+ channel (Figure 1.14:(4)). This channel is located basolaterally and reduces the intracellular build up of K^+. Cl^- exits the cell via an apical Cl^- anion channel or CFTR (cystic fibrosis transmembrane receptor) (Figure 1.14:(1)). An apically-located transepithelial electrical potential moves Na^+ (Figure 1.14:(5)) through the leaky paracellular pathway between MRCs and ACs via a cation-selective

paracellular pathway (Degnan and Zadunaisky, 1980) to exit due to the negative potential created by transcellular Cl^- flux (Sardet *et al.*, 1979).
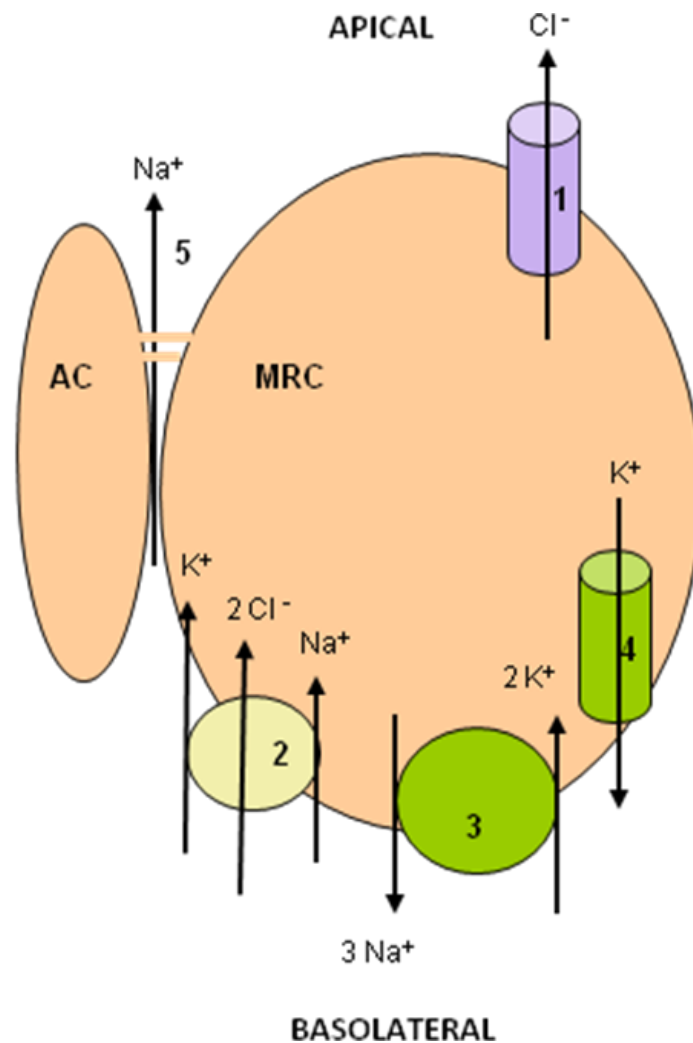
Figure 1. 14 Schematic diagram of transepithelial Cl^- secretion in a mitochondria-rich cell. **(1)** CFTR or Cl^- channel, **(2)** NKCC, **(3)** Na^+/K^+-ATPase, **(4)** K^+ channel and **(5)** tight junction through which paracellular flow of Na^+ occurs. **AC**: accessory cell; **MRC**: mitochondria-rich cell. Adapted from Hirose *et al.* (2003).

1.3.6 Mitochondria-rich cells in freshwater teleosts or euryhaline teleosts acclimated to freshwater

The electrochemical gradients that exist in freshwater produce a net diffusional loss of Na^+ Cl^- from fishes and ionic homeostasis must be corrected by an active branchial Na^+ Cl^- uptake system (Motais and Garcia-Romeu, 1972; McDonald and Wood, 1981) (see Figure 1.7.).

1.3.6.1 Morphology

Mitochondria-rich cells in freshwater usually lack an apical crypt and have their apical surfaces forming microvilli above the adjacent PVCs, which is consistent with their ion absorptive nature (Marshall *et al.,* 1997; Hwang, 1988; Perry *et al.,* 1992). However an invaginated, crypt-like structure has been reported in MRCs of the euryhaline Mangrove killifish (*Rivulus marmoratus)* in 1 ppt (King *et al.,* 1989) and a slightly invaginated apical opening in the β – MRCs in the freshwater adapted guppy (*Lebistes reticulatus*) (Pisam *et al.,* 1987), the loach (*Cobitis taenia*) and the gudgeon (*Gobio gobio*) (Pisam *et al.,* 1990). This has similarly been reported in freshwater adapted Tilapiine species *e.g.* the Mozambique tilapia (*Oreochromis mossambicus)* (Lee *et al.,* 1996, van der Heijden *et al.,* 1997; Uchida *et al.,* 2000; Inokuchi *et al*., 2008) and the Nile tilapia (*Oreochromis niloticus*) (Pisam *et al.,* 1993). The basolateral tubular system is less well developed in freshwater than in seawater adapted MRCs, and MRCs form extensive tight, multi-stranded junctions with adjacent PVC cells (Hwang, 1988).

1.3.6.2   Ion uptake

- Na^+

The theory of the mechanism of active ion uptake by MRCs has been a controversial subject over the past 30 years (Hiroi *et al.,* 2008). Krogh's (1939) original proposition that the mechanism for Na^+ Cl^- uptake coupled Na^+ influx with NH_4^+ secretion and Cl^- uptake with HCO_3^- extrusion was first challenged by Kerstetter *et al.* (1970) who suggested that Na^+ was, in fact, exchanged apically for H^+ rather than NH_4^+ with basolateral Na^+/K^+-ATPase providing the electromotive force. This hypothesis was later developed by numerous authors into an alternative model for Na^+ entry via an epithelial Na^+ conductive channel coupled electrochemically to an H^+-ATPase (Avella and Bournancin, 1990; Lin and Randall, 1995).

However, the viability of an apical electroneutral exchanger was later questioned as external Na^+ concentration was found to be lower than intracellular concentrations, so an alternative model was developed (Figure 1.15.). Evidence for the sodium uptake pathway is suggested by the existence of an epithelial sodium channel (ENaC) in the apical membrane of the MRC (Evans *et al.,* 2005). Indeed an ENaC-like protein had previously been immunolocalised to apical surfaces of MRCs in gills of the tilapia (*O. mossambicus*) and rainbow trout (*O. mykiss*) (Wilson *et al.*, 2000 a and b). It was suggested that the apical entry of Na^+ is dependant on an apical vacuolar or V-type proton ATPase (V-H^+-ATPase) which is electrochemically coupled to the Na^+ channels (Fenwick *et al.*, 1999; Reid *et al.,* 2003). This V-H^+-ATPase is an ubiquitous enzyme in organelles and of the plasma membrane (Nelson and Harvey, 1999).

Immunohistochemical techniques were used in an attempt to define the cellular localisation of these transport systems in the rainbow trout using the antibody against the bovine brain V-type ATPase and found it to be localised specifically to the apical regions of the cell (Sullivan *et al*., 1995; Wilson *et al.,* 2000 b).
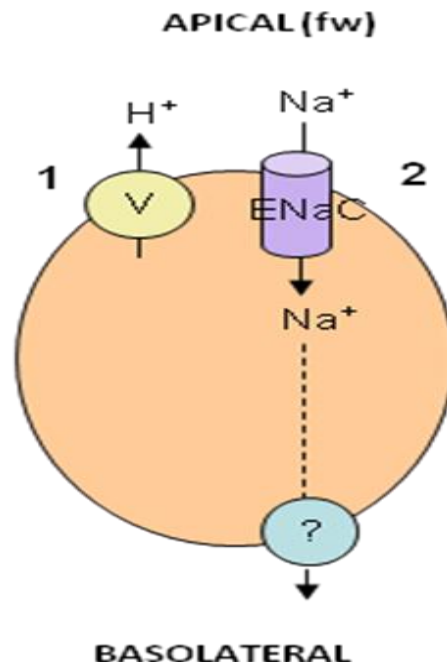
Figure 1. 15 Schematic diagram of Na^+ uptake mechanism proposed for freshwater rainbow trout and tilapia. (**1**) Apical proton extrusion by vacuolar-type or $V-H^+$-ATPase provides the electrical gradient to draw in (**2**) Na^+ across the apical surface via an epithelial sodium channel (ENaC-like channel). The expected role of Na^+-K^+-ATPase in basolateral Na^+ is unclear. Adapted from Evans *et al.* (2005).

- *Cl⁻*

The relationship between Cl^- uptake and acid-base secretion was first suggested by Krogh in 1939 and subsequent work established this link with several fish species. Although Krogh's original hypothesis of Cl^- uptake by a Cl^-/HCO_3^- apical exchange

mechanism had largely remained unchallenged (Tresguerres *et al.,* 2005), it is now proposed that Cl$^-$ uptake takes place via an apical anion exchanger or AE (Cl$^-$/HCO$_3^-$) which is functionally linked to intracellular carbonic anhydrase (CA). In this model, V-H$^+$-ATPase provides the driving force to overcome the unfavourable gradient for Cl$^-$ uptake via the AE. This arrangement of proteins has been named 'the freshwater chloride uptake metabolon' (Tresguerres *et al.,* 2005). This model proposes that the combined action of the apical anion exchangers (AEs), carbonic anhydrase (CA) and V-H$^+$-ATPase would create a local intracellular HCO$_3^-$ high enough to drive Cl$^-$ uptake from the freshwater via an AE and to exit the cell basolaterally through a chloride channel (Figure 1.16.).

The expected role of Na$^+$/K$^+$-ATPase in Na$^+$ and Cl$^-$ exit in the basolateral membrane is unclear. There is, however, clear evidence that Na$^+$/K$^+$-ATPase is expressed in MRCs of freshwater fishes or euryhaline fishes in freshwater; immunocytochemical studies using heterologous antibodies to Na$^+$/K$^+$-ATPase localised expression to basolateral and/or tubulovesicular components of MRCs of tilapia (*O. mossambicus*) (Hiroi *et al.,* 2008) and tilapia (*O. mossambicus*) and rainbow trout (Wilson *et al.,* 2000 a). It is presumed to provide an exit step for Na$^+$ from the MRC into the extracellular fluids.
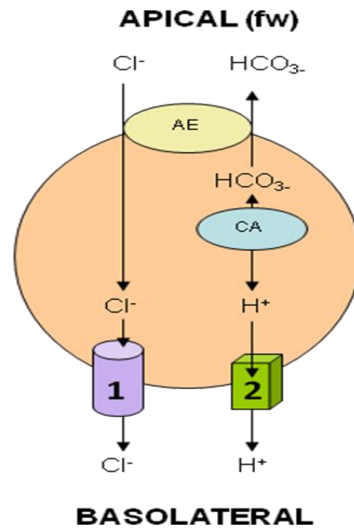
Figure 1. 16 Schematic diagram of the 'freshwater chloride uptake metabolon' in MRCs. AE; anion exchanger, CA; carbonic anhydrase. (**1**) Chloride channel and (**2**) V-H$^+$-ATPase. Adapted from Tresguerres *et al*. (2005).

1.3.6.3   Recent advances in the ion uptake model

Tresguerres *et al.* (2005) states that, despite the technological advances during recent years, the complete cellular mechanisms for branchial chloride uptake in freshwater fish remains unclear. Hiroi *et al.* (2005) had described a previously unreported apical localisation of the Na$^+$/Cl$^-$ co-transporter or NKCC in MRCs of embryos of *O. mossambicus* in freshwater. However an active Na$^+$/Cl$^-$ uptake mechanism with apical NKCC had been reported prior to this in the crabs *Carcinus maenas* and *Chasmagnathus granulatus* in brackish water (Riestenpatt *et al.,* 1996; Onken *et al*., 2003) and the suggestion that a similar mechanism had been proposed by Kirschner (2004) for estuarine fishes.   The existence of this apical NKCC was further examined by Hiroi *et al.* (2008). The expression of mRNA following transfer in *O. mossambicus* embryos was investigated and an mRNA encoding NCC was found to be exclusively expressed in the yolk-sac membranes and gills of freshwater acclimatised *O.*

mossambicus larvae. Antibodies were therefore generated with whole-mount immunofluorescence staining in combination with Na^+/K^+-ATPase, CFTR and Na^+/H^+ exchanger (NHE_3) and results suggested that NCC was specifically restricted, at the protein level, to the apical membrane of freshwater specific MRCs. They therefore proposed a novel ion uptake model with NCC (Figure 1. 17.(1)) co-transporting Na^+ and Cl^- from the external environment into the cells with a basolateral Cl^- channel exporting Cl^- out of the cell.
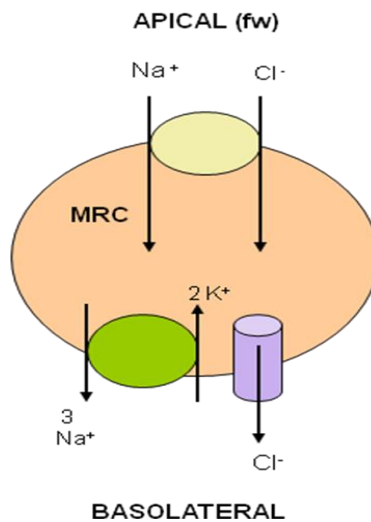
Figure 1. 17 Schematic diagram of the novel ion uptake model utilising NCC. Adapted from Hiroi *et al*. (2008).

1.4 Osmoregulation in Embryonic and Post-Embryonic Teleosts

1.4.1   Introduction

The ontogenetic development of osmoregulatory capacity, moving from a somewhat limited trans-membrane particle exchange at a cellular level in the embryonic blastular stage, to the fully-functioning regulatory tissues in juvenile and adult, such as the renal complex, the gut and the branchial epithelium, is described succinctly by Alderdice (1988; p.225) as a process which displays 'continuity, with increasing complexity'.

It is well established that teleost embryos and larvae are able to maintain osmotic and ionic gradients between their internal and external environments (Guggino, 1980 a and b; Alderdice, 1988; Kaneko *et al.,* 1995), although full adult osmoregulatory capacity is not reached in these early developmental stages as organs are under-developed or absent (Varsamos *et al.,* 2005). Compared to adult teleosts (see above, Section 1.2.2.), larvae are able to maintain their blood osmolality in a less narrow range of $\approx$ 240 - 540 mOsmol kg^{-1}, and this adaptive ability is accomplished by an early acquisition of osmoregulatory mechanisms that are different from those in adult fish. In general, the ability of early stages of fish to tolerate salinity through osmoregulation depends initially on integumental MRCs and then shifts to rely on the developing digestive tract and controlled drinking rate, the urinary organs and the developing branchial tissues and the MRCs which they support.

While osmoregulation in the adult teleost fish has been extensively studied, much less information, however, exists regarding osmoregulation in the early stages of development (Holliday, 1965, Alderdice, 1988; Tytler *at al.,,* 1993; Schreiber, 2001; Evans, 2005; Varsamos *et al.,* 2005). In general, the complexity of the gill anatomy, compounded by the small size of larval fish, has precluded such studies. Recently improved availability of precisely staged young fish, due to both the improved rearing methods by aquaculture and less stressful capture techniques for wild populations has contributed to developments in the field (Evans, 2005). In addition, the development and application of new immunological techniques allowing visualisation of delicate early life stages, has allowed the progression of ontogenetic studies.

1.4.2   Ontogeny of osmoregulatory mechanisms in embryonic teleosts

Leading up to ovulation, the transfer of nutrients and ions occurs through the contact between oocyte and follicular cell microvilli and, therefore, their ionic and osmotic control are a function of the parental regulatory system. At ovulation or release from the follicular cells, the mature eggs become free in the ovary of the adult and surrounded by ovarian fluid are still under the control of the adult regulatory system. During this period their plasma membrane appears to be relatively permeable to water and responds to changes in the ovarian fluid (Sower and Schreck, 1982); osmotically the ovarian fluid is very similar to the blood plasma (Hirano *et al.*, 1978) and the blood plasma is in physiological balance osmotically with the external environment (Sower and Schreck, 1982).

However, at spawning, the mature eggs are hypotonic to sea water and hypertonic to fresh water. Independent regulatory capacity is first evident with activation of the embryo occurring in teleosts at metaphase II, the stage of meiosis following the extrusion of the polar body. During activation, the cortical alveoli, underlying the oocyte plasma membrane, discharge their contents into the presumptive perivitelline space between the chorion and the plasma membrane, by a process called cortical alveolar exocytosis causing an uptake of water from the external environment across the chorion, lifting it away from the plasma membrane by displacement and blocking the micropyle therefore preventing polyspermy. Subsequent regulation and maintenance of the integrity of the egg appears to be achieved by the resistive maintenance of a tight plasma membrane and limited trans-membrane water and ion fluxes (Bennett *et al.*, 1981).

Following this is the transitory developmental blastula stage, characterised by the formation and development of the blastoderm or overgrowth of the yolk by a single layer of cells called blastomeres which spreads out as a flat plate over the upper surface of the yolk mass. There is little evidence to suggest that there is much control over water and ion exchange between egg and external environment at this stage and any regulatory capacity that does exist is presumed to arise from low trans-membrane fluxes and appears to be 'neither modulated nor selective' (Alderdice, 1988; p. 241). Indeed, Alderdice (1988) concludes that the establishment of osmotic or systemic regulation begins during gastrulation, and is in place by yolk-plug closure; an increase in the permeability of the plasma membrane during gastrulation coincides with the appearance of integumetal or cutaneous MRCs on the epithelium of the body surface and yolk-sac of the developing embryo, marking the start of the selective restriction of ions and water

transfer or active ionoregulation (Guggino, 1980 a). Epiboly, or cellular overgrowth of the yolk and pericardial regions of the embryo, occurs when the developing ectodermal layer of the blastoderm, along with the marginal ridge of the blastodisc and its inner layer or 'germ ring', grows to form an epiblast. This, combined with the periblast, which is the initial covering of the yolk, forms the yolk sac. The opening called the yolk-plug or blastopore overgrows when gastrulation is complete.

1.4.3   Ontogeny of osmoregulatory processes during post-embryonic development

Anatomical, physiological and cellular changes, occurring after hatch and throughout the early larval period, account for the ontogenetic variations in their capacity to osmoregulate.

1.4.3.1   Digestive tract

Existing studies have focused on the ontogeny of the digestive tract in larvae, generally as a result of aquaculture development and the need to understand the transition from endogenous to exogenous feeding. The mouth is closed and the stomach and intestine are not totally developed at hatching and undergo morphological and functional changes during larval development (Zambonino Infante and Cahu 2001). Yolk-sac larvae rely on endogenous feeding, utilising the yolk-sac nutrients until first feeding commences. Tytler *et al.* (1993) reported the development of the gut from a simple tube at hatch during the yolk-sac period in the turbot (*S. maximus*) and Varsamos *et al.* (2002 a) noted the digestive tract of the sea bass (*D. labrax*) at hatch to be closed at both ends.

The study of drinking as a part of hydromineral homestasis in larval fish is not well documented and has concentrated mainly on seawater species. Data does suggest that larvae are able to drink seawater and absorb water as part of their osmoregulatory strategy even though the mouth and gut are neither fully formed nor functional for digestion. Active drinking was reported by Guggino (1980 a) in sea-water adapted killifish embryos (*F. heteroclitus* and *F. bermudae*) and was thought to take place through the opercular openings as the mouth was still closed.

Drinking rate is found to increase from hatching to yolk-sac absorption in most of the seawater species studied *e.g.* turbot (*S. maximus*) (Reitan *et al.,* 1993), sea-water adapted tilapia (*O. mossambicus*) (Miyazaki *et al.,* 1998) and cod (*G. morhua*) (Mangor-Jensen, 1987; Tytler *et al.,* 1993) also demonstrating that the rate of water absorption from the larval intestine is similar to measurements for adult fish. This led Schreiber (2001) to suggest that, before exogenous feeding commences, the early larval gut is primarily ionoregulatory not digestive in function.

An age-related increase in drinking rate during early post-embryonic development has also been reported in freshwater species *e.g.* Mozambique tilapia (*O. mossambicus*) (Miyazaki *et al*., 1998) and the European eel (*Anguilla anguilla*) (Birrell *et al.,* 2000). While it is accepted that fish drink mainly in hyper-osmotic environments to maintain water balance, other possible explanations are suggested for drinking in iso- or hypo-osmotic environments; to clear yolk-sac debris from the digestive tract as a result of stress (Wendelaar Bonga, 1997) *i.e.* it has been reported that cortisol induces a gulping reflex and suggests an osmoregulatory functions for intestinal absorption of divalent

ions such as Ca^{2+} (Wendelaar Bonga, 1997). Data comparing drinking rates between sea and freshwater hatched tilapia (*O. mossambicus*) found seawater-hatched larvae commenced drinking at 1 day post-hatch as compared to freshwater-hatched larvae which commenced drinking at 2 days post-hatch, with drinking rates higher in seawater as compared to freshwater at all stages (Miyazaki *et al.,* 1998). Other studies have shown that seawater larvae are able to modulate their water ingestion according to salinity; Tytler and Blaxter (1988) showed in cod (*G. morhua*) plaice (*Pleuronectes platessa*) and herring (*Clupea harengus*) drinking rates were significantly higher at 32 ppt than at 16 ppt.

1.4.3.2   Urinary system

Much less is known about the involvement of the urinary system in osmoregulation during ontogeny in teleosts. The primordial kidney or 'pronephros' in fish embryos and larvae comprises of a closed system consisting of a pair of rudimentary tubules, a single renal corpuscle and, in some cases, a urinary bladder (Holstvoogd, 1957; Takahashi *et al.,* 1978; Tytler and Blaxter, 1988; Tytler *et al.,* 1996; Drummond *et al*., 1998). It appears to become progressively more complex, being replaced with the 'metanephros' at a later developmental stage (Vize *et al*., 1997) and has been reported in several species *e.g.* chum salmon (O*nchorynchus keta*) (Takahashi *et al.,* 1978), guppy (*Lebistes reticulates*) (Agarwal and John, 1988), herring (*C. harengus*) (Tytler *et al*., 1996), zebrafish (*Danio rerio*) (Drummond *et al*., 1998), turbot (*S. maximus*) (Tytler *et al*. 1996) and the sea bass (*Dicentrachus labrax*) (Nebel *et al.,* 2005). The trajectory of the transition from the pronephros to the mesonephros is species-specific. Generally speaking the mesonephric tubules bud from the pronephric tubules at around 20 dph in

the sea bass (*D. labrax*) (Nebel *et al*., 2005) and herring (*C. harengus*) (Holstvoogd, 1957).

1.4.4   Role of gills in embryonic and post-embryonic development

1.4.4.1   Ontogeny of gill development in developing larvae

A general feature of early fish larvae is the absence of fully developed gills (Segner *et al.,* 1994), and the ontogeny of the gills forms an important part of the developmental process of the embryonic and larval fish. The sequence of gill development is described by Hughes (1984) as 'continuous' with the epithelium that forms the surface of the gill arches becoming the surface of the filament and afterwards the surface of the lamellae (Figure 1.18.). Coinciding with this development is the maturation of other parts of the respiratory and cardiovascular system and coordination of the pumping systems for water and blood flow through the gills immediately prior to metamorphosis (Rombough, 2004).
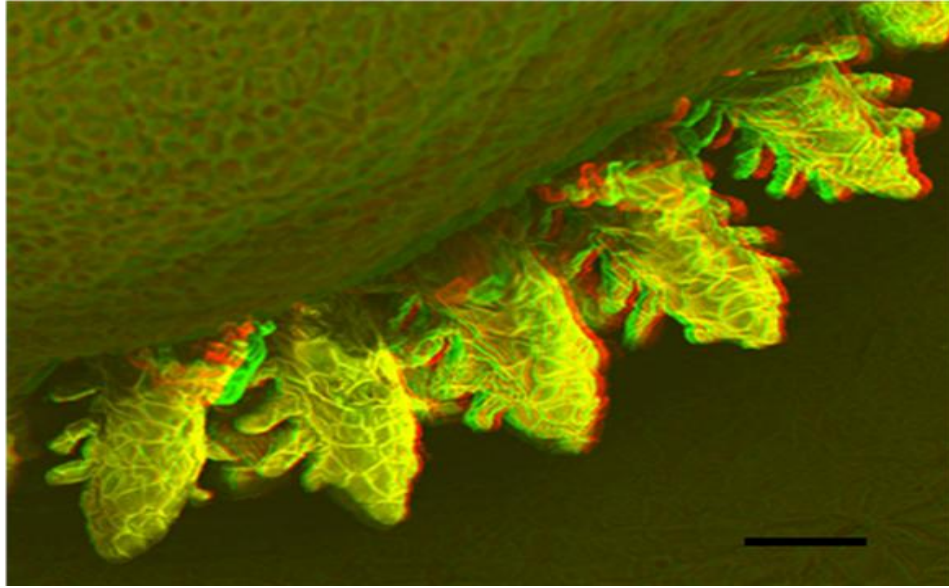
Figure 1. 18 3-D scanning electron micrograph of developing gills in yolk-sac larvae of Nile tilapia at hatch showing filaments with budding secondary lamellae [Bar = 50 μm].

Studies on the development of the gills as respiratory organs have found that ontogeny of their functionality is species specific, but the process can still be seen to be one of progressive development. Fishelson and Bresler's (2002) comparative studies on Tilapiine fish with different reproductive styles gives a good, general overview of this process. Embryos of the substrate-brooder *Tilapia zillii* at 34 h post-fertilization were found to possess rudimentary opercular folds, with the beginnings of the most anterior rudimentary gill arches. Similar developments were observed in mouth-brooding *Oreochromis spp*. embryos at a later stage of 52 h post-fertilisation and the mouth-brooding *Sarotherodon galileus* at 60 hours post-fertilisation. At hatch, all species had sealed mouths and minute operculi, with all four gill arches visible externally with short, budding filaments. At 1 day post-hatch (dph) in all species, mouths were found to

be slightly opened, and irregular swallowing motions were noted. The operculum could be seen to cover the first two gill arches and signs of short lamellae on the filaments were visible. At 2 dph in *T. zilli* and 3 days post-hatch in the mouth-brooding species, mouths were more widely open and moved in unison with moving opercula that almost covered all 4 gill arches. At 4 dph in *T. zilli* and 6 days post-hatch in mouth-brooding species, lamellae were fully developed and larvae had begun active feeding. In contrast, Li *et al.* (1995) reports gills in *O. mossambicus* developing at a later stage, with lamellae starting to form at 8 dph, and still poorly formed in 10 dph, although the presence of high densities of MRCs on the gills suggested that they were participating in active transport.

In other teleost species, a similar pattern has been observed in gill development, marking the transition between cutaneous and branchial respiration. In the walleye (*Stizostedion vitreum*), gill filaments are present at mouth opening (3 dph) with lamellae developing once active feeding is initiated (10 days post-hatch) (Phillips and Summerfelt, 1999). A comparable development pattern has been observed in the smallmouth bass (*Micropterus dolomieui*) (Coughlan and Gloss, 1984) and in killifish (*Fundulus heteroclitus*) (Katoh *et al.,* 2000) with gill filaments developing at hatch or in early yolk-sac larvae and lamellae appearing later in the free-swimming larvae. Rombough's study (1999) on rainbow trout larvae (*O. mykis*s) observed the formation of gill arches at 3 dph and the appearance of filaments on the gill arches at 6 dph, with filament surface area expanding rapidly thereafter, due to an increase in filament size rather than increase in filament number. Secondary lamellae were observed at 8 dph and total lamellar surface area expanded more rapidly, exceeding that of the filaments at 17 dph. Varsamos *et al.* (2002 b) in the sea bass (*D. labrax*) found four branchial arches

present at mouth opening at 5 dph with filaments showing buds that form the lamellae. The study of Segner *et al*. (1994) on the turbot (*S. maximus*) found gill filaments present at the transition from yolk sac larvae to first-feeding, and the lamellae appearing

1.4.5 The extrabranchial mitochondria-rich cell

1.4.5.1 Introduction

After hatch, post-embryonic larvae are able to live in media whose osmolality differs from their own blood osmolality, and this tolerance is based on ability to osmoregulate. This is due to the presence of numerous integumental MRCs commonly observed in the yolk-sac membrane and other body surfaces of fish embryos and larvae *i.e.* head, trunk and fins. These extrabranchial MRCs are considered to play a definitive role in osmoregulation during early development until the time when gills become fully developed and branchial MRCs become functional. In addition, the absence of gills in early larvae and the comparatively low skin permeability tends to decrease the passive movement of water and ions (Alderdice 1988; Tytler *et al*. 1993). The first report of localisation of ionoregulation to the integument of teleost larvae was that of Shelbourne (1957) who investigated chloride regulation sites in marine plaice larvae (*P. platessa*). Subsequent and similar reports are summarized in Table 1.1.

Table 1. 1 Reports on the presence of extrabranchial mitochondria-rich cells during embryonic and post-embryonic stages of teleosts.

Common name	Species	Reference
plaice	*Pleuronectes platessa*	Shelbourne (1957); Roberts *et al.* (1973)
Pacific sardine	*Sardinops caerulea*	Lasker and Threadgold (1968)
puffer	*Fugu niphobles*	Iwai (1969)
guppy	*Poecilia reticulate*	Depeche (1973)
plaice	*Pleuronectes platessa*	Shelbourne (1957); Roberts *et al.* (1973)
rainbow trout	*O. mykiss*	Rombough (1999)
killifish spp.	*Fundulus heteroclitus* and *Fundulus bermudae*	Guggino (1980b); Katoh *et al.,* (2000)
anchovy	*Engraulis mordax*	O'Connell (1981)
ayu, flounder and carp	*Plecoglossus altivelis, Kareius bicoloratus*, *Cyprinus carpio*	Hwang (1989)
Mozambique tilapia	*Oreochromis mossambicus*	Ayson *et al.* (1994a); Hwang *et al.* (1994); Shiraishi *et al.* (1997); Hiroi *et al.* (1999; 2005; 2008); Li *et al.* (1995); van der Heijden *et al.* (1997;1999); Kaneko and Shiraishi (2001); Lin and Hwang (2004).
tilapia *spp*.	*T. zillii, O. aureus, O. niloticus, Tristramella sacra, Saratherodon galileus*	Fishelson and Bresler (2002)
turbot	*Scopthalamus maximus*	Tytler and Ireland (1995)
herring	*Clupea harengus*	Wales and Tytler (1996); Wales, (1997)
Japanese eel	*Anguilla japonicus*	Sasai *et al.* (1998)
Japanese flounder	*Paralichhys olivaceu*	Hiroi *et al.*(1998)
seaweed pipefish	*Syngnathus schlegeli*	Watanabe *et al.* (1999)
sea bass	*Dicentrarchus labrax*	Varsamos (2001); Varsamos (2002a); Varsamos (2002b)

1.4.5.2 General structure and distribution of MRCs during early life stages

In general, embryonic and larval integumental MRCs appear structurally and biochemically similar to adult branchial MRCs (see Section 1.3.3). Ayson *et al.* (1994), using transmission electron microscope to examine MRCs in the yolk-sac membrane of freshwater and seawater-adapted *O. mossambicus* tilapia embryos and larvae, noted a similarity with MRCs in branchial and opercular epithelium of the adult fish; the cytoplasm of the MRCs was seen to contain numerous mitochondria and Na^+/K^+-ATPase located on the extensive and well-developed tubular system. In addition, SEM indicated clear changes in the size and structure of integumental MRC apical opening as a response to changes in salinity, as displayed in adult species.

Correspondingly, van der Heijden *et al.* (1999), using immunostaining of cross sections of whole tilapia larvae (*O. mossambicus*) with an antibody against the α -subunit of Na^+/K^+- ATPase, found extrabranchial MRCs (from 24 h post-hatch onwards) in both freshwater and seawater adapted larvae to be ultrastructurally similar to that of MRCs in the branchial epithelium of adult fish, and similarly MRCs resembled the different developmental stages of the MRC cycle that were observed in adults. In addition, Shiraishi *et al*. (1997) reported the presence of multicellular complexes (MCCs) in the yolk-sac membrane of seawater–adapted tilapia larvae *O. mossambicus*.

The extrabranchial integument that can potentially be occupied by larval MRCs comprises the yolk-sac, head, trunk and fins (Varsamos *et al*., 2005). Distribution of MRCs in the integuments can also clearly be seen to be species-dependant (Varsamos *et*

al., 2005) and vary ontogenetically (Wales and Tytler, 1996, Fishelson and Bresler, 2002).

1.5   Overall aims and objectives

In recent times it has become increasingly clear that long-term sustainability of aquaculture must be based on an efficient use of natural resources. Improved and efficient farming practices, scope and efficiency of culture systems and knowledge of the adaptability of cultured fish species must keep pace with growing world aquaculture consumption without compromising the overall integrity of our ecosystems. As the earth's climate warms and large-scale atmospheric circulation patterns change, a physical impact in fresh water and marine environments is expected, bringing about a network of ecological changes. The existing balance of ground waters will alter due to infiltration of saline waters, putting pressure on available agricultural land and fresh water resources. These biotope changes may have profound effect upon fish stocks in both capture fisheries and culture, and it is likely that the greatest impact will be on the sensitive early stages of fish biology. Therefore conventional aquaculture management practices will need to be adapted and modified. Indeed, improvements in larval rearing techniques can significantly contribute to improved aquatic management practices and the ability to predict responses of critical life-history stages to environmental changes will improve conditions for transportation of young fish for replenishment of wild stocks, and for movement of fish outside endemic ranges for artificial culture.

This work will address the physiological adaptability during the early life stages of the Nile tilapia (*Oreochromis niloticus)*, a species that displays a wide range of physiological tolerances and hardiness in captivity, as well as being an economically important aquaculture species in many countries. The overall aim of this study was to explore the scope of tolerance and the nature of the related mechanisms that provide osmoregulatory capacity during the early life stages of the Nile tilapia, when faced with the osmoregulatory challenge of low salinity or brackish water environments. An increased understanding of salinity tolerance of this species could improve hatchery management practices and extend the geographic scope of this species as well as providing a vital understanding of underlying adaptive mechanisms of ionoregulatory processes during the early life stages of teleost fishes.

The principal objectives of the study were:

- To study the ontogenic changes in the physiological responses to osmoregulatory challenge during early life stages of the Nile tilapia throughout a range of salinities (freshwater to 32 ppt). (**Chapter 3**).

- To examine the effects of salinity (freshwater to 25 ppt) on embryogenesis, survival, growth and metabolic burden during early life stages of the Nile tilapia (**Chapter 4**).

- To investigate ontogenetic changes in location and morphology of mitochondria-rich cells in the Nile tilapia adapted to freshwater and brackish water (15 ppt) (**Chapter 5**).

- To explore the effects of osmotic challenge on structural differentiation of apical openings in active mitochondria-rich cells (MRCs) in the Nile tilapia (**Chapter 6**).

- To assess the effects of transfer to elevated salinities on mitochondria-rich cell functional differentiation during early life stages using a correlative microscopy approach (**Chapter 7**).

2 Chapter 2 General Materials and Methods

Techniques common to all experimental chapters in the present study are described below. Materials and methods specific to individual experiments are outlined in the relevant chapters.

2.1 Broodstock maintenance and egg supply

2.1.1 Broodstock maintenance

In all experiments, eggs were obtained from Nile tilapia (*Oreochromis niloticus*) breeding populations held at the Tropical Aquarium, Institute of Aquaculture, University of Stirling. This population was originally isolated from Lake Manzala in Egypt and imported to the University of Stirling in 1979.

Broodstock were either maintained individually in 50 L freshwater aquaria or in partitioned 200 L aquaria (Coward and Bromage, 1999). All fish were maintained in gravity-fed recirculation systems linked to several settling tanks, faecal traps and filtration units incorporating filter brushes and bio-rings (Dryden aquaculture, UK). Pre-conditioned tap water (local tap water aerated and heated to 28 ºC ± 1 for 24 h prior to use) was used. Water was pumped from the system collector tanks to a sand filter tank and then sent to a header tank (227 L capacity) via a water pump (Beresford Pumps, UK). To maintain good water quality, a partial change of pre-conditioned water (10% of total volume) was carried out once a week. Temperature was maintained at 26 - 28 ºC

using a 3-kW thermostatically controlled water heater and water was oxygenated via air-stones in the header tank and in each aquaria by a low-pressure blower. Water quality was monitored twice a month, including dissolved oxygen (O_2). Broodstock were fed on artificial pellets (#5 trout pellet, Trouw Aquaculture Limited, Skretting, U.K.). The light regime was maintained at a 12:12 hour day: night photoperiod.

2.1.2   Egg supply

When females were observed to be ripe and at the point of spawning, *i.e.* displayed protruding genital papillae they were removed from the tanks and eggs were obtained by manually stripping into a Petri dish. This was followed by the addition of freshly collected milt from two males per female. After 1 - 2 minutes, water was added and gently mixed and the eggs were placed in their respective incubation unit.

2.2 Preparation of experimental salinities

The experimental media was prepared using conditioned freshwater (local tap water aerated and heated to 28 ºC ± 1 for 24 h prior to use) and commercial salt (Tropic Marin, Aquarientechnic, D-36367, Germany) and salinity was measured using a salinity refractometer (Instant Ocean Hydrometer, Marineland Labs., US) accurate to 1 ppt. Media with the following salinities and corresponding osmolalities were prepared (Table 2.1.).

Table 2. 1 Media salinity and corresponding osmolality.

Salinity (ppt)	Osmolality (mOsmol kg^{-1})
7.5	220.6
12.5	367.6
15	441.1
17.5	514.7
20	588.2
25	735.2

2.3 Artificial incubation of eggs and yolk-sac fry

2.3.1 Freshwater unit

The incubation of eggs and rearing of yolk-sac larvae in freshwater was carried out in the existing down-welling incubation system (Rana, 1986) (Figure 2.1). Water supply was maintained with a gravity-fed recirculation system as described above (Section 2.1.1.) with conditioned freshwater. Fertilised eggs were placed in round bottom plastic bottles of 1 L and water flow rates in bottles was controlled by regulatory valves. During development, daily monitoring was carried out and any dead eggs or larvae were removed. Temperature was maintained at 28 ºC ± 1.

Figure 2. 1 Freshwater, down-welling incubation system in the Tropical Aquarium, University of Stirling.

2.3.2　　Experimental salinity units

Independent test incubation units consisted of 20 L plastic aquaria, each with an individual Eheim pump (Series 94051) and with 6 x 1 L plastic bottles with a down-welling system were designed in order to challenge eggs and larvae to experimental salinities (Figure 2.2.). Temperature in the incubation units was maintained at 28 ºC ± 1 with individual 300 W thermostatically controlled heaters (Visi-therm, Aquarium-systems, Mentor, Ohio, U.S.). Approximately 10% of water was replaced daily in the incubation aquaria to compensate for evaporation and salinity was adjusted accordingly.

For both systems, dead eggs and larvae were regularly removed to prevent fungal infection. The light régime was maintained as for broodstock (Section 2.1.1.). Larvae were not fed during the experiment as they still possessed endogenous yolk reserves.

61
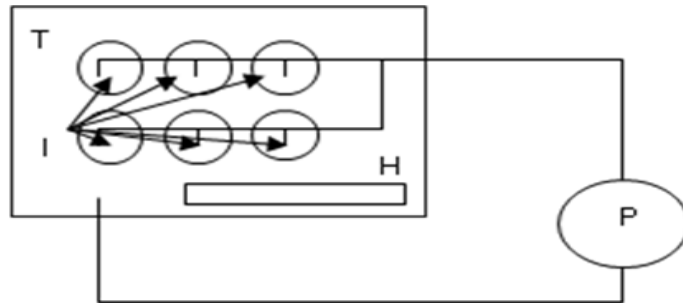
A)

B)

C)

Figure 2. 2 Independent test incubation and yolk-sac rearing units used in the evaluation of the effects of salinity on Nile tilapia egg and yolk-sac larvae. **A)** Schematic representation of individual unit consisting of a water pump (P), six plastic round-bottom incubators (I) and a thermostatically controlled heater (H) in a 20 L plastic aquarium (T), **B)** General view of units and **C)** Individual 20 L plastic aquarium with incubators and down-welling system.

2.4 Definition of stages during embryogenesis and yolk-sac period

The developmental staging system for embryonic and early larval development at 28 °C, as defined by Rana (1988), was used (Table 2.2).

Table 2. 2 Developmental stages of Nile tilapia (*Oreochromis niloticus*) at 28 °C ± 1 in freshwater. Age is recorded in hours post-fertilization (hpf) and days post-fertilisation (dpf), counting the time of fertilization as 0 h and the day of fertilization as the first day and days post-hatch (dph), counting the time of hatch as day 0. Adapted from Rana (1988).

Stage	Stage #	dpf	hpf	dph	Characteristics
Zygote	1	1	0-1.5		1-cell
Cleavage	2	1	1.5-2		2-cell
	3	1	2		4-cell
	4	1	4		8-cell
	5	1	5		16-cell
	6	1	6		32-cell
Blastula	7	1	10		Flattening of blastoderm forming cap at animal pole
Gastrula	8		10-12		Blastoderm grows over yolk with germ ring forming leading edge, thickening of region forming embryonic shield
	9	1-2	14-30		Commencement of epiboly; extension of gastrula, elongation of embryonic shield, head fold lifts from cephalic end of embryo and development of keel of central nervous system, germ ring encloses blastopore, heart begins contracting
	10	2	30		Completion of epiboly *i.e.* yolk plug closure, brain divisions visible and development of keel
Somitogenesis	11	2	30-48		Segmentation period; development of somites, tail under cut, rapid heartbeat and onset of blood circulation
		2	48		Eye pigmentation
		3	72		Appearance of pectoral buds, larvae flexing
Hatching	12	4-5	90-120	0	Hatching of embryo
				1	Mouth opening, appearance of ventral and caudal fin folds

63

Table 2.1.cont.

Yolk-sac larvae	13	2-9	Yolk consumed, fins and fin rays differentiate, development of digestive system and inflation of swim bladder, swim-up
Juvenile	14	9-12	Exhaustion of yolk reserves

2.5 Statistical analysis

All statistical analyses were carried out using the programme Minitab version 16 (Coventry, U.K.).

2.5.1 Statistical assumptions

For parametric analyses, normal distribution of data is a prerequisite, therefore the Anderson-Darling test was used prior to statistical analysis in order to determine if the data deviated significantly from a normal distribution ($p < 0.05$). If data were not found to be normally distributed, transformation of data was carried out and is discussed in the appropriate chapter. Homogeneity of variance was tested using Levene's Test for non-normally distributed data.

All other statistical tests used in this thesis are discussed within the appropriate chapters.

3 Chapter 3 Ontogenic changes in the osmoregulatory capacity of early life stages of Nile tilapia in elevated salinities.

3.1 Introduction

It has long been established that measurement of blood or body fluid osmolality in teleosts provides functional information that offers a valuable contribution to the understanding of osmoregulatory status and the ensuing ability to withstand osmotic stress (Alderdice, 1988). This information is of enormous interest in the euryhaline Nile tilapia, where knowledge of the adaptive ability to hypo- and hyper-osmoregulate during early life stages could allow expansion of culture into brackish water environments and optimisation of aquaculture practices in areas where fresh water is limiting.

Salinity is known to exert selective pressure on all developmental stages on fish species influencing reproduction, dispersal and larval recruitment in marine, coastal and estuarine habitats (Anger, 2003). To date, reports on ontogenic changes in the osmoregulatory capacity, as a result of physiological adjustments during early life stage, have been mainly confined to marine teleost species in an attempt to explain species and developmental stage-specific distribution, and are summarised below in Table 3.1.

Variations in salinity can induce larval deformities and are a useful indicator of osmoregulatory stress. Malformations, as a result of salinity challenge during early life

stages have been reported, mostly in the larvae of marine teleost species *e.g.* the navaga (*Eleginus nava*), polar cod (*Boreofadus saida*) and Arctic flounder (*Liopsetta glacialis*) (Doroshev and Aronovich, 1974), the pomfret (*Pampus punctatissimus*) (Shi *et al.,* 2008), the Japanese eel (Okamoto *et al.*, 2009) and the Atlantic halibut (*H. hippoglossus*) (Bolla and Ottensen, 1998). The detrimental effects of high salinity have been previously reported in adult and juvenile tilapiine *spp*. *e.g.* the development of skin lesions (Vine, 1980; Hopkins *et al.,* 1989; Likongwe *et al.,* 1996; Ridha, 2006) and haemorrhaging of internal organs (McGeachin *et al*., 1987). Additionally, various structural abnormalities, generally characterised by an underdevelopment of organs that resulted in a low hatchability, have been described in Nile tilapia eggs incubated at full strength seawater (Watanabe *et al.,* 1985 b).

3.1.1   Aims of the study

The ability of Nile tilapia larvae to withstand variations in salinity is due to their capacity to osmoregulate, therefore the objective of the work described in the present chapter was to investigate the basis of the osmoregulatory capacity during early life stages.

The following areas of study were conducted to:

- Establish whether the measurement of egg and whole-body osmolality provides a valuable evaluation of osmoregulatory status during ontogeny.

66

- Assess the impact of abrupt osmotic challenge (0 – 25 ppt) during early life stages on mortality and osmoregulatory status during ontogeny.

- Document the physical effects of osmoregulatory stress during the yolk-sac period in terms of incidence of larval malformation.

Table 3. 1 Summary of reports of teleost osmoregulatory capacity (osmolality) during early life stages.

Common name	Scientific name	Stage	Reference
herring	*Clupea harengus*	eggs and larvae	Holliday and Blaxter (1960 b); Holliday and Jones (1965)
Pacific sardine	*Sardinops caerulea*	eggs and larvae	Lasker and Theilacker (1962)
plaice	*Pleuronectes platessa*	pre-metamorphic larvae	Holliday (1965); Holliday and Jones (1967)
Pacific salmon *spp.*		eggs and fry	Weisbart (1968)
Navaga, polar cod and Arctic flounder	*Eleginus nava, Boreogadus saida, Liopsetta glacialis*	larvae	Doroshev and Aronovich (1974)
eels	*Ariosoma balearicum*	pre-metamorphic larvae	Hulet (1978)
long rough dab	*Hippoglossoides platessoides limandoides*	eggs	Lonning and Davenport (1980)
cod	*Gadus morhua*	eggs	Davenport *et al.* (1981); Mangor-Jensen (1987)
Atlantic halibut	*Hippoglossus hippoglossus*	yolk-sac larvae	Riis-Vestergaard (1982); Hahnenkamp *et al.* (1993)
lumpfish	*Cyclopterus lumpus*	eggs and larvae	Kjorsvik *et al.* (1984)
bonefish	(Albula *sp.*) leptocephali larvae	larvae	Pfeiler (1984)
turbot	*Scophthalmus maximus*	larvae	Brown and Tytler (1993)
chum salmon	*Oncorhynchus keta*	eggs	Kaneko *et al.* (1995)

Table 3.1. cont.

sea bass	*Dicentrachus labrax*	larvae	Varsamos *et al.* (2001)
Japanese eel	*Anquilla japonica*	eggs and larvae	Unuma *et al.* (2005); Okamoto *et al.* (2009)
Mozambique tilapia	*Oreochromis mossambicus*	eggs and larvae	Yanagie *et al.* (2009)
Gilt-head sea bream	*Spaurus aurata*	larvae and juveniles	Bodinier *et al.* (2010)

3.2 Materials and methods

3.2.1   Broodstock care, egg supply and artificial incubation systems

Broodstock were maintained as outlined in Section 2.1.1. and eggs were obtained by manual stripping as outlined in Section 2.1.2. Preparation of experimental salinities and artificial incubation of eggs and yolk-sac fry were carried out as detailed in Sections 2.2 and 2.3.

3.2.2   Development of a feasible method for the measurement of tissue fluid osmolality of embryos and yolk-sac larvae

3.2.2.1   To establish whether tissue osmolality was equivalent to blood and plasma osmolality of juvenile Nile tilapia

Nile tilapia maintained in freshwater, weighing *c.* 150 g, were euthanised following the approved Home Office Schedule 1 method of killing *i.e.* destruction of the brain as well as overdose in anaesthetic with an overdose of MS222 (tricaine methane sulphonate). Blood was removed from the caudal artery with a heparinised 0.6 x 25 mm needle and 5 ml syringe and stored in Eppendorf tubes which were kept moving on a Stuart Scientific blood tube rotator (SBI) at room temperature until sampled. Analysis of blood was performed on an Advanced 3MO Plus MicroOsmometer (Advanced Instruments, MA, US) by measurement of 3 replicates from each fish of 20 µl aliquots. The remaining blood was centrifuged for 3 min at 10 °C at 14 000 g and osmolality of plasma was

measured as above. Tissue was de-scaled and de-skinned and ground in an eppendorf with rotary blade homegeniser (Ultra-Turex T8 IKA, Labortecnic), centrifuged as above and the supernatant checked for osmolality as above. A total of 6 fish were sampled.

3.2.2.2   To establish whether osmolality of whole-body homogenates was equivalent to tissue osmolality during yolk-sac stages

The small size of Nile tilapia embryos and yolk-sac larvae prevented efficient collection of blood or specific body fluids for osmolality measurements therefore whole-body measurements were used for osmolality measurements. In order to assess the effects of contamination of yolk-material on whole-body measurement of larvae, yolk osmolality and body compartment osmolality were compared separately against whole-body (including yolk) osmolality.

Six pooled samples of 60 individuals that had been maintained in freshwater were collected at 2 days post-hatch (dph) and a further six pooled samples of 60 individuals that had been incubated and reared in 20 ppt were collected at 4 dph. Each sample was divided into 2 groups of 30 individuals. One group of 30 larvae was blotted with filter paper and transferred to an Eppendorf tube and frozen immediately at -70 °C. From the remaining 30 individuals, each yolk-sac was carefully removed under a dissecting microscope and the resulting body compartment and yolk-sac were placed in two separate Eppendorfs and frozen immediately at -70 °C. Due to yolk shrinkage by 4 dph insufficient amounts of yolk could be collected therefore only body compartment was compared with whole-body osmolality.

For osmolality measurements, the pools of whole larvae, body compartment and yolk were thawed on ice, homogenised with a motorised Teflon pestle (Pellet Pestle® Motor, Kontes) and the homogenate centrifuged at 10 °C for 10 min at 14 000 g (Eppendorf centrifuge 5417R). The supernatant overlying the pellet was carefully removed by pipette into a single well of a 96-well plate and thoroughly mixed by pipetting to ensure homogeneity of sample. Three replicates of 20 µl aliquots of supernatant from each pool were measured for osmolality. Accuracy of the machine was regularly checked against calibration standards of 50 and 850 mOsm kg^{-1}.

3.2.3   Experiment 1: To determine the ontogenic profile of osmoregulatory capacity of embryos and yolk-sac larvae reared in freshwater and water of elevated salinity

Eggs were obtained by the manual stripping method and both ovarian fluid and un-fertilised eggs were sampled for osmolality. Eggs were then fertilised in freshwater and transferred at 3 - 4 h post-fertilisation to the experimental salinities *i.e.* 7.5, 12.5, 17.5, 20 and 25 ppt. Control eggs remained in freshwater. Sampling was initially performed at time of transfer *i.e.* 3 - 4 h post-fertilisation and, subsequently, at developmental points during embryogenesis *i.e.* gastrula (*c.* 24 h post-fertilisation) and completion of segmentation period (*c.* 48 h post-fertilisation) and then at hatch, 2, 4 and 6 dph and finally at yolk-sac absorption. Triplicate experiments were conducted using different batches of eggs, and each batch was divided into three replicate round-bottomed incubators within each incubation unit. A pooled sample of 30 eggs or larvae was collected at each sampling point (10 from each replicate) and immediately frozen at -70

°C. Osmolality was determined as above (Section 3.2.2.2.) and expressed either as whole-body osmolality (mOsmol kg^{-1}) or as osmoregulatory capacity (OC; mOsmol kg^{-1}), defined as the difference between the mean osmolality of the pooled larvae to that of the osmolality of their corresponding incubation or rearing media.

3.2.4 Experiment 2: To examine the osmotic effects of abrupt transfer to elevated salinities on yolk-sac larvae

3.2.4.1 To ascertain adaptation time of yolk-sac larvae to abrupt salinity challenge

This experiment, using yolk-sac larvae at hatch, 3 and 6 dph, was carried out to determine the time necessary for whole-body osmolality to reach a steady-state after abrupt transfer from the rearing medium (freshwater) to two experimental salinities (12.5 and 20 ppt). Triplicate experiments were conducted using different batches of eggs. Pooled samples, consisting of 30 whole larvae collected prior to transfer (0 h) and at 1.5, 3, 6, 12, 24, 48 and 72 hours post-transfer were immediately frozen at -70 °C. Whole-body osmolality (mOsmol kg^{-1}) was determined as above (Section 3.2.2.2.).

3.2.4.2 To establish whole-body tissue osmolality of Nile tilapia yolk-sac larvae following abrupt transfer to elevated salinities

Healthy yolk-sac larvae were transferred directly from freshwater to 7.5, 12.5, 17.5 or 25 ppt at hatch, 2, 4, 6 and 8 dph. Larvae were exposed to their experimental salinity for 48 h prior to sampling. Control larvae remained in freshwater. Triplicate experiments

were conducted using different batches of eggs. Pooled samples, consisting of 30 whole larvae, were immediately frozen at -70 °C. Osmolality was determined (as above Section 3.2.2.2.) and expressed either as whole-body osmolality (mOsmol kg^{-1}) or as osmoregulatory capacity (OC; mOsmol kg^{-1}), defined as the difference between the osmolality of the larvae to that of the medium.

3.2.4.3 To establish survival of Nile tilapia yolk-sac larvae following abrupt transfer to elevated salinities

Survival at 48 h post-transfer was also recorded. Triplicate experiments were conducted using different batches of eggs. Healthy yolk-sac larvae were transferred directly from freshwater to 7.5, 12.5, 17.5 or 25 ppt at hatch, 2, 4, 6 and 8 dph. A total of 90 larvae were transferred to triplicate incubation bottles (30 larvae per incubation bottle) and mortality was recorded after 48 h. Control larvae remained in freshwater.

3.2.5 Effects of elevated salinities on larval malformations

Thirty newly hatched larvae from each of the three batches were selected at random from each of the experimental salinities (freshwater, 12.5 and 20 ppt) and examined under a dissecting microscope for malformations. Thereafter, thirty live larvae were selected at regular time points during yolk-sac absorption *i.e.* 2 dph, 4 dph, 6 dph and yolk-sac absorption and malformations were noted. The percentage of abnormality was calculated, based on the numbers of normal and malformed larva as follows:

percentage of malformed larvae (%) = 100 * (number malformed larvae/total number of larvae *i.e.* normal and malformed)

3.2.6   Statistical analyses

Statistical analyses were carried out with Minitab 16 using a General Linear Model (GLM) or One-way analysis of variance (ANOVA) with Tukey's post-hoc pair-wise comparisons ($p < 0.05$). Homogeneity of variance was tested using Levene's test and normality was tested using the Anderson-Darling test. Where data failed these assumptions, they were transformed using an appropriate transformation *i.e.* squareroot. All percentage data were normalised by arcsine square transformation prior to statistical analyses to homogenise the variation and data are presented as back-transformed mean and upper and lower 95% confidence limits. Significance was accepted when $p < 0.05$.

3.3 Results

3.3.1 Development of a viable method for measurement of tissue fluid osmolality of embryos and yolk-sac larvae

3.3.1.1 Relationship between tissue and blood or plasma osmolality in juvenile Nile tilapia

In Nile tilapia juveniles, the osmolality of the muscle tissue was 334.5 ± 1.87 mOsmol kg^{-1} and the blood and plasma osmolality were 335.3 ± 1.87 and 330.7 ± 2.50 mOsmol kg^{-1} respectively. Since no significant difference (One-way ANOVA with Tukey's post-hoc pair-wise comparisons; $p < 0.05$) was found between them, tissue osmolality was considered to be equivalent to blood osmolality in juvenile Nile tilapia.

3.3.1.2 Relationship between tissue and yolk osmolality in yolk-sac Nile tilapia larvae

In freshwater maintained larvae at 2 dph, there was no significant difference (One-way ANOVA with Tukey's post-hoc pair-wise comparisons; $p < 0.05$) found between yolk osmolality (234.2 ± 2.60 mOsmol kg^{-1}), tissue osmolality (body compartment) (222.7 ± 3.64 mOsmol kg^{-1}) and whole-body (yolk + body compartment) (220.7 ± 3.2 mOsmol kg^{-1}). Similarly at 4 dph, there was no significant difference ($p < 0.05$) between tissue osmolality (body compartment) (398.3 ± 3.25 mOsmol kg^{-1}) and whole-body (yolk + body compartment) (397.7 ± 2.91 mOsmol kg^{-1}) of larvae maintained in 20 ppt.

It was, therefore, concluded that blood osmolality was similar to tissue osmolality which was in turn similar to whole-body osmolality in yolk-sac larvae in Nile tilapia.

3.3.2 Experiment 1: Ontogenic profile of osmolality and osmoregulatory capacity of embryos and yolk-sac larvae reared in freshwater and elevated salinities

Osmolality was measured in eggs and yolk-sac larvae at selected points from spawning to yolk-sac absorption. Data were combined from all three batches as variances were homogeneous and no statistical differences were observed between batches (GLM; $p < 0.001$). There was an overall significant effect of salinity, age and their interaction on osmolality which is summarised in Table 3.2. and Figure 3.1.

Table 3. 2 Analysis of Variance for whole-body osmolality (mOsmol kg^{-1}) (General Linear Model; $p < 0.001$).

Source	DF	F	P-value
Salinity	4	1140.8	0.001
Age	6	113.9	0.001
Age vs. salinity	24	48.6	0.001
Error	278		

A)   B)
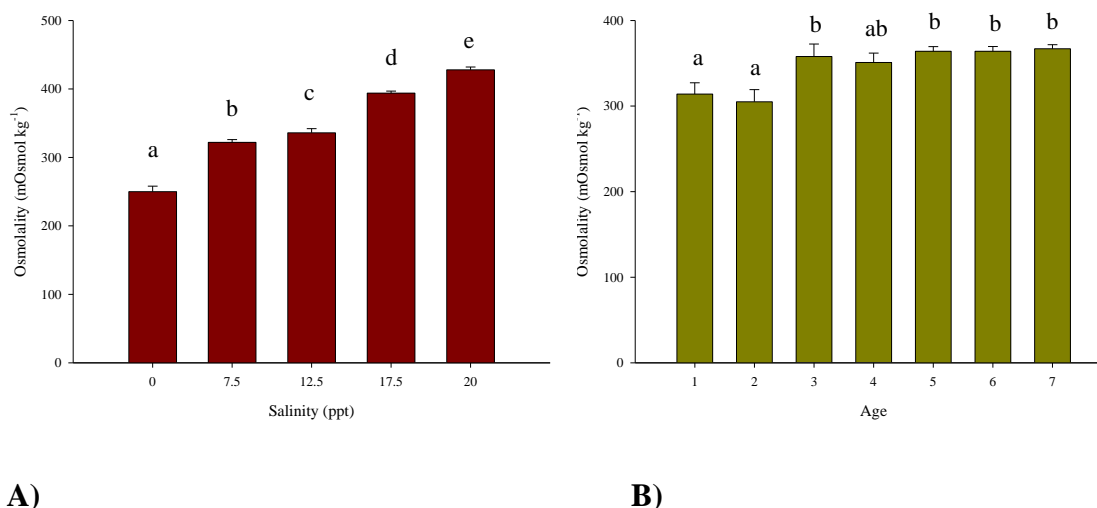
Figure 3. 1 Overall effects on whole-body osmolality (mOsmol kg^{-1}) of Nile tilapia during early life stages of **A)** Salinity and **B)** Stage; *x* axis: 1- 24 h post-fertilisation; 2 – 48 h post-fertilisation; 3 - hatch; 4 - 2 dph; 5 - 4 dph; 6 - 6 dph; 7 - yolk-sac absorption. Mean ± S.E. Different letters indicate significant differences between treatments (General Linear Model with Tukey's post-hoc pairwise comparisons; p < 0.05).

Similarly, there was an overall effect of salinity, age and their interaction on osmoregulatory capacity (OC) *i.e.* difference between osmolality of body fluids and that of the media, which is summarised in Table 3.3. and Figure 3.2.

Table 3. 3 Analysis of Variance for osmoregulatory capacity (OC) (General Linear Model; p < 0.001).

Source	*DF*	*F*	*P-value*
Salinity	4	66.9	0.001
Age	6	42.3	0.001
Age vs. salinity	24	4.2	0.001
Error	46		

A)

B)
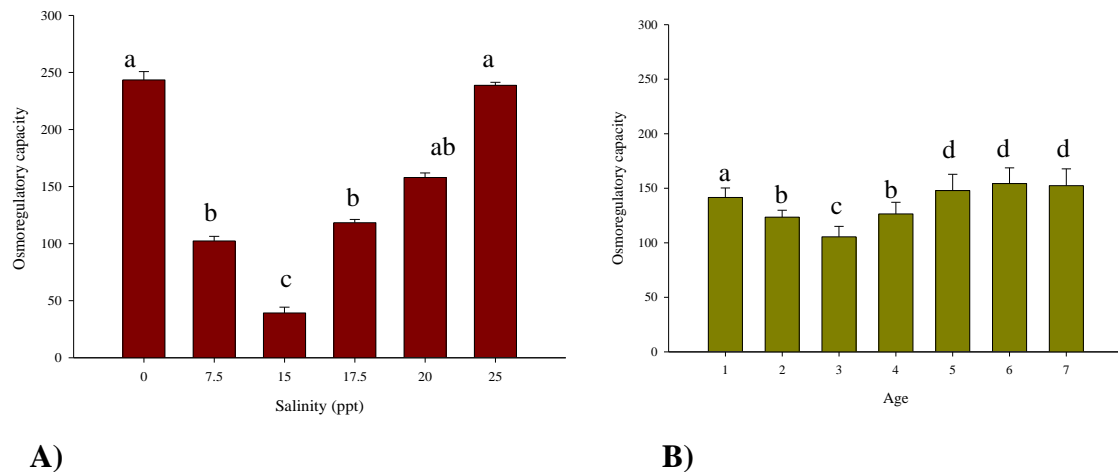
Figure 3. 2 Overall effects on osmoregulatory capacity (OC) (mOsmol kg^{-1}) of Nile tilapia during early life stages of **A)** Salinity and **B)** Stage; *x* axis: 1- gastrula; 2 – end of segmentation period; 3 - hatch; 4 - 2 dph; 5 - 4 dph; 6 - 6 dph; 7 - yolk-sac absorption. Mean ± S.E. Different letters indicate significant differences between treatments (General Linear Model with Tukey's post-hoc pairwise comparisons; $p < 0.05$).

Osmolality of unfertilised eggs (358.2 ± 4.95 mOsmol kg^{-1}) was similar to that of ovarian fluid (370.7 ± 2.30 mOsmol kg^{-1}) but was seen to drop significantly (One-way ANOVA with Tukey's post-hoc pair-wise comparisons; $p < 0.05$) to 216.9 ± 8.89 mOsmol kg^{-1}) after 3 - 4 hours post-fertilisation in freshwater. Osmolality during embryogenesis in freshwater dropped further to a low of 174.6 ± 4.15 mOsmol kg^{-1} at completion of segmentation period at *c.* 48 h post-fertilisation, and then was seen to increase by hatching to 230.3 ± 2.53 mOsmol kg^{-1}. Osmolality of larvae in freshwater was then seen to rise abruptly (GLM with Tukey's post-hoc pairwise comparisons; $p < 0.05$) by 4 dph and, thereafter, maintained a relatively constant level of 319.5 ± 4.91 – 324.8 ± 7.41 mOsmol kg^{-1} until yolk-sac absorption (Table 3.4.; Figure 3.3.).

In contrast, the osmolality of eggs transferred to elevated salinities at 3 - 4 h post-fertilisation increased with increasing salinity immediately upon transfer. Transfer to 25 ppt induced 100% mortality by 48 h post-fertilisation. In the higher salinities of 17.5 and 20 ppt, osmolality was seen, after the initial abrupt rise, to steadily increase, reaching a maximal value of 434.0 ± 2.07 mOsmol kg^{-1} and 497.8 ± 2.79 mOsmol kg^{-1} at hatch for larvae maintained in 17.5 and 20 ppt, respectively, declining at 2 dph and thereafter maintaining a relatively constant level until yolk-sac absorption. For the lower salinities of 7.5 and 15 ppt, following a similar, abrupt rise at transfer, osmolality appears to drop slightly at *c.* 48 h post-fertilisation and then steadily rise until 4 dph, maintaining a relatively constant level thereafter until yolk-sac absorption. There was always a significantly higher whole-body osmolality in eggs and larvae maintained in elevated salinities as compared to those in freshwater (Table 3.4.; Figure 3.3.).
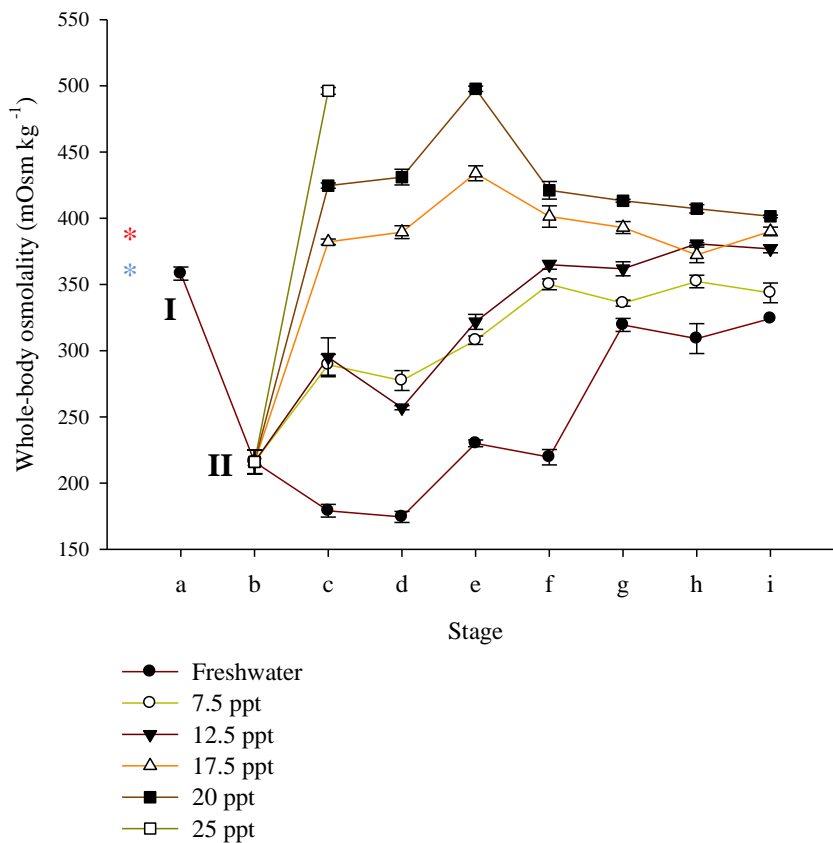
Figure 3. 3 Ontogenic changes in whole-body osmolality of Nile tilapia larvae. Mean ± S.E. *: un-fertilised eggs (358.2 ± 4.95 mOsmol kg^{-1}); *: ovarian fluid (370.7 ± 2.30 mOsmol kg^{-1}). *x* axis (Stage): a; un-fertilised eggs; b: 3 – 4 h post-fertilisation; c: 24 h post-fertilisation; d: 48 h post-fertilisation; e: hatch; f: 2 dph; g: 4 dph; h: 6 dph; i: yolk-sac absorption. Different numerals indicate significant difference between pre-fertilised eggs and those at 3 - 4 h post-fertilisation (One-way ANOVA with Tukey's post-hoc pair-wise comparisons; $p < 0.05$). Statistical differences between sampling points are included in corresponding Table 3.4. rather than in graph for clarity of presentation.

Larvae within all developmental stages hyper-regulated at low salinities (*i.e.* freshwater to 7.5 ppt) and hypo-regulated at higher salinities (*i.e.* 17.5 – 20 ppt). Complete mortality of embryos transferred to 25 ppt occurred following 24 h post-fertilisation.

During embryogenesis in the iso-osmotic salinity of 12.5 ppt, embryos either hypo-regulated or were iso-osmotic with their environmental salinity and from hatch until yolk-sac absorption larvae hyper-regulated (Figure 3.4.). The ability to osmoregulate increased throughout the developmental period studied, as evidenced by variations in osmoregulatory capacity (OC; defined as the difference between the mean osmolality of the pooled larvae to that of the osmolality of their corresponding incubation or rearing media). A higher OC indicates the greater the ability to maintain homeostasis (Table 3.4.; Figure 3.5.).

Hyper-OC in freshwater increased progressively in absolute value from 176.1 ± 3.66 mOsmol kg^{-1} at 24 h post-fertilisation to 321.2 ± 4.99 mOsmol kg^{-1} until yolk-sac absorption; OC values during embryogenesis remained similar but rose significantly at hatch (GLM; $p< 0.05$). Osmoregulatory capacity was again seen to increase significantly (GLM; $p< 0.05$) by 4 dph to 316.4 ± 2.92 with levels remaining constant thereafter until yolk-sac absorption. A similar pattern was observed for embryos and yolk-sac larvae adapted to 7.5 ppt, although OC levels were significantly lower throughout ontogeny than corresponding freshwater values (GLM; $p < 0.05$) (Table 3.4.; Figure 3.5.). Whilst at the elevated salinities of 17.5 and 20 ppt, OC levels remained constant during embryogenesis with no significant change in absolute value from 24 hours post-fertilisation until yolk-sac absorption, a significant drop in OC (GLM; $p < 0.05$) was observed at hatch (Table 3.4; Figure 3.5), but which then rose again by 2 dph. In the iso-osmotic salinity of 12.5, embryos hypo-regulated until hatch, and thereafter were either iso-osmotic to the environmental salinity or slightly hyper-gulated (Table 3.4.; Figure 3.5.).
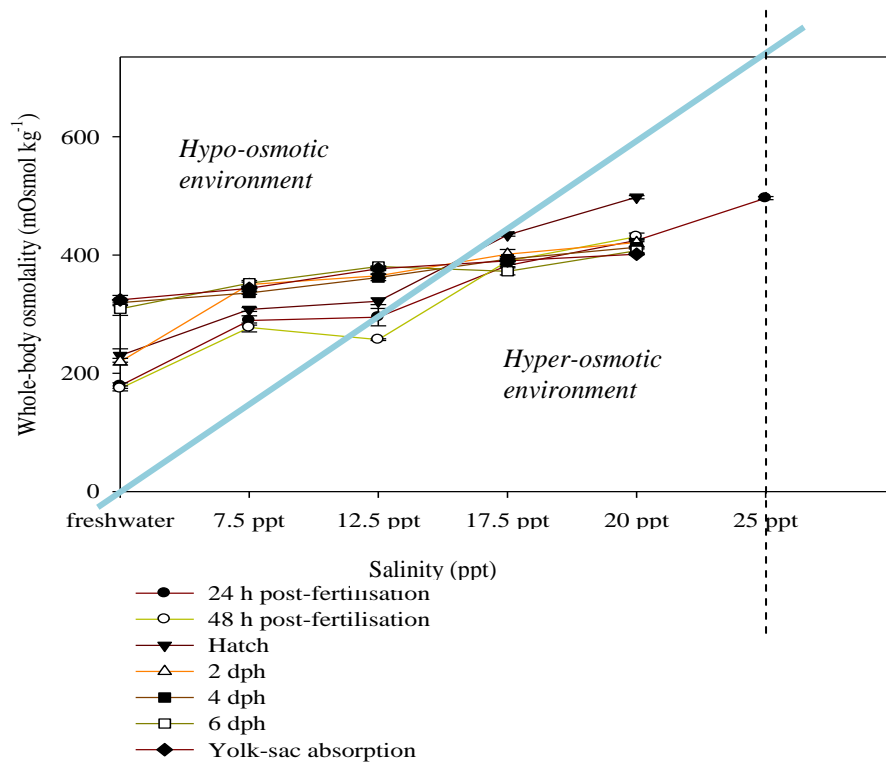
Figure 3. 4 Variations in whole-body osmolality during ontogeny in relation to the osmolality of the media. Blue line; iso-osmotic concentration. Mean $\pm$ S.E.; statistical differences between salinities are included in corresponding Table 3.4. rather than in graph for clari
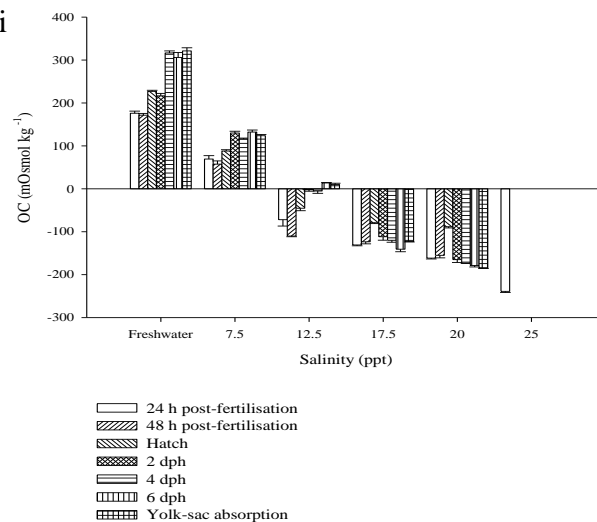
Figure 3. 5 Variations in osmoregulatory capacity (OC) during ontogeny in relation to the osmolality of the medium. Mean $\pm$ S.E; statistical differences between salinities are included in corresponding Table 3.4. rather than in graph for clarity of presentation.

Table 3. 4 Ontogenic variations in whole-body osmolality (mOsmol kg^{-1}) and osmoregulatory capacity (OC) at various developmental points from fertilisation until yolk-sac absorption Different superscript letters represent significant differences between treatments; different subscript letters represent significant differences between sampling points (General Linear Model with Tukey's post-hoc pairwise comparisons; p < 0.05). Complete mortality occurred from 48 h post-fertilisation onwards in 25 ppt.

Media osmolality/mOsmol kg^{-1}	0	221	368	519	588	735
Salinity (ppt)	0	7.5	12.5	17.5	20	25

Whole-body osmolality (mOsmol kg^{-1}):

Stage:

	0	221	368	519	588	735
24 h post-fertilisation	$179.1 \pm 4.80\ ^{a}_{a}$	$289.3 \pm 7.87\ ^{b}_{ab}$	$295 \pm 14.68\ ^{b}_{a}$	$382.2 \pm 2.07\ ^{c}_{a}$	$424.6 \pm 1.99\ ^{d}_{a}$	$496.2 \pm 2.60\ ^{e}$
48 h post-fertilisation	$174.4 \pm 4.15\ ^{a}_{a}$	$277.4 \pm 7.53\ ^{b}_{a}$	$256.9 \pm 1.51\ ^{b}_{a}$	$389.5 \pm 4.86\ ^{c}_{a}$	$431.1 \pm 5.96\ ^{d}_{a}$	-
Hatch	$230.3 \pm 2.53\ ^{a}_{b}$	$307.9 \pm 3.21\ ^{b}_{b}$	$321.8 \pm 5.67\ ^{b}_{b}$	$434.0 \pm 2.07\ ^{c}_{b}$	$497.8 \pm 2.79\ ^{d}_{b}$	-
2 dph	$219.5 \pm 5.77\ ^{a}_{b}$	$350.1 \pm 4.02\ ^{b}_{c}$	$364.9 \pm 3.32\ ^{b}_{c}$	$401.3 \pm 8.06\ ^{c}_{a}$	$421.1 \pm 6.67\ ^{c}_{a}$	-
4 dph	$319.4 \pm 4.91\ ^{a}_{c}$	$335.9 \pm 2.26\ ^{b}_{c}$	$361.9 \pm 5.28\ ^{c}_{c}$	$393 \pm 4.51\ ^{bc}_{a}$	$413.2 \pm 1.10\ ^{d}_{a}$	-
6 dph	$309.1 \pm 11.31\ ^{a}_{c}$	$352.2 \pm 4.73\ ^{b}_{c}$	$380.7 \pm 0.97\ ^{c}_{c}$	$392.3 \pm 5.90\ ^{cd}_{a}$	$407.2 \pm 3.11\ ^{d}_{a}$	-
Yolk-sac absorption	$324.8 \pm 7.41\ ^{a}_{c}$	$343.7 \pm 1.02\ ^{b}_{c}$	$376.9 \pm 3.11\ ^{c}_{c}$	$390.1 \pm 6.34\ ^{c}_{c}$	$401.44 \pm 0.99\ ^{c}_{c}$	-

Table 3.4. cont.

Media osmolality (mOsmol kg^{-1})	0	221	368	519	588	735
Salinity (ppt)	0	7.5	12.5	17.5	20	25

Osmoregulatory capacity (OC) (mOsmol kg^{-1}):

Stage:

	0	221	368	519	588	735
24 h post-fertilisation	176.1 ± 3.66 $^{a}_{a}$	69.33 ± 3.22 $^{b}_{a}$	-72.0 ± 3.06 $^{c}_{ab}$	-130.8 ± 0.99$^{cd}_{a}$	-161.3 ± 2.06 $^{d}_{a}$	-238.8 ± 3.60 ^{e}
48 h post-fertilisation	171.4 ± 6.15 $^{a}_{a}$	57.4 ± 2.333 $^{b}_{a}$	-110.1 ± 3.51 $^{c}_{a}$	-123.4 ± 2.55 $^{c}_{a}$	-154.9 ± 5.23 $^{d}_{a}$	-
Hatch	227.0 ± 9.54 $^{a}_{b}$	87.8 ± 2.37 $^{b}_{b}$	-45.2 ± 2.67 $^{c}_{b}$	-79.0 ± 0.97 $^{d}_{b}$	-88.2 ± 1.44 $^{d}_{b}$	-
2 dph	216.5 ± 2.88 $^{a}_{b}$	130.1 ± 3.02 $^{b}_{c}$	-2.1 ± 3.32 $^{c}_{c}$	-111.7 ± 3.06 $^{d}_{a}$	-164.9 ± 5.33 $^{e}_{a}$	-
4 dph	316.4 ± 2.92 $^{a}_{c}$	115.8 ± 1.22 $^{b}_{bc}$	-5.11 ± 2.28 $^{c}_{c}$	-120.0 ± 3.52 $^{d}_{a}$	-172.3 ± 1.13 $^{e}_{a}$	-
6 dph	306.1 ± 10.61$^{a}_{c}$	132.2 ± 3.98 $^{b}_{c}$	13.66 ± 2.97 $^{c}_{d}$	-140.0 ± 6.90 $^{d}_{a}$	-178.8 ± 2.56 $^{d}_{a}$	-
Yolk-sac absorption	321.2 ± 4.99 $^{a}_{c}$	123.7 ± 1.23 $^{b}_{c}$	9.88 ± 2.33 $^{c}_{d}$	-122.9 ± 2.45 $^{d}_{a}$	-184.6 ± 1.44 $^{e}_{a}$	-

3.3.3 Experiment 2: To establish whole-body tissue osmolality of yolk-sac larvae following abrupt transfer to low salinities

3.3.3.1 Establishment of adaptation time

The time required for whole-body osmolality to stabilise following an abrupt transfer to an elevated salinity did not appear to vary according to age at transfer (Figure 3.6.). There was a significant initial rise in osmolality at 1.5 h following transfer (One-way ANOVA with Tukey's post-hoc pairwise comparisons; $p < 0.05$) for all developmental stages tested, which was proportional to the salinity; larvae transferred to 20 ppt exhibited an osmolality in the range of 513.3 ± 5.30 - 482.7 ± 5.04 mOsmol kg^{-1} whilst those transferred to 12.5 ppt exhibited an osmolality in the range of 414.3 ± 3.21 - 387.7 mOsmol kg^{-1} after 1.5 h. The difference in osmolality between the two treatment ranges was about 100 mOsmol kg^{-1}. In general, the changes in osmolality appeared to follow a pattern of crisis and regulation, with values for larvae stabilising at *c.* 48 h for all treatments, regardless of age at time of transfer, and subsequently remaining the same with no significant change ($p < 0.05$) until 72 h post-transfer. According to these results, the subsequent experiments on osmolality and osmoregulatory capacity were made on larvae having reached a steady-state osmolality following 48 h exposure to experimental salinities.
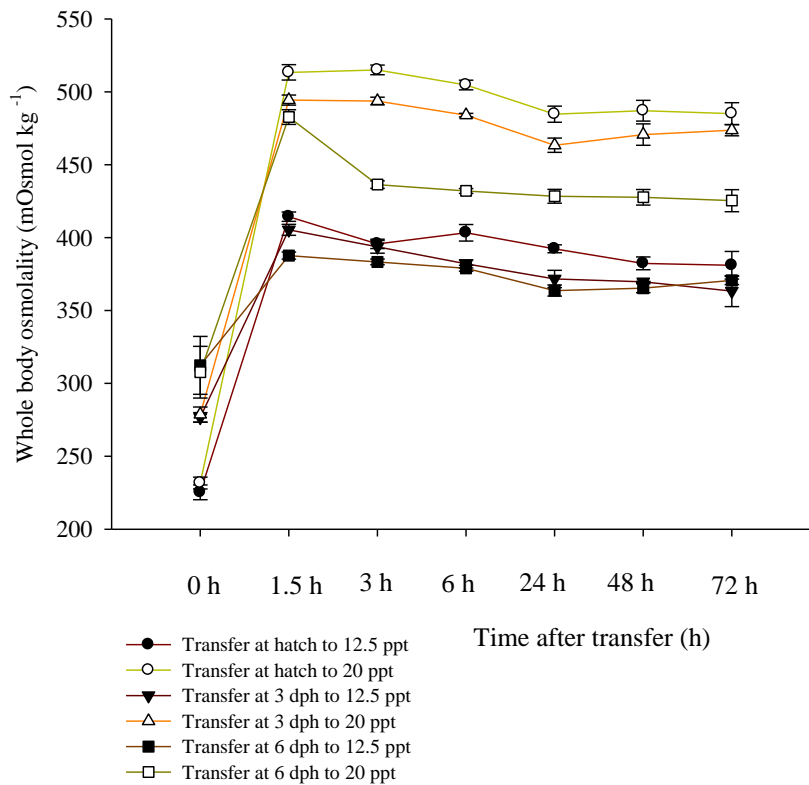
Figure 3. 6 Time-course of whole-body osmolality in Nile tilapia yolk-sac larvae following direct transfer from freshwater to 12.5 and 20 ppt at hatch, 3 dph and 6 dph. Mean ± S.E.

3.3.3.2 Osmolality and osmoregulatory capacity following abrupt transfer to elevated salinities

Post-embryonic stages were abruptly transferred from freshwater to varying low salinities (range 7.5 ppt - 20 ppt) and osmolality measured after 48 h. Data were combined from all three batches as no statistical differences were observed between batches (GLM; $p < 0.001$). There was an overall significant effect of salinity but not of age at transfer or their interaction on whole-body osmolality which is summarised in Table 3.5. and Figure 3.7.

Table 3. 5 Analysis of Variance for whole-body osmolality (General Linear Model; p < 0.001).

Source	DF	F	P-value
Salinity	4	618.08	0.001
Age	4	51.96	0.324
Age vs. salinity	16	6.57	0.121
Error	198		
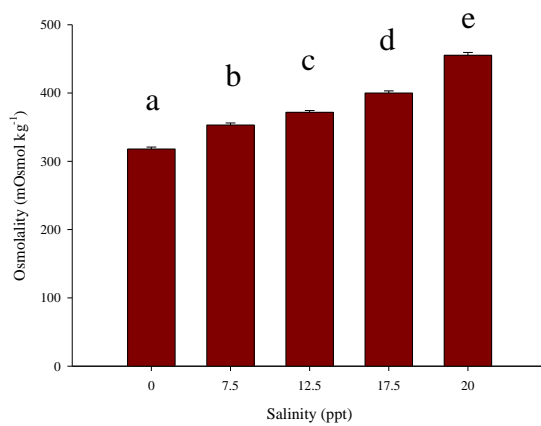
Figure 3. 7 Overall effects on whole-body osmolality (mOsmol kg^{-1}) following transfer to elevated salinities. Mean ± S.E. Different letters indicate significant differences between treatments (General Linear Model with Tukey's post-hoc pairwise comparisons; $p < 0.05$).

There was an overall effect of salinity, but not of age or their interaction on osmoregulatory capacity (OC) which is summarised in Table 3.6. and Figure 3.8.

Table 3. 6 Analysis of Variance for osmoregulatory capacity (OC) (General Linear Model; p < 0.001)

Source	DF	F	P-value
Salinity	4	429.6	0.001
Age	4	4.13	0.087
Age vs. salinity	16	0.59	0.837
Error	211		
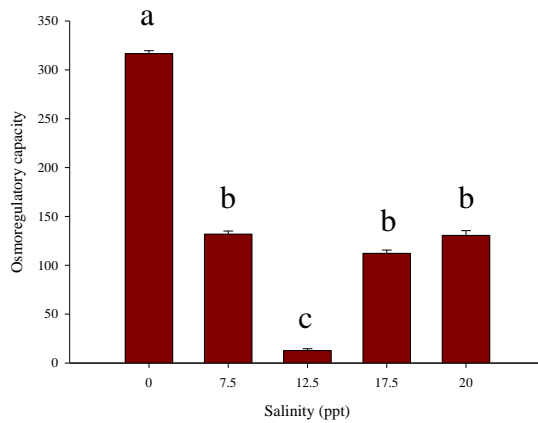
Figure 3. 8 Overall effect of salinity on osmoregulatory capacity (OC) (mOsmol kg^{-1}) of Nile tilapia during early life stages. Mean ± S.E. Different letters indicate significant differences between treatments (General Linear Model with Tukey's post-hoc pairwise comparisons; p < 0.05).

All stages (*i.e*. from hatch to 8 dph) hyper-regulated in freshwater, 7.5 and 12.5 ppt and hypo-regulated at 20 ppt. Larvae transferred to 17.5 ppt had an osmolality close to that of the media (iso-osmotic) (Table 3.7.; Figure 3.9.). Ontogeny had a significant effect (GLM; p < 0.05) on larval ability to withstand abrupt osmotic challenge; larvae at 8 dph maintained a more constant osmolality over the experimental salinities tested (range 341.1 ± 11.06 to 427.0 ± 2.34 mOsmol kg^{-1}) than larvae transferred at hatch (360.9 ±

3.33 to 487.7 $\pm$ 4.92 mOsmol kg^{-1}) (Table 3.7.; Figure 3.10.). Similarly, a statistical comparison of OC values showed a clear pattern of age at transfer positively influencing osmoregulatory status. However, there was no significant effect of age of transfer on osmoregulatory capacity (OC) to the lower salinity of 7.5 ppt (Table 3.7.; Figure 3.11.).
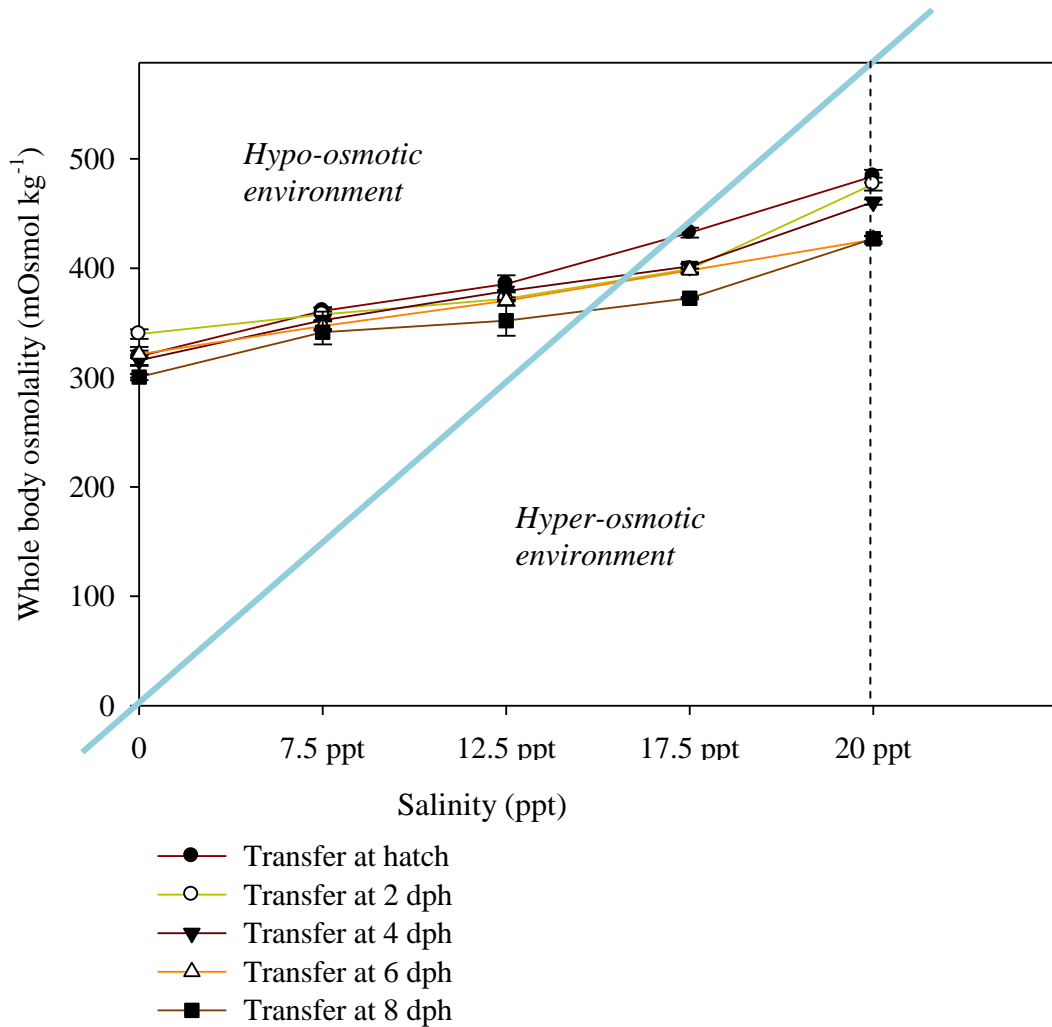
Figure 3. 9 Variations in whole-body osmolality at different post-embryonic stages in relation to the osmolality of the medium following 48 h exposure to experimental salinity. Blue line; iso-osmotic concentration. Mean $\pm$ S.E.; statistical differences between salinities are included in corresponding Table 3.7. rather than in graph for clarity of presentation.

Table 3. 7 Variations in whole-body osmolality (mOsmol kg^{-1}) and osmoregulatory capacity (OC) at different post-embryonic stages in relation to the osmolality of the medium following 48 h exposure to experimental salinity. Different superscript letters represent significant differences between treatments; different subscript letters represent significant differences between time of transfer (General Linear Model with Tukey's post-hoc pairwise comparisons; $p < 0.05$).

Media osmolality (mOsmol kg^{-1})	30-40	221	368	515	588
Salinity (ppt)	0	7.5	12.5	17.5	20

Whole-body osmolality (mOsmol kg^{-1}):

Age at transfer:

Hatch	$219.4 \pm 8.65^{a}_{a}$	$360.9 \pm 3.33^{b}_{a}$	$385.7 \pm 7.82^{c}_{a}$	$432.5 \pm 4.55^{d}_{a}$	$487.7 \pm 4.97^{e}_{a}$
2 dph	$229.7 \pm 4.44^{a}_{a}$	$357.8 \pm 6.11^{b}_{a}$	$372.1 \pm 1.28^{b}_{b}$	$399.2 \pm 4.48^{b}_{b}$	$476.9 \pm 5.89^{c}_{a}$
4 dph	$315.8 \pm 4.27^{a}_{b}$	$352.3 \pm 9.01^{b}_{a}$	$379.2 \pm 0.90^{b}_{ab}$	$401.8 \pm 2.25^{b}_{b}$	$460.5 \pm 2.5^{c}_{b}$
6 dph	$321.3 \pm 3.40^{a}_{b}$	$347.2 \pm 4.19^{b}_{a}$	$370.3 \pm 0.72^{b}_{b}$	$398.0 \pm 1.69^{bc}_{b}$	$426.1 \pm 3.57^{c}_{c}$
8 dph	$300.4 \pm 2.88^{a}_{b}$	$341.4 \pm 11.06^{b}_{a}$	$352.0 \pm 11.06^{b}_{c}$	$372.5 \pm 0.98^{b}_{c}$	$427.0 \pm 2.34^{c}_{c}$

Table 3.7. cont.

Media osmolality (mOsmol kg^{-1})	30-40	221	368	515	588
Salinity (ppt)	0	7.5	12.5	17.5	20

Osmoregulatory capacity (OC) (mOsmol kg^{-1}):

Age at transfer:

Hatch	$216.4 \pm 2.65^{a}_{a}$	$140.8 \pm 3.63^{b}_{a}$	$18.7 \pm 0.66^{b}_{a}$	$-80.44 \pm 3.65^{c}_{a}$	$-98.3 \pm 3.12^{c}_{a}$
2 dph	$236.8 \pm 3.72^{a}_{b}$	$137.7 \pm 2.50^{b}_{a}$	$5.1 \pm 1.68^{c}_{a}$	$-113.8 \pm 3.68^{d}_{b}$	$-109.1 \pm 2.55^{d}_{ab}$
4 dph	$312.8 \pm 4.07^{a}_{a}$	$132.3 \pm 5.63^{b}_{a}$	$12.2 \pm 0.90^{c}_{a}$	$-111.2 \pm 1.25^{d}_{b}$	$-125.5 \pm 1.95^{d}_{b}$
6 dph	$318.3 \pm 2.21^{a}_{a}$	$127.2 \pm 3.22^{b}_{a}$	$3.3 \pm 2.71^{c}_{a}$	$-115.0 \pm 0.65^{d}_{b}$	$-159.9 \pm 2.99^{e}_{c}$
8 dph	$297.4 \pm 2.88^{c}_{c}$	$121.4 \pm 7.99^{a}_{a}$	$-15.00 \pm 2.06^{b}_{b}$	$-140.4 \pm 1.07^{b}_{c}$	$-159.0 \pm 2.04^{c}_{c}$
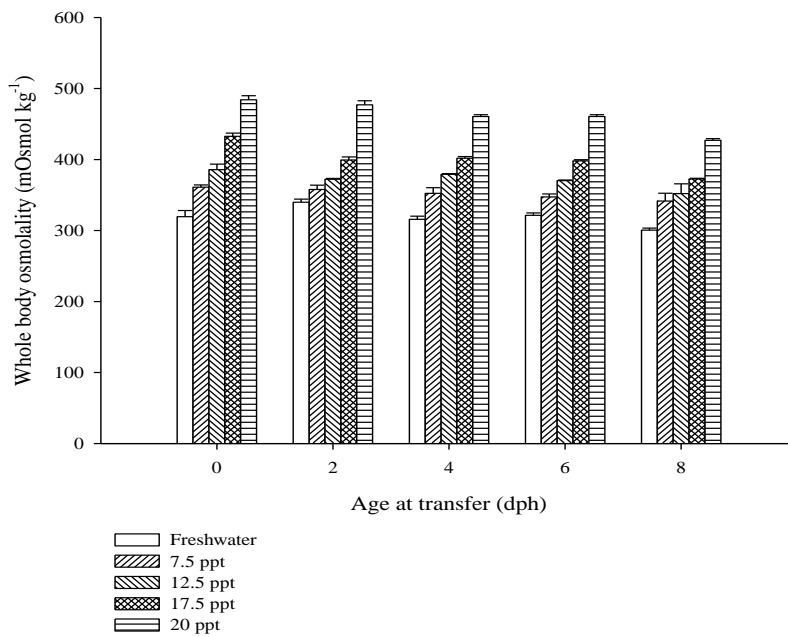
Figure 3. 10   Whole-body osmolality following 48 h after transfer to elevated salinities. Mean ± S.E.; statistical differences between salinities are included in corresponding Table 3.7. rather than in graph for clarity of presentation.
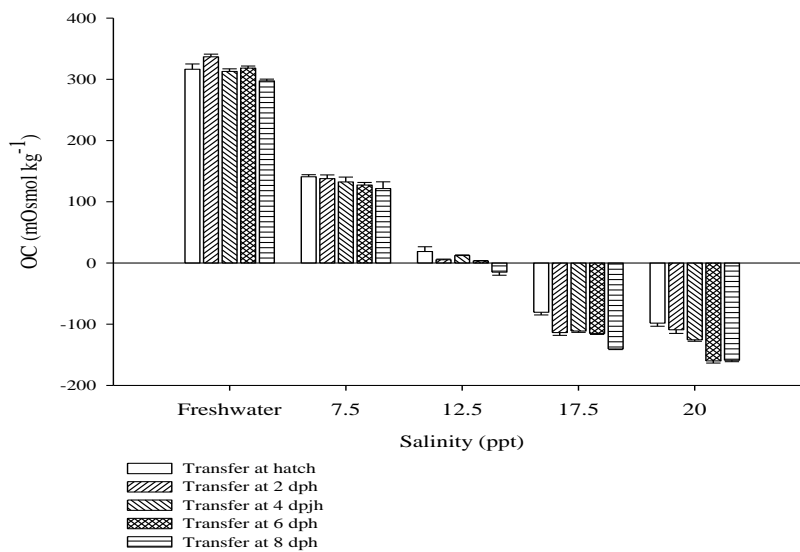
Figure 3. 11 Variations in osmoregulatory capacity (OC) at different post-embryonic stages in relation to the osmolality of the medium following 48 h exposure to experimental salinities. Mean ± S.E; statistical differences between salinities are included in corresponding Table 3.7. rather than in graph for clarity of presentation.

3.3.3.3 Survival

Data were combined from all three batches as variances were homogeneous and no statistical differences were observed between batches (GLM; $p < 0.001$). There was an overall significant effect of salinity, age at time of transfer and their interaction on survival rates which is summarised in Table 3.8. and Figure 3.12.

Table 3. 8 Analysis of Variance for survival (%) (General Linear Model; $p < 0.001$).

Source	*DF*	*F*	*P-value*
Salinity	4	6.97	0.001
Age	4	11.56	0.001
Age vs. salinity	16	2.45	0.001
Error	200		

A)   B)
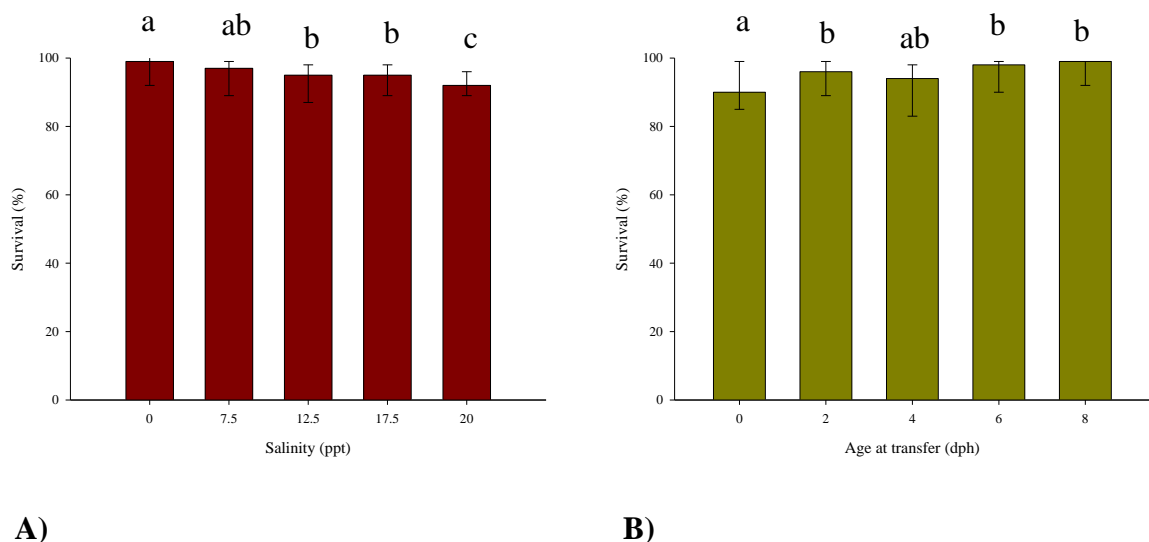
Figure 3. 12 Overall effects of **A)** Salinity and **B)** Time of transfer on survival rates of Nile tilapia larvae (General Linear Model; $p < 0.001$). Statistical analysis, mean and 95% confidence limits were calculated on arcsine square transformed data.

Survival generally decreased with increasing salinity but increased with successive developmental stages (Figure 3.13.; Table 3.9.). Survival rates of 98 % were recorded for larvae maintained in freshwater at hatch yet lower survival rates, in the range of 83 - 92 %, were recorded for those transferred, at hatch, to elevated salinities. Larvae transferred to salinities of 7.5 – 17.5 ppt at 2 and 4 dph exhibited an improved survival rate than at hatch, yet larvae transferred to 20 ppt still displayed a significantly lower survival rate (GLM; $p < 0.05$) than other salinities. From 6 dph onwards, no significant differences were observed between survival rates amongst salinities (GLM; $p < 0.05$) (Table 3.9.; Figure 3.13.).
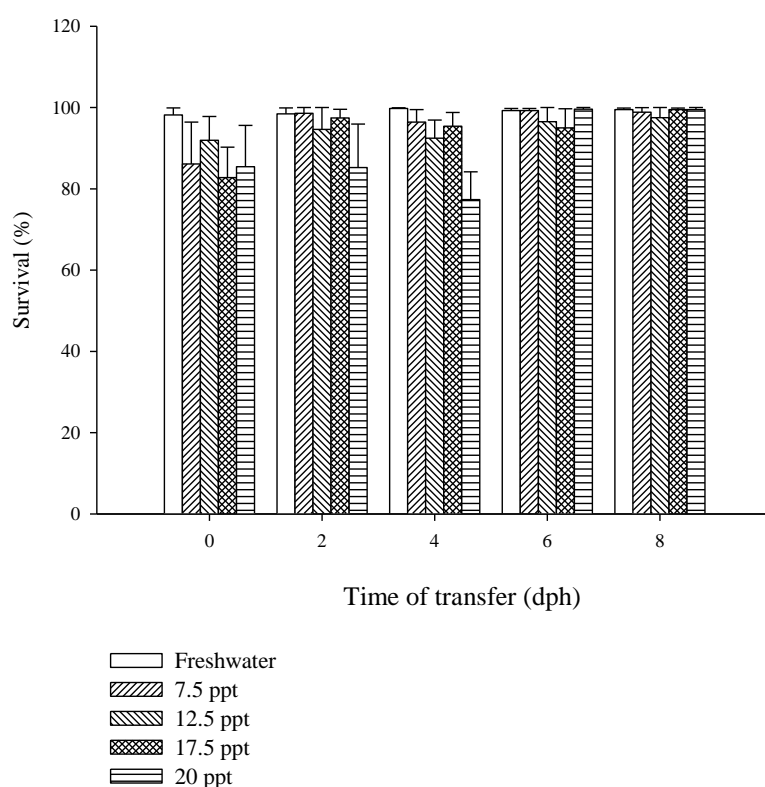
Figure 3. 13 Effect of elevated salinities on larval survival (%) at 48 h post-transfer at various developmental stages during yolk-sac period. Mean and 95% confidence limits were calculated on arcsine square transformed data. Statistical differences between salinities and between sampling points are included in corresponding Table 3.9. rather than in graph for clarity of presentation.

Table 3. 9 Effect of various salinities on larval survival (%) at 48 h post-transfer at various developmental stages during yolk-sac period. Mean and 95% confidence limits were calculated on arcsine square transformed data of three batches with three replicates per batch (n = 30) larvae per replicate). Different superscript letters represent significant differences between treatments; different subscript letters represent significant differences between times of transfer (General Linear Model with Tukey's post-hoc pairwise comparisons; $p < 0.05$).

Larval survival (%):

Salinity	Freshwater	7.5 ppt	12.5 ppt	17.5 ppt	20 ppt
Time of transfer:					
Hatch	98	86	92	83	85
	$(94.4 - 99.9)^{a}_{a}$	$(70.6 - 96.4)^{b}_{a}$	$(82.9 - 97.8)^{ab}_{a}$	$(73.7 - 90.2)^{b}_{a}$	$(70.7 - 95.6)^{b}_{a}$
2 dph	98	98	95	97	85
	$(95.4 - 99.9)^{a}_{a}$	$(94.5 - 99.9)^{a}_{b}$	$(79.5 - 99.9)^{a}_{a}$	$(93.5 - 99.6)^{a}_{b}$	$(69.4 - 95.9)^{b}_{a}$
4 dph	99	96	92	95	77
	$(98.4 - 99.9)^{a}_{a}$	$(90.7 - 99.5)^{a}_{b}$	$(86.2 - 96.9)^{a}_{a}$	$(90.1 - 98.8)^{a}_{b}$	$(69.6 - 84.2)^{b}_{a}$
6 dph	99	98	96	95	99
	$(95.1 - 99.8)^{a}_{a}$	$(94.8 - 99.9)^{a}_{b}$	$(87.1 - 99.9)^{a}_{a}$	$(85.1 - 99.7)^{a}_{b}$	$(95.5 - 99.3)^{a}_{b}$
8 dph	99	99	97	99	99
	$(96.8 - 99.9)^{a}_{a}$	$(94.8 - 99.9)^{a}_{b}$	$(90.8 - 99.9)^{a}_{a}$	$(96.8 - 99.9)^{a}_{b}$	$(96.8 - 99.9)^{a}_{b}$

3.3.4   Larval malformation

Gross larval malformation was defined as pericardial oedema, sub-epithelial oedema of the yolk-sac, non-specific haemorrhaging of blood vessels associated with the yolk-sac syncytium and body or abnormal neurocranium (Figure 3.14.). There was a significant effect of salinity, age and their interaction on the incidence of malformation, which is summarised in Table 3.10. and Figure 3.15.

Table 3. 10 Analysis of Variance for incidence of malformation (%) (General Linear Model; $p < 0.001$).

Source	*DF*	*F*	*P-value*
Salinity	2	11.44	0.001
Age	4	13.85	0.001
Age vs. salinity	8	3.39	0.007
Error	44		

Incidence of malformation of yolk-sac larvae was always significantly higher in salinities than in freshwater at all stages (GLM; $p < 0.05$). Incidence of malformation was seen to decline significantly (GLM; $p < 0.05$) from hatch until yolk-sac absorption (Table 3.11.).

Table 3. 11 Effect of salinity on larval malformation during yolk-sac period. Mean and 95% confidence limits were calculated on arcsine square transformed data. Different superscript letters represent significant differences between treatments; different subscript letters represent significant differences between days (General Linear Model with Tukey's post-hoc pairwise comparisons; $p < 0.05$).

Incidence of malformation (%)

Salinity	Freshwater	12.5 ppt	20 ppt
Time of transfer:			
Hatch	14	22	23
	$(12 - 59.6)^{a}_{a}$	$(20.6 - 41.9)^{b}_{a}$	$(19.9 - 32)^{b}_{a}$
2 dph	2	8	29
	$(0.5 - 17.6)^{a}_{b}$	$(6.2 - 34.8)^{b}_{ab}$	$(22.6 - 35.6)^{c}_{a}$
4 dph	2	8	10
	$(0.4 - 4.7)^{a}_{b}$	$(2.23 - 18.1)^{b}_{ab}$	$(2.4 - 23.6)^{b}_{b}$
6 dph	1	2	6
	$(0.1 - 15.1)^{a}_{b}$	$(0.1 - 15.1)^{a}_{b}$	$(1.9 - 13.6)^{b}_{b}$
Yolk-sac absorption	1	7	9
	$(0.5 - 6.0)^{a}_{b}$	$(5.6 - 8.5)^{b}_{ab}$	$(7.5 - 11.7)^{b}_{b}$
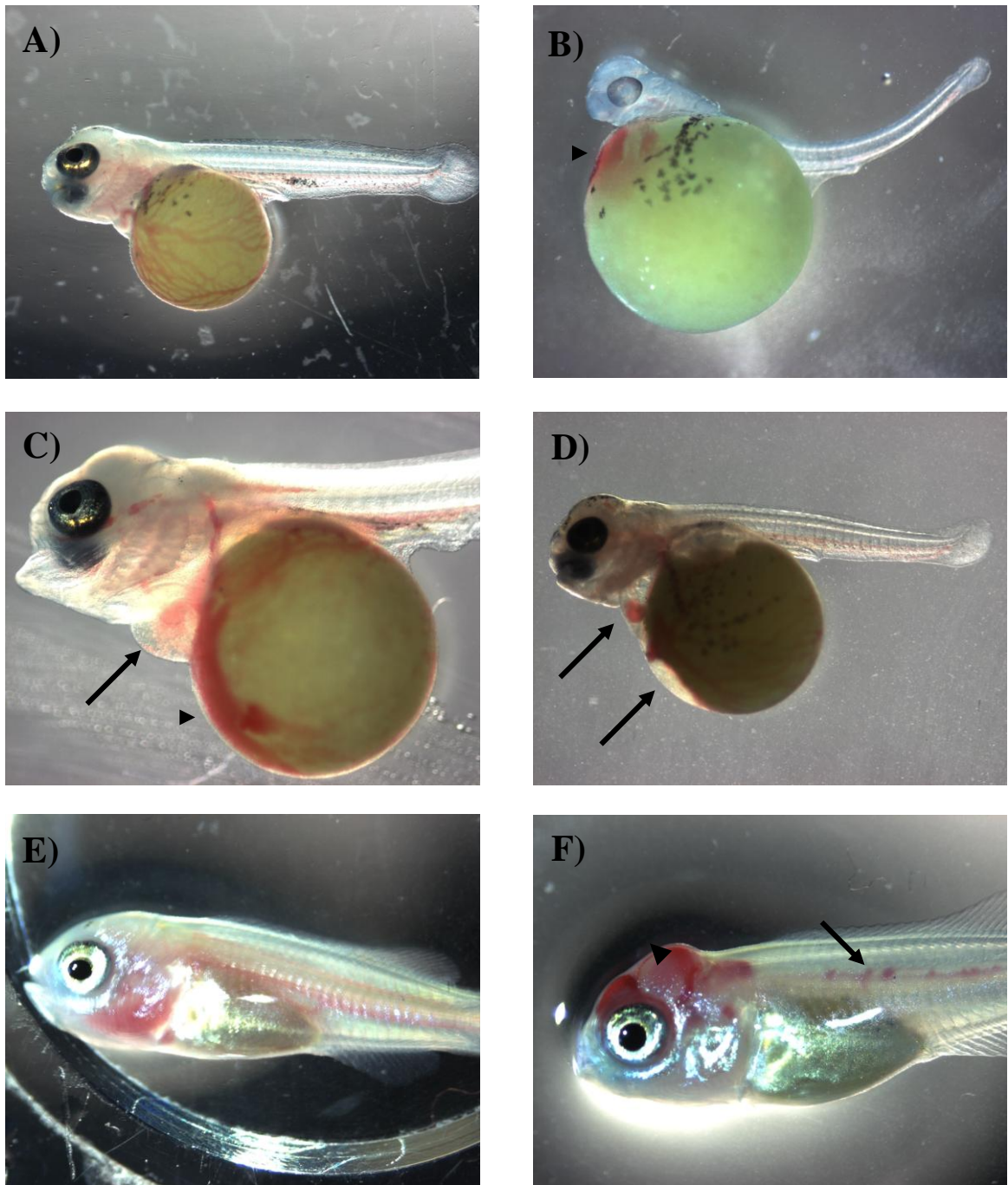
Figure 3. 14 Malformation during yolk-sac absorption period in Nile tilapia. **A)** Normal larvae at hatch in freshwater showing network of blood vessels associated with yolk-sac syncytium, **B)** Malformed larvae at hatch maintained in 17.5 ppt showing curvature of stunted tail and pericardial haemorrhaging (arrowhead), **C)** 2 dph larvae maintained in 20 ppt showing pericardial oedema (arrow) and haemorrhaging of blood vessels associated with the yolk-sac syncytium (arrowhead), **D)** 2 dph larvae maintained in 20 ppt with pericardial oedema, enlarged heart (arrow) and sub-epithelium oedema of the yolk-sac (arrowhead), **E)** Normally developing larvae at yolk-sac absorption maintained in freshwater, **F)** 8 dph larvae maintained in 20 ppt showing distortion of neurocranium

(arrowhead) and pooling of blood along spine (arrow).
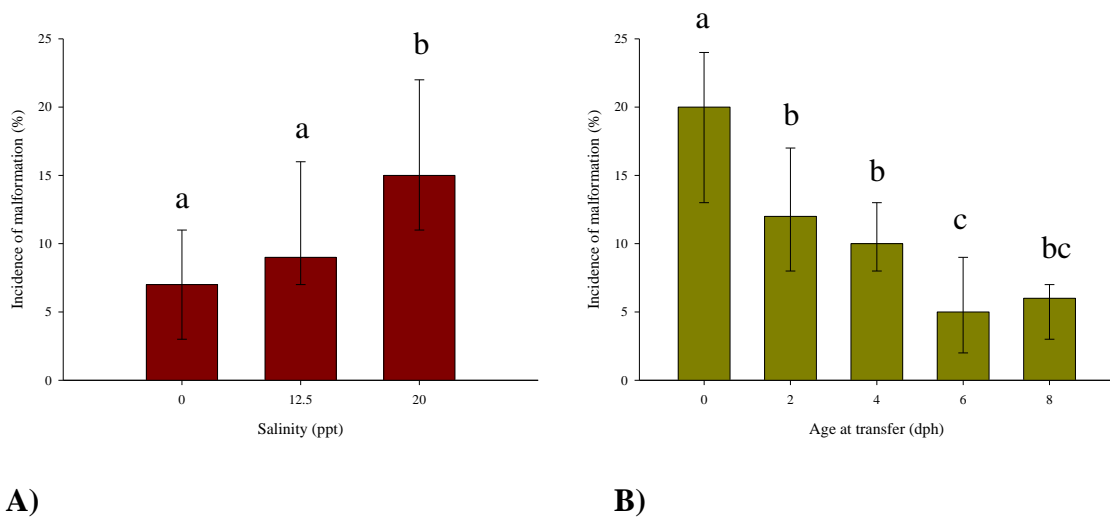
A) **B)**

Figure 3. 15 Overall effects of **A)** Salinity and **B)** Age on incidence of malformation (%). Statistical analysis, mean and 95% confidence limits were calculated on arcsine square transformed data. Different letters above each bar indicate significant differences (General Linear Model with Tukey's post-hoc pairwise comparisons; $p < 0.05$)

3.4 Discussion

3.4.1   Methodology

Osmolality is the measurement of the concentration of a solution in terms of osmoles of solute per kilogram of solvent (Osmol kg^{-1}). Whereas blood or plasma osmolality is commonly measured in adult fishes, where adequate amounts of blood can easily be obtained, it is generally unfeasible during early life stages of fishes, because of their small size (Yanagie *et al.,* 2009). Methods used to overcome these technical difficulties have often produced contradictory results.

Reports of the direct measurement of the ion content of individual eggs and larvae are scarce. Holliday and Blaxter (1960 a) were the first to report osmolar concentrations of individual eggs and yolk-sac larvae of the Pacific sardine (*Sardinops caerulea*) using a melting point apparatus (Gross, 1954; Giese, 1957), in which *c.* 1 μl of yolk or perivitelline fluid (PVF) was drawn into a capillary tube, rapidly frozen on dry ice then cooled in brine frozen to -10 °C. Time of thawing was plotted with a range of standard sodium chloride solutions and results expressed in molarities. This method was subsequently used by Lasker and Theilacker (1962) on eggs and yolk-sac larvae of the Pacific sardine (*S. caerulea*) and by Davenport *et al.* (1981) for eggs and yolk-sac larvae of the cod (*Gadus morhua*), in order to check reliability of the "egg squash" method described below. It is likely that this method was time consuming (due to the small number of single eggs or larvae used in these studies) although the range of osmolarities do suggest that this method produced standardised results. However, the advantages of using samples from individual larvae, in terms of significance of the data,

were clear leading to the use of the Nanolitre Osmometer, which used the freezing point depression method (Prager and Bowman, 1963; Kalber and Costlow, 1966; Frick and Sauer, 1973) requiring only a few drop of fluid . This method was subsequently used for osmolality measurements of eggs of cod (*G. morhua*) (Mangor-Jensen, 1987), eggs of chum salmon (*Oncorhynchus keta*) (Kaneko *et al.,* 1995) and larvae of sea bass (*Dicentrachus labrax*) (Varsamos *et al.,* 2001).

With the availability of this machine as a limiting factor, alternative methods were devised. Pooled samples were used with existing vapour pressure osmometers and, it would seem, techniques were developed accordingly. Lonning and Davenport (1980; p. 317) report 'a novel (if crude) "egg squash" technique' in which pools of eggs (50 – 200 eggs) of the long rough dab (*Hippoglossoides platessoides limandoides*) were blotted dry and compressed through the fine needle of a syringe into a glass vial which was then centrifuged for 2 min and the osmolarity of the supernatant was measured. This approach was subsequently used by the same authors on both freshly spawned eggs and whole yolk-sac larvae of the cod (*G. morhua*) (Davenport *et al.,* 1981) and on eggs and larvae of the lumpfish (*Cyclopterus lumpus*) (Kjorsvik *et al.,* 1984).

This method was subsequently adapted for measurement of whole-body osmolality of larvae of the Mozambique tilapia (*Oreochromis mossambicus*), with pooled larvae homogenised and then centrifuged and the resulting supernatant measured using a vapour pressure osmometer (Hwang and Wu, 1993; Wu *et al*., 2003). It was subsequently slightly modified by Yanagie *et al.* (2009), who squashed *O. mossambicus* larvae between Parafilm and measured the resulting tissue fluid also using a vapour

pressure osmometer.

In the present study, homogenates of whole larvae were used which obviously included yolk, blood and extracellular and intracellular fluids, therefore the effects of the contamination of these materials on yolk-sac larvae were tested. It had already been established by Yanagie *et al.* (2009) that blood plasma in juvenile *O. mossambicus* was equal to extracellular and intracellular fluids and the current study is in agreement that blood and plasma osmolality is equal to tissue fluid osmolality collected from muscle tissue in the juvenile Nile tilapia (*Oreochromis niloticus*). The effect of yolk materials on osmolality values was also tested in this study by compartmentalising larvae and measuring the osmolality of the body compartment (*i.e.* body minus yolk) and the yolk and no significant difference was found. Indeed, Lasker and Theilacker (1962) remarks that larval yolk is isotonic with the circulating body fluids concurring with Yanagie *et al.* (2009), who similarly concluded that yolk osmolality could represent blood osmolality in yolk-sac larvae of the Chum salmon (*O. keta*).

3.4.2   Ontogenic pattern of osmoregulatory capacity

This study is the first to consider the ontogeny of osmoregulatory capacity in a tilapiine species over a range of salinities. It is well established that unfertilised teleost eggs generally appear to be almost iso-osmotic with the blood and ovarian fluid of the mother (Holliday 1969) *e.g.* herring (*Clupea harengus*) (Holliday and Blaxter, 1960a; Alderdice *et al.,* 1979), plaice (*Pleuronectes platessa*) (Holliday and Jones, 1967), long rough dab (*Hippoglossoides platessoides limandoides*) (Lonning and Davenport, 1980), cod (*G. morhua*) (Davenport *et al.,* 1981; Mangor-Jensen, 1987), lumpfish (*C. lumpus*)

(Kjorsvik *et al.,* 1984) and Atlantic halibut (*Hippoglossus hippoglossus*) (Østby *et al*., 2000). This study confirms that newly extruded Nile tilapia eggs, prior to fertilisation, have the same osmo-concentration to that of the ovarian fluid and that of the tissue of the mother. Indeed, it has been recognised that marine teleost oocytes, prior to ovulation take up a large amount of water leading to swelling of 4 - 7 times resulting in a relative water content of 90 -92 % (Craik and Harvey, 1987; Østby *et al.*, 2000). Indeed, both prior to and post ovulation, the plasma membrane of eggs are relatively permeable to water and respond to changes in the ovarian fluid (Sower *et al.,* 1982) and they are therefore assumed to be iso-osmotic with maternal blood.

After spawning, fertilisation and activation of the egg results in cortical alveolar exocytosis, a process that causes imbibition of water from the external environment across the chorion to form the perivitelline fluid (PVF), blocking the micropyle and therefore preventing polyspermy (Yamamoto, 1944). Lonning and Davenport, (1980) report swelling to be complete at 24 h post-fertilisation, but may have ceased between 4 – 24 h in the eggs of the long rough dab (*H. platessoides limandoides*). Shanklin (1959) comments that the PVF of the egg, upon spawning, rapidly establishes equilibrium with the external media, and this is confirmed by Lasker and Theilacker (1962) in the developing eggs of the Pacific sardine (*S. caerulea*). Similarly, a rapid increase in osmolality after spawning into sea water is reported in newly extruded eggs in the Atlantic herring (*C. harengus*) (Holliday and Jones, (1965), the cod (*G. morhua*) (Davenport *et al.,* 1981), the long rough dab (*H. platessoides limandoides*) (Lonning and Davenport, 1980) and the lumpfish (*C. lumpus*) (Kjorsvik *et al.*, 1984). This could explain the abrupt decline in osmolality of eggs at 3 - 4 h post fertilisation into hypo-osmotic freshwater that is described in this study.

It has been demonstrated in this study that during embryogenesis, regardless of the external media, a constant osmolality is maintained, with no statistical differences observed in whole-body osmolality until 48 h post-fertilisation (Table 3.4.). Therefore the question arises, how do embryos maintain some sort of osmoregulatory control during the early stages of embryogenesis. At spawning the yolk is enclosed by a double membrane enclosing a thin layer of cytoplasm which concentrates on the animal pole forming a blastodisc. During gastrulation the peripheral cells of the morula begin to cover the yolk sac coinciding with the appearance of cutaneous mitochondria-rich cells (MRCs) *i.e.* on the epithelium of the body surface and yolk-sac of the developing embryo, thus marking the start of the selective restriction of ions and water transfer or active ionoregulation (Guggino, 1980a). The first appearance of MRCs on the yolk-sac epithelium of dechorionated freshwater maintained *O. mossambicus* embryos was reported at 26 h post-fertilization but no apical crypt was found until 48 h post-fertilization (Lin *et al.*, 1999). Similarly, Ayson *et al.* (1994) observed MRCs on the yolk-sac epithelium of *O. mossambicus* embryos at 30 h post-fertilization in both freshwater and seawater, but apical openings of MRCs were first observed at a low density at 48 h post-fertilization or half-way to hatching. The presence of functional MRCs therefore may offer some explanation for the ability of embryos, as demonstrated in this study, to maintain osmotic control *i.e.* to hyper-regulate in low salinity waters (*i.e.* freshwater and 7.5 ppt) and to hypo-regulate in elevated salinities (*i.e.* 12.5 – 20 ppt) at 48 h post-fertilisation following completion of epiboly. Whilst osmolality levels of embryos initially showed a rapid rise following transfer to hyper-osmotic environments, embryos still displayed some sort of regulative control, with the exception of embryos transferred to 25 ppt, which were unable to survive.

However, the only report of ontogenic changes in osmoregulatory ability in a tilapiine species maintained in freshwater to date describes contradictory results to those in the current study (Yanagie *et al.,* 2009). They report an increase in the osmolality of freshwater maintained *O. mossambicus* embryos from *c.* 300 mOsmol kg^{-1} on day of fertilisation to a maximal value of *c.* 370 mOsmol kg^{-1} at 3 days post-fertilisation, and then to decrease by hatching to 320 - 335 mOsmol kg^{-1}, remaining at this relatively constant level until 13 dph. These authors suggested that this increase in osmolality in a hypo-osmotic environment was due to an accumulation of metabolic products of yolk materials that the undeveloped kidney is unable to extrude, with the development of kidney and other organs from just before hatching onwards being responsible for the increasing ability to maintain stable osmolality levels. However, it is suggested here that the methodology used may be responsible for the contradictory results; eggs and yolk-sac larvae in the study of Yanagie *et al.* (2009) were simply squashed between Parafilm and the resulting 'squash' was not homogenised, as it was in previous studies and also in the current study and, therefore, may have given different results. In the present study, it was observed that inaccurate and varying results were obtained if the supernatant was not sufficiently mixed before sampling.

The effect of perivitelline fluid on overall osmolality measurement of eggs should be considered here. Lonning and Davenport (1980) recognised the drawbacks of the 'egg squash' method in the long rough dab (*H. platessoides limandoides*) which, although rapid and convenient, gave a mixture of PVF, yolk and, as development progressed, embryonic body fluids. In order assess the contribution of the different parts of the eggs, separate sub-samples of PVF and yolk were taken and osmolarities determined by the melting point method (Gross, 1954). They found that while osmo-concentrations of all

types of sample rose after spawning into seawater, both whole egg squashes and yolk osmolarity began to decline after 24 h, although not to the same levels *i.e.* yolk osmolarity declined to 396 mOmol kg^{-1} by day 11 post-fertilisation and whole egg squash declined to *c.* 650 mOsmol kg^{-1}. During this time osmolarity of the PVF remained similar to that of the surrounding water (*c.* 980 mOmol kg^{-1}). A similar pattern was reported by Kaneko *et al.* (1995) in their evaluation of the osmoregulatory ability of eyed-stage eggs of the chum salmon (*O. keta*) following transfer from freshwater to elevated salinities, describing an immediate increase in the osmolality of both PVF and embryonic blood at 3 h post-transfer, however, whilst levels in PVF osmolality remained high, blood levels began to drop gradually after 3 h but still remained higher than the freshwater control. In agreement, Mangor-Jensen (1987) reported a 20 % increase in yolk osmolality from values of 342 ± 5 mOsmol kg^{-1} to *c.* 420 mOsmol kg^{-1} in developing cod eggs (*G. morhua*) during the first 48 h of development, which by 6 days post-fertilisation had reverted back to initial values. It should be noted that the relative volume of PVF varies amongst species *e.g. c.* 18 % of total eggs of cod (*G. morhua*) volume after 1 - 2 days (Mangor-Jensen, 1987) to up to 80 % of total egg volume in eggs of long rough dab (*H. platessoides limandoides*) (Lonning and Davenport, 1980), so the influence of PVF in the 'egg squash' method, as used in this study, should be taken into account.

The current study reports a significant increase in osmoregulatory capacity upon hatching for larvae in freshwater and 7.5 ppt but a significant drop in osmoregulatory capacity for larvae reared in salinities of 12.5 ppt and above (Figure 3.5.). This pattern can be seen to be reflected in the overall effects of larval stage on osmoregulatory capacity in Figure 3.2.B. The regulative ability of larvae at hatch to maintain

osmoregulatory control has already been reported in other marine teleost species through measurement of body-fluid concentration *e.g.* Pacific salmon *spp.* (Weisbart, 1968), herring (*C. harengus*) (Holliday and Blaxter, 1960a), plaice (*P. platessa*) (Holliday, 1965; Holliday and Jones, 1967), Atlantic halibut (*H. hippoglossus*) (Riis-Vestergaard, 1982; Hahnenkamp *et al.,* 1993) and turbot (*Scophathalmus maximus*) (Brown and Tytler, 1993) and is likely to be related to the osmoregulatory ability conferred by extrabranchial MRCs that has already been discussed above. Therefore the abrupt rise in whole-body osmolality and a concomitant decrease in osmoregulatory ability in elevated salinities of 12.5 ppt and above reported in the present study at hatch is surprising. The difference in osmolality between the embryo prior to hatching (*i.e.* 48 h post-fertilisation) and that of the external media is similar for each treatment (*c.* 150-200 mOsmol kg^{-1}, except for 7.5 ppt which is *c.* 50 mOsmol kg^{-1}), which discounts the theory that larvae hatching into an environment with a larger difference in osmolality as compared to their whole-body osmolality would experience a greater osmotic shock which would, in turn, be reflected in their whole-body osmolality measurements. To answer this question, additional measurements should be made between 48 h post-transfer and hatching to identify whether whole-body osmolality continues to increase at a steady state rather than abruptly upon hatch.

Results from the present study illustrate that, once hatching occurs, osmolality levels begin to move towards a more constant range from 4 dph until yolk-sac absorption for all larvae both in freshwater and elevated salinities (7.5 − 20 ppt) suggesting an improvement in ability to osmoregulate as larvae develop. Indeed, Yanagie *et al*. (2009) reports a similar maintenance of osmolality at a relatively constant level for yolk-sac *O. mossambicus* larvae maintained in freshwater from hatch until yolk-sac absorption at

around 320 mOsmol kg^{-1}.

3.4.3   Abrupt transfer to elevated salinities

The short-term iono-regulatory responses of yolk-sac larvae to abrupt transfer to elevated salinities (7.5 – 20 ppt) were assessed. Preliminary trials for estimation of adaptation time in this study, as defined by whole-body osmolality measurements, showed larvae at all stages displaying a crisis followed by recovery period to reach a steady state after 48 h post-transfer. Results in other species have shown a similar pattern in body-fluid osmolality *e.g.* Mozambique tilapia (*O. mossambicus*) 48 h post-transfer from freshwater to 26 ppt for osmolality levels to reach original levels (Hwang and Wu, 1993), sea bass (*D. labrax*) a crisis and recovery period for 27 d larvae is reported after abrupt transfer from 25 ppt to 39.5 ppt and 5.3 ppt to reach a steady state by 48 h post-transfer (Varsamos *et al.,* 2001) and juvenile red drum (*Sciaenops ocellatus*) a stabilisation in blood osmolality levels occurs following direct transfer from sea water to freshwater after 96 h (Crocker *et al.,* 1983).

Ontogenic changes in salinity tolerance appear, in this study, to be related to developmental stage. Results suggest that abrupt osmotic challenge gave rise to different osmoregulatory responses which were dependant on the ontogenic stage of the larvae and, moreover, a gradual improvement in ability to osmoregulate occurs during ontogeny. Indeed this ability to maintain osmotic homeostasis is reflected in survival patterns of larvae following transfer; from 4 dph onwards, no significant difference is evident in survival between salinities. The study by Watanabe *et al.* (1985a) on the ontogeny of salinity tolerance in tilapia *spp.* (*e.g. Oreochromis aureus*, *O. niloticus* and

O. mossambicus x *O. niloticus* hybrid) spawned and reared in freshwater but transferred to elevated salinities (0 − 32 ppt) from 7 − 120 dph suggested that changes in salinity tolerance were more closely related to body size than chronological age, and was probably related to maturational events such as the functional development of the osmoregulatory system. Although the fish in that study were older than those used in the present study, it is still interesting to note that ontogenic physiological changes may confer osmoregulatory ability and salinity tolerance.

Therefore it is apparent that ontogenic changes occur in the osmoregulatory capacity of eggs and yolk-sac larvae of the euryhaline Nile tilapia. Osmolality levels of embryos immediately post-transfer to elevated salinities appear to be proportional to and directly related to the osmolality of the external media, but then drop to a more steady state during embryogenesis and yolk-sac period, suggesting that an ontogenic regulatory control is evident which is, in turn, reflected in larval ability to withstand transfer to elevated salinities.

3.4.4   Effects of salinity on larval malformation

In this study, there was a significant negative effect ($p < 0.05$) of increasing salinity on the occurrence of larval malformations during the yolk-sac period. A high incidence of larval abnormalities has been previously reported during early life stages of marine teleosts, when challenged with variations in salinity. Larvae of the navaga (*Eleginus nava*), polar cod (*Boreofadus saida*) and Arctic flounder (*Liopsetta glacialis*) exhibited a high incidence of malformation in low salinities (Doroshev and Aronovich, 1974), as did the Atlantic halibut (*H. hippoglossus*) (Bolla and Ottensen, 1998). Indeed, a lower

percentage of abnormalities in the newly hatched larvae of the pomfret (*Pampus punctatissimus*) was similarly reported at 29 – 30 ppt than either at < 25 ppt or > 40 ppt (Shi *et al.,* 2008) and, similarly, the percentage of deformities was significantly lower at 36 ppt than at either lower (24 – 33 ppt) or higher (36 - 42 ppt) salinities in the Japanese eel (*A. japonica*) (Okamoto *et al*., 2009). These results would therefore seem to suggest that, once the incubation and rearing salinity moves away from that which is encountered in nature, detrimental effects become more pronounced, a trend that is apparent in the current study.

It is clear from this study that there also exists a significant effect of ontogeny on the incidence of malformation during the yolk-sac period. The reported development of the branchial system and the appearance of branchial MRCs would appear to confer an increasing osmoregulatory capacity which is apparent in the pattern of survival in elevated salinities following hatch. This appears to be reflected in an increasing ability to maintain ionic and osmotic balance and the observed reduction of pericardial and sub-epithelial oedema as yolk-sac larvae develop. In agreement, oedema is not observed in zebrafish larvae after exposure to contaminants if exposure is delayed during ontogeny suggesting that larvae are particularly vulnerable shortly after hatching (Belair *et al.,* 2001).

Haemorrhaging and pooling of blood during yolk-sac stages appears to be linked to oedematous build up in the current study. It is possible that oedema may compress the delicate blood capillary network on the yolk-sac syncytium, and have a damaging, systemic effect on whole larvae by impairing circulation. It has been suggested that

alteration in overall shape of kidney in the zebrafish larvae may be a consequence of compression by oedema (Hill *et al.,* 2003).

Interestingly, it has previously been reported that lower salinites tend to increase the occurrence of pericardial oedema during early life stages in marine species. Lasker and Theilacker (1962; p. 30) make the first reference to abnormalities in a teleost fish, the Pacific sardine (*S. caerulae*), with embryos in distilled water displaying 'a somewhat enlarged yolk-sac sinus' and, when transferred at hatch to distilled water, experience a swelling and bursting of the brain area. In addition, Doroshev and Aronovich (1974) describe a higher incidence of pericardial oedema at low salinities in the navaga (*Eleginus nava*), polar cod (*Boreofadus saida*) and Arctic flounder (*Liopsetta glacialis*) and Kjorsvik *et al.* (1984; p. 319) describe 'considerable embryonic irregularities' in lumpfish embryos (*C. lumpus*) after only 24 h incubation at lower salinities. Moreover, in larvae of the Japanese eel (*A. japonica*), a higher proportion of pericardial oedema was reported at lower salinites (24 - 33 ppt) with no evidence of severe pericardial oedema at 42 ppt (Okamoto *et al.,* 2009). Indeed, in freshwater, the cellular and extra-cellular fluids of eggs and larvae are hyper-osmotic to their environment and therefore undergo an osmotic gain of water and a diffusional loss of ions. It would, therefore, be anticipated that early stages, with a limited capability to osmoregulate, would indeed be unable to maintain an osmotic balance in the face of increased water flux and water would accumulate as oedematous fluid. However, in the present study, such abnormalities occur in larvae challenged with both iso-osmotic conditions (12.5 ppt) and hyper-osmotic conditions (12.5 - 20 ppt). A possible explanation is that, as mentioned above, once conditions move away from that which is naturally faced, then the organism will encounter difficulties in maintaining homeostasis.

It is true that embryos and larvae have been widely used in experimental toxicity studies because of their sensitivity during early life stages (Andreasen *et al.,* 2002) and there are numerous reports of the occurrence of embryonic and larval malformations occurring naturally in contaminated areas (von Westernhagen *et al.,* 1988). Villalobos (1996) reports a clear correlation between exposure to toxic compounds and occurrence of oedematous larvae in the Medaka (*Oryzias latipes*). Moreover, similar effects of sub-lethal and lethal levels of ammonia and nitrite (*i.e.* sub-epithelial oedema of the yolk-sac, and non-specific haemorrhaging of blood vessels of the yolk-sac syncytium) to those of salinity in the present study have been reported in the yolk-sac larvae of *O. niloticus* (Rana, 1988). In addition, histo-pathological changes in the gills of 9 dph *O. niloticus* were also evident *i.e.* oedema of filaments and secondary lamellae, hyperplasia and inter-lamellar fusion following sub-lethal ammonia concentrations of 6.2 mg l^{-1} (Rana, 1988) and in *O. mossambicus* (Subasinghe, 1986). To further expand this idea, the study by Hill *et al*. (2003) on the effects of exposure of early stage zebrafish to the contaminants Polychlorinated dibenzo-*p*-dioxins (PCDDs) offers insights into the potential causes of oedema. They proposed a model which combined the negative impacts of the contaminant on the epithelium during early life stages, leading to the build up of oedema, and the resulting organ compression leading to decreased kidney and circulatory function as ontogeny progresses (see Figure 3.16.). They conclude that this model also predicts that many different types of stresses, within which salinity must be included, might lead to the same outcome, and this therefore offers a possible explanation of what is happening in this study.
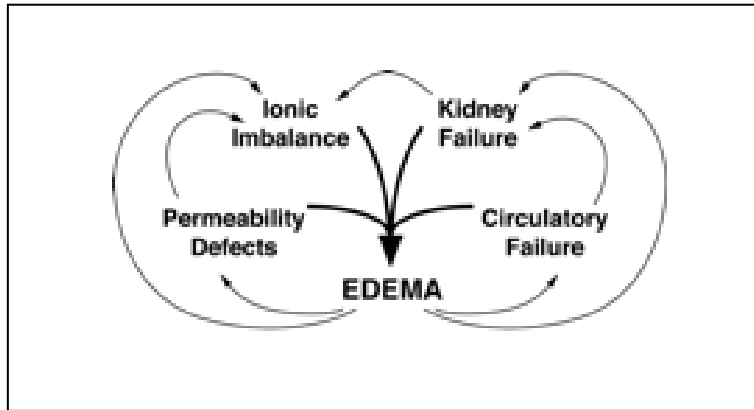
Figure 3. 1 Model of proposed positive feedback loop through which stresses can lead to irreversible oedema (= edema). Adapted from Hill *et al.,* (2003).

To conclude, assessment of whole-body osmolality has provided a method that has allowed an evaluation of the osmoregulatory status during the early life stages of the Nile tilapia; these measurements appear to offer valuable insight into the emerging pattern of the adaptive capacity to hypo- and hyper-regulate during ontogeny. The failure of yolk-sac larvae to maintain a viable osmotic balance, when challenged with hyper-osmotic conditions, are in turn reflected in an increase in larval mortality and incidence of malformation following salinity challenge.

4 Chapter 4 Effects of salinity on embryogenesis, survival and growth in embryos and yolk-sac larvae of the Nile tilapia

4.1 Introduction

4.1.1 Salinity tolerance of the Nile tilapia and its relevance to aquaculture

Tilapiine fishes, despite being freshwater species, display an ability to tolerate a broad range of naturally occurring variations in environmental salinities (Philippart and Ruwet, 1982). As has already been outlined in Section 1.1.5., relatively few species of aquacultural interest offer a potential for culture in waters of elevated salinity. With increasing pressure on freshwater resources, the ability to withstand and adapt to variations in environmental salinity is a vital factor when choosing a euryhaline species for aquaculture, especially during the sensitive early life stages. Investigations into salinity tolerance of tilapiine fish include both basic research on the physiology of osmoregulatory capacity and more practical research into aquacultural practices. These applied approaches to investigating the salinity tolerance of the Nile tilapia are summarised in Table 4.1.

Table 4. 1 Summarised data on salinity tolerance of the Nile tilapia (*Oreochromis niloticus*)

Reference	Source of fish	Stage/size	Range (ppt), Temp. (°C) and duration	Acclimation régime	Performance and Optimum salinity	Parameters measured
Reproductive performance						
Watanabe and Kuo, 1985	Broodstock from TFRI [a]	Broodstock. Mean initial wt.: 2-3 year broodstock 99 – 277 g; 1 year-old broodstock 12.6 – 18.8 g.	0 – 32 ppt. 24 – 31 °C. 140 days	**Gradual transfer:** 2-3 year old broodstock kept in freshwater; 1 year-old group had gradual acclimation from freshwater to 32 ppt at rate of 5 ppt/day, followed by direct reduction of salinity to 5, 10, and 15 ppt .	Spawning observed in all salinies in 1 year-old group from freshwater to 32 ppt however normal reproduction was inhibited with increasing salinity. Higher total number of spawnings in 5, 10 and 15 ppt than 32 ppt or freshwater; mean number of eggs per spawning or per gram body weight similar in all salinities. Optimum salinity: up to 15 ppt.	Reproductive performance of broodstock monitored throughout experiment *i.e.* # spawnings, # eggs/spawning and per female per g body weight.
Fineman-Kalio, 1988	Broodstock from Philippines	Broodstock Mean initial wt. 2.8 g	Rising from 25 to 50 ppt. 14.8 – 34 °C. 120 days	**Gradual transfer:** Initial acclimation from 0 to 25 ppt carried out at rate of 5 ppt/day. *Note* during experiment, salinity in ponds rose from 25 to 50 ppt.	Spawning observed at all salinities below 30 ppt but inhibited above. At end of experiment 95 % gravid females but no spawning occurred.	20 % protein diet fed at 5 and 3 % of total fish biomass; after 120 days gonads of females examined for reproductive performance.
El-Sayed *et al.*, 2003	Juveniles obtained from native Egyptian stocks	Broodstock Mean. wt. of broodstock 25.7 g	0 – 14 ppt. 30 °C. 195 days	**Gradual transfer:** Gradual acclimation of broodstock from freshwater to experimental salinities of 7 and 14 ppt over 7 – 10 days before start of experiment.	Spawning occurred at all salinities and no adverse effect on size at first maturation or spawning interval was observed at 40 % dietary protein. Fecundity significantly lower for fish reared in 7 and 14 ppt even at highest protein ration (40 %). Spawning performance better in freshwater than 7 and 14 ppt.	Reproductive performance monitored throughout experiment with combination of varying water salinity and different protein levels of broodstock diets e.g. 25 and 40% protein.
Stage: Eggs						
Watanabe and Kuo, 1985	Broodstock from TFRI [a]	Eggs	0 - 32 ppt. 24 – 31 °C	Eggs removed from brooding females in 0, 5, 10, and 15 and 32 ppt at 1 -2 days post-spawning and incubated at equivalent salinity.	Very low hatching success for eggs spawned at 32 ppt with deformed larvae; hatching success higher for eggs spawned at 5 ppt (54.2%) than freshwater (30.9%) or 10 (32.7%) and 15 ppt (36.9%).	Hatching rate (%) and deformity.

Table 4.1. cont.

Reference	Source of fish	Stage/size	Range (ppt), Temp. (°C) and duration	Acclimation régime	Performance and Optimum salinity	Parameters measured
Stage: Eggs						
Watanabe *et al,* 1985 b	Broodstock from TFRI[a]	Eggs	0 – 32 ppt 27.2 – 31.5 °C	**Direct transfer:** Freshwater-spawned eggs removed from female at 1 day post-spawning and transferred directly to experimental salinities 0, 5, 10, 15, 20, 25, 32 ppt for artificial incubation. Hatching occurred at 3 days post-spawning and yolk-sac absorption at 6 – 7 days post-hatch.	No hatching at 32 ppt; similar hatching rate for 0 – 15 ppt with mortality during incubation increasing with higher salinities. Structural abnormalities and under-development of organs observed at higher salinities.	Hatching rate (%) and deformity.
El-Sayed *et al.*, 2003	Broodstock obtained from native Egyptian stocks	Eggs	0 – 14 ppt 30 °C	Eggs removed from brooding females held in experimental salinities of freshwater, 7 and 14 ppt and incubated at equivalent salinity.	Hatching rate significantly higher for eggs of broodstock held in freshwater than 7 and 14 ppt and fed low protein diets (25% protein) , but comparable to hatching rates of eggs held in 7 and 14 ppt fed high protein diets (40% protein). Time to hatch and yolk-sac absorption longer in eggs from broodstock held in 7 and 14 ppt and fed 25 % protein diet.	Hatching success, time to hatch and time to yolk-sac absorption.
Stage: Fry						
Watanabe *et al.,* 1985 b	Broodstock from TFRI[a]	<u>Exp.1</u>; Fry 7 days post-hatch	0 – 32 ppt	**Gradual transfer:** Freshwater-spawned eggs removed from female at 1 day post-spawning and transferred directly to experimental salinities of 0, 5, 10, 15, 20, 25, 32 ppt for artificial incubation and resulting hatched fry transferred to varying test experimental salinities of 0, 5, 10, 15, 20, 25 and 32 ppt at 7 days post-hatch.	Increased salinity of incubation and early rearing increased salinity tolerance upon subsequent transfer *i.e.* MLS-96 of freshwater incubated eggs and reared fry was 19.2 ppt whereas MLS-96 of eggs incubated and fry reared in 10 ppt was 25 ppt and MLS-96 of eggs incubated in 20 and 25 ppt was > 32 ppt.	Survival index *i.e.* **MLS-96** salinity at which survival falls to 50% 96 hours following direct transfer from pre-exposed salinity to test salinities.
' '	' '	<u>Exp.2</u>; Fry 6 – 7 days post-hatch	0 – 32 ppt	**Direct transfer:** Broodstock maintained in experimental salinities of 0, 5, 10 and 15 ppt. Eggs were removed from mouth at 1 day post-spawning and artificially incubated at equivalent salinity of spawning until 6-7 days post-hatch followed by direct transfer to test salinities of 0,7.5, 15, 17.5, 20, 22.5, 25, 27.5, 30 and 32 ppt.	Increasing MLS-96 with increasing spawning salinity *i.e.* eggs spawned at 5 ppt showed MLS-96 of 28.1 ppt, eggs spawned at 10 ppt showed MLS-96 of 32 ppt and eggs spawned at 15 ppt showed MLS-96 > 32 ppt.	**MLS-96** (*as above*).

117

Table 4.1. cont.

Reference	Source of fish	Stage/size	Range (ppt), Temp. (°C) and duration	Acclimation régime	Performance and Optimum salinity	Parameters measured
Stage: Fry cont.						
Watanabe *et al.,* 1985 b	Broodstock from TFRI [a]	<u>Exp.3</u>; Fry 12 – 18 days post-hatch	0 – 32 ppt	**Gradual transfer:** Fry from freshwater maintained broodstock transferred directly at 4 – 10 dph to experimental salinities of 5, 10, and 15 ppt and after 7-8 days following acclimation again transferred to full-strength sea-water *i.e.* 32 ppt.	Increasing salinity of pre-acclimation increased **MST** or salinity tolerance to full strength seawater.	Mean survival time (**MST**) *i.e.* mean survival time over 96 h following direct transfer from salinity of pre-exposure to full sea-water (32 ppt).
Watanabe *et al.,* 1985 a	Broodstock from TFRI [a]	Fry to fingerling, 7-120 dph.	0 – 32 ppt 24 – 32 °C Variable	**Direct transfer:** Direct transfer of varying aged fry and fingerlings from freshwater to experimental salinities of 5, 15, 17.5 20, 22.5, 25 27.5 30 and 32 ppt.	Salinity tolerance increased with age; mean MLS-96 values from 7 – 120 days post-hatch were 18.9 ppt. MST complete mortality ranging from 52 mins to 200 mins post-transfer and 50% survival times ranging from 23 mins to 105 mins.	Various survival *i.e.* **MLS-96** as above, Mean Survival time (**MST**) as above and Median Survival time (**ST$_{50}$**) time at which survival fall to 50% following transfer to 32 ppt.
Villegas, 1990	Broodstock from stocks of Taiwan-Singapore	Fry and fingerlings, 1-90 dph	0 – 32 ppt 24 -31°C Variable	**Direct transfer:** Direct transfer of varying aged fry and fingerlings from freshwater to 10, 15, 20, 25 and 32 ppt.	Time of death following transfer increasing with age; 100 % mortality for all ages transferred directly to 32 ppt. Salinity tolerance related to age and body size. Optimum salinity: 15 ppt for direct transfer at all ages.	Survival indices *i.e.* mortality.
El Sayed *et al.*, 2003	Broodstock obtained from native Egyptian stocks	Fry Initial wt. 12 – 16 mg	0 – 14 ppt 30 °C 30 days	Fry obtained from broodstock held in experimental salinities of 7 and 14 ppt.	Larval growth reduced (p < 0.5) in 7 and 14 ppt compared to 0 ppt.	Growth and feed utilisation efficiency of fry.
Stage: Fingerlings and juveniles						
Al-Amoudi, 1987	Broodstock originating from Stirling, Scotland	Fingerlings Mean initial wt. 4 g	0 - 32 ppt 26 – 28 °C 2 days	**Gradual transfer:** Exp.1: direct transfer from freshwater to 18 ppt for 48 hours then gradual acclimation to 27 ppt and 36 ppt**.** **Direct transfer:** Exp.2: direct transfer from freshwater to 18, 21.6, 23.4, 25.2, 27, 28.8 and 30.6 ppt.	Exp 1: 100 % survival for fish gradually transferred to 36 ppt after 4 days acclimation in 18 ppt and 4 days acclimation in 27 ppt. Exp.2: Able to tolerate direct transfer to 18 ppt without mortality, 30% mortality at 21.6 ppt ,81.7% mortality at 23.4 ppt and 100% mortality in higher salinities.	Survival 2 days post- transfer

118

Table 4.1. cont.

Reference	Source of fish	Stage/size	Range (ppt), Temp. (°C) and duration	Acclimation régime	Performance and Optimum salinity	Parameters measured
Stage: Fingerlings and juveniles (cont.)						
Avella *et al.,* 1993	2 strains of *O. niloticus* from Ivory Coast: 'lab strain' and 'field strain'	Juvenile Mean wt. 30 g	0 - 30 ppt 27 °C Direct: 6-9 days; gradual: 13 days	**Direct transfer:** 'fast challenge' *i.e.* 2 steps:freshwater control to 20 ppt (2 days) to 30 ppt (4-7days). **Gradual transfer:** 'progressive challenge' *i.e.* 2 steps: freshwater control to 10 ppt (6 days) to 20 ppt (7 days).	'field strain' progressive challenge showed 65% mortality, and 'fast challenge' showed 100% mortality; 'lab. strain' progressive challenge showed no mortality, and 'fast challenge' showed 25 % mortality. Inter-species variation apparent.	Survival (%) at end of challenge.
Likongwe *et al.,* 1996	Fry from Alabama, US.	Fingerlings Av. wt. 4.6 – 4.83 g	0 - 16 ppt 24 – 32 °C 56 days	**Gradual transfer:** Gradual acclimation from freshwater at a rate of 2 ppt/day to 0, 8, 12, 16 ppt before start of experiment	Increase in salinity generally inhibited growth. At 32 °C and 16 ppt fish developed body lesions. Comparable growth rates at 28 or 32 °C in 0, 8 and 12 ppt.. Optimum: Highest FCR at 32 °C and 8 ppt.	Combined effects of salinity and temperature (24, 28 and 32 °C) on growth and feed utilisation monitored.
Lemarie *et al.,* 2004	Broodstock (Bouake strain) from Ivory Coast	Juveniles Initial wt. 5 – 20 g	0 - > 70 ppt 28 °C Variable	**Gradual transfer:** Daily increments of salinity of 2, 4, 6, 8, 10,12 and 14 ppt from freshwater	MLS was 46.3 ± 3.5 ppt for daily increases of 2 to 8 ppt decreasingly significantly (P < 0.5) above this level. Optimum: daily increment of 8 ppt/day	Index of salinity resistance = Median Lethal Salinity (**MLS**) defined at each daily increment rate as salinity at which 50% of fish died.
Kamal and Mair, 2005	2 pure strain *O. niloticus* originating from GIFT project and Fishgen-selected (N2) Philippines	Juveniles	0 – 30 ppt On-growing for 75 days	**Gradual transfer:** Gradual acclimation of 5 ppt every 2 days to 0, 7.5, 15, 22.5 and 30 ppt before start of experiment	Higher growth at lower salinites than higher salinities or freshwater. Optimal < 15 ppt.	Survival, growth, FCR and biomass gain/cage over experimental period
Ridha, 2006	Non-improved (NS) Nile tilapia from Florida and (GIFT) from Philippines	Juvenile to adult	37 – 40 ppt 29 ± 2 °C . 34 days	**Gradual transfer:** Salinity increased from freshwater to full-strength seawater (37 – 40 ppt) at 2-3 ppt day	Both strains able to survive in seawater (37-40 ppt) displaying 89% > survival but reduced growth, FCR and skin lesions with higher salinities. Gift fish showed better performance in full strength seawater for all sizes than NS strain. Optimum salinity: Brackish water < 20 ppt.	2 acclimation régimes and 3 sizes of fish: Survival (%), mean body weight, daily growth rate (DGR), specific growth rate (SGR) and feed conversion rate (FCR).

Table 4.1. cont.

Reference	Source of fish	Stage/size	Range (ppt), Temp. (°C) and duration	Acclimation régime		Performance and Optimum salinity	Parameters measured
Stage: Adult							
Lotan, 1960	*Broodstock* from Israel	Adult 30 – 50 g	0- 150% seawater 24 h	**Direct transfer:** Exp.1: Freshwater to 30 , 40, 50, 60 and 70% seawater	**Gradual transfer:** Exp.2: gradual increase to 148% seawater	Exp.1: 100 % mortality at direct transfer to 80% seawater, 100% survival after 24 hours at 30 – 50 % seawater. Exp.2: Fish can withstand up to 150% seawater after gradual acclimation. Optimum salinity: Direct transfer 60-70 % seawater	Survival after transfer .
Kabir Chowdhury *et al.,* 2006	Sex-reversed all male fry of Chitralda strain	Adult Mean initial wt. 144 g	8 - 25 ppt 30 °C 88 days	**Gradual transfer:** Freshwater fish gradually acclimated to experimental salinities of 8, 15 and 25 ppt at rate of 5 ppt/day before start of experiment		Survival significantly reduced with increasing salinity; significant mortality at 15 and 25 ppt. SGR not significantly affected (p < 0.05) yet overall biomass growth significantly affected (p < 0.05) by salinity. Optimum performance salinity 8 ppt declining at or above 15 ppt.	Survival, growth and FCR monitored at end of experiment.

[a] TFRI Taiwan Fisheries Research Institute

4.1.2   Effects of salinity on reproductive performance of tilapia *spp.*

The principal aim of research into the effects of salinity on seed production on suitable Tilapiine species was to establish an appropriate balance between minimising freshwater requirements by maintaining broodstock at elevated salinities, whilst still producing seed at a commercially viable level. With experimental evidence on the reproductive performance of tilapias at various salinities lacking, Watanabe and Kuo (1985) undertook the first research with Nile tilapia (*O. niloticus*) broodstock under laboratory conditions. Spawning was observed in all salinities up to full strength seawater, but, salinity above 15 ppt was found to have an inhibitory effect on both seed production and hatching success. Interestingly, mean hatching success was considerably higher for females spawning in salinities of 5 ppt (54.2 %) than in freshwater (30.9 %).

Further studies by Watanabe *et al*. (1989) on the effects of salinity on the reproductive performance of the *O. mossambicus* x *O. hornorum* hybrid or Florida Red tilapia (see Section 1.1.5.5.) suggested that, while egg production and spawning were feasible in this fish at all salinities up to 36 ppt, a similar inhibitory effect of salinity on reproductive performance was found at 18 ppt and above, reflected in a marked decline in both fertilisation and hatching success. Nevertheless, in contrast to *O. niloticus*, viable yolk-sac fry were still produced at salinities as high as 36 ppt, suggesting the suitability of culture of this hybrid in areas where low salinity water is lacking may be practical, therefore broadening the scope of culture of this hybrid. Subsequent research (Ernst *et al.,* 1991) attempted to further define the variations in seed production of the Florida Red tilapia in salinities less than 18 ppt. A comparison of the reproductive performance of year class 1 broodstock held in low salinity (5 ppt) and brackish water (15 ppt) was made; seed production was amongst the highest reported for tilapia *spp.* in

121

the low salinity (5 ppt), whilst seed production in brackish water (15 ppt) was still within reported ranges for both fresh and low-salinity tilapia culture hatcheries. The lower seed production in brackish water as compared to low-salinity was due to both a smaller proportion of brooding females at any one time and a smaller average clutch size. Smaller clutch size suggested either lower numbers of eggs per spawn or a lower fertilisation success and fry survival at the higher salinity, in agreement with the findings of Watanabe and Kuo (1985) and El-Sayed *et al.* (2003) in the Nile tilapia.

4.1.3   Ontogeny of salinity tolerance in tilapia *spp*.

Research carried out into the development of seawater acclimation methods during the early hatchery phase of production of tilapia *spp*. that minimise the requirement of freshwater, has focused specifically on two areas; the influence of spawning and incubation salinity on hatchability and growth during early life stages and the influence of timing of transfer on subsequent culture performance.

4.1.3.1   The influence of spawning and incubation salinity on hatchability and growth during early life stages

The early approach to saline water culture of tilapia was to produce seed and juveniles in freshwater and then on-grow in brackish water. Therefore initial research (Watanabe *et al.,* 1985 a) was carried out to study the ontogeny of salinity tolerance of various *Oreochromis* spp. and the varying effects of age or size of fry (7 – 120 dph) at transfer on subsequent survival and growth, in order to allow culturists to implement transfer at the earliest possible time. The advantages of early salinity exposure to reduce freshwater requirements were evident, and further work with Nile tilapia (Watanabe *et*

al., 1985 b) showed that progeny spawned in waters of elevated salinity displayed higher survival indices than progeny spawned in freshwater and hatched in elevated salinities. In addition, progeny spawned in freshwater and hatched at elevated salinities exhibited a higher salinity tolerance than those spawned and hatched in freshwater but acclimatised at an elevated salinity at a later stage (see Table 4.1).

Further studies to test the hypothesis that early salinity exposure through spawning and hatching under elevated salinities could increase the salinity tolerance of Florida red tilapia fry were carried out (Watanabe *et al.,* 1989 a). Growth of fry (mean wt. 1.57 g) spawned and sex reversed at 4 and 18 ppt was compared upon transfer to rearing salinities of 18 and 36 ppt. SGR was higher for progeny spawned and hatched in 18 ppt with no significant difference observed between 18 and 36 ppt as compared to SGR of progeny spawned and hatched in 4 ppt and reared under 18 and 36 ppt.

In an attempt to assess relative performance under practical culture conditions, growth of juvenile Florida Red tilapia (mean wt. 0.98 g) spawned and sex reversed at salinities of 2 and 18 ppt were compared at 36 ppt in outside pools. When temperatures fell below 25 °C, growth and survival was significantly higher amongst progeny spawned at 18 ppt, suggesting Florida Red tilapia spawned and reared through early development in brackish water have an improved resistance to cold-stress in sea water (Watanabe *et al.*, 1989 b).

4.1.3.2 The influence of timing of transfer and method of transfer to increased salinities on subsequent culture performance

Optimal age or size at transfer to elevated salinities is critical in order to allow minimisation of freshwater requirements whilst still maximising growth and survival. Ontogenic variation in salinity tolerance and therefore age at transfer affected culture performance and, indeed, a trend towards increased salinity tolerance with age was seen to exist with Florida red tilapia fry. Survival indices displayed an improved tolerance following transfer from 40 days post-hatch onwards, suggesting that a more premature transfer from spawning and early rearing salinity to higher salinities for grow-out could significantly impair survival in the Florida red tilapia (Watanabe, 1990). Further research into effects of transfer régime highlighted the importance of a pre-acclimation period to a lower salinity before transfer to a higher salinity on subsequent survival of fingerlings and juvenile Nile tilapia (Al-Amoudi, 1987; Avella *et al.,* 1993; Lemarie *et al.,* 2004 (see Table 4.1).

4.1.4 Effect of salinity on metabolic burden

Oxygen consumption has been used as an indirect indicator of rate of metabolism in fishes (Cech, 1990) and consumption rates, in response to variations in environmental salinities, have been employed in an attempt to assess the energetic costs of osmoregulation in a wide range of teleost species. Unfortunately, results appear contradictory and have often led to confusion (Swanson, 1998). The assumptions that metabolic rates are lowest at iso-osmotic salinities because of minimal osmoregulatory costs and that the extra oxygen consumed in increasingly non iso-osmotic media is proportional to the increase in osmoregulatory requirements can be supported by studies carried out in juvenile and adult teleosts *e.g.* Nile tilapia (*Oreochromis*

niloticus) (Farmer and Beamish, 1969), rainbow trout (*Oncorhynchus mykiss*) (Rao, 1968), sea bream (*Sparus sarba*) (Woo and Kelly, 1995) and O*reochromis mossambicus* x *Oreochromis hornorum* hybrids (Febry and Lutz, 1987). However, contrary results have also been reported by Morgan and Iwama (1991) in the juvenile rainbow trout (*O. mykiss*) and Chinook salmon (*Oncorhynchus tshawytscha*) describing a lower oxygen consumption in freshwater with increasing consumption in increasing salinity. In tilapiine species, Job (1969 a and b) describes a higher oxygen uptake in 12.5 ppt than in either fresh water or 100 ppt seawater in *O. mossambicus,* whereas Ron *et al*. (1995) reports a significantly (p < 0.05) lower oxygen consumption in 20 month old *O. mossambicus* reared in seawater than in freshwater. Iwama *et al*. (1997) similarly demonstrated lower oxygen consumption rates in *O. mossambicus* acclimated to sea water as compared to fresh water and hyper-saline water (1.6 x sea water).

Variations in oxygen consumption relative to external salinity have also been reported for teleost embryos and larval stages. No salinity-related differences in oxygen consumption rates have been observed in embryos and larvae of the Pacific sardine (*Sardinops caerula*) (Lasker and Theilacker, 1962), embryos and larvae of the herring (*Clupea harengus*) (Holliday *et al.,* 1964), embryos of the grubby (*Myoxocephalus aenaeus*) and longhorn sculpin (*Myoxocephalus octodecemspinosus*) (Walsh and Lund, 1989), embryos and larvae of the striped mullet (*M. cephalus*) (Walsh *et al*., 1991 a), embryos and yolk-sac larvae of the milkfish (*Chanos chanos*) (Walsh *et al.,* 1991 b), embryos and alevins of Rainbow trout (*O. mykiss*), Chinook salmon (*O. tshawytsha*) (Morgan *et al.,* 1992) and hatch to 35 day old fry in the Nile tilapia (*O. niloticus*) (De Silva *et al.,* 1986).

In general, these discrepancies may be due to limitations in accurately estimating osmoregulatory costs due to both methodological and physiological factors (Swanson, 1998). They include a lack of standardisation in methods or systems of oxygen measurement as well as inconsistency of acclimation régimes that often result in the confounding effect of stress, often combined with variations in age and size of species investigated. In this study, oxygen consumption rates of individual larvae, and individual dry weight and standard length, were monitored in order to give a full picture of the energetic costs of salinity during early life stages.

4.1.5   Aims of the chapter

It has been demonstrated in Chapter 3 that ontogenic variation exisst in osmoregulatory capacity during early life stages of the Nile tilapia. Therefore, in this chapter, the following areas were tested; whether the developmental stage of embryos and yolk-sac larvae combined with varied acclimation conditions influences their ability to withstand transfer to elevated salinities.

The following aspects were investigated:

- The effects of timing of transfer of freshwater spawned eggs to rearing salinities (range 0 - 32 ppt) on embryonic viability.

- The effect of varying rearing salinities (range 0 - 25 ppt) on embryonic development rates, and dry weight and embryonic survival at hatch.

- The effect of salinity (range 0 - 25 ppt) on yolk-sac absorption, growth and survival of larvae until yolk-sac absorption.

- The influence of salinities (range 0 - 25 ppt) on the metabolic burden of larvae during yolk-sac period.

4.2 Materials and methods

4.2.1 Broodstock care, egg supply and artificial incubation systems

Broodstock were maintained as outlined in Section 2.1.1. and eggs were obtained by the manual stripping method outlined in Section 2.1.2. Preparation of experimental salinities and artificial incubation of eggs and yolk-sac fry were carried out as detailed in Sections 2.2 and 2.3.

4.2.2 Egg dry weight

For each spawning, immediately post-fertilisation, 30 eggs were randomly sampled from each batch, rinsed in distilled water, placed on a pre-weighed foil and oven dried at 60 °C for 24 h, followed by desiccation for 3 h. Measurements were made to the nearest 0.1 mg on an Oxford G21050 balance and mean dry egg weight (mg) was calculated.

4.2.3 Experiment 1. The effect of salinity on egg viability

Due to the asynchronous spawning nature of Nile tilapia, simultaneous batches of eggs at precisely the same developmental stage could not be obtained so three separate trials were run, each with an individual batch of eggs. Eggs from a freshly stripped batch of eggs were fertilised with freshly stripped milt (3 replicates per batch with 40 eggs per replicate) and were exposed to elevated salinities (0, 7.5, 15, 20, 25 and 32 ppt) according to two transfer régimes; Group A eggs were exposed to experimental salinities immediately following stripping and addition of milt and Group B eggs were

exposed to freshwater and incubated for 4 h before being transferred to experimental salinities. Egg viability *i.e.* embryos showing expected developmental features (see Table 2.2.) was determined by examination of eggs under a dissecting microscope at 4 and 9 h post-fertilisation for Group A or at 9 h post-fertilisation for Group B.

4.2.4 Experiment 2. The effects of salinity on embryogenesis and hatching success

As above, due to the asynchronous spawning nature of Nile tilapia, simultaneous batches of eggs at precisely the same developmental stage could not be obtained so three separate trials were run, each with an individual batch of eggs. Eggs from a newly fertilised batch were placed in the freshwater incubation system and allowed to develop to the 8 - 16 cell blastula stage (*i.e.* 3 - 4 h post-fertilisation). Healthy, normally developing embryos were chosen and randomly allocated to each experimental treatment (0, 7.5, 15, 20 and 25 ppt) with three replicates per treatment and 40 eggs per replicate. Thereafter, normally developing embryos were then taken from the freshwater system at 24 h post-fertilisation (gastrula) and again at 48 h post-fertilisation (at completion of segmentation period) and transferred, as above, to the experimental treatments.

Developmental rates of embryos *i.e.* time to acquisition of selected ontogenetic characteristics, time until hatching (> 50% hatch and 100% hatching) and embryonic survival patterns were noted. In addition, 10 newly hatched larvae were removed randomly from each replicate (n = 30), euthanised in MS222 (tricaine methane sulphonate), immediately rinsed in distilled water and dissected using a binocular

microscope; the yolk was separated from the larval body and yolk-sac epithelium *i.e.* body compartment, and both were placed separately on pre-weighed foils and oven dried at 60 °C for 24 h, followed by 3 h desiccation and then weighed to the nearest 0.0001 g on an Oxford G2105D balance.

4.2.5   Experiment 3. The effect of salinity on survival and growth rate from hatch to yolk-sac absorption

This experiment studied the effect of rearing salinity on larval performance from hatch until complete yolk-sac absorption. Three separate batches of eggs were used and designated as Trial 1, Trial 2 and Trial 3. Initial egg dry mean weights were calculated (see Section 4.2.2) for each batch. Embryos were allowed to develop to 8 - 16 cell stage (3 - 4 h) in the freshwater incubation system and then normally developing embryos were randomly allocated to each of the five experimental treatments *i.e.* freshwater, 7.5, 15, 20 and 25 ppt, with three replicates per treatment and 40 eggs per replicate. Survival was monitored daily until complete yolk-sac absorption occurred. Further eggs from each batch were also transferred at 3 - 4 h post-fertilisation to an additional three replicate bottles per treatment for growth measurements; a total of 30 larvae per treatment (10 from each bottle) were randomly removed at hatch and subsequently on days 3, 6, 9 post-hatch, euthanised in an overdose of MS222 and rinsed in distilled water. Half of the sample was allocated for larval whole weight whilst the other half were dissected from their yolk and the resulting body compartment was weighed. Samples were oven dried at 60 °C for 24 h followed by 3 h desiccation and weighed to the nearest 0.0001 g on an Oxford G2105D balance. YAE (%) was calculated (see Section 4.2.7.).

4.2.6   Experiment 4. To determine the effect of salinity on oxygen consumption of yolk-sac larvae

This experiment investigated the effects of salinity on the metabolic rate of yolk-sac larvae from hatch to yolk-sac absorption. A Strathkelvin microcathode electrode (Model SI130) attached to a Strathkelvin dissolved oxygen meter (Model 782) was used to measure oxygen consumption of individual yolk-sac larvae. A Strathkelvin glass respiration chamber (Model RC300) with a volume of 3 ml was maintained at a constant temperature by pumping water from a temperature controlled water bath through the glass jacket surrounding the chamber (Figure 4.1.). The chamber was placed on a magnetic stirrer (Gallenkamp Magnetic Stirrer Hotplate) and was provided with a stirrer bar to ensure adequate but gentle mixing of the water. A screen was placed above the stirrer bar to protect the larvae (Figure 4.1.B. and C.). Calibration to zero and 100% saturation for each salinity was assumed to be equivalent to oxygen levels calculated according to the formula described in Forstner and Gnaiger (1983).

Trials were run to see the effects of stress on oxygen consumption. Transfer of larvae to the respiration chamber appeared to increase O_2 consumption rates which were seen to level out after 5 minutes within the chamber. Therefore two respiration chambers were used alternatively - an individual larva was placed in the spare respiration chamber (see Figure 4.1.B.) 5 min prior to measurement of O_2 consumption so as to allow larvae to acclimitise.

Oxygen respiration rates were measured for 5 min per larvae and results given as

oxygen consumption (expressed as $\mu l \ O_2 \ h^{-1}$). Preliminary trials had indicated that 5 min was sufficient to give a representative value of O_2 consumed without allowing O_2 to become a limiting factor. A control run was made for each experimental salinity (*i.e.* treatment water and no larvae) due to an observed decline in the amount of oxygen in the chamber not due to the metabolism of the larvae and the value of this blank was subtracted from the respective respiration values. The respiration chamber was washed with a mild bleach solution and then rinsed thoroughly with distilled water after every 3 runs to prevent build up of bacteria that would negatively affect O_2 consumption rates.

Embryos from three separate batches were allowed to develop to 8 - 16 cell stage (3 - 4 h post-fertilisation) in the freshwater incubation system, normally developing embryos were chosen using a dissecting microscope and were then randomly allocated to each of the five experimental treatments *i.e.* freshwater, 7.5, 15, 20 and 25 ppt. Oxygen consumption rates for individual larvae were subsequently measured at selected time points during the yolk-sac absorption period *e.g.* hatch, 3 dph, 6 dph and 9 dph. A minimum of 4 larvae per batch was measured. Larvae were then euthanised in an overdose of MS222 (tricaine methane sulphonate), rinsed in distilled water and standard length measurements were taken according to May (1971). Individuals were immediately frozen at -70 °C and subsequently oven dried, desiccated and weighed to the nearest 0.0001 g on an Oxford G21050 balance. Data was calculated as QO_2 *i.e.* μl O_2 mg dry weight $^{-1} \ h^{-1}$.
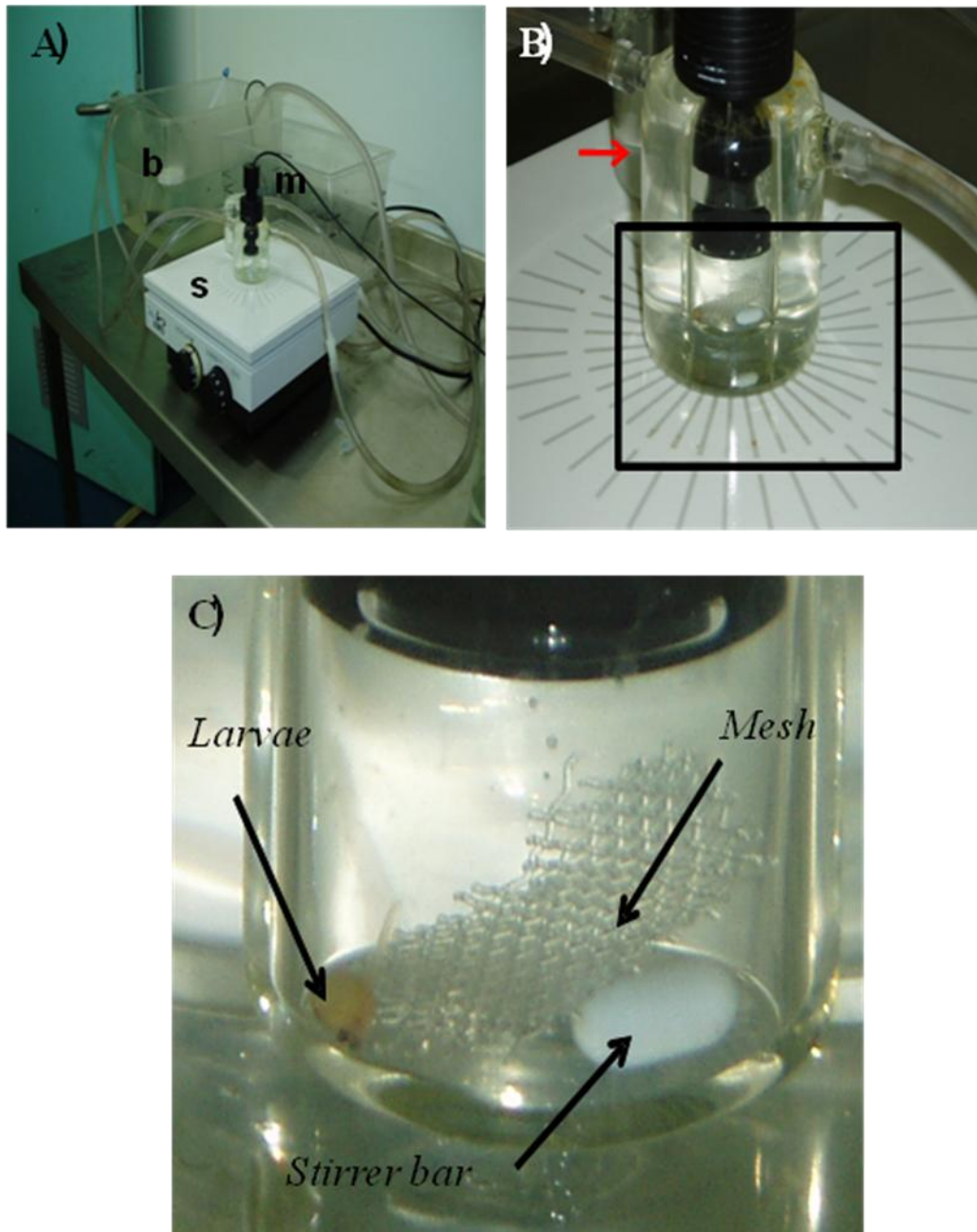
Figure 4. 1 System used in the evaluation of the effects of salinity on oxygen consumption for individual yolk-sac larvae. **A)** Temperature controlled water bath (b), magnetic stirrer (s) with Strathkelvin dissolved oxygen meter (m), **B)** Strathkelvin glass respiration chamber showing stir bar and screen protecting larvae, spare respiration chamber (arrowhead) and **C)** Close up of respiration chamber (boxed area from B).

4.2.7 Performance indices

Yolk absorption efficiency was calculated using the following formula:

YAE (%) = (mean body compartment gain (dry weight) – mean yolk consumed   during yolk absorption period (dry weight)) x 100.

4.2.8 Statistical analyses

Statistical analyses were carried out with Minitab 16 software using a General Linear Model or one-way analysis of variance (ANOVA) with Tukey's post-hoc pair-wise comparisons. Homogeneity of variance was tested using Levene's test and normality was tested using the Anderson-Darling test. Where data failed these assumptions, they were transformed using an appropriate transformation *i.e.* squareroot. All percentage data were normalised by arcsine square transformation prior to statistical analyses to homogenise the variation and data are presented as back-transformed mean and upper and lower 95% confidence limits.

4.3 Results

4.3.1   Experiment 1. The effect of salinity on egg viability

There was an overall inverse significant effect of elevated salinity on egg viability (GLM; $F_{5,131} = 51.45$; $p < 0.05$) but not of batch (GLM; $F_{1,131} = 6.89$; $p > 0.05$) therefore data were combined for the three batches for each group a and b. Embryo viability after 9 h was significantly affected (One-way ANOVA with Tukey's post-hoc pairwise comparisons; $p < 0.05$) by salinity, regardless of the timing of post-spawning exposure to treatment salinities; embryos incubated at elevated salinities always displayed a lower viability than those incubated in freshwater (Table 4.2.; Figure 4.2.). Egg development was severely inhibited at 32 ppt with no development observed after 9 h, regardless of transfer time. The timing of exposure to elevated salinities had a significant effect (One-way ANOVA with Tukey's post-hoc pairwise comparisons; $p < 0.05$) on egg viability after 9 h, with immediate exposure to an elevated salinity (Group a) negatively affecting egg viability compared with exposure after 4 h (Group b) (Table 4.2.; Figure 4.2.). However, the effects of immediate exposure of embryos to experimental salinities were more apparent after 9 h than after 4 h, with embryos after 4 h displaying a significantly reduced viability (One-way ANOVA with Tukey's post-hoc pairwise comparisons; $p < 0.05$) only for salinities of 20 ppt and above, whereas embryos after 9 h displayed a significantly reduced viability (One-way ANOVA with Tukey's post-hoc pairwise comparisons; $p < 0.05$) for all salinities.

Table 4. 2 Effects of salinity on embryo viability (%) of Nile tilapia embryos according to transfer time to experimental salinities. Statistical analyses, means and 95% confidence limits were calculated on arcsine square transformed data of three batches with three replicates per batches). Values in the same column sharing a common superscript are not significantly different (One-way ANOVA with Tukey's post-hoc pairwise comparisons; $p < 0.05$); asterisks next to values for 9 h post-spawning sampling in Group b denote a significant difference between corresponding value in Group a ($p < 0.05$).

Incubation salinity (ppt)	Embryo viability (%): mean and 95% confidence limits (upper – lower)	
Group a: eggs fertilized in experimental salinities [A]		
Sampling point (h post-fertilisation):	**4**	**9**
Freshwater	94 (92 - 96) [a]	94 (91-96) [a]
7.5 ppt	93 (91 – 94) [a]	65 (63-67) c
15 ppt	94 (91 – 96) [a]	73 (71 -74) [b]
20 ppt	86 (84 – 87) [b]	56 (53 -57) [d]
25 ppt	63 (60 – 64) [c]	23 (21 -23) [e]
32 ppt	7 (4 – 8) [d]	0
Group b: eggs fertilized in freshwater and transferred to experimental salinities after 4 h [B]		
Sampling point (h post-fertilisation):	**4**	**9**
Freshwater	96 (93 – 97)	99 (97 - 99) [a]
7.5 ppt	-	97 (96 - 98) [a]*
15 ppt	-	85 (84 - 86) [b]*
20 ppt	-	87 (86 -87) [b]*
25 ppt	-	57 (55 -57) [c]*
32 ppt [C]	-	0

[A] Group a: initial egg weight (mg) = 3.2 ± 0.02; [B] Group b: initial egg weight (mg) = 3.6 ± 0.03.
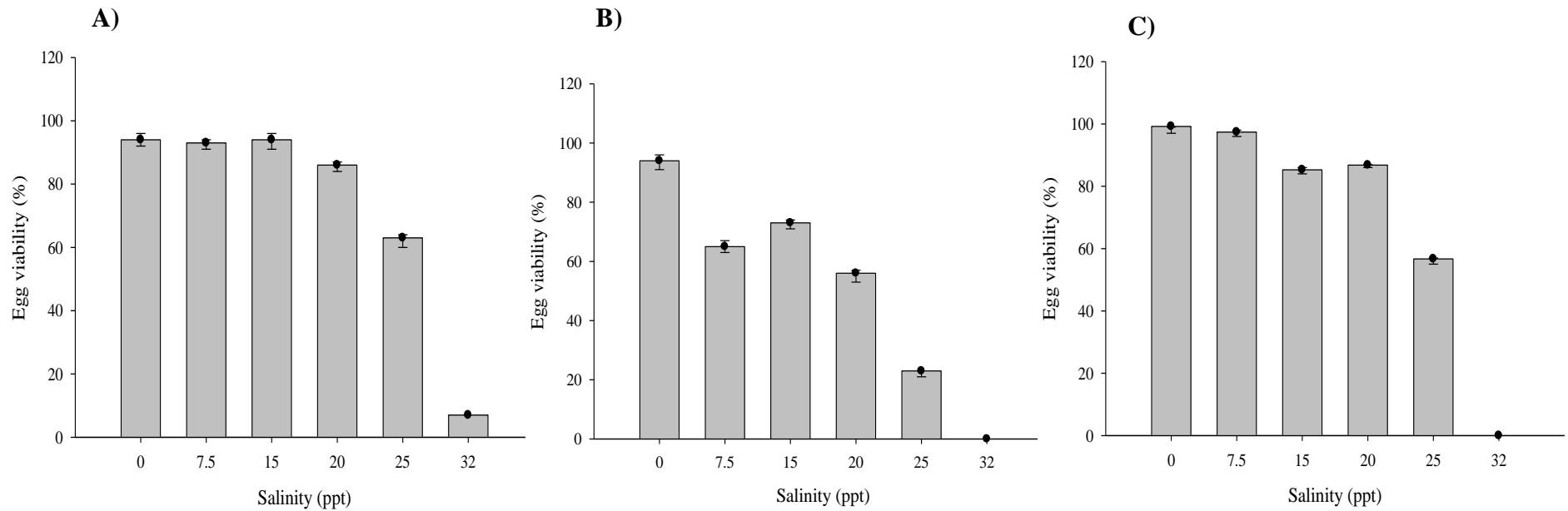
Figure 4. 2 Effects of salinity on egg viability (%) of Nile tilapia embryos according to transfer time to experimental salinities. **Group a**: **A)** Eggs fertilized in experimental salinities sampled at 4 h, **B)** Eggs fertilized in experimental salinities sampled at 9h. **Group b**: **C)** Embryos transferred after 4 h incubation in freshwater and sampled after 9 h. Mean and 95% confidence limits were calculated on arcsine square transformed data. Statistical differences between treatments are presented in Table 4.2.

4.3.2   Experiment 2

4.3.2.1. The effects of salinity on embryonic development and hatching success

There was a significant overall effect of salinity, transfer régime of embryos and their interaction on hatching rates, but not between batches. Effects are summarised in Table 4.3. and Figure 4.3.

Table 4. 3 Analysis of Variance for effect of salinity, timing of transfer and their interaction on hatching rate (General Linear Model; $p < 0.001$).

Source	DF	F	P-value
Dry weight (mg):			
Batch	2	7.55	0.134
Salinity	4	782.77	0.001
Timing of transfer	2	629	0.001
Salinity vs. timing of transfer	8	21.96	0.001
Error	120		

Nile tilapia embryos developed and hatched at all salinities tested, however hatching rate, regardless of transfer time, was always significantly inversely related to salinity (GLM; $p < 0.05$) (Figure 4.4.A.). Acclimation régime *i.e.* time of transfer, similarly, had a significant effect (GLM; $p < 0.05$) on hatching rates; embryos transferred from freshwater to elevated salinities either at 24 h post-fertilisation or at 48 h post-fertilisation displayed a lower hatching rate, compared with those transferred at the 3 - 4 h stage, significantly in the case of 20 ppt (GLM; $p < 0.05$) (Figure 4.4.B.).
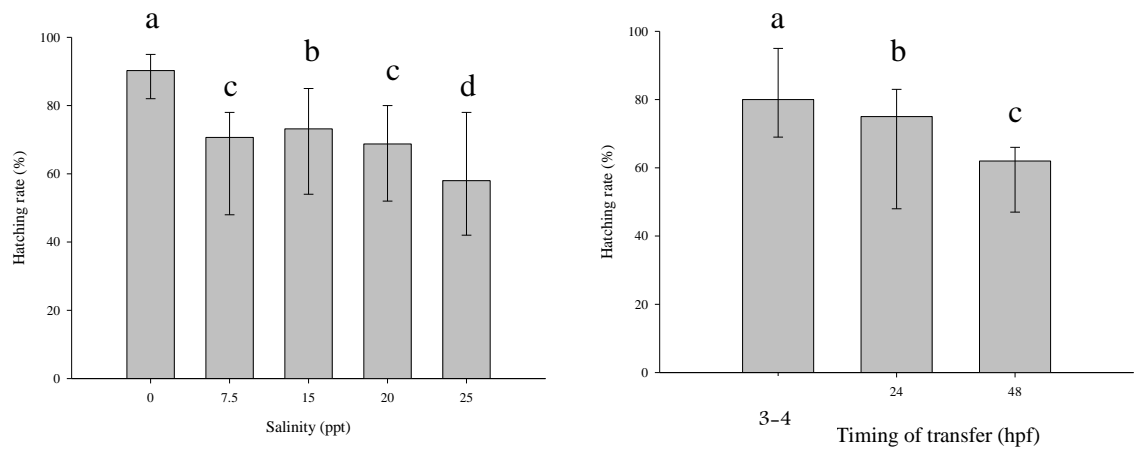
Figure 4. 3 Overall effects of **A)** Salinity and **B)** Timing of transfer on hatching rates of Nile tilapia larvae. Statistical analysis, mean and 95% confidence limits were calculated on arcsine square transformed data. Different letters indicate significant differences between treatments (General Linear Model with Tukey's post-hoc pairwise comparison; $p < 0.05$).

Survival curves are shown in Figure 4.5.A., B. and C. Mortalities occurred immediately after transfer to elevated salinities for embryos transferred at 3 - 4 h post-fertilisation, showing a gradual decline in survival thereafter until hatch. Survival of embryos transferred at a later stage *i.e.* 24 h and 48 h post-fertilisation declined rapidly within the first 24 h following transfer in all salinities and then showed a gradual decline over the remaining days until hatch. For embryos transferred at 48 h post-fertilisation there was a further drop in survival at *c*. 82 h post-fertilisation, especially in the elevated salinities (*i.e.* 20 and 25 ppt).

Increasing incubation salinity significantly (GLM; $p < 0.05$) lengthened the time taken to reach selected embryonic stages. Time to 100% hatch for embryos transferred at 3 - 4 h post-fertilisation was inversely related to incubation salinity (Figure 4.6.) with hatching times ranging from 120 h for embryos incubated in 15, 20 and 25 ppt to 93 h for embryos incubated in freshwater.
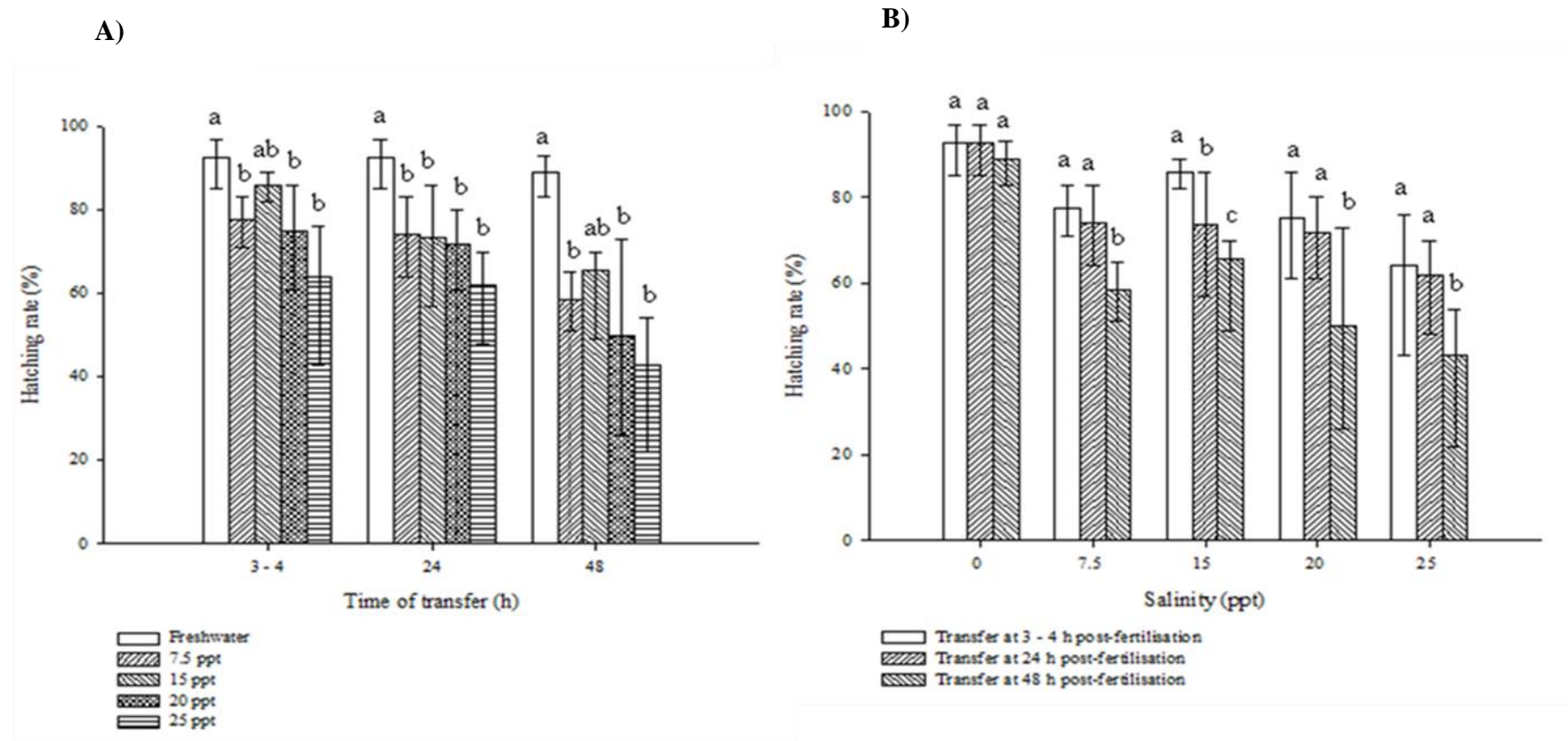
Figure 4. 4 Comparison of hatching rates (%) of Nile tilapia embryos in varying salinities subjected to varying post-fertilisation acclimation régimes. Mean and 95% confidence limits were calculated on arcsine square transformed data of three batches with three replicates per batch (n = 40 eggs per replicate). **A)** Hatching rates according to time of transfer, **B)** Hatching rates according to salinity. Different letters indicate significant differences between timing of treatments (GLM with Tukey's post-hoc pairwise comparisons; $p < 0.05$).
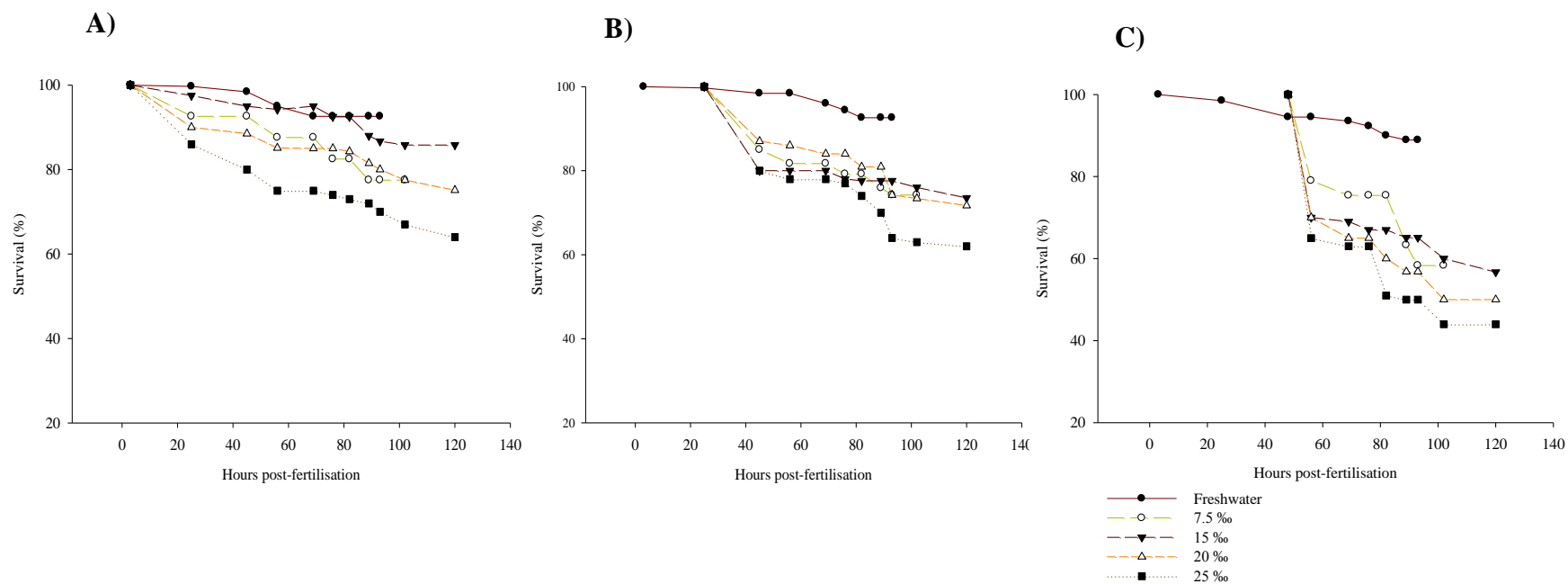
Figure 4. 5 Survival curves of Nile tilapia embryos incubated at various salinities. Data points are mean calculated on arcsine square transformed data of three batches with three replicates per batch (n = 40 eggs per replicate). **A)** Embryos transferred at 3 - 4 h post-fertilisation, **B)** Embryos transferred at 24 h post-fertilisation and **C)** Embryos transferred at 48 h post-fertilisation. 95% confidence limits removed for clarity of presentation.
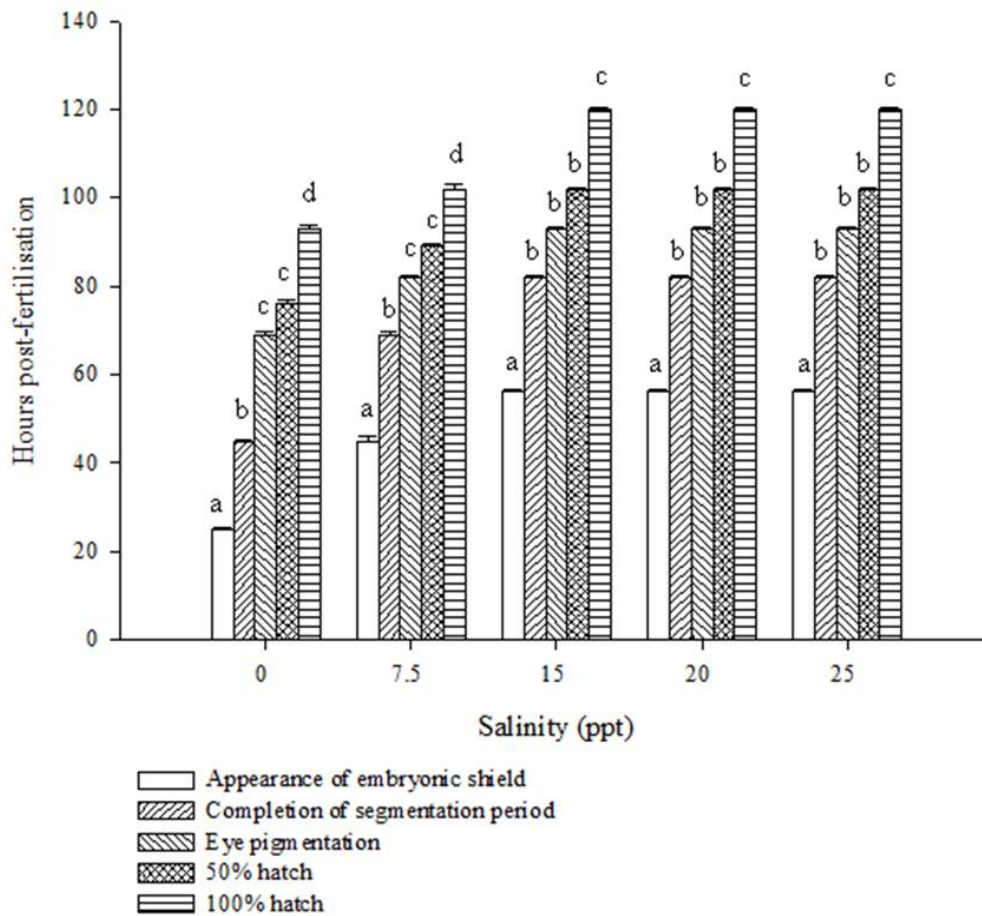
Figure 4. 6 Effect of incubation salinity on the developmental rate of Nile tilapia embryos transferred to experimental salinites at 3 - 4 h post-fertilisation. Data points are means ± S.E. of three batches with three replicates per batch (n = 40 eggs per replicate). Different letters indicate significant differences between developmental stages (GLM with Tukey's post-hoc pairwise comparisons; $p < 0.05$).

4.3.2.2. The effect of salinity on dry weights of fry at hatch

Dry weight data of yolk-sac larvae at hatch from embryos transferred to experimental salinites at 3 - 4 h post-fertilisation were combined from all three batches as variances were homogeneous and no statistical differences were observed between batches (GLM with Tukey's post-hoc pairwise comparisons; $p > 0.05$). Body compartment weight and

yolk weight were inversely related in salinities above 15 ppt and produced fry at hatching with a lower mean dry body compartment weight but containing greater yolk reserves (One-way ANOVA; p < 0.05) (Figure 4.7.).
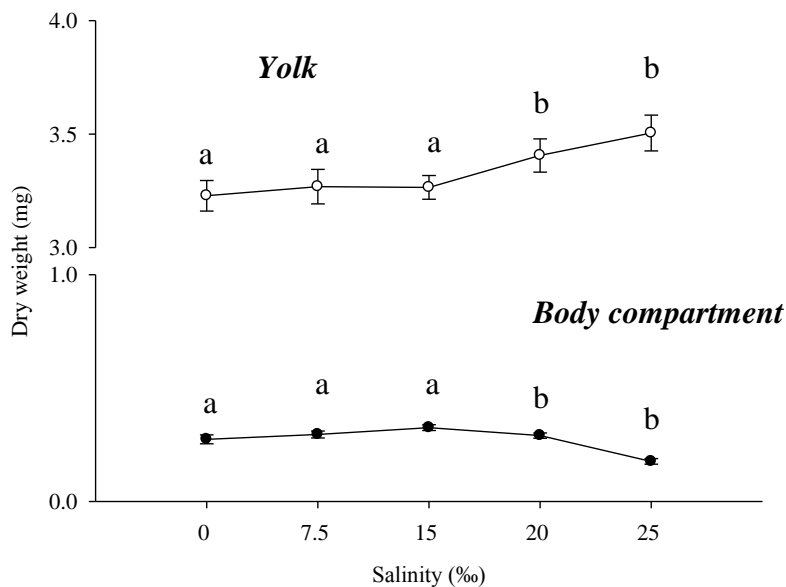
Figure 4. 7 Effect of incubation salinity on mean dry body compartment (total weight minus yolk) and mean dry yolk weight of newly hatched Nile tilapia larvae. Embryos were transferred 3 - 4 h post-fertilisation. Data points are mean ± S.E. of three batches with three replicates per batch (n = 40 eggs per replicate). Different letters denote significant differences between treatments (One-way ANOVA with Tukey's post-hoc pairwise comparisons; p < 0.05).

4.3.3 Experiment 3: The effect of salinity on growth rate and survival of yolk-sac larvae from hatch to yolk-sac absorption

Data from the three trials are presented separately as variances were non-homogeneous and statistical differences were observed between three batches (GLM: $F_{2,42} = 1.65$; p < 0.001). An overall significant effect of salinity on survival at yolk-sac absorption was

observed (GLM: $F_{4,44} = 9.44$; $p < 0.001$) which is summarised in Figure 4.8.
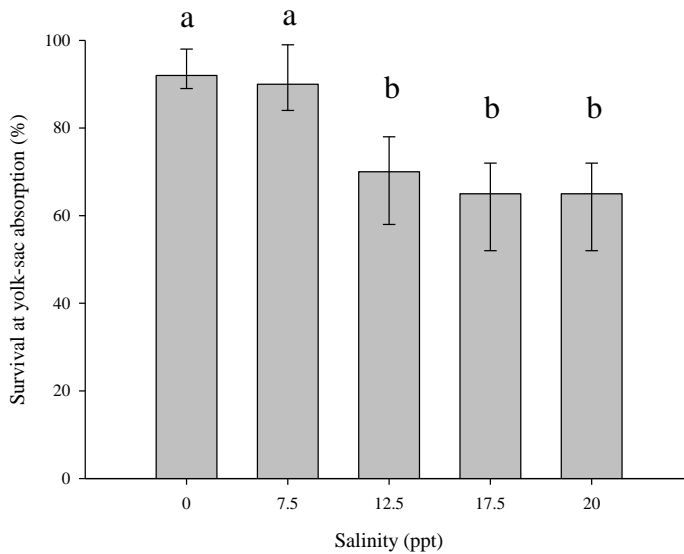
Figure 4. 8 Overall effects of salinity on survival at yolk-sac absorption of Nile tilapia larvae. Statistical analysis, mean and 95% confidence limits were calculated on arcsine square transformed data. Different letters indicate significant differences between treatments (General Linear Model with Tukey's post-hoc pairwise comparison; $p < 0.001$).

Fry survival at complete yolk-sac absorption displayed a significant (One-way ANOVA with Tukey's post-hoc pairwise comparisons; $p < 0.05$) inverse relationship with increasing salinity at the salinities tested for all trials (Table 4.4.). Survival curves of fry up to yolk-sac absorption are shown for the three trials in Figure 4.9. Mortality occurred in all treatments, primarily during early development *i.e.* from hatch to 5 dph. Mortalities increased with increasing salinity and were particularly heavy in the higher salinities of 15, 20 and 25 ppt. Following the period of early mortality, survival generally stabilised from 5 dph. In general, the pattern of survival for fry reared in 7.5 ppt was similar to that observed for fry reared in freshwater.

The mean dry body compartment weight and whole dry fry weight for larvae at hatch

and mean dry weight at end of yolk-sac absorption period at 9 dph are shown in Table 4.4. Generally at hatch, fry had a greater whole dry body weight in elevated salinities (> 15 ppt) compared with those in freshwater. Similarly, at yolk-sac absorption, fry incubated and reared in elevated salinities (> 15 ppt) had a higher whole body weight than those in freshwater, and fry incubated and reared in 7.5 ppt in all trials showed a smaller whole dry body weight compared with fry incubated and reared in 20 or 25 ppt ($p < 0.05$). Yolk-sac absorption efficiency (YAE) was salinity dependant. Fry reared in 20 and 25 ppt showed a lower YAE than those reared in freshwater, 7.5 and 15 ppt in all Trials. There was no effect of salinity on time taken to yolk-sac absorption (Table 4.4.).

Table 4. 4 Influence of salinity on growth characteristics of Nile tilapia larvae from hatch to yolk-sac absorption. Values for weight are mean ± S.E.; values for survival data are mean and 95% confidence limits calculated on arcsine square transformed data with three replicates per treatment (n = 30 larvae per replicate). Different superscript letters indicate significant differences between treatments (One-way ANOVA with Tukey's post-hoc pairwise comparisons; $p < 0.05$).

Treatment	Dry weight at hatch (mg)		Weight at yolk-sac absorption (mg)	Time to yolk-sac absorption (days)	Yolk-sac absorption efficiency (%)[D]	Survival (%) at yolk-sac absorption: mean and 95% confidence limits (upper – lower)
Trial 1[A]	**Whole**	**Body compartment**				
Freshwater	4.0 ± 0.11[ab]	0.2 ± 0.01[a]	2.9 ± 0.06[ab]	9	71	95 (97 – 92)[a]
7.5 ppt	3.8 ± 0.03[a]	0.3 ± 0.05[ab]	2.8 ± 0.11[b]	9	72	90 (97 – 80)[a]
15 ppt	4.1 ± 0.18[ab]	0.3 ± 0.06[ab]	3.0 ± 0.07[a]	9	73	89 (99 – 60)[a]
20 ppt	4.3 ± 0.13[b]	0.4 ± 0.03[b]	3.1 ± 0.07[a]	9	69	82 (92 – 67)[b]
25 ppt	4.4 ± 0.12[b]	0.4 ± 0.01[b]	3.2 ± 0.08[a]	9	68	81 (91 – 70)[b]
Trial 2[B]						
Freshwater	3.5 ± 0.03[a]	0.2 ± 0.01[a]	2.3 ± 0.01[a]	9	65	98 (99 – 58)[a]
7.5 ppt	3.5 ± 0.04[a]	0.3 ± 0.01[a]	2.2 ± 0.11[a]	9	66	98 (99 – 58)[a]
15 ppt	3.4 ± 0.06[a]	0.3 ± 0.05[a]	2.4 ± 0.03[a]	9	66	50 (62 – 38)[b]
20 ppt	3.4 ± 0.06[a]	0.2 ± 0.02[a]	2.3 ± 0.08[a]	9	69	48 (62 – 34)[b]
25 ppt	3.5 ± 0.05[a]	0.2 ± 0.03[a]	2.3 ± 0.04[a]	9	69	46 (60 – 33)[b]

Table 4.4. cont.

Trial 3[C]

Freshwater	3.9± 0.06[ab]	0.2 ± 0.09[a]	2.8 ± 0.11[ab]	9	61	80 (96 – 56)[a]
7.5 ppt	3.8 ± 0.02[a]	0.3 ± 0.04[a]	2.7 ± 0.03[b]	9	64	80 (99 – 39)[a]
15 ppt	4.0 ± 0.01[ab]	0.5 ± 0.10[b]	3.1 ± 0.07[a]	9	64	67 (75 – 58)[b]
20 ppt	4.2 ± 0.17[b]	0.4 ± 0.03[b]	3.1 ± 0.12[a]	9	59	68 (86 – 46)[b]
25 ppt	4.1 ± 0.02[b]	0.3 ± 0.02[b]	3.1 ± 0.09[a]	9	57	68 (90 – 47)[b]

[A] Initial egg weight (mg) = 4.23 ± 0.07; [B] Initial egg weight (mg) = 4.14 ± 0.06; [C] Initial egg weight (mg) = 3.88 ± 0.11 (mg).

[D] Yolk Absorption Efficiency, YAE (%) = ((mean body compartment gain (dry weight) – mean yolk consumed during yolk absorption period (dry weight)) x 100).

147

A)　　　　　　　　　　　　　　　　　　　　　**B)**　　　　　　　　　　　　　　　　　　　　　**C)**
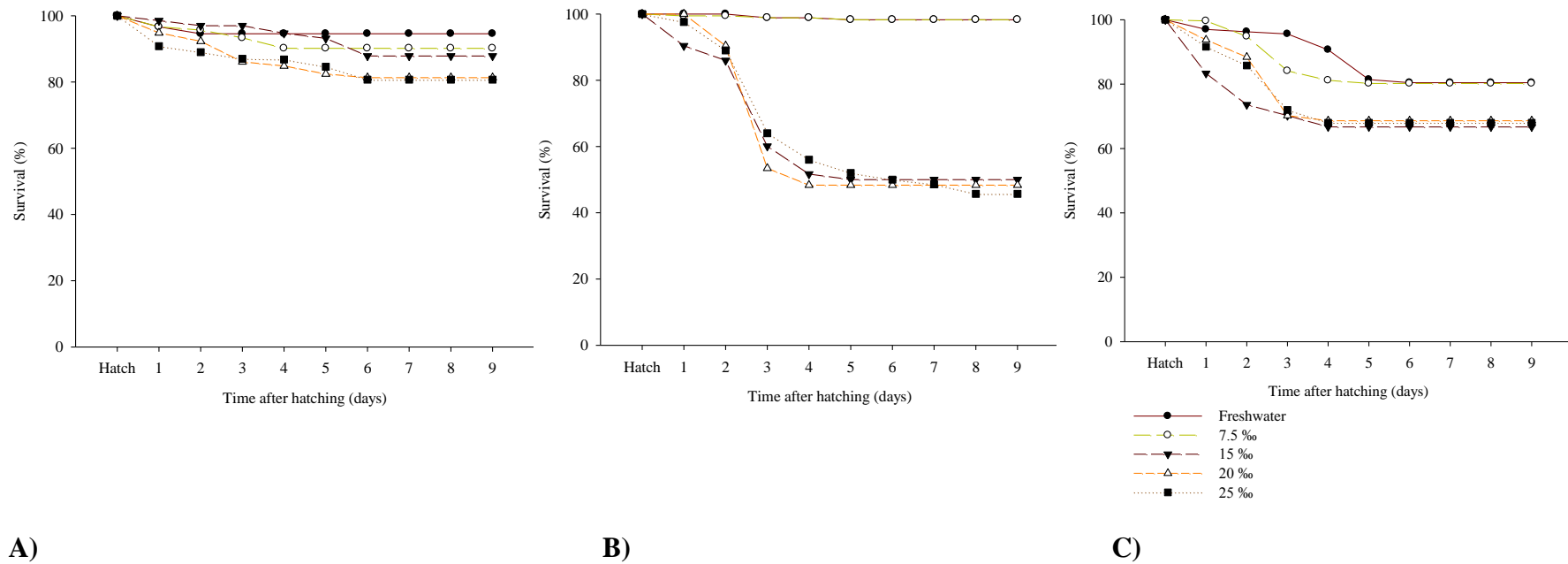
Figure 4. 9 Survival curves for Nile tilapia larvae reared at different salinities following transfer at 3 - 4 h post-fertilisation. **A)** Trial 1, **B)** Trial 2 and **C)** Trial 3. Data points are mean of individual batches of three separate trials with three replicates per trial (n = 30 yolk-sac larvae per replicate) calculated on arcsine square transformed data. 95% confidence limits have been removed for clarity of presentation.

4.3.4　The effect of salinity on oxygen consumption of yolk-sac larvae

Data were combined from all three batches as variances were homogeneous and no statistical differences were observed between batches. There was a significant overall effect of age, salinity and their interaction on QO_2. Effects are summarised in Table 4.5. and Figure 4.10.

Table 4. 5 Analysis of Variance for QO_2 (General Linear Model; $p < 0.001$).

Source	DF	F	P-value
QO_2:			
Batch	2	2.66	0.381
Age	3	24.62	0.001
Salinity	3	6.19	0.001
Age vs. salinity	9	20.63	0.001
Error	128		

A)　　　　　　　　　　　　　　　**B)**
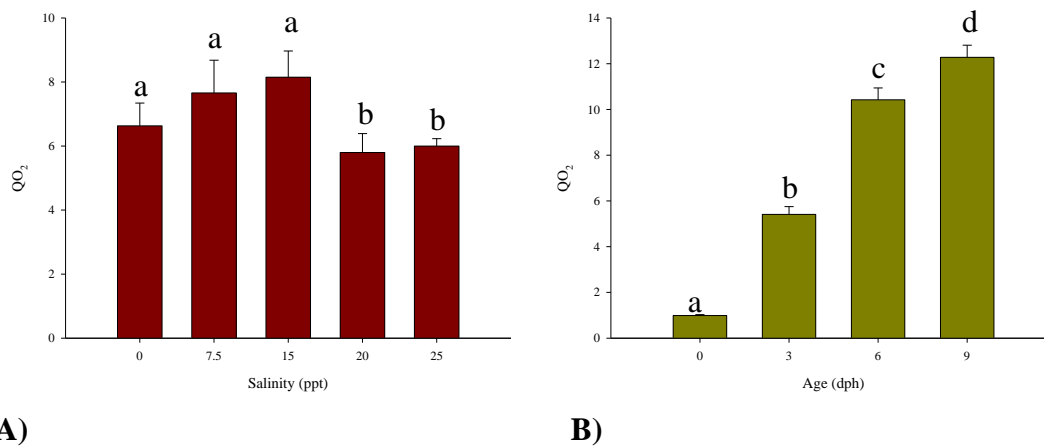
Figure 4. 10 Overall effect of **A)** Salinity and **B)** Age on QO_2. Mean ± S.E. (General Linear Model with Tukey's post-hoc pairwise comparisons; $p < 0.001$).

Salinity-related differences in oxygen consumption rates were not detectable until 3 dph and, thereafter, mean QO_2 rates varied between salinities (Figure 4.11.A.). The QO_2 of larvae in freshwater between $3-6$ dph were always significantly higher (GLM; $p < 0.05$) than those in 7.5, 15, 20 and 25 ppt however, on 9 dph, this pattern was reversed and freshwater larvae showed a significantly lower QO_2 than those in elevated salinities (Figure 4.11.). Salinity always displayed a significant effect on QO_2 regardless of age (Figure 4.11.B.).
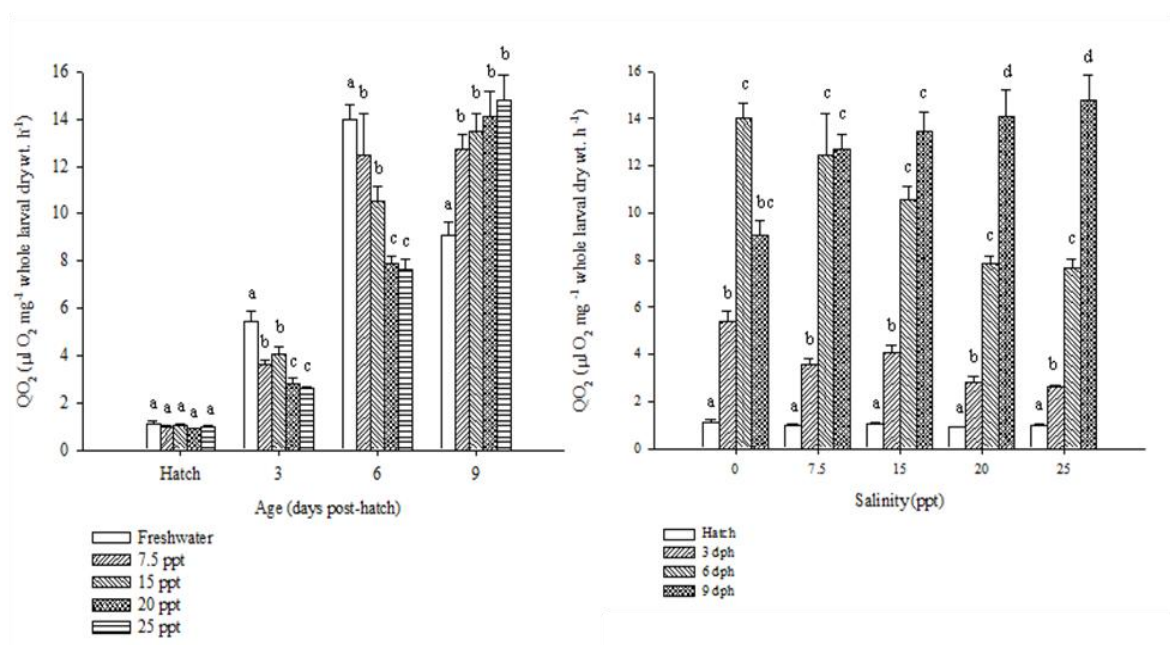
A)   B)

Figure 4. 11 Effect on oxygen consumption expressed as QO_2 ($\mu l\ O_2\ mg^{-1}$ whole larval dry wt. h^{-1}) of yolk-sac larvae during yolk-sac period of **A)** Age; different letters indicate significant differences between treatments and **B)** Salinity; different letters indicate significant differences between days (GLM with Tukey's post-hoc pairwise comparisons; $p < 0.001$). Values represent mean $\pm$ S.E. of data from three Trials.

4.3.5 The effect of salinity on larval dry weight and standard length

. Salinity, age and their interaction had an overall significant effect on larval dry weight and on larval standard length, but no significant effect of batch was observed. Effects are summarised in Table 4.6. and Figure 4.12.

Table 4. 6 Analysis of Variance for effect of salinity on dry weight and standard length (General Linear Model; p < 0.001).

Source	DF	F	P
Dry weight (mg):			
Batch	2	1.08	0.724
Salinity	4	16.25	0.001
Age	3	14.58	0.001
Salinity vs. age	12	3.98	0.001
Error	126		
Standard length (mm):			
Batch	2	0.76	1.03
Salinity	4	21.02	0.001
Age	3	787.66	0.001
Salinity vs. age	12	4.61	0.001
Error	129		

A)

B)

C)

D)
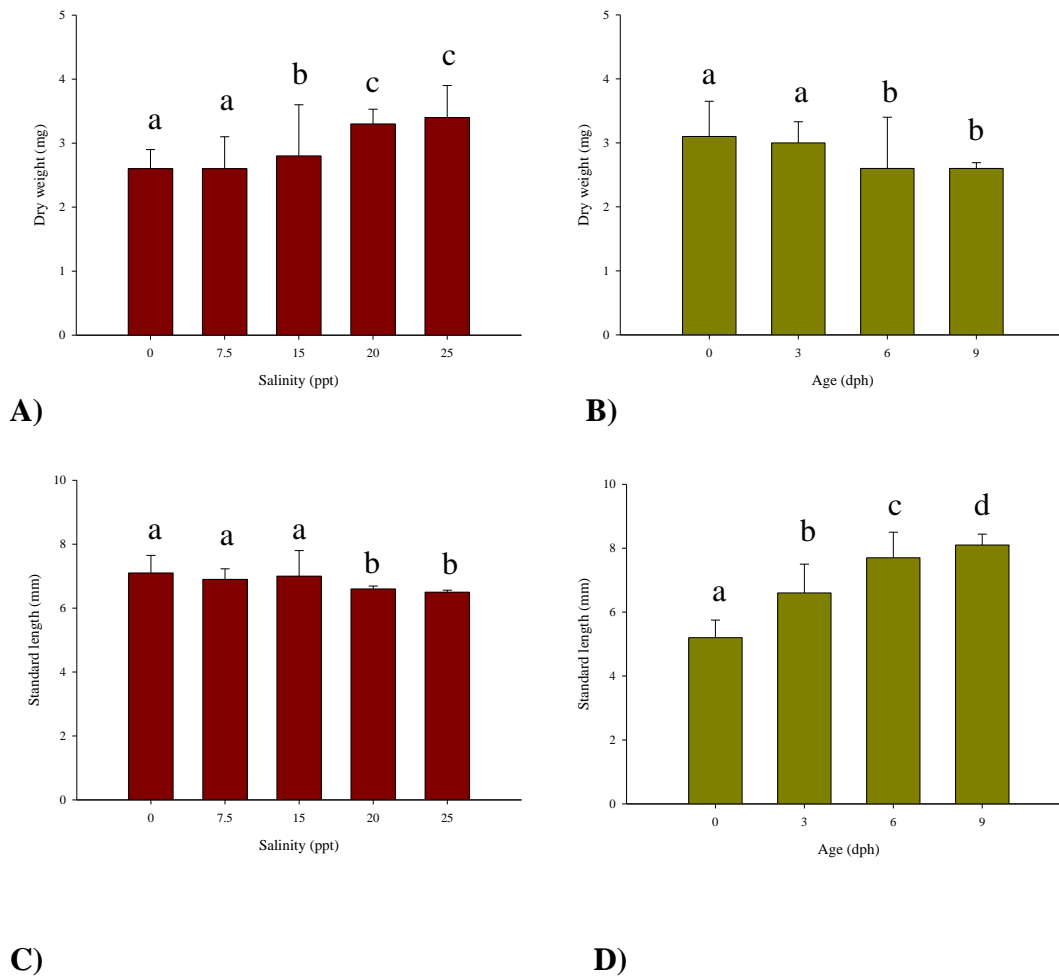
Figure 4. 12 Overall effect of **A)** Salinity and **B)** Age on larval dry weight (mg) and **C)** Salinity and **D)** Age on larval standard length (mm). Mean ± S.E. Different letters indicate significant differences between treatments (General Linear Model with Tukey's post-hoc pairwise comparison; $p < 0.001$).

Salinity appeared to have a significant detrimental effect (GLM with Tukey's post-hoc pairwise comparison; $p < 0.05$) on larval standard length, with elevated salinities producing shorter larvae from hatch until 6 dph, after which time there was no significant differences

between treatments (Table 4.7.). Similarly salinity had a significant effect on larval dry weight, with heavier larvae in elevated salinities throughout the yolk-sac period (GLM; $p < 0.05$) (Table 4.7.).

Table 4. 7 Effect of salinity on larval standard length (mm) and larval dry weight (mg). Values represent mean ± S.E. of data from three Trials (n = 9 larvae per Trial). Different superscripts indicate significant differences between treatments; different subscripts indicate significant differences between days (GLM with Tukey's post-hoc pair-wise comparison; $p < 0.05$).

Salinity:	Freshwater	7.5 ppt	15 ppt	20 ppt	25 ppt
Standard length (mm):					
Hatch	$5.4 \pm 0.08\,^a_a$	$5.3 \pm 0.04\,^a_a$	$5.3 \pm 0.08\,^a_a$	$4.9 \pm 0.08\,^b_a$	$4.6 \pm 0.06\,^b_a$
3 dph	$7.1 \pm 0.05\,^a_b$	$6.5 \pm 0.07\,^b_b$	$6.8 \pm 0.12\,^{ab}_b$	$6.0 \pm 0.08\,^c_b$	$6.1 \pm 0.79\,^c_b$
6 dph	$7.8 \pm 0.08\,^a_c$	$7.7 \pm 0.11\,^a_c$	$7.7 \pm 0.08\,^a_c$	$7.3 \pm 0.07\,^b_c$	$7.4 \pm 0.07\,^b_c$
9 dp	$8.0 \pm 0.04\,^a_c$	$8.1 \pm 0.11\,^a_d$	$8.1 \pm 0.13\,^a_c$	$8.2 \pm 0.06\,^a_d$	$8.2 \pm 0.05\,^a_d$
Dry weight (mg):					
Hatch	$2.8 \pm 0.13\,^a_c$	$3.0 \pm 0.15\,^b_b$	$3.4 \pm 0.13\,^b_d$	$3.5 \pm 0.15\,^b_c$	$3.6 \pm 0.14\,^b_c$
3 dph	$2.4 \pm 0.07\,^a_b$	$2.8 \pm 0.20\,^b_b$	$3.1 \pm 0.12\,^b_c$	$3.6 \pm 0.11\,^b_c$	$3.6 \pm 0.12\,^b_c$
6 dph	$2.0 \pm 0.13\,^a_a$	$2.4 \pm 0.24\,^a_a$	$2.6 \pm 0.10\,^a_b$	$3.3 \pm 0.14\,^b_b$	$3.4 \pm 0.11\,^b_b$
9 dph	$2.4 \pm 0.16\,^a_b$	$2.4 \pm 0.09\,^a_a$	$2.3 \pm 0.11\,^a_a$	$2.7 \pm 0.11\,^b_a$	$2.8 \pm 0.14\,^b_a$

4.4 Discussion

4.4.1　　Effects of salinity on embryogenesis

The results presented in this study indicate that freshly fertilised eggs from freshwater maintained parents transferred immediately to test salinities of 7.5, 15, 20 and 25 ppt displayed a significantly lower hatching rate after 9 h than those transferred after 4 h prior incubation in freshwater. In addition, mortality was 100% after 9 h for embryos transferred to 32 ppt, regardless of time of transfer. Failure of Nile tilapia embryos to develop at this salinity has previously been reported (Watanabe and Kuo, 1985, Watanabe *et al.,* 1985 b).

Alderdice (1988; p. 237) suggests that, at spawning, eggs face 'the first major regulatory challenge' as they are subjected to any major changes in the osmotic and ionic properties of the spawning water. Prior to this, they are subject to homeostatic regulation by the adult regulatory system, with contacts between oocyte and follicular cell microvilli allowing transfer of nutrients and ions. Post-ovulation but pre-spawning, their plasma membrane appears to be relatively permeable to water and responds to changes in the ovarian fluid (Sower *et al.,* 1982) and they are therefore iso-osmotic with the blood of the parents. After spawning and activation of the egg following fertilisation, cortical alveolar exocytosis causes imbibition of water from the external environment across the chorion, forming the perivitelline space. Immediately following this, regulation and maintenance of the integrity of the egg appears to be achieved by the resistive maintenance of a tight plasma membrane

154

and limited trans-membrane water and ion fluxes (Kao *et al.,* 1954), making the egg 'rather impermeant' (Bennett *et al,* 1981). This theory of egg impermeability is supported by Swanson (1996) who transferred eggs of milkfish (*Chanos chanos*), spawned at 32 – 36 ppt to lower and higher salinities at the cleavage-blastula stage (*i.e.* 2 – 5 h post-fertilisation) and observed no swelling or shrinkage of the eggs in response to osmotic gradients. In the present study, the reduced viability of embryos transferred immediately upon spawning to elevated salinities as compared with those transferred at 4 h post-fertilisation *i.e.* once eggs have become impermeant, would suggest the resulting osmotic shock following uptake of water from the external media could affect fertilisation and egg viability. However, once eggs have 'hardened' they are more resistant to changes in the osmotic concentration of the external media.

In the present study, Nile tilapia embryos were able to tolerate salinity challenge across the full range of salinities tested *i.e.* 7.5 to 25 ppt, but results indicate that salinity had a significant negative effect on hatching rates. There is generally a paucity of work on the effects of salinity on the embryogenesis of teleosts that mainly focuses on euryhaline marine species. Studies on these marine species generally show that hatching rates of embryos are adversely affected as salinity moves from the normal salinity range encountered in nature *e.g.* embryos of milkfish (*C. chanos*), spawned in 32 – 36 ppt, but transferred 2-5 h post-fertilisation to varying salinities showed a reduced hatching success (50% hatch) in both lower (15 and 20 ppt) and higher (50 and 55 ppt) salinities (Swanson, 1996), and embryos of mullet (*Mugil cephalus*) transferred at the gastrula stage from a

spawning salinity of 30 ppt showed an optimum salinity range for hatching of 30 to 40 ppt and reduced hatching rates in lower (10 – 25 ppt) and higher (45 – 50 ppt) salinities (Lee and Menu, 1981). Interestingly, Hu and Liao (1979) reported a lower optimum range of hatching for embryos of mullet (*M. cephalus*) of 22 – 23 ppt, but, in this case, the spawning salinity was lower, at 24.5 – 25.5 ppt, suggesting that the salinity of spawning influences the tolerance range of subsequent egg transfer. In agreement with this theory, Zhang *et al.* (2010) explained the optimal salinity for tawny puffer (*Takifugu flavidus*) eggs in their experiment to be lower than in nature to the fact that the long term acclimation of broodstock to a lower than natural salinity influenced the eggs before release.

It is therefore suggested that the maternal osmotic environment has an effect on subsequent osmoregulatory capability of offspring and their ensuing ability to withstand osmotic challenge. In general, freshwater teleosts have a lower osmotic range than teleosts in water of elevated salinity therefore it follows that the media in which the females are held during oocyte maturation and ovulation will influence the subsequent osmolality of the eggs. Indeed, Schofield *et al*. (2007) reported a decline in the number of ovulated vitellogenic oocytes at above 30 ppt in *O. niloticus* which would suggest that high environmental salinity can have a negative effect on oocyte viability during final maturation, possibly through hydration due to osmotic strain. Indeed this hypothesis could be supported by Watanabe *et al.* (1985 b) who found that when *O. niloticus* larvae, spawned and incubated at 0, 5, 10 and 15 ppt, were directly transferred at 6 – 7 days post-hatch to salinities in the range of 0 – 32 ppt, an increased in Median Lethal Salinity-96 (MLS-96), *i.e.* salinity at

which survival falls to 50% 96 h following direct transfer from freshwater to test salinity, was seen in those eggs spawned and incubated at 15 ppt (MLS-96 >32 ppt) compared with those spawned in 5 ppt (MLS-96 of 28.1 ppt).

The ability of *O. niloticus* to tolerate changes in salinity during embryogenesis in the present study was, likewise, clearly influenced by the stage of embryonic development at transfer. The results of the current study report a significant increase in hatching rate of Nile tilapia eggs transferred at 3 – 4 h post-fertilisation compared with eggs transferred at a later stage *i.e.* 24 or 48 h post-fertilisation. The pattern of embryonic survival seemed to follow the same trend, with mortalities increasing rapidly following transfer, this being especially pronounced in those embryos transferred at later stages of embryonic development (48 h). These results are contrary to previously published reports on marine telosts; Lee and Menu (1981) reported that embryos of grey mullet (*M. cephalus*) transferred from the salinity of spawning (30 ppt) at the late gastrula stage (approx. 12 h post-spawning) showed a wider range in tolerance *i.e.* 20 – 45 ppt than embryos transferred at the 2-blastomere stage (approx. 1 h post-spawning) to the test salinities where the best hatching was reported at the reduced salinity of 35 ppt. In agreement, Lee *et al.* (1981) reported that fertilised embryos of the euryhaline Northern whiting (*Sillago sihama*) were more tolerant to salinity change at later stages of development.

Alderdice (1988) describes the establishment of osmotic regulation during embryogenesis as beginning during gastrulation and being in place by yolk-plug closure or completion of epiboly. Indeed, a reported increase in the permeability of the plasma membrane during gastrulation coincides with the appearance of extrabranchial or integumental mitochondria-rich cells (MRCs), thus marking the start of the selective restriction of ions and water transfer or active ionoregulation (Guggino, 1980 a and b). The first appearance of MRCs on the yolk-sac epithelium of dechorionated Mozambique tilapia (*Oreochromis mossambicus*) embryos has been reported at 26 h post-fertilization but only at 48 h post-fertilisation has the presence of apical crypts indicated functionality (Lin *et al.,* 1999). Ayson *et al.* (1994) likewise observed MRCs on the yolk-sac epithelium of *O. mossambicus* embryos at 30 h post-fertilization in both fresh and seawater, distributed underneath the pavement cells, with functional apical openings noted at 48 h post-fertilization or half-way to hatching. Similar observations were made by Hwang *et al.* (1994) in *O. mossambicus*. It would be expected, therefore, that if ontogenetic changes in appearance of MRCs confer adaptability during this period of development, embryos should be more tolerant to transfer to elevated salinities as embryogenesis progresses.

However, this is contrary to what has been reported in the present chapter. It has already been demonstrated in Chapter 3 that a distinct ontogenic pattern in embryonic osmoregulatory ability is apparent until hatch; in hyper-osmotic environments (*e.g.* elevated salinities), after an initial and abrupt rise in osmolality following transfer at 3 - 4 h post-fertilisation until 24 h post-fertilisation, levels continue to gradually rise until hatch,

and, conversely, in hypo-osmotic environments (*e.g.* freshwater) a sharp decline in osmolality values is seen immediately post-spawning, which continue to decline until 48 h post-fertilisation and then rise until hatch (Figure 3.3.). This would appear to suggest that the egg remains permeable to water after fertilisation, suggesting that the chorion is not offering any sort of protective barrier to osmotic entry or loss of water. Indeed chorion permeability to dyes has been reported in 16 – 17 days post-fertilisation eggs of the cod (*Gadus morhua*) (Davenport *et al.*, 1981) and 7 – 8 days post-fertilisation eggs of the long rough dab (*Hippoglossoides platessoides limandoides)* (Lonning and Davenport, 1980). Therefore it follows that eggs in hyper-osmotic salinities would lose water thus increasing their osmolality, and, in contrast, eggs in the hypoosmotic environment would osmotically gain water. The increased incidence of embryonic mortality immediately post-transfer at 48 h and the subsequently significantly reduced hatching rate as compared to those transferred at 3 – 4 h post-fertilisation, as seen in this study, supports the theory that the increase in permeability of the chorion allows passage of the external water into the developing egg and puts an osmoregulatory strain on an embryo that is not yet able to cope, as MRCs are only just beginning to gain full functionality. Indeed, in this study, mortality is directly related to increasing salinity, most likely due to the fact that the developing embryo is unable to maintain homeostasis in the face of an increasingly hyper-osmotic environment.

In addition to affecting embryonic mortality, salinity also influenced rates of embryonic development and time to hatching in this study. No effect of salinity on hatching times was reported for Greenback flounder embryos (*Rombosolea tapirina*) (Hart and Purser, 1995)

159

or tawny puffer embryos (*Takifugu. flavidus*) (Zhang *et al.,* 2010) however influence of salinity on hatching rates has been observed by Swanson (1996) for milkfish embryos (*C. chanos*) with salinity influencing hatching time by 1-2 h. No salinity-related differences were observed in timing to yolk-sac absorption in the present study. It is notable that Collins and Nelson (1993) found an increased rate of development in embryos of Randall's rabbitfish (*Siganus randalli*) resulting from temperature variation but no difference in the timing of the development of yolk-sac larvae, suggesting that temperature may be more critical for embryonic development than for larval development in this species. It is suggested that salinity may similarly be less influential during larval stages than during embryogenesis.

4.4.2   Effects of salinity on survival and growth of yolk-sac larvae

In this study, mortalities occurred in all salinities during the first few days after hatching, but declined by 3 dph and then levelled out by 5 dph up to yolk-sac absorption. Mortality was especially pronounced at higher salinities. This suggests that Nile tilapia face the greatest osmoregulatory challenge immediately after hatching, yet show an increasing capacity to maintain ionic and osmotic balance that is conferred ontogenically through the yolk-sac period. This is contrary to previous studies that looked at the ability of newly-hatched yolk-sac larvae of marine teleost species to withstand abrupt salinity challenge. Young and Dueñas (1993) reported that 12 h post-hatch larvae of rabbitfish (*Siganus guttatus*) could tolerate transfer to salinity ranges of 10 – 45 ppt and at 24 h post-hatch to the reduced salinity range of 14 – 37 ppt and Banks *et al.* (1991) reported that 1 dph

spotted sea trout larvae (*Cynoscion nebulosus*) could tolerate salinity ranges of $4 - 40$ ppt and that at 3 dph they could tolerate $8 - 32$ ppt. Similarly, Estudillo *et al.* (2000) reported a longer LT_{50} for newly-hatched larvae of the red snapper (*Lutjanus argentimaculatus*) than for larvae of 7, 14 or 21 days post-hatch when abruptly transferred from 32 ppt to a lower salinity.

It is well documented that teleost yolk-sac larvae are able to maintain osmotic and ionic gradients between their internal and external environments (Guggino, 1980 a and b; Alderdice, 1988; Kaneko *et al.*, 1995), due mainly to the presence of numerous extrabranchial MRCs commonly observed on the abdominal epithelium of the yolk-sac and other body surfaces of fish larvae. Integumental mitochondria-rich cells have been reported in the post-embryonic stages of several teleost species. A distinct spatial shift in MRC distribution from body surface to branchial areas during ontogeny is acknowledged and has been reported in several species *e.g.* the European sea bass (*Dicentrachus labrax*) (Varsamos *et al.*, 2002 a), the killifish (*Fundulus hereroclitus*) (Katoh *et al.,* 2000), the Japanese flounder (*Paralichthys olivaceus*) (Hiroi *et al.,* 1998) and the Mozambique tilapia (*O. mossambicus*) (van der Heijden *et al.,* 1999; Yanagie *et al.,* 2009; Li *et al.*, 1995). Therefore it is suggested that the temporal patterns of survival following hatching that were observed in this study may indicate that, with the development of the branchial system and the increase in numbers of MRCs by 3 dph onwards, the larvae are better able to cope with osmoregulatory challenge.

Growth is highly dependent on environmental conditions and numerous studies have reported an influence of water salinity on fish development during early life stages (Boeuf and Payan, 2001). Effects of salinity on growth in juveniles and adults has also been reported in a number of species *e.g.* Rainbow trout (*Oncorhynchus mykiss*) (Rao, 1968; Morgan and Iwama, 1991), Chinook salmon (*Oncorhynchus tshawytscha*) (Morgan and Iwama, 1991), Coho salmon (O. *kisutch*) (Otto, 1971) supporting the hypothesis that the energetic cost of osmoregulation is lower in an iso-osmotic environment, where the gradients between blood and water are minimal, and that these energy savings are substantial enough to increase growth. Indeed, many sensitive juvenile stages of marine species will opt for intermediary brackish water salinities in estuaries and coastal systems in order to optimise growth. It would therefore follow that the proportion of metabolic energy from yolk reserves which is available for somatic growth is greater at iso-osmotic salinities, and reduced at both freshwater and higher salinities with their corresponding increased osmoregulatory burden. This is reflected in the current study with the highest yolk absorption efficiency (YAE) observed at 7.5 and 15 ppt in trials 1 and 3, and a lower YAE at 20 ppt and above. This is in agreement with May (1974) who reported, in the euryhaline croaker (*Bairdiella icistia*), YAE to be reduced at higher salinities of 30 and 40 ppt compared to 20 ppt. Swanson (1996) also reported a deleterious effect of high salinity on yolk conversion efficiency in milk fish (*C. chanos*). The higher YAE observed in Trial 2 maybe a reflection of external factors influencing the larvae *i.e.* water quality, infection as survival rates at salinities above 15ppt were considerably reduced in this batch.

162

4.4.3 Effects of salinity on metabolism of yolk-sac larvae

In the present study, weight-specific oxygen consumption rates (QO_2) ($\mu l\ O_2$ mg dry wt. $^{-1}$ h $^{-1}$) were seen to increase during the yolk-sac period. Metabolic rates are strongly influenced by developmental stage and by the amount of metabolically active tissue (Swanson, 1996) and indeed, linear relationships of oxygen consumption with age during embryogenesis have already been demonstrated for embryos and newly hatched larvae of milkfish (*C. chanos*) (Swanson, 1996), embryos and yolk-sac larvae of milkfish (*C. chanos*) (Walsh *et al.,* 1991 b), embryos and larvae of striped mullet (*M. cephalus*) (Walsh *et al*., 1991 a), early life stages of the common carp (*Cyprinus carpio*) (Kaushik *et al.,* 1982). On the other hand, non-linear relationships have been reported for Atlantic halibut embryos (*Hippoglossus hippoglossus*) (Finn *et al.,* 1991), yolk-sac larvae of large mouth bass (*Micropterus salmoides*) (Laurence, 1969), embryos and larvae of cod (*G. morhua*) (Davenport and Lonning, 1980) and yolk-sac larvae of Randall's rabbitfish (*Siganus randalli*) (Collins and Nelson, 1993). However, the limitations resulting from variations in estimation methods and non-uniformity in developmental stages measured may be the cause of variation in oxygen consumption rates.

In this study, a significant effect ($p < 0.05$) of salinity was observed for weight-specific oxygen consumption rates (QO_2) from 3 dph onwards (Figure 4.11.A.). However, salinity related variations in QO_2 do not appear to reflect a direct metabolic cost of osmoregulation, as differences were not apparently related to the magnitude of the osmotic gradient between the larvae and the surrounding water (Figure 4.11.B). This is in agreement with

observations in milkfish embryos (*C. chanos*) transferred from a spawning salinity of 32 – 36 ppt to either a hypo-osmotic range of 15 - 20 ppt or to a strongly hyper-osmotic range of 50 - 55 ppt, where equally low oxygen consumption rates were measured for both ranges (Swanson, 1996). Nevertheless, salinity during early life stages may indirectly influence larval development rate and hence activity levels and resulting energetic cost (Swanson, 1996). It has been suggested that muscular activity increases the metabolic rate of yolk-sac larvae by mixing the perivitelline fluid which in turn facilitates gas exchange (Peterson and Martin-Robichaud, 1983). Salinity-related differences observed in this study from 3 dph onwards support this theory, since they occurred only once larval movement has commenced; salinity clearly had an effect on rate of yolk absorption and growth between 3 and 6 dph. Whilst fish in freshwater had a lower mean dry weight than those in elevated salinities, they had a greater standard length, indicating that more yolk-sac had been absorbed and used for somatic growth.

The salinity-related differences in oxygen consumption rates (QO_2) were only detectable from 3 – 9 dph. Between 3 – 6 dph QO_2 was always significantly higher ($p < 0.05$) in freshwater adapted larvae than those in 7.5, 15 and 20 and 25 ppt (Figure 4.11.A). However, at 9 dph this pattern was reversed and freshwater larvae had a significantly lower QO_2 than those in elevated salinities. The reduction of the diffusive capacity of the epithelia and the resulting dependency on branchial respiration as larvae develop (Kamler, 1992) could explain why the more developed larvae in freshwater were more active and showed a higher metabolic rate, this being supported by branchial respiration. Depressed activity of

heavier larvae with larger yolk-reserves at higher salinities could account for the significantly lower QO_2 value for 7.5, 15 and 20 ppt compared with freshwater on day 3 and day 6. Tsuzuki *et al.* (2008) reported that larvae of the silversides (*Odontesthes hatcheri* and *Odontesthes bonariensis*) were visibly less active at 30 ppt than at lower salinities. De Silva *et al.* (1986) similarly demonstrated that larval activity may be responsible for increasing metabolic consumption; their study of un-anaesthetised fresh water *O. niloticus* larvae showed a 3-fold increase in oxygen consumption from 3.4 to 10.09 μl O_2 indv.$^{-1}$ h^{-1} between $0 - 14$ h post-hatch and $2 - 3$ days post-hatch, yet basal oxygen consumption measured for anaesthetised larvae did not show such a large change, increasing from 2.55 to 3.06 μl O_2 indv.$^{-1}$ h^{-1}.

Therefore, to conclude, this work confirms the euryhaline nature of the early life stages of the Nile tilapia, showing that salinities up to 20 ppt are tolerable, although reduced hatching rates at 15 and 20 ppt suggest that these salinities may be less than optimal. Optimum timing of transfer of embryos from freshwater to elevated salinities was 3 - 4 h post-fertilisation, following manual stripping and fertilisation of embryos, however increasing incubation salinity lengthened the time taken to hatch. Survival at yolk-sac absorption displayed a significant ($p < 0.05$) inverse relationship with increasing salinity were particularly heavy in the higher salinities of 15, 20 and 25 ppt. Mortalities occurred primarily during early yolk-sac development, stabilising from 5 dph onwards. Salinity-related differences in oxygen consumption rates (QO_2) were only detectable from $3 - 9$ dph; between $3 - 6$ dph, QO_2 was always significantly higher ($p < 0.05$) in freshwater

adapted larvae than those in 7.5, 15 and 20 and 25 ppt, however, at 9 dph this pattern was reversed and freshwater larvae had a significantly lower QO_2 than those in elevated salinities.

5 Chapter 5 Ontogenic changes in location and morphology of mitochondria-rich cells during early life stages of the Nile tilapia adapted to freshwater and brackish water.

5.1 Introduction

5.1.1 Background

As has already been established, the euryhaline Nile tilapia (*Oreochromis niloticus*) is an important culture species that displays an ability to thrive in a range of salinities, thus providing enormous flexibility of culture conditions. In addition to its importance for aquaculture, this adaptability of the Nile tilapia makes it an ideal model for studies on the biological mechanisms of adaptation during early life stages. As has already been seen in Section 1.4., embryonic and post-embryonic teleost larvae are able to live in media whose osmolality differs from their own blood osmolality, and this tolerance is due to the presence of numerous integumental or cutaneous mitochondria-rich cells (MRCs) commonly observed in the yolk-sac membrane and other body surfaces of fish embryos and larvae which play a definitive role in osmoregulation during early development. There exists an ontogenic transfer of regulative, osmoregulatory function from the integumental system to the developing branchial epithelial sites, culminating in the fully-functioning, branchial MRCs.

Although a large amount of literature exists on osmoregulation in the adult teleost (reviews Evans, 1999; 2005) much less data exist regarding osmoregulation during the more sensitive early life stages. Whilst the majority of studies on Tilapiine species have been carried out on the Mozambique tilapia (*Oreochromis mossambicus*), the only study to date conducted on the Nile tilapia is Fishelson and Bresler's (2002) comparative study on various Tilapiine *spp.*, despite that fact that this species dominates global Tilapia aquaculture. The current chapter aims to undertake key ontogenetic studies in order to address the important question of the timing of the appearance of MRCs that provide osmoregulatory capacity during critical early life stages.

5.1.2 Ontogeny of integumental mitochondria-rich cells during embryogenesis and post-embryonic development

The first appearance of MRCs in fish embryos was reported on the yolk-sac epithelia of dechorionated Mozambique tilapia (*O. mossambicus*) embryos as early as 26 h post-fertilisation, but no apical crypt to indicate functionality was apparent until 48 h post-fertilisation (Lin *et al*., 1999). Similarly, Ayson *et al.* (1994), using SEM and TEM, observed MRCs distributed underneath the pavement cells on the yolk-sac epithelium of Mozambique tilapia (*O. mossambicus*) embryos at 30 h post-fertilization in both freshwater and seawater but were presumed to be not yet functional as no apical openings were noted. MRC apical openings were first observed, albeit at a low density, at 48 h post-fertilization or half-way to hatching.

The site of active ionoregulation in the integument of post-hatch or post-embryonic teleost larvae was first demonstrated by Shelbourne (1957) who investigated the chloride regulation sites in the European plaice larvae (*Pleuronectes platessa*). Since then, integumental MRCs have been reported in the post-embryonic stages of several species (see Section 1.4.5.1 and Table 1.1).

5.1.3 Ontogeny of branchial mitochondria-rich cells during the post-embryonic period

Less is known about the ontogeny of branchial MRCs in fish larvae, with the majority of osmoregulatory studies in embryos and larvae focusing on integumental MRCs. It would seem that there is a shift in distribution of MRCs in the post-embryonic stage, from integumental to branchial sites, coinciding with yolk-sac absorption and the beginning of exogenous feeding (see Section 1.4.4). Indeed, it is widely accepted that that gills in fish larvae have an iono-regulatory function before a respiratory function. Li *et al*. (1995) identified fully-functioning MRCs at an ultrastructural level in branchial tissue of developing larvae of freshwater Mozambique tilapia (*O. mossambicus*) at 3 dph, before secondary lamellae were fully formed. MRC numbers on branchial epithelia, thereafter, showed a 50 % increase by 10 dph (at yolk-sac absorption) with this density remaining constant up to the adult stage. In agreement, the study by van der Heijden *et al*. (1999) on the fresh-water Mozambique tilapia (*O. mossambicus*) showed a similar ontogenic shift in location of active MRCs from extrabranchial to branchial sites from 24 hrs post-hatch until yolk-sac absorption; the majority of MRCs (66%) were located extrabranchially up to 2 dph

with this number declining as the majority of MRCs (80%) were found in the buccal cavity at 5 dph, before lamellae were fully formed.

5.1.4   Aims of the chapter

It has been demonstrated in the preceding chapters that ontogenic variations exist in osmoregulatory capacity during early life stages of the Nile tilapia which, in turn, is reflected in survival, growth and metabolic burden. The work presented in the current chapter will therefore explore the hypothesis that the ability of the Nile tilapia to withstand elevated salinities, during early life stages, is due to the presence of extrabranchial mitochondria-rich cells (MRCs) that confer an osmoregulatory capacity before the development of the adult branchial osmoregulatory system, and will offer a more comprehensive study on the ontogenetic development of osmoregulatory system of this less studied species.

In order to test this hypothesis, the following aspects were investigated:

- The pattern of ontogenic changes in the location, size and density of integumental MRCs in the Nile tilapia adapted to freshwater and brackish water (15 ppt) using Na^+/K^+-ATPase immunohistochemistry with light microscopy and confocal scanning laser microscopy.

- The role of the developing gills and branchial regions during the post-embryonic period.

- The effect of salinity on the morphology of the apical structure of MRCs using scanning electron microscopy.

5.2 Materials and Methods

5.2.1   Egg supply, artificial incubation systems and transfer regime

Broodstock were maintained as outlined in Section 2.1.1. and eggs were obtained by the manual stripping method, as outlined in Section 2.1.2. The experimental salinity (15 ppt) was prepared as outlined in Section 2.2. Batches of eggs from several females were combined to provide a heterogeneous sample. Half a batch of eggs were incubated in freshwater and the other half were transferred to brackish water (15 ± 1 ppt) at 3 - 4 h post-fertilisation, according to methods outlined in Section 2.3. Post-embryonic larvae were sampled from both freshwater and brackish water at hatch (designated day 0), and subsequently at 1, 3, 5 and 7 days post-hatch (dph).

5.2.2   Antibody

A mouse monoclonal antibody raised against the α-subunit of chicken Na^+/K^+-ATPase (mouse anti-chicken IgG α5, Takeyasu *et al*. 1988) that cross-reacts with fish tissue (van der Heijden *et al*. 1999) was used to detect integumental MRCs in yolk-sac larvae. This antibody, developed by D.M. Fambrough (John Hopkins University, MD, US), was obtained from the Development Studies Hybridoma Bank developed under the auspices of the NICHD and maintained by the University of Iowa, Department of Biological Sciences, Iowa City, IA 52242, US).

5.2.3   Whole mount immunohistochemistry

5.2.3.1   Light microscopy

Whole-mount post-embryonic larvae were fixed and labelled according to the following protocol:

(i) Fixed in a 4% (w/v) paraformaldehyde in 0.1 M phosphate buffer (PB; pH 7.4) (see Appendix 1) for 24 h at 4 $^{\circ}$C,

(ii) Preserved in 70% ethanol at 4 $^{\circ}$C,

(iii) Rinsed twice for 20 min each time with phosphate buffered saline (PBS) (see Appendix 1) at room temperature,

(iv) Incubated with monoclonal antibody against α5-subunit of chicken Na$^+$/K$^+$-ATPase (IgG α5) diluted 1:200 with PBS containing blocking agents; 10% normal goat serum (NGS) and 1% bovine serum albumin overnight (BSA) at 4 $^{\circ}$C,

(v) Rinsed twice for 20 min each time in PBS at room temperature,

(vi) Incubated with secondary antibody peroxidase conjugated goat anti-mouse IgG (Molecular Probes, Invitrogen) diluted in PBS (1:100) at room temperature for 1 hour,

(vii) Rinsed twice for 20 min each time in PBS at room temperature,

(viii) Incubated with freshly prepared chromogen stain Nova Red for 10 min at room temperature (Vector$^{®}$ Nova Red Substrate Kit for peroxidase, Vector Laboratories Inc., California, U.S.),

(ix) Rinsed twice briefly in distilled water and kept in the dark at 4 ℃ until observation.

Control samples were prepared without the primary antibody.

Control and labelled samples were mounted in glycerin on a slide and photographed using a JVC KY-F30B 3CCD camera with an interfacing × 2.5 top lens fitted to an Olympus BH2 compound microscope under a x40 objective lens. MRGrab version 1.0 (Zeiss) software was used to capture and save images. ImageJ version version 1.43 (National Institutes of Health, U.S.) software and a slide graticule allowed calibration of scale bar on images.

5.2.3.2   Confocal Scanning Laser Microscopy

To reveal the three dimensional structure and orientation of the MRCs using confocal scanning laser microscopy (CSLM), whole mount preparations of larvae from freshwater and brackish water (day 3) were prepared as above (stages (i) − (v)). Stage (vi) onwards was replaced with incubation with goat anti-mouse IgG conjugated with Alexa Fluor 488 (Molecular Probes, Invitrogen) (1:100) for 2 h in PBS at room temperature followed by washing twice for 20 min each time in PBS at room temperature. This was followed by a 30 min incubation at room temperature with the actin stain Texas Red (594) phalloidin (Molecular Probes, Invitrogen) (4 µl of 0.2 U µl^{-1} phalloidin in 200 µl PBS). The nuclear stain DAPI (4',6-Diamidino-2-phenylindole) was added to the samples immediately prior to observation. Samples were kept in the dark at 4 ℃ until observation. Control samples without the primary antibody were prepared to determine the auto-fluorescence of the sample.

Control and labeled samples were mounted in glycerin on a 35 mm glass base dish (Iwaki, Scitech Div., Japan) and observed using a Leica TCS SP2 AOBS confocal scanning laser microscope (CSLM) (Leica Microsystems, Milton Keynes, U.K.) coupled to a DM TRE2 inverted miscroscope (Leica Microsystems, Milton Keynes, U.K.) and employing a x 63 oil/glycerol immersion objective, in conjunction with Leica Confocal Software (v. 6.21). Images were captured using grey, red, green and blue channels using recommended excitation and emission wavelengths for the different fluorescent dyes (Table 5.1). To avoid cross talk, a sequential configuration was used with images collected successively rather than simultaneously on three separate channels.

Table 5. 1 Properties of fluorescent dyes used to identify MRCs in integument of Nile tilapia larvae.

Target label	Probe	Channel	Excitation maximum (nm)	Emission maximum (nm)	Laser Line
Na^+/K^+-ATPase	Alexa Fluor	Green	488	498	488
Nuclei	DAPI	Blue	405	411	405
Actin	Phalloidin – Texas Red	Red	594	600	594

5.2.4   Mitochondria-rich cell number and size

Quantitative changes in diameter (μm) and density (number of MRCs mm^{-2}) of cutaneous MRCs were estimated on pre-defined areas of yolk sac larvae (Figure 3.1): three standardised fields on the yolk-sac, one standardised field at mid-point on the tail and one standardised field on the outer opercular region of the head were examined on a minimum of 5 larvae per developmental stage from each adaptive treatment on 0, 1, 3 and 5 days post-hatch (dph). Inner operculum quantifications were carried out by dissecting out the operculum on 3, 5, 7 and 9 dph.

Cell density was determined as number of immunoreactive cells per micrograph and final values were expressed as number of immunoreactive cells mm^{-2}.

- Mean 2-D Na$^+$/K$^+$-ATPase immunoreactive area of MRCs was calculated on the yolk-sac and inner opercular area as follows: Mean 2-D Na$^+$/K$^+$-ATPase immunoreactive area of cell (μm^{-2}) = Π r^2.

- Percentage (%) of skin (mm^{-2}) occupied by immunoreactive cells on the yolk-sac and inner opercular area was calculated as follows: % 2-D Na$^+$/K$^+$-ATPase immunoreactive cell area /mm^{-2} skin = (mean 2-D Na$^+$/K$^+$-ATPase immunoreactive area of MRCs (μm^{-2}) x mean density of MRC mm^{-2})/1000000)*100.
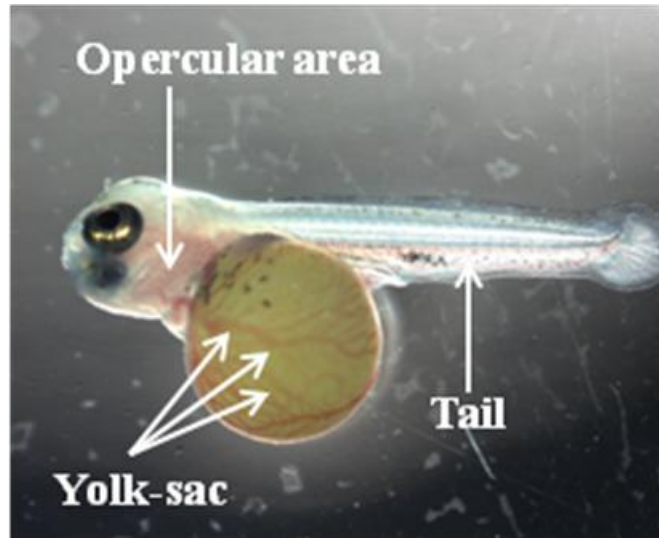
Figure 5. 1 Pre-defined areas of Nile tilapia larvae used for measurement of quantitative changes in MRC distribution.

5.2.5   Scanning electron microscopy

Scanning electron microscopy was used for external morphological studies. Whole yolk-sac larvae (day 0, 3 and 7) and excised gills (day 3 and 7) from freshwater and brackish water were fixed in 2.5 % (v/v) glutaraldehyde in 0.1 M sodium cacodylate buffer (see Appendix 1) and fixed at 4° C for two days. Samples were then transferred to buffer rinse (see Appendix 1) and stored at 4 °C. Samples were then transferred to 1% (w/v) osmium tetroxide in 0.1 M sodium cacodylate buffer (see Appendix 1) for 2 h. They were then dehydrated through an ethanol series (30% for 30 min, 60% for 30 min, 90% for 30 min and 100% twice for 30 min each) before critical point drying in a Bal-Tec 030 critical point dryer. Samples were mounted on specimen stubs using double-faced tape and gold sputter-

coated for 1.5 min at 40 mA to coat to a thickness of *c.* 2 -3 nm (Edwards sputter coater, S150B, BOC Edwards, Wilmington, MA, US). Images were collected with a Scanning Electron Microscope (SEM; JEOL JSM6460LV; Jeol, Welwyn Garden City, UK). Images were taken at between 5 - 10 kV and a working distance of 10 mm.

5.2.6   Statistical methods

Statistical analyses were carried out with Minitab 16 software using a General Linear Model or One-way analysis of variance (ANOVA) with Tukey's post-hoc pair-wise comparisons. Homogeneity of variance was tested using Levene's test and normality was tested using the Anderson-Darling test. Where data failed these assumptions, they were transformed using an appropriate transformation *i.e.* logbase $_{10}$. Significance was accepted when $p < 0.05$.

5.3 Results

5.3.1   Gill and larval development

At hatch, both freshwater and brackish water adapted larvae possessed a large yolk-sac, budding pectoral fins and growing teguments of the primordial opercula that partly covered the emergent gills. By 1 dph, four gill arches were clearly distinguished by light microscopy with short filaments that displayed budding lamellae and clearly defined vasculature (Figure 5.2.A and B). By 3 dph, the yolk-sac was much reduced in size and still showed a complex blood-plexus system overlying the epithelium of the yolk-sac. The blood network was fully developed on the caudal fin (Figure 5.2.C). The mouth was fully open and slight jaw movement could be observed. The operculum almost completely covered the gills and the prominent thymus was visible (Figure 5.2.D). At 7 dph, yolk-sac absorption was almost complete and the operculum completely covered the gill filaments and adult-type fin organisation was evident (Figure 5.2.E).
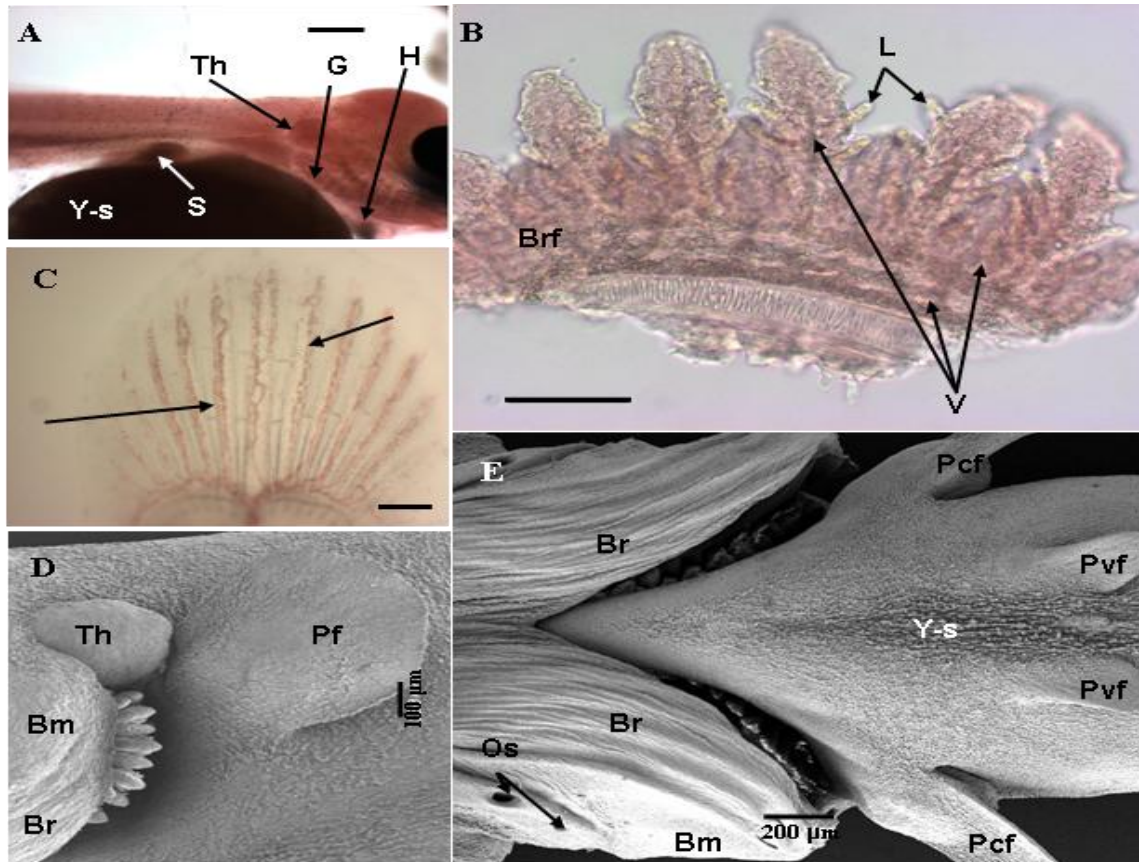
Figure 5. 2 Development of branchial system and vasculature in Nile tilapia. **A)** Freshwater adapted larvae at 1 dph showing gills (G), budding thymus (Th), heart (H), yolk-sac (Y-s) and stomach (S) [Bar = 500 μm] (LM), **B)** Detail of branchial arch of freshwater adapted larvae at 1 dph showing pairs of hemibranchs or branchial filaments (Brf) with emergent lamellae (L) with clearly defined vasculature (V) (arrows) [Bar = 100 μm] (LM), **C)** Developing caudal fin of larvae adapted to brackish water at 3 dph showing vasculature (arrow) [Bar = 200 μm] (LM), **D)** Freshwater adapted larvae 3 dph showing pectoral fin (Pf), prominent thymus (Th) and branchiostegal membrane or operculum with visible branchiostegal rays (Br) partly covering gill arches and developing gills [Bar = 100 μm] (SEM) and **E)** Underside of brackish water adapted larvae at 7 dph showing gills completely covered by the fully-defined branchiostegal membrane (Bm) with branchiostegal rays (Br), opercular spiracles (Os) and pectoral (Pcf) and pelvic fins (Pvf) developing on shrunken yolk-sac (Y-s) [Bar = 200 μm] (SEM).

5.3.2 Ontogenic changes in size of mitochondria-rich cells in freshwater and brackish water

Mitochondria-rich cells were detected by whole-mount immunohistochemistry with anti-Na^+/K^+-ATPase on the integument of both freshwater and brackish water adapted larvae from 0 - 7 dph and on the inner opercular area from 3 - 9 dph. The overall effects of age, treatment and their interaction and also location of MRCs on MRC diameter (μm) are summarised in Table 5.2. and Figure 5.3.

Table 5. 2 Analysis of Variance for MRC diameter (μm) (General Linear Model; p < 0.001).

Source	DF	F	P-value
MRC diameter:			
Age	4	14.15	0.001
Treatment	1	436.56	0.001
Age vs. treatment	4	85.79	0.001
Area on fish	3	139.66	0.001
Error	5634		
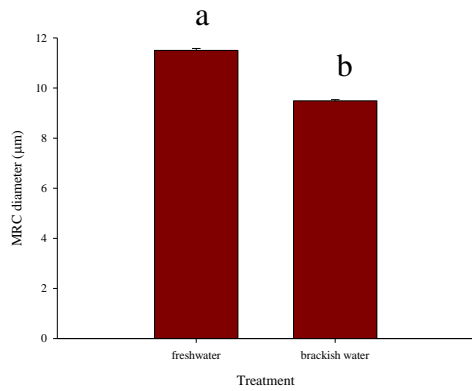
A)
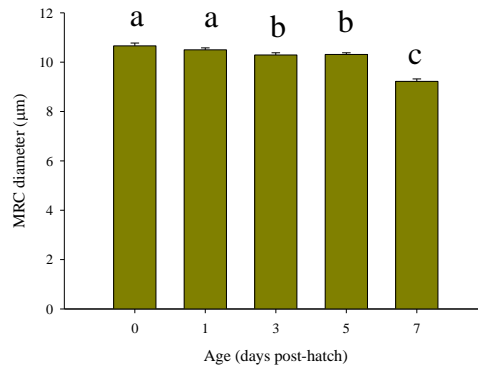
B)
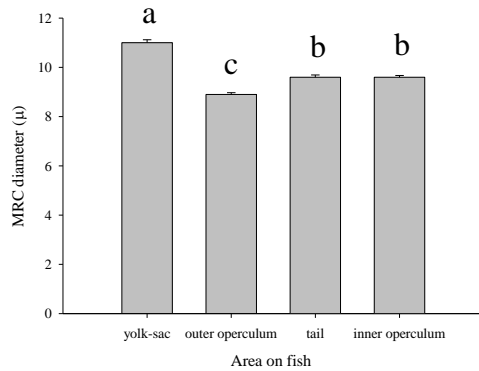
C)

Figure 5. 3 Overall effects of **A)** Treatment **B)** Age and **C)** Location of MRC on fish on MRC diameter. Mean ±S.E. Different letters above each bar indicate significant differences (General Linear Model with Tukey's post-hoc pairwise comparison; $p < 0.05$).

In freshwater adapted larvae, Na^+/K^+-ATPase immunoreactive cells located on the outer operculum and tail increased in size between hatch and 5 dph, significantly in the case of the outer operculum (General Linear Model with Tukey's post-hoc pairwise comparisons; $p < 0.05$). In contrast, immunoreactive cells located on the abdominal epithelium of the yolk-sac, decreased in size significantly (GLM; $p < 0.05$) between hatch and 5 dph (Table 5.3;

Figure 5.4; Figure 5.5.). A similar pattern was displayed in brackish water adapted larvae where immunoreactive cells located on the outer operculum and tail showed a significant increase in size (GLM; $p < 0.05$) between hatch and 5 dph, but, on the abdominal epithelium of the yolk-sac, decreased significantly ($p < 0.05$) over the developmental period studied (Table 5.3; Figure 5.4; Figure 5.5.). The diameter of immunoreactive cells on the yolk-sac epithelium of brackish water adapted larvae was significantly greater (GLM; $p < 0.05$) from 1 to 5 dph than those hatched in freshwater (Table 5.3; Figure 5.4; Figure 5.5.; Figure 5.6.)

Immunopositive cells located on the inner epithelium of the opercular membrane in both fresh and brackish water decreased in size over time from 3 dph onwards, significantly in the case of brackish water (GLM; $p < 0.05$). In addition, immunopositive cells on the inner epithelium of the opercular membrane from brackish water adapted larvae were always significantly larger (GLM; $p < 0.05$) than freshwater for all days (Table 5.3).

Table 5. 3 Diameter of Na^+/ K^+-ATPase immunoreactive cells at different developmental stages of Nile tilapia. Mean ± S.E. Different superscript notations within the same column indicate significant differences between hatch and subsequent days for outer operculum, tail and yolk-sac and between 3 dph and subsequent days for inner operculum; asterisks in brackish water column indicate a significant difference from the corresponding freshwater value (GLM with Tukey's post-hoc pairwise comparisons; $p < 0.05$).

	Na^+/K^+-ATPase immunoreactive cell diameter (μm) ± S.E.	# fish measured/ total # Na^+/K^+-ATPase immunoreactive cells measured	Na^+/K^+-ATPase immunoreactive cell diameter (μm) ± S.E.	# fish measured/ total # Na^+/K^+-ATPase immunoreactive cells measured
Location of NKA-IR cells:	*Freshwater*		*Brackish water*	
Outer operculum:				
Hatch	$7.7^a \pm 0.17$	8/175	$7.7^a \pm 0.19$	8/85
1 day post-hatch	$8.8^b \pm 0.11$	7/212	$10.1^{b*} \pm 0.20$	5/105
3 days post-hatch	$7.6^a \pm 0.16$	6/118	$10.0^{b*} \pm 0.27$	6/97
5 days post-hatch	$9.8^b \pm 0.19$	5/148	$11.0^{b*} \pm 0.31$	8/58
7 days post-hatch	Not detectable	9	Not detectable	8

Table 5.3. cont.

	Na⁺/K⁺-ATPase immunoreactive cell diameter (µm) ± S.E.	# fish measured/ total # Na⁺/K⁺-ATPase immunoreactive cells measured	Na⁺/K⁺-ATPase immunoreactive cell diameter (µm) ± S.E.	# fish measured/ total # Na⁺/K⁺-ATPase immunoreactive cells measured
Location of NKA-IR cells:	*Freshwater*		*Brackish water*	
Tail :				
Hatch	9.5 ^{a} ± 0.16	8/167	8.6 ^{a*} ± 0.20	8/84
1 day post-hatch	9.2 ^{a} ± 0.14	7/132	11.1 ^{b*} ± 0.33	0.175/70
3 days post-hatch	7.9 ^{b} ± 0.19	6/89	11.8 ^{b*} ± 0.31	6/70
5 days post-hatch	9.7 ^{a} ± 0.20	5/57	10.4 ^{b} ± 0.20	8/59
7 days post-hatch	Not detectable	9	Not detectable	8
Yolk-sac:				
Hatch	12.3 ^{a} ± 0.17	8/306	13.4 ^{a} ± 0.31	8/234
1 day post-hatch	10.9 ^{b} ± 0.15	7/219	12.6 ^{a*} ± 0.27	5/187
3 days post-hatch	9.0 ^{b} ± 0.11	6/252	14.5 ^{a*} ± 0.27	6/214
5 days post-hatch	9.5 ^{b} ± 0.08	5/260	11.3 ^{b*} ± 0.17	8/178
7 days post-hatch	Not detectable	9	Not detectable	8

Table 5.3. cont.

	Na^+/K^+-ATPase immunoreactive cell diameter (μm) ± S.E.	# fish measured/ total # Na^+/K^+-ATPase immunoreactive cells measured	Na^+/K^+-ATPase immunoreactive cell diameter (μm) ± S.E.	# fish measured/ total # Na^+/K^+-ATPase immunoreactive cells measured
Location of NKA-IR cells:	*Freshwater*		*Brackish water*	
Inner operculum:				
Hatch	Not detectable	8	Not detectable	8
1 day post-hatch	Not detectable	7	Not detectable	5
3 days post-hatch	8.9[b] ± 1.10	6/123	11.7[a*] ± 0.31	7/116
5 days post-hatch	9.4[a] ± 0.13	5/133	11.0[a*] ± 0.21	8/105
7 days post-hatch	8.6[b] ± 0.09	9/269	10.4[b*] ± 0.21	8/119
9 days post-hatch	8.0[c] ± 0.10	7/239	10.1[b*] ± 0.21	6/107
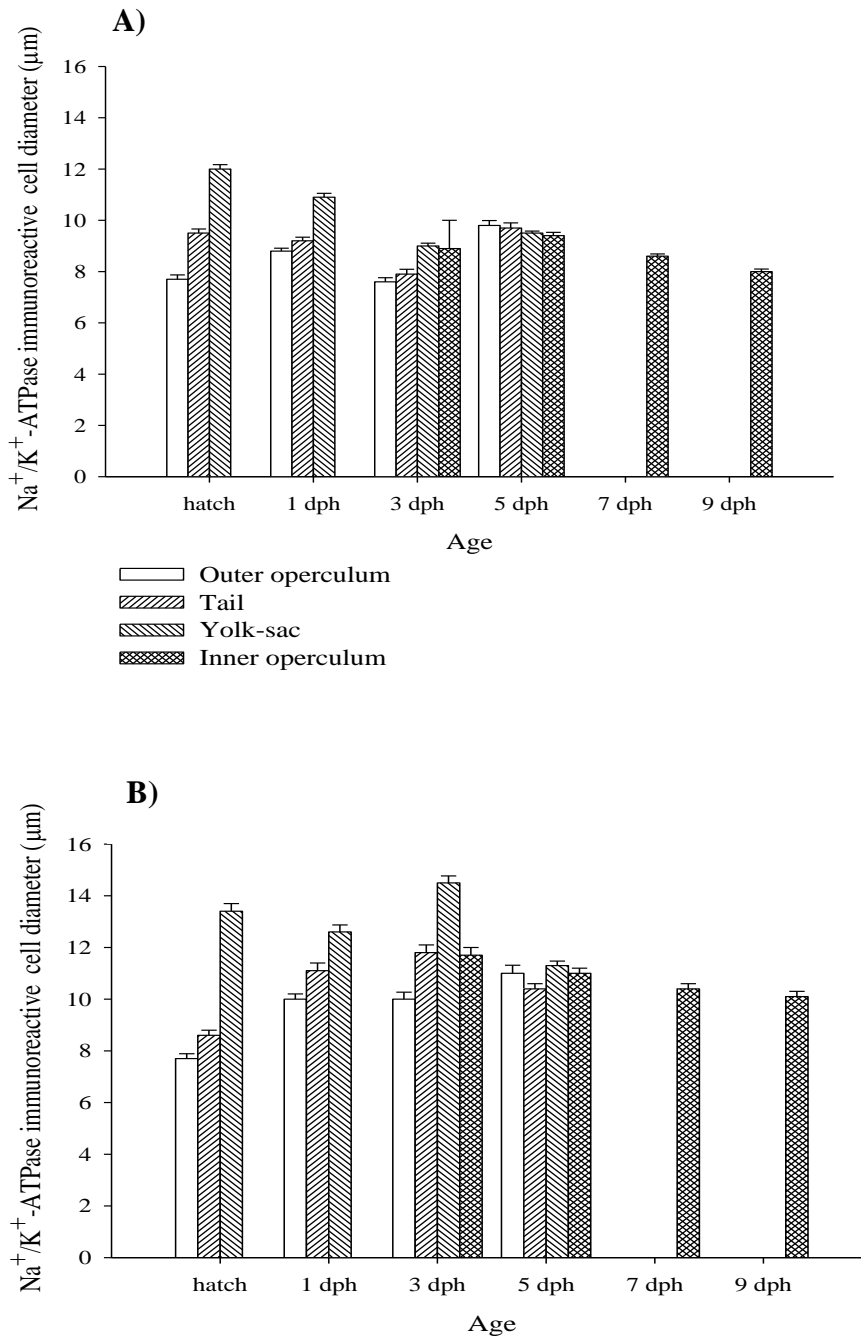
Figure 5. 4 Diameter of Na^+/ K^+-ATPase immunoreactive cells (µm) at different developmental stages in Nile tilapia. Mean ± S.E. **A)** Freshwater and **B)** Brackish water. Statistical differences between days are presented in corresponding Table 5.3. rather than in graph for clarity of presentation.
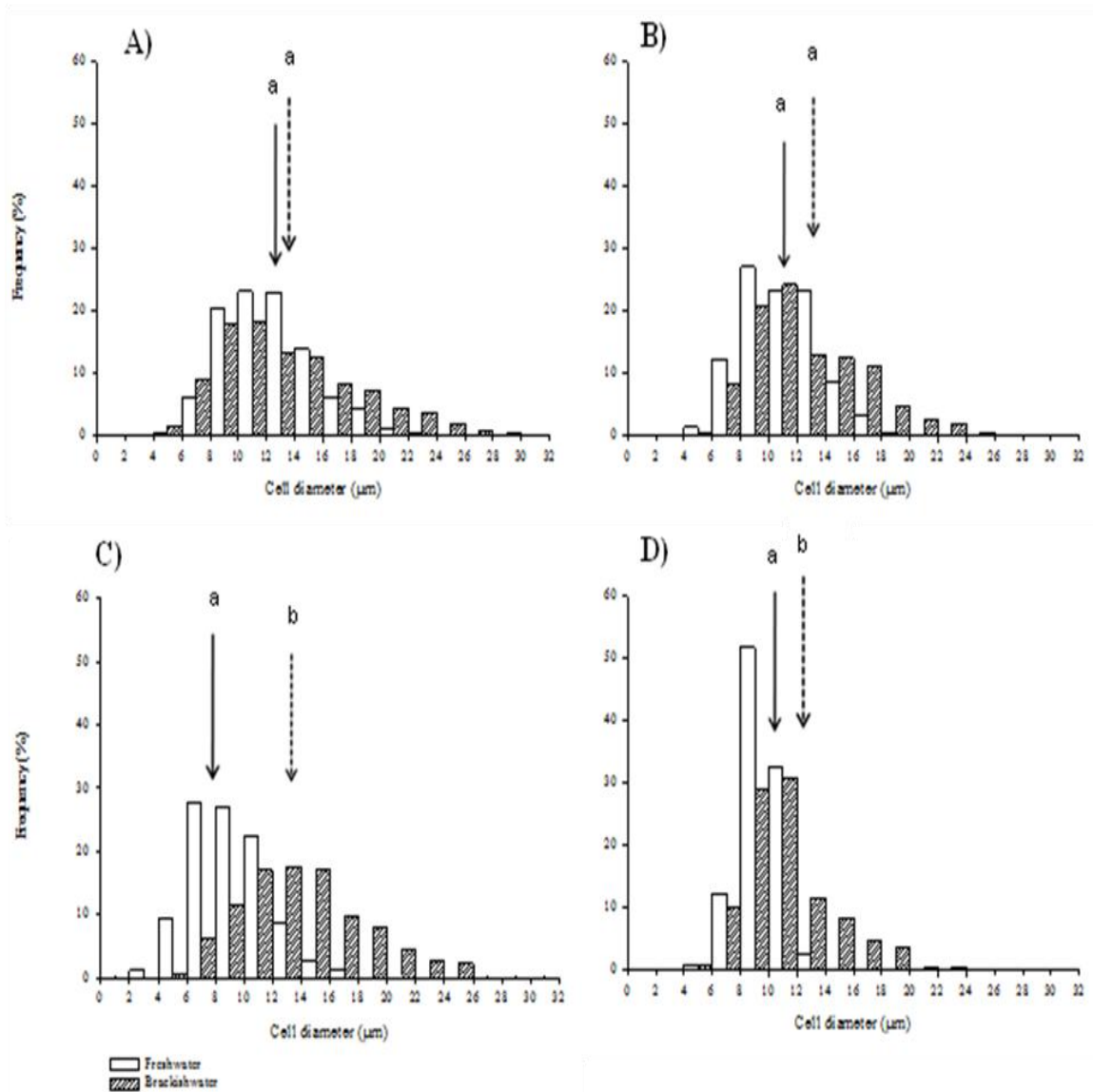
Figure 5. 5 Size-frequency distributions of Na$^+$/ K$^+$-ATPase immunoreactive MRCs on the yolk-sac epithelia of Nile tilapia in freshwater and brackish water at different times during development. **A)** Hatch, **B)** 1 dph, **C)** 3 dph and **D)** 5 dph. Arrows indicate mean MRCs diameter (µm) (solid arrows = freshwater and dashed arrows = brackish water), different letters indicate a significant difference between treatments (GLM with Tukey's post-hoc pairwise comparison; p < 0.05).
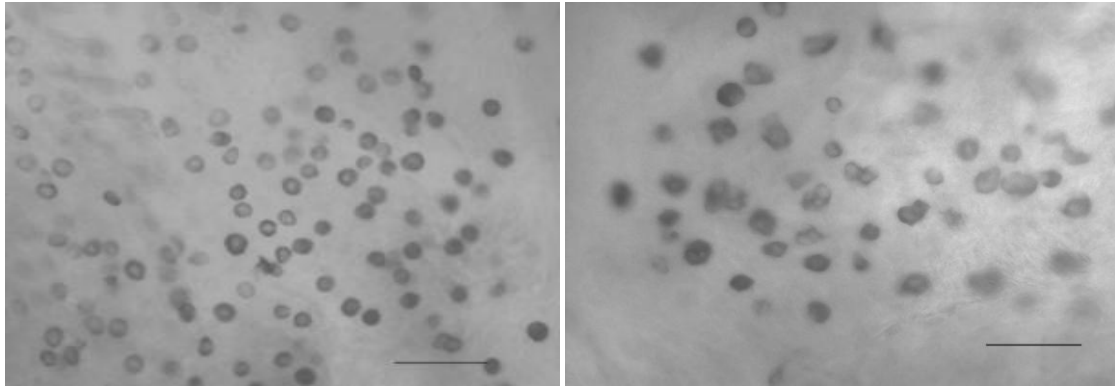
A)   **B)**

Figure 5. 6 Variations in size and distribution of Na^+/ K^+-ATPase immunoreactive MRCs on yolk-sac epithelium of Nile tilapia adapted to freshwater and brackish water using light microscopy. **A)** Densely packed, smaller MRCs from freshwater adapted larvae at 5 dph [Bar = 50 µm] and **B)** Larger, more dispersed MRCs from brackish water adapted larvae at 5 dph [Bar = 50 um).

5.3.3   Ontogenic changes in distribution and numerical density of mitochondria-rich cells in freshwater and brackish water

The overall effects of age, treatment and their interaction and also location on fish on MRC density (# MRCs/mm^{-2}) are summarised in Table 5.4. and Figure 5.7.

Table 5. 4 Analysis of Variance for density (#MRCs/mm^{-2}) (General Linear Model; p < 0.001).

Source	DF	F	P-value
MRC density:			
Age	4	62.35	0.001
Treatment	1	66.59	0.001
Age vs. treatment	4	1.06	0.375
Area on fish	3	29.47	0.001
Error	333		

A)

B)

C)
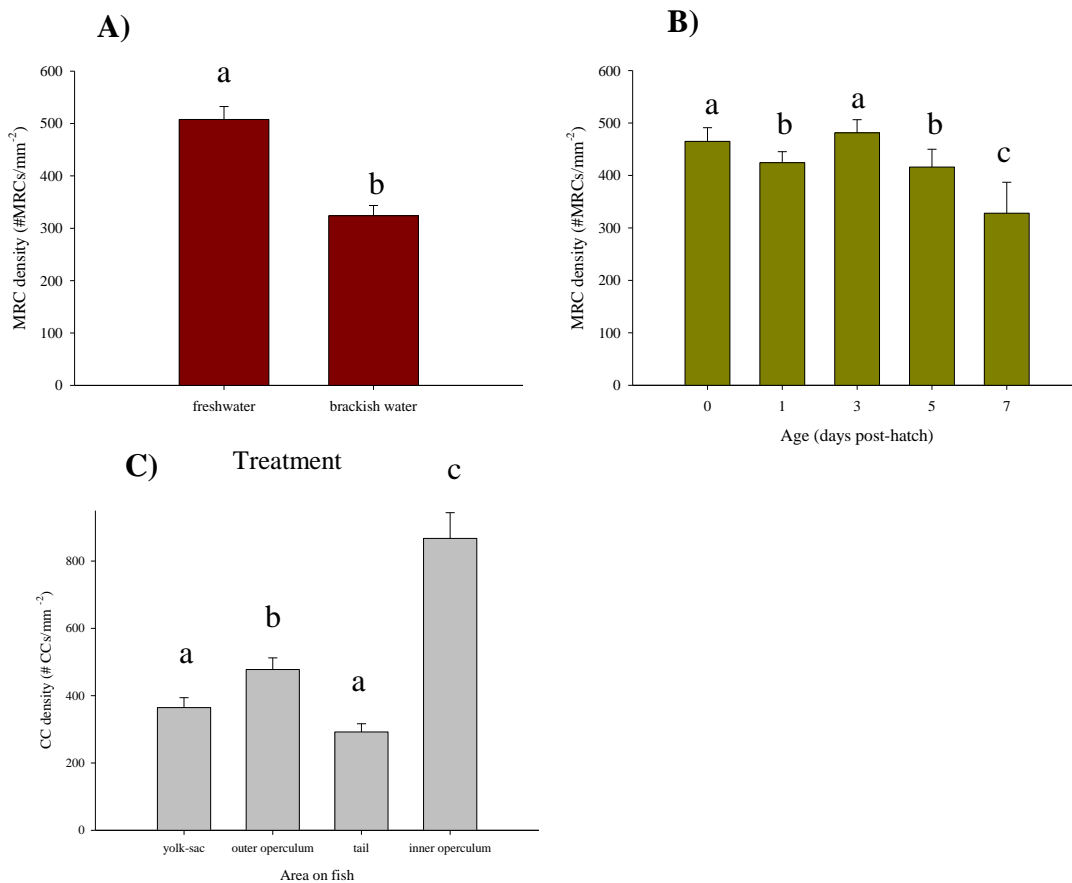
Figure 5. 7 Overall effects of **A)** Treatment **B)** Age and **C)** Location of MRC on fish on MRC density. Mean ±S.E. Different letters above each bar indicate significant differences (General Linear Model with Tukey's post-hoc pairwise comparison; $p < 0.05$).

At hatching, before the full development of the gills and opening of the digestive tract and mouth, immunoreactive MRCs were only observed on the body surface of freshwater and brackish water adapted larvae. They were evenly distributed over the body from the head to the tail but were relatively less dense on the abdominal epithelium of the yolk-sac (Table 5.5.; Figure 5.8.).

By 3 dph, fewer MRCs were observed on the head and tail area than on the yolk-sac in both treatments (Table 5.5.; Figure 5.8.), with a marked concentration observed at the posterior and anterior end of the yolk-sac *i.e.* overlying the vessel network near the anal opening (Figure 5.9.A) and pericardial membrane (Figure 5.9.B). Punctate, tear-drop shape immunoreactive cells were visible on caudal and pectoral fins of both freshwater and brackish water adapted larvae coinciding with the formation of the blood network (Figure 5.9.C and D).

Corresponding to the onset of mouth movements and ventilation, a rich population of MRCs was observed at 3 dph onwards on the inner opercular area of both freshwater and brackish water adapted larvae (Figure 5.9.E). Likewise, confocal scanning laser microscopy revealed a population of MRCs on the forming gills (Figure 5.10.A) at 3 dph with SEM

revealing apical openings suggesting functionality (Figure 3.11.C). Coinciding with this, integumental MRCs became scarcer, disappearing completely on the outer opercular region by 7 dph. In addition, clustered MRCs were visible at the base of developing fins on the posterior section of larvae (Figure 5.9.F).

Freshwater MRCs density decreased significantly (GLM; $p < 0.05$) in all areas examined on larval integument between hatch and 7 dph. However, on the outer operculum, cell density rose slightly between hatch and 1 dph and thereafter decreased, with immunoreactive cells disappearing completely by 7 dph. Similarly, on the abdominal epithelium of the yolk-sac, a significant increase in density between hatch and day 3 was evident (GLM; $p < 0.05$), decreasing thereafter. In the tail area, a steady decrease was seen over time. Correspondingly, in brackish water, a significant decrease in final density was apparent on all areas between hatch and 7 dph (GLM; $p < 0.05$). On the outer operculum and tail area, a continuous decrease in density was evident whereas, in the yolk-sac, a significant increase in cell density between hatch and day 3 (GLM; $p < 0.005$) was followed by a decrease to day 7. In both freshwater and brackish water adapted larvae, density of immunoreactive cells on the inner opercular area increased significantly between 3 to 9 dph. Integumental and inner opercular immunoreactive cells were always denser in freshwater larvae than brackish water larvae on all areas examined throughout the developmental period studied (Table 5.5.; Figure 5.8.).
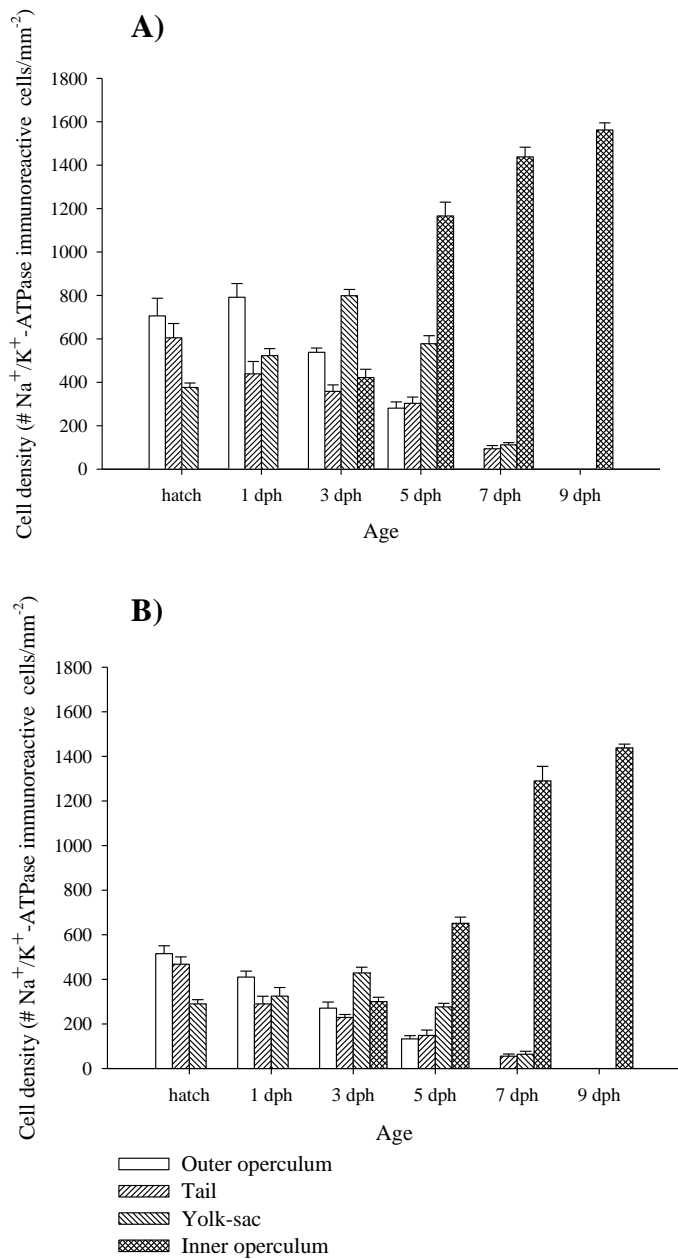
Figure 5. 8 Density of Na^+/ K^+-ATPase immunoreactive cells (# Na+/K+-ATPase immunoreactive cells /mm^{-2}) at different developmental stages in Nile tilapia. Mean ± S.E. **A)** Freshwater adapted and **B)** Brackish water adapted. Statistical differences between days are presented in corresponding Table 5.5. rather than in graph for clarity of presentation.
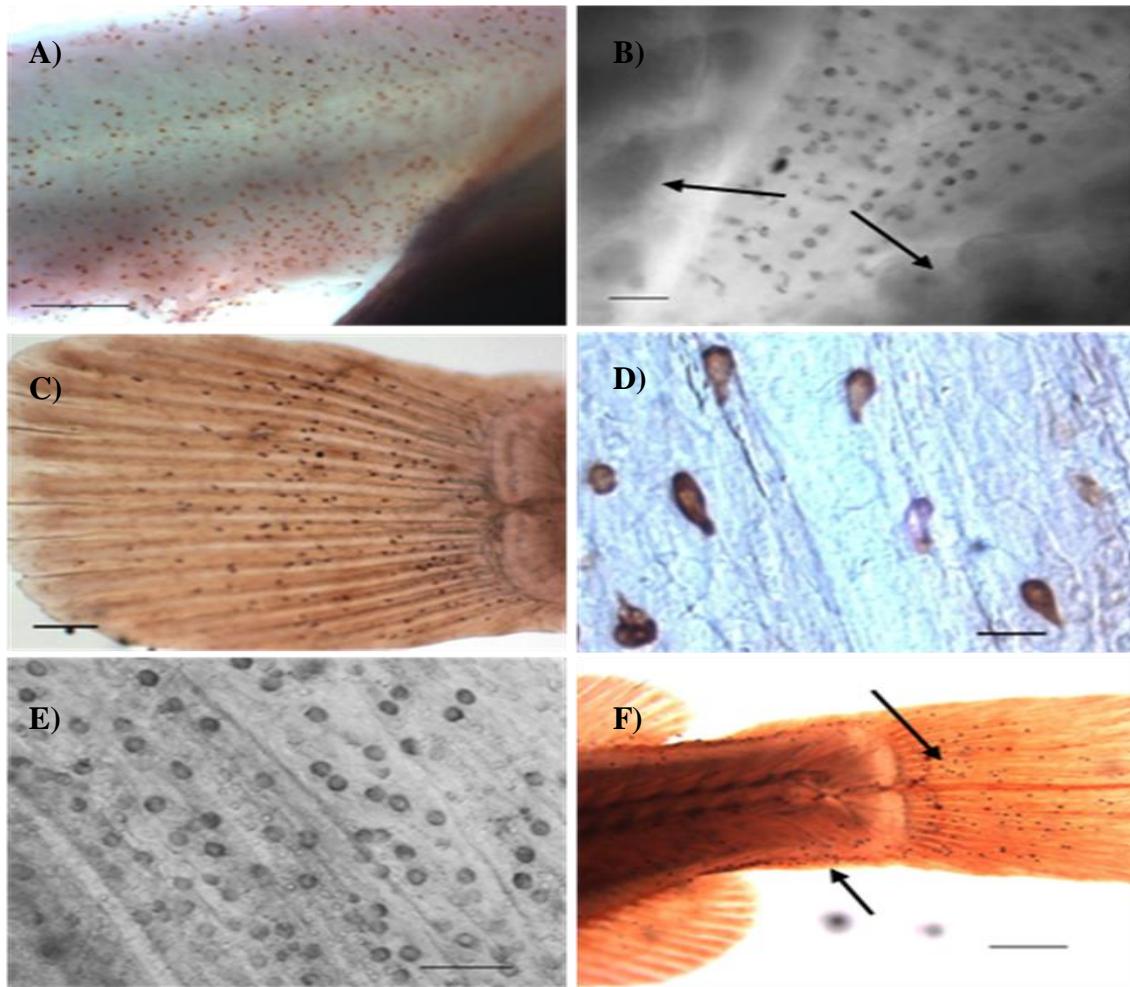
Figure 5. 9 Distribution of mitochondria-rich cells (MRCs) as revealed by anti-Na$^+$/K$^+$-ATPase antibody during post-embryonic development of Nile tilapia using light microscopy. **A)** Detail of anal region of freshwater adapted larvae at 3 dph showing clustered immunoreactive MRCs [Bar = 200 μm], **B)** MRCs on ventral region of brackish water adapted larvae at 3 dph. Arrows indicates presence of gills underlying opercula [Bar = 30 μm], **C)** Caudal fin of freshwater adapted larvae at 3 dph showing immunoreactive MRCs [Bar = 200 μm] (LM), **D)** Detail of immunoreactive MRCs on caudal fin of brackish water adapted larvae at 3 dph [Bar = 20 μm], **E)** Inner opercular area of freshwater adapted larvae at 5 dph showing immunoreactive MRCs [Bar = 50 μm] (LM) and **F)** Caudal extremity of brackish water adapted larvae at 7 dph. Arrows indicate location of clustered immunoreactive MRCs [Bar = 300 μm].
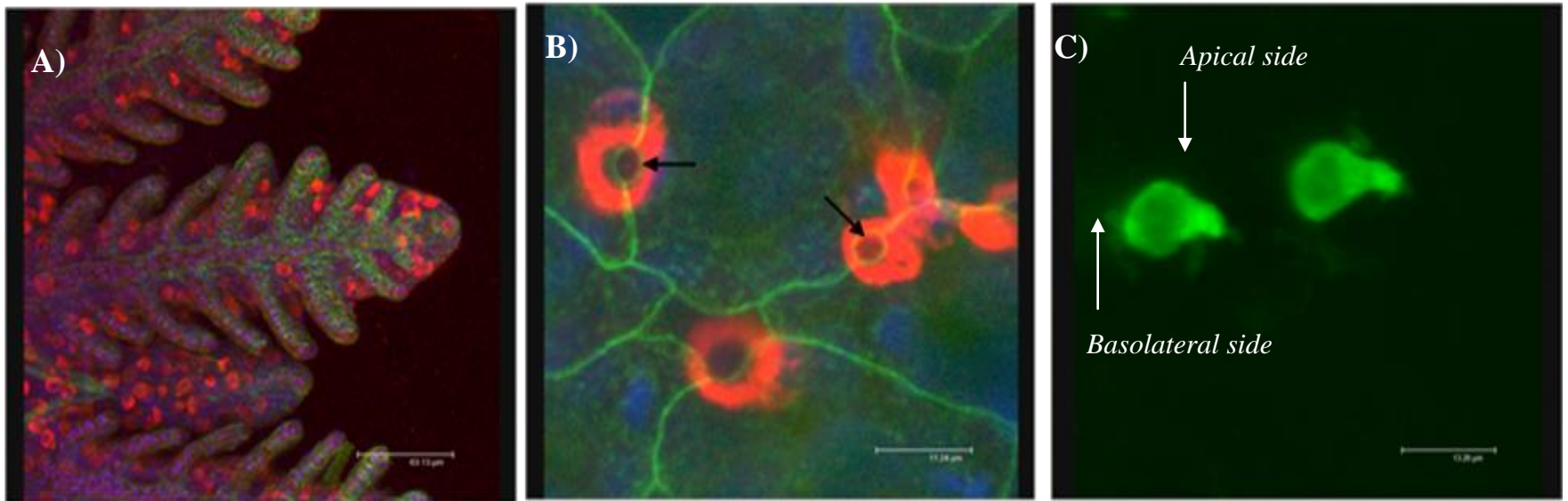
Figure 5. 10 Mitochondria-rich cells (MRCs) as visualised by confocal scanning laser microscopy. **A)** Developing gills brackish water adapted larvae at 3 dph showing clustered MRCs at base of lamellae as detected by triple staining (anti-Na$^+$/K$^+$-ATPase (red), actin-staining phalloidin (green) and nuclear staining DAPI (blue)) [Bar = 63.13 μm], **B)** Detail of MRC on the yolk-sac epithelium of brackish water adapted larvae at 3 dph as detected by triple staining (anti-Na$^+$/K$^+$-ATPase (red), actin-staining phalloidin (green) and nuclear staining DAPI (blue)) - *note* arrows indicating actin-rich border surrounding apical pores [Bar = 11.24 μm] and **C)** Individual tear-drop shape MRCs on the yolk-sac epithelium of brackish water adapted larvae at 3 dph as detected by anti-Na$^+$/K$^+$-ATPase (green) showing orientation of cell [Bar = 13.26 μm].
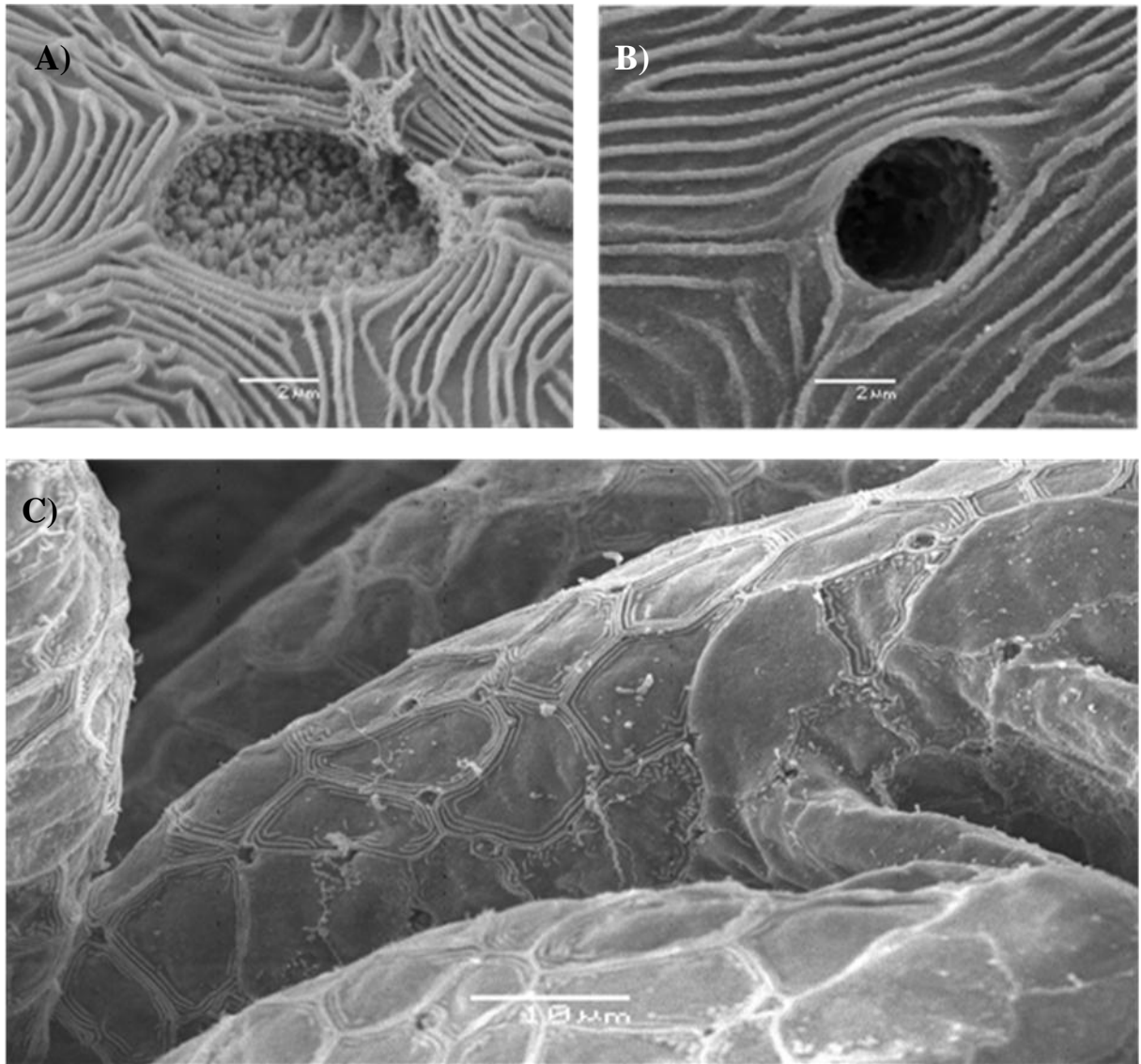
Figure 5. 11 Scanning electron micrographs of external morphology of mitochondria-rich cells (MRCs). **A)** Apical opening of MRC on yolk-sac epithelia of Nile tilapia in freshwater adapted larvae at hatch [Bar = 2 μm), **B)** Apical opening of MRC on yolk-sac epithelia of Nile tilapia in brackish water adapted larvae at hatch [Bar = 2 μm] and **C)** Lower magnification of apical openings of MRCs on gill filaments of freshwater larvae at 3 dph [Bar = 10 μm]

.

Table 5. 5 Density of Na$^+$/ K$^+$-ATPase immunoreactive cells at different developmental stages of Nile tilapia. Mean $\pm$ S.E.; different superscript letters within the same column indicate significant differences between hatch and subsequent days for outer operculum, tail and yolk-sac and between 3 dph and subsequent days for inner operculum; asterisks in brackish water column indicate a significant difference from the corresponding freshwater value (General Linear Model with Tukey's post-hoc pairwise comparisons; $p < 0.05$).

	Cell density (# Na$^+$/K$^+$-ATPase immunoreactive cells/mm $^{-2}$) + S.E.	# fish measured	Cell density (# Na$^+$/K$^+$-ATPase immunoreactive cells/mm $^{-2}$) + S.E.	# fish measured
Location of NKA-IR cells:	*Freshwater*		*Brackish water*	
Outer operculum:				
Hatch	706.8^a $\pm$ 81.75	8	515.3^a $\pm$ 35.20	8
1 day post-hatch	792.6^a $\pm$ 63.36	7	410.9^{a*} $\pm$ 27.68	6
3 days post-hatch	538.7^a $\pm$ 20.61	6	271.4^{a*} $\pm$ 27.28	6
5 days post-hatch	281.4^b $\pm$ 29.74	5	132.8^b $\pm$ 14.66	8
7 days post-hatch	Not detectable	9	Not detectable	8

Table 5.5 cont.

	Cell density (# Na$^+$/K$^+$-ATPase immunoreactive cells/mm^{-2}) + S.E.	# fish measured	Cell density (# Na$^+$/K$^+$-ATPase immunoreactive cells/mm^{-2}) + S.E.	# fish measured
Location of NKA-IR cells:	*Freshwater*		*Brackish water*	
Tail:				
Hatch	605.2^a ± 66.60	8	468.9^a ± 32.82	8
1 day post-hatch	439.9^a ± 57.49	7	289.8^a ± 34.31	6
3 days post-hatch	358.3^b ± 30.99	6	229.2^b ± 13.10	6
5 days post-hatch	303.5^b ± 29.74	5	148.6^b ± 24.79	8
7 days post-hatch	94.8^b ± 15.52	9	55.3^b ± 9.91	8
Yolk-sac:				
Hatch	376.1^a ± 21.13	8	290.5^a ± 18.75	8
1 day post-hatch	523.1^b ± 32.25	7	324.6^{a*} ± 38.62	6
3 days post-hatch	799.1^b ± 29.67	6	428.5^{b*} ± 25.78	6
5 days post-hatch	578.5^b ± 37.72	5	276.6^{a*} ± 15.98	8
7 days post-hatch	112.4^b ± 10.88	9	64.1^b ± 13.31	8

Table 5.5 cont.

	Cell density (# Na$^+$/K$^+$-ATPase immunoreactive cells/mm^{-2}) + S.E.	# fish measured	Cell density (# Na$^+$/K$^+$-ATPase immunoreactive cells/mm^{-2}) + S.E.	# fish measured
Location of NKA-IR cells:	*Freshwater*		*Brackish water*	
Inner operculum:				
Hatch	Not detectable	8	Not detectable	8
1 day post-hatch	Not detectable	7	Not detectable	6
3 days post-hatch	422.8^a ± 38.57	6	300.3^a ± 19.51	7
5 days post-hatch	1166.6^b ± 64.87	5	651.3^{b*} ± 28.01	8
7 days post-hatch	1438.4^b ± 45.10	9	1290.9^b ± 65.51	8
9 days post-hatch	1562.3^b ± 33.09	7	1438.2^b ± 16.99	6

5.3.4 2-D Na$^+$/ K$^+$-ATPase immunoreactive area and percentage Na$^+$/K$^+$-ATPase immunoreactive area/mm^{-2} skin

The overall effects of age, treatment and their interaction and also location on fish on 2-D Na$^+$/ K$^+$-ATPase immunoreactive area (μm^{-2}) and percentage Na$^+$/ K$^+$-ATPase immunoreactive area/mm^{-2} skin on the yolk-sac epithelium and inner opercular area are summarised in Table 5.6.

Table 5. 6 Analysis of Variance for 2-D Na$^+$/ K$^+$-ATPase immunoreactive area (μm^{-2}) and percentage Na$^+$/K$^+$-ATPase immunoreactive area /mm^{-2} skin (General Linear Model; p < 0.001).

Source	DF	F	P-value	DF	F	P-value
		Yolk-sac			Inner operculum	
2-D Na$^+$/ K$^+$-ATPase immunoreactive area :						
Age	3	14.37	0.001	2	2.5	0.100
Treatment	1	96.72	0.001	1	55.6	0.001
Age vs. treatment	3	16.48	0.001	2	2.14	0.135
Error	139			31		
Percentage (%) Na$^+$/ K$^+$-ATPase immunoreactive area/mm^{-2} skin:						
Age	3	25.14	0.001	2	132.16	0.001
Treatment	1	2.06	0.153	1	2.25	0.144
Age vs. treatment	3	6.29	0.001	2	13.57	0.001
Error	137			31		

Mean 2-D Na^+/K^+-ATPase immunoreactive area (μm^{-2}) on both the epithelium of the yolk-sac and inner operculum was always significantly larger (GLM; $p < 0.05$) for brackish water adapted larvae than for freshwater larvae (Table 5.7.; Figure 5.12.). The percentage Na^+/K^+-ATPase immunoreactive area/mm^{-2} skin was significantly greater (GLM; $p < 0.05$) in brackish water than in freshwater on the yolk-sac only on 3 dph and, on inner operculum, from 7 dph onwards. There was a significant decrease in mean 2-D Na^+/K^+-ATPase immunoreactive area between hatch and 5 dph on the epithelium of the yolk-sac for both freshwater and brackish water adapted larvae. Similarly, in the inner operculum, mean 2-D Na^+/K^+-ATPase immunoreactive area between 3 dph and 9 dph showed a decrease in size but was not, however, significant (GLM; $p < 0.05$). The percentage Na^+/K^+-ATPase immunoreactive area/mm^{-2} skin showed a decrease in size on yolk-sac, significantly in brackish water and, in contrast, a significant increase in both freshwater and brackish water on the inner operculum (GLM; $p < 0.05$) (Table 5.7.; Figure 5.12.).
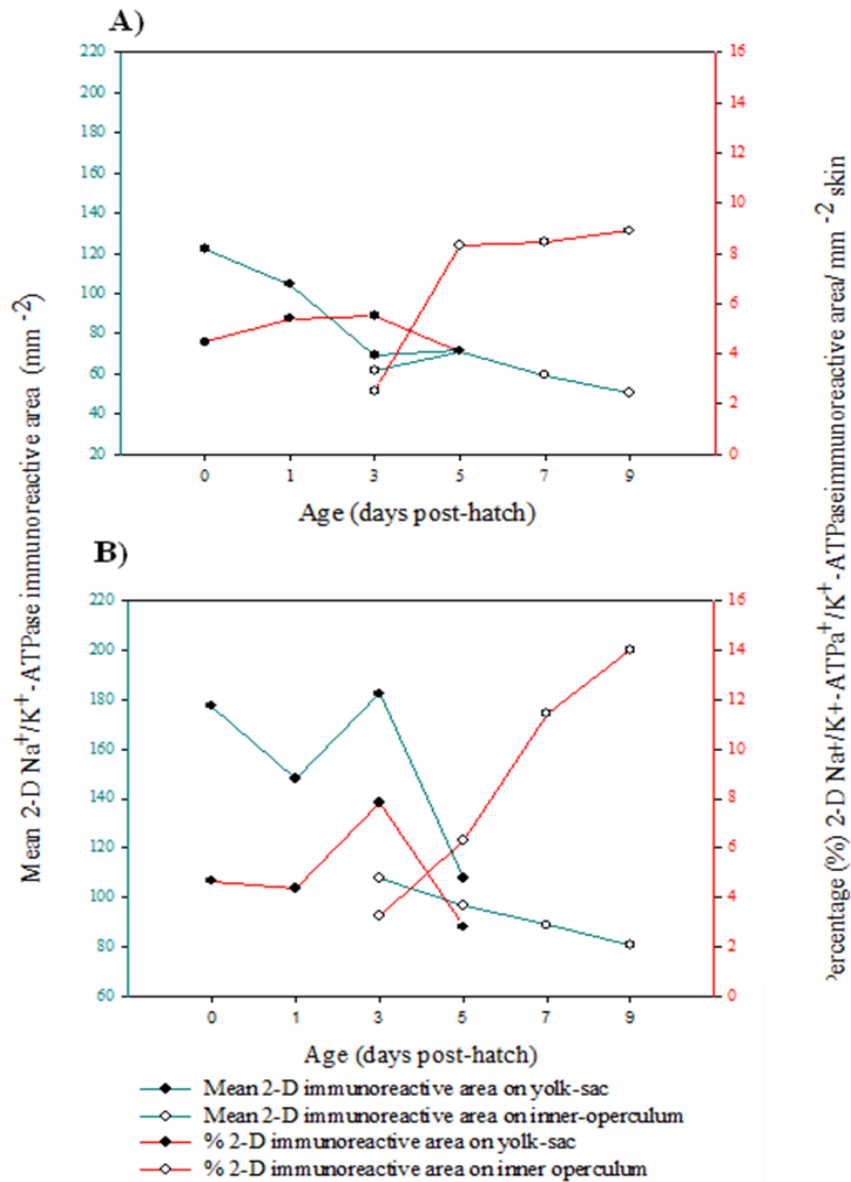
Figure 5. 12 2-D Na$^+$/K$^+$-ATPase immunoreactive cell area (μm^{-2}) and percentage (%) 2-D Na$^+$/K$^+$-ATPase immunoreactive cell area /mm^{-2} skin on yolk-sac and inner operculum as a function of time during post-embryonic development. **A)** Freshwater adapted Nile tilapia and **B)** Brackish water adapted Nile tilapia. Data points indicate mean, error bars have been removed for clarity and S.E. and statistical differences are presented in Table 5.7.

Table 5. 7 2-D Na$^+$/K$^+$-ATPase immunoreactive cell area (μm^{-2}) and percentage (%) 2-D Na$^+$/K$^+$-ATPase immunoreactive cell area /mm^{-2} skin on yolk-sac and inner operculum as a function of time during post-embryonic development. Mean $\pm$ S.E.; different letters indicate significant differences (p < 0.05) between hatch and 5 dph for yolk-sac and between 3 dph and 9 dph for inner operculum; asterisks for brackish water values indicate a significant difference (p < 0.05) from the corresponding freshwater value (General Linear Model with Tukey's post-hoc pairwise comparisons; p < 0.05).

Mean $\pm$ S.E. surface area of MRC immunoreactive area (μm^{-2}):

	Yolk-sac		Inner operculum	
Age	*Freshwater*	*Brackish water*	*Freshwater*	*Brackish water*
Hatch	122.20 $\pm$ 7.19^a	177.33 $\pm$ 19.87^{ab}*		
1 day post-hatch	104.64 $\pm$ 5.74^b	148.14 $\pm$ 12.02^b*		
3 days post-hatch	69.11 $\pm$ 2.05^c	182.44 $\pm$ 9.75^a*	61.69 $\pm$ 2.1^a	108.45 $\pm$ 9.1^a *
5 days post-hatch	71.49 $\pm$ 7.37^c	107.77 $\pm$ 7.37^c*	71.31 $\pm$ 4.06^b	96.94 $\pm$ 8.06^b*
7 days post-hatch	Not detectable	Not detectable	59.42 $\pm$ 1.63^a	88.92 $\pm$ 3.74^b*
9 dph	Not detectable	Not detectable	50.55 $\pm$ 2.56^c	80.66 $\pm$ 1.56^c*

Mean $\pm$ S.E. % 2-D immunoreactive area /mm^{-2} skin:

	Yolk-sac		Inner operculum	
Age	*Freshwater*	*Brackish water*	*Freshwater*	*Brackish water*
Hatch	4.46 $\pm$ 0.01^a	4.67 $\pm$ 0.01^a	Not detectable	Not detectable
1 day post-hatch	5.40 $\pm$ 0.001^b	4.36 $\pm$ 0.01^a	Not detectable	Not detectable
3 days post-hatch	5.51 $\pm$ 0.001^b	7.82 $\pm$ 0.01^b*	2.52 $\pm$ 0.31^a	3.26 $\pm$ 0.38^a
5 days post-hatch	4.01 $\pm$ 0.001^c	2.81 $\pm$ 0.01^c*	8.31 $\pm$ 0.68^b	6.30 $\pm$ 0.59^b*
7 days post-hatch	Not detectable	Not detectable	8.45 $\pm$ 0.27^b	11.42 $\pm$ 0.59^c*
9 dph	Not detectable	Not detectable	8.90 $\pm$ 0.004^b	14.00 $\pm$ 0.01^c*

5.3.5   MRC structure in freshwater and brackish water

Apical openings of MRCs in contact with the external environment were observed using scanning electron microscopy; they were interspersed between pavement cells (PVCs) which were characterised by an array of microridges. Marked morphological differences between the apical openings were observed between freshwater and brackish water adapted larvae at hatch, day 3 and day 7 post-hatch. In freshwater adapted larvae, MRCs lacked an apical crypt and had their mucosal surfaces forming microvilli above the adjacent PVCs (Figure 5.11.A). In contrast, brackish water adapted larvae displayed an apical membrane recessed below the surface of the surrounding pavement cells forming a concave pore or 'crypt' (Figure 5.11.B).

Confocal microscopy confirmed the presence of MRCs on the epithelium of the yolk-sac at 3 dph in both freshwater and brackish water (Figure 5.10.B). They were found to possess a tear-drop configuration (Figure 5.10.C).

5.4 Discussion

Although full adult osmoregulatory capacity is not reached during early life stages because organs are either under-developed or absent (Varsamos *et al.,* 2005), it is well established that teleost embryos and larvae are able to maintain osmotic and ionic gradients between their internal and external environments (Guggino, 1980 a and b; Alderdice, 1988; Kaneko *et al.*, 1995) due mainly to the presence of numerous extrabranchial cutaneous MRCs commonly observed on the abdominal epithelium of the yolk-sac and other body surfaces of fish embryos and larvae. Alderdice (1988; p.225) succinctly describes the ontogenetic development of teleost osmoregulatory capacity from a somewhat limited trans-membrane cellular particle exchange in the embryonic blastular stage to the fully-functioning regulatory tissues in the juvenile and adult, as a process which displays 'continuity, with increasing complexity'.

The site of initial ionoregulation in the integument of teleost larvae was first demonstrated by Shelbourne (1957) who investigated the chloride regulation sites in the European plaice larvae (*Pleuronectes platessa*) and other marine teleost larvae. Since then, integumental MRCs have been reported in the post-embryonic stages of several species, more specifically for tilapiine fishes *i.e.* Mozambique tilapia (*Oreochromis mossambicus*) (Ayson *et al.,* 1994; Hwang *et al.,* 1994; Shiraishi *et al.,* 1997; Hiroi *et al.*, 1999; Li *et al.*, 1995; van der Heijden *et al.,* 1997;1999; Kaneko and Shiraishi, 2001) and other tilapiine species (*Tilapia zilli, Oreochromis aureus, Oreochromis niloticus, Tristramella sacra, Saratherodon galileus*) (Fishelson and Bresler, 2002).

In this study integumental MRCs in the Nile tilapia (*O. niloticus)* were always larger in brackish water larvae than freshwater from 1 dph until yolk-sac absorption. These changes in MRC size as a response to variations in environmental salinity are well documented in the adult teleost *e.g. Oreochromis mossambicus* (Uchida *et al.,* 2000), *Oreochromis niloticus* (Guner *et el*., 2005), Atlantic salmon (*Salmo salar*) (Langdon and Thorpe, 1985), Coho salmon (*Oncorhynchus kisutch*) (Richman and Zaugg, 1987), chum salmon (*Oncorhynchus keta)* (Uchida *et al*., 1996) and killifish *(F. heteroclitus)* (Katoh *et al*., 2000). Similarly, the larger size of MRCs in water of elevated salinity have been confirmed in teleost embryos and larvae; most studies on the effects of salinity on larval integumental MRCs having been carried out on the tilapia *Oreochromis mossambicus* (van der Heijden *et al*., 1999; Li *et al.,* 1995), especially focusing on the epithelium of the yolk-sac (Ayson *et al.,* 1994; Shiraishi *et al*., 1997; Hiroi *et al.,* 1999). Our observations on MRCc on the yolk-sac and inner operculum are in agreement with existing studies, and show that, regardless of location, from hatch onwards MRC surface area is always greater in larvae adapted to brackish water than freshwater.

The sodium pump Na^+-K^+-ATPase has been localised to teleost and elasmobranch MRCs (Cutler *et al.,* 1995; Shikano and Fujio, 1998 a and b; Piermarini and Evans, 2000; Feng *et al.,* 2002) and, more specifically, to the basolateral aspect of the cell (Lee *et al*., 1998; Cutler *et al*., 2000; Piermarini and Evans, 2000; Varsamos *et al*., 2002 b), where it is localised densely on the membranes of the tubular network and generates the driving force for other salt transport systems operating in the MRC in both freshwater and seawater models (Hirose *et al*., 2003). This is in agreement with the present

immunocytochemical staining which resulted in cytoplasmic labelling throughout the cell but left the nucleus unstained. Increased expression and activity of Na^+/K^+-ATPase in teleosts is often directly correlated with enhanced salinity (Cutler *et al*., 1995; D'Cotta *et al*., 2000; Feng *et al*., 2002; Wilson and Laurent, 2002), therefore an increase in size of the cell can be explained by an expansion of the tubular network for the incorporation of Na^+/K^+-ATPase (Uchida *et al.,* 2000; Lee *et al*., 2003) in order for osmotic homeostasis to be maintained in waters of elevated salinity. Salinity dependant expression of Na^+/K^+-ATPase has also been demonstrated at the transcriptome level in terms of increased expression of the α1 and α3 subunits of the Na^+/K^+-ATPase molecule in tilapia larvae *O. mossambicus* (Hwang *et al.,* 1998; Feng *et al*., 2002).

Increased size of MRCs in brackish water can also be explained by the presence of multi-cellular complexes (MCCs); a main cell with accessory MRCs sharing an apical pit. MCCs have been frequently observed on gills of adult fish in seawater and, to a lesser extent, in freshwater (*i.e.* Sardet *et al*., 1979; Hootman and Philpott, 1980; Chretien and Pisam, 1986; Hwang, 1987; Wendelaar Bonga *et al*., 1990; Pisam and Rombourg, 1991; Fishelson and Bresler, 2002) and in the yolk-sac membrane and body skin of larval killifish (*Fundulus heteroclitus*) (Katoh *et al.*, 2000); sea bass (*D. labrax)* (Varsamos *et al.,* 2002 a); Japanese flounder (*Paralichthys olivaceus*) (Hiroi *et al.,* 1998) and Japanese eels (*Anguilla japonica*) (Sasai *et al.,* 1998). Shiraishi *et al*. (1997), using TEM, demonstrated that the complexes on the yolk-sac of seawater adapted *O. mossambicus* larvae possessed multiple shallow junctions on the cytoplasmic processes of the accessory cell that extended into the apex of the main cell, suggesting that an enlarged surface area around the apical pit would enhance sodium

extrusion, since sodium is probably excreted through a paracellular pathway down its electrical gradient in sea water (Silva *et al*., 1977; Zadunaisky, 1984; Marshall, 1997; McCormick, 1995).

The present study found an increase in MRC size on the outer opercular and tail region from hatch to yolk-sac absorption for both fresh and brackish water adapted larvae but a decrease in size of MRCs located on the epithelium of the yolk-sac, suggesting that morphological changes are occurring during ontogeny. A number of structural changes in MRCs have been reported during ontogeny: Varsamos *et al.* (2002 a) used transmission electron microscopy (TEM) to demonstrate morphological changes in integumental MRCs from hatching to juvenile stage of larval sea bass (*D. labrax*) in seawater. Three stages of MRC differentiation were suggested, characterised by a differentiation of the organelles and development of a segmentation of the cytoplasm and accompanied by significant growth of the tubular network, endoplasmic reticulum and enlargement of mitochondria, as seen in adult branchial MRCs. Similarly in Fishelson and Bresler's (2002) comparative study on the development of MRCs in freshwater tilapiine species, the first visible MRCs on the abdominal epithelium of the yolk-sac in the embryonic substrate-brooder *Tilapia zillii* at 24 hrs post-fertilization are described as 'young', possessing the rudiments of microtubules and tubules of rough endoplasmic reticulum with only a few mitochondria interspersed amongst them. In the same study, in the juvenile *T. zillii,* two morphotypes of MRCs were observed with results suggesting they were not functionally different MRCs but one type that changes structure during ageing. Ultrastructural changes resulting in ontogenetic differentiation of MRCs are also suggested by Specker *et al*. (1999) in the Summer flounder (*P.*

dentatus) and by Wales (1997) in the herring (*Clupea harengus)*. This would confirm Alderdice's assumption that osmoregulatory capacity displays an ontogenic continuum.

Newly-hatched teleost larval skin is a thin, 2 cell layer lying on a basal membrane and overlying an extensive haemocoel (Bullock and Roberts, 1975), and its thinness is determined by the fact that its role in respiration and osmoregulatory exchange is more important than its protective role before the gills are fully formed. If, as Alderdice (1988) suggests, the two requirements of MRCs in order to be functional are 1/ to have contact with external medium via an apical opening and 2/ to have contact with blood at basolateral level, it would suggest that, in order to maintain its functionality, the shape and depth of the integumental MRC is limited by the thickness of the epidermis in which it is located (Ayson *et al*., 1994). Katoh *et al.* (2000) noted that the integumental MRCs of seawater-adapted larval killifish (*F. heteroclitus*) were flattened whereas branchial MRCs at later stage in development were spherical or columnar in shape. Similar morphological differences were observed in post embryonic MRC populations in the flounder (*Kareius bicoloratus*) and ayu (*Plecoglossus altivelis* (Hwang, 1989), the Mozambique tilapia (*O. mossambicus*) (Ayson *et al.*, 1994), the turbot (*Scophathalmus maximus)* (Tytler and Ireland, 1995) and the Japanese flounder (*P. olivaceus*) (Hiroi *et al*., 1998). Therefore, if it can be assumed that a development of the internal organisation of the MRC is taking place during ontogeny, its shape is nevertheless in part defined by its location; where the skin remains thin, as on the integumetal opercular area and tail of *O. niloticus,* the expanding MRCs appear flat in shape and increase in size by lateral expansion. The significant decrease in MRC size on the yolk-sac during the yolk sac absorption period for both treatments could be due to a thickening of the

209

body wall over the shrinking yolk sac (Fishelson, 1995), causing MRCs, in order to fulfil their functionality, to appear more elongated or tear-drop shaped.

One feature of the ontogeny of osmoregulatory capability in *O. niloticus* was a distinct spatial shift in chloride cell distribution in both freshwater and brackish water. It is generally accepted that integumental MRCs are initially responsible for osmoregulation prior to development of the adult osmoregulatory organs in *O. mossambicus* (Ayson *et al*., 1994; Shiraishi *et al*., 1997; Hiroi *et al.,* 1999) and killifish (Katoh *et al.,* 2000) and similarly density diminishes with age in the Japanese flounder (Hiroi *et al.,* 1998), disappearing completely in adulthood (Whitear, 1970; Bullock and Roberts, 1975). If, as previously stated, Alderdice's (1988) assumption that larval MRC functionality is subject to the requirement of proximity to 'sub-epithelial circulatory vessels', then the timing of the distribution dynamics of MRCs could be explained by their close association with the changing blood network system of the developing larvae. The pattern of progressive absorption of the yolk-sac synyctium and associated blood network system is reflected in the disappearance of MRCs in this area during ontogeny.

In the present study, a higher density of MRCs was seen in the outer opercular and tail areas than in the epithelium of the yolk sac at hatch in both freshwater and brackish water. However all areas displayed a decline in MRC numbers over the yolk sac absorption period, with a concomitant rise in MRC density on the inner opercular area from day 3 post-hatch onwards following mouth opening and development of the gills and related blood network system. Wales and Tytler (1996), investigating the ontogeny

of MRC distribution in the herring (*C. harengus*), found most MRCs at 1 dph to be associated with the haemocoel or primordial blood vessels. They found that MRCs exhibited a distribution gradient with a lower concentration on the yolk-sac proper and with a higher density on the integument joining the yolk-sac dorsally and anteriorly, with the highest density seen around the pectoral fin bud, close to the pericardial cavity. In the current study, a peak in MRC numbers was observed at 3 dph on the epithelium of the yolk sac followed by a subsequent decline, in both freshwater and brackish water. A similar increase in MRC numbers was reported in *T. zillii* (Fishelson and Bresler, 2002) on the yolk sac and pre-anal fin fold during initial stages of larval ontogeny that was concomitant with an enlargement of the localised vascular system. Integumental MRC numbers then decreased in conjunction with the development of the larvae, the yolk diminishment and disappearance of the yolk-sac syncytium and a progressive development of the gills and operculum. Therefore an important factor influencing MRC distribution appears to be the presence of the underlying and developing circulatory system; as gill development progresses with an increase in size and number of primary and secondary lamellae and an extension of the developing operculum, the larger epithelial surface facilitates an increase in the number and size of differentiating MRCs (Fishelson and Bresler, 2002).

Early fish larvae are characterised by an absence of fully developed gills (Segner *et al.*, 1994), however, the exact timing of MRC functionality in the fish gill is a matter of debate (Alderdice, 1988). Functional branchial MRCs have been identified in larval teleosts in the sea water flounder (*K. bicoloratus*) (Hwang, 1989), the summer flounder (*P. dentatus*) (Schreiber and Specker, 1998), the rainbow trout *O. mykiss* (Gonzalez *et*

al., 1996; Rombough, 1999), the trout (*S. trutta*) (*Rojo et al*., 1997), the Japanese flounder (*P. olivaceus)* (Hiroi *et al.,* 1998), the guppy (*P. reticulata*) (Shikano and Fujio, 1999) and the killifish *(F. heteroclitus*) (Katoh *et al*., 2000). The current study reports that at 3 dph functional MRCs were present in the gills which is in agreement with Li *et al.* (1995) who found numerous functional filamental MRCs at 3 dph in *O. mossambicus* (approximately 4000 cells mm^{-2}) before lamellae had formed, and approximately 6000 cells mm^{-2} at 10 dph, with this density remaining constant up to the adult stage, suggesting the gills to have an early role as a functional ionoregulatory organ before it starts functioning as a gas-exchange organ. However in this study, as early as 1 dph, secondary lamellae were present on the gills in *O. niloticus* and it can also be noted that the absence of a fully formed brachiostegal membrane at 3 dph suggests that the gills are already exposed to the external environment at this point, even though mouth opening has not taken place. The gills of *O. niloticus* may therefore have a functional role as ionoregulatory organs earlier than previously thought.

To conclude, the findings of the research presented in this chapter on the lesser studied Nile tilapia would suggest that osmoregulatory capacity is evident as early as hatch, due to the presence of MRCs on the epithelium of the yolk-sac and other body surfaces. The morphological observations suggest evidence of both freshwater type and brackish water type MRCs whose ontogenetic development appears to confer an ability to cope with varying environmental conditions during early development. This is of particular interest as the appearance of MRCs in the Nile tilapia appears analogous to the pattern observed in the Mozambique tilapia, a cultured species whose broader tolerance for salinity allows direct transfer of embryos and larvae from freshwater to seawater and

vice versa (Ayson *et al*., 1994). In addition, integumental MRCs in the Nile tilapia potentially provide excellent models for future sequential studies on alteration of structure and function of mitochondria-rich cells following exposure to different osmotic environments.

6 Chapter 6   Effects of osmotic challenge on structural differentiation of apical openings in active mitochondria-rich cells in the Nile tilapia.

6.1 Introduction

6.1.1   Background

It is well established that trans-epithelial ion transport is differentially regulated in the MRC. If the requirement of a functional MRC is that it is in contact with the external environment via its apical surface (Zadunaisky, 1984), it therefore follows that structural MRC differentiation, allowing modification of its role in ion secretion or absorption depending on its external environment, could also be reflected in the morphological appearance of its apical openings. Copeland (1948), using light microscopy, was the first to describe the apical structure of the MRC in seawater-adapted killifish as an 'excretory vesicle', suggesting a role in fishes' adaptation to high salinity living conditions. The study of alterations in MRC crypt morphology, therefore, offers valuable insights into the relationship between structure to function during adaptation following osmotic challenge.

6.1.2 Quantification and classification of different MRC 'sub-types' using electron microscopy

The use of scanning electron microscopy (SEM) has allowed the identification of openings or pores on the apical surface of active or functional mitochondria-rich cells (MRCs) *i.e.* with an apical opening to the external environment, as a response to variations in environmental ion compositions or salinities. Numerous attempts have been made to classify and sub-divide the distinctive apical structures of MRCs for euryhaline species, based on their external morphological appearance, including studies on Sockeye salmon (*Onchorhynchus nerka*) (Franklin and Davison, 1989), rainbow trout (*Onchorhynchus mykiss*) (Perry and Laurent, 1989; Goss and Perry, 1994), Japanese eel (*Anguilla japonica*) (Wong and Chan, 1999), Brown trout (*Salmo trutta*) (Brown, 1992), Killifish (*Fundulus heteroclitus*) (Hossler *et al.,* 1985; Katoh *et al.,* 2001; Scott *et al.,* 2004), Mullet (*Mugil cephalus*) (Hossler *et al.,* 1979), Striped bass (*Morone saxatilis*) (King and Hossler, 1991). Scanning electron microscopic studies (SEM) for Tilapiine species are summarised in Table 6.1.

Goss *et al.* (1995), describing the varying apical surface morphologies of MRCs in salmonid *spp.* in freshwater environments, points out that they do not represent different 'populations' of MRCs but merely 'a continuum across which an arbitrary division has been placed'. Perry (1997) describes the marked inter-specific differences in surface morphology of MRCs as 'profound'. It would therefore seem that attempts to classify MRC 'sub-types', based on their surface morphological appearance, has often resulted

in arbitrary and conflicting classifications that appear to be dependant on species, age, external media and transfer regime, even within a same-species group (see Table 6.1.).

SEM has also been used to quantify changes in density of MRC apical openings following salinity transfer in a range of euryhaline teleost species including killifish (*F. heteroclitus*) (Daborn *et al.,* 2001; Scott *et al.,* 2004), adult Mozambique tilapia (*Oreochromis mossambicus*) (Inokuchi *et al.,* 2008; Wang *et al*., 2009; Sardella *et al.* 2004; Shieh *et al.,* 2003; Lee *et al*., 1996, 2000, 2003; van der Heijden *et al.,* 1997; Wendelaar Bonga *et al.,* 1990) and Mozambique tilapia yolk-sac larvae (Lin and Hwang, 2001). In addition, diameter of apical crypts has been measured at maximal apical opening or greatest linear diameter according to Franklin (1990) and Brown 1992) for herring (*Clupea harengus*) (Wales, 1997), the adult Mozambique tilapia (*O. mossambicus*) (Shieh *et al.,* 2003; Lee *et al*., 1996; 2000; van der Heijden *et al.,* 1997) and Mozambique tilapia (*O. mossambicus*) yolk-sac larvae (Lin and Hwang, 2001). However, fewer studies have measured surface area of apical openings or area of MRC exposure as a response to salinity challenge *e.g.* Kultz *et al*., 1995 Shiraishi *et al*., 1997 (*O. mossambicus*).

Transmission electron microscopy (TEM) has been used to observe MRC ultrastructural modifications, in order to examine change in ionoregulatory function occurring when fishes are transferred to seawater. TEM is often used in conjunction with surface scanning electron microscopy (SEM) to support the hypothesis that variations in MRC 'sub-type', occurring in response to alterations in external salinity, are reflected both in

apical morphology, in ultrastructural modification and presumed functional characteristics *e.g.* Japanese eel (*Anguilla japonica*) (Shirai and Utida, 1970), Atlantic salmon (*Salmo salar*) (Pisam *et al.,* 1988), guppy (*Poecilia reticulata*) (Pisam *et al.,* 1987), Rainbow trout (*O. mykiss*) (Pisam *et al.,* 1989) and in tilapiine spp. (see Table 6.1).

Table 6. 1 Classification of different types of mitochondria-rich cells as a response to environmental changes in tilapia *spp.* using CSLM, SEM and TEM.

Common name	Scientific name	Stage/ age	Media	Types of MRCs	Methods of observation	Observations	Reference
Lake Magadi tilapia	*Oreochromis alcalicus grahami*	Adult	High salinity Lake Magadi lake water and diluted lake water.	Light staining, less electron dense MRCs with apical pit and deep MRCs and dark staining electron dense MRCs, both with apical pit.	TEM/SEM	No change in location of types after transfer to diluted media, but signs of cellular degradation.	Maina (1990; 1991)
Nile tilapia	*Oreochromis niloticus*	Adult	Freshwater (control)	Dark and light stained MRCs with apical pit.		Reduced numbers of MRCs.	"
Nile tilapia	*Oreochromis niloticus*		FW, deionised water and BW (20 ppt)	α and β type cells.	TEM	α and β type cells in FW and deionised water, only α type in BW	Pisam *et al.* (1995)
Mozambique tilapia	*Oreochromis mossambicus*	Adult	FW, BW (20ppt) and SW (35ppt)	3 subtypes: wavy-convex (subtype 1), shallow-basin (subtype II) and deep-hole (subtype III).	SEM	FW: all subtypes, BW and SW: subtype II and III	Wang *et al.* (2009)
"	"	Adult	FW, normal Na^+/low Cl^-, low Na^+/normal Cl^-, low Na^+/low Cl^-	3 types: (1) small pit, (2) concave surface (3) convex surface.	SEM/CSLM	Small pit predominated in FW, concave and convex predominated in low Na^+/ and low Cl^- respectively	Inokuchi *et al.* (2009 b)

Table 6.1. cont.

Common name	Scientific name	Stage/ age	Media	Types of MRCs	Methods of observation	Observations	Reference
Mozambique tilapia	*Oreochromis mossambicus*	Adult	FW and SW	4 types: I, II, III, IV, depending on distribution of Na^+/K^+-ATPase, NKCC and CFTR, NHE_3, NKCC1a, NCC.	CSLM	FW displayed Type I, II and III. Following transfer to SW Type IV appeared	Hiroi *et al.* (2008)
"	"	Adult	FW and SW	4 types: I, II, III, IV depending on distribution of Na^+/K^+-ATPase, NKCC and CFTR	CSLM	FW displayed Type I, II and III. Following transfer to SW Type IV appeared.	Hiroi *et al.* (2005)
"	"	"	SW (35 - 95 ppt)	Mature, accessory, immature and apoptotic MRCs	TEM	35 - 55 ppt showed consistent numbers of MRC types. At 65 - 95 ppt, number of ACCs and apoptotic cells significantly increased and 75 - 95 ppt significant increase in immature cells and reduction in mature cells.	Sardella *et al.* (2004)
"	"	"	3 FW types; High Na/high Cl; high Na/low Cl; low Na/low Cl	3 sub-types: wavy-convex (sub-type 1), shallow-basin (sub-type II) and deep-hole (sub-type III)	SEM	Wavy convex type predominate in low Cl^- but Na^+ uptake showed no changes in MRC apical morphology	Chang *et al.* (2003)
"	"	"	3 FW types; low Na^+/low Cl^-, high Na^+/low Cl^-, high Na^+/high Cl^-.	"	SEM	low Na^+/low Cl^- and high Na^+/low Cl^-: all types high Na^+/high Cl^-: no wavy-convex	Shieh *et al.* (2003)

Table 6.1. cont.

Common name	Scientific name	Stage/ age	Media	Types of MRCs	Methods of observation	Observations	Reference
Mozambique tilapia	*Oreochromis mossambicus*	Adult	3 FW types; high-Ca^+, mid-Ca^+, low-Ca^+ and low Na^+Cl^-	3 sub-types: wavy-convex (sub-type 1), shallow-basin (sub-type II) and deep-hole (sub-type III)	SEM, TEM	Wavy convex and shallow basin increased with enhanced Na^+/Cl^- and Ca^{2+} uptake	Chang *et al.* (2001)
"	"	Juveniles	FW and SW	"	SEM/TEM/ CSLM	FW; all types, SW only type III	Lee *et al.* (2003)
"	"	Adult	FW and BW *i.e.* 5, 10, 20, 30 ppt.	"	SEM	Deep hole type increase with increasing salinity	Lee *et al.* (2000)
"	"	Larvae	FW and high Na/high Cl, high Na/low Cl, Normal na/low Cl	"	SEM	Wavy convex predominate in low Cl acclimated larvae, deep hole only in high Cl	Lin and Hwang (2001)
"	"	Yolk-sac larvae	FW and SW	Mature, immature, and degenerating *i.e.* necrotic, apoptotic and mitochondria-poor' cells (MP)	TEM	Mature MRCs decreased following transfer to SW with increase in immature and apoptotic cells	Van der Heijden *et al.* (1999)

Table 6.1. cont.

Common name	Scientific name	Stage/ age	Media	Types of MRCs	Methods of observation	Observations	Reference
Mozambique tilapia	*Oreochromis mossambicus*	Adult	Freshwater and 3.2 µmol l-1 copper (Cu)	Apoptotic and necrotic MRCs	TEM	Increase in number of apoptotic and necrotic MRCs following transfer to Cu	Li *et al.* (1998)
"	"	Adult	FW and SW	Type I pit with small cellular extension, Type II pit with globular extensions, Type III smaller with deeper invaginated exposed surface.	SEM	FW; all types, SW only type III	Van der Heijden *et al.* (1997)
"	"	Adult	FW, hard freshwater (HFW) and BW (5ppt)	3 subtypes: wavy-convex (subtype 1), shallow-basin (subtype II) and deep-hole (subtype III).	SEM/TEM	Wavy convex predominate in HFW, shallow-basin in FW and deep-hole in BW.	Lee *et al.* (1996)
"	"	Adult	FW and acidified FW	Accessory cells (ACs), immature, mature and degenerating cells	TEM	Acidification decreased numbers of mature cells and increased numbers of immature and apoptotic cells.	Wendelaar Bonga *et al.* (1990)

6.1.3   Aims of the chapter

It has been demonstrated in the preceding chapters that osmoregulatory capacity varies according to age during early life stages (Chapters 3 and 4). In addition, it has been shown that this ability to withstand variation in salinity is most likely due to the osmoregulatory function of extrabranchially located MRCs that possess a clearly defined temporal staging in their location, size, density and morphology that varies according to the environmental salinity (Chapter 5). Therefore the hypothesis that changes in density, abundance, size and appearance of MRC apical openings as a response to changes in ionic composition of the external media do in fact reflect cellular differentiation, either as an expression of their developmental stage or as a modulation of their function, will be investigated in this chapter through the examination of:

- Short-term changes in size and density of MRC apical crypts *i.e.* those in contact with the external environment via their apical openings, following salinity challenge during early life stages of the Nile tilapia using SEM.

- Morphological variations in type of apical crypts using SEM.

- The relationship of structure to function of MRCs apical openings combining SEM quantitative measurements and morphological variations in combination with composite TEM studies and re-classification of apical crypts into 'sub-types'.

6.2 Materials and methods

6.2.1   Egg supply, artificial incubation systems and transfer régime

Broodstock were maintained as outlined in Section 2.1.1. and eggs were obtained by the manual stripping method outlined in Section 2.1.2. Preparation of experimental salinities and artificial incubation of eggs and yolk-sac fry were carried out as detailed in Sections 2.2 and 2.3. Batches of eggs were fertilized and incubated in freshwater until 3 dph when yolk-sac larvae were transferred immediately to 12.5 and 20 ppt incubation units and sampled after 24 and 48 hours.

6.2.2   Scanning electron microscopy

6.2.2.1   Sampling and fixation

Scanning electron microscopy was used for examination of MRC apical openings of whole yolk-sac larvae. Freshwater larvae were sampled at time of transfer (3 dph) and at 24 and 48 h post-transfer to elevated salinities (*i.e.*12.5 and 20 ppt). Controls *i.e.* larvae remaining in freshwater were also sampled at the same time points.

Larvae were fixed in 2.5 % (v/v) glutaraldehyde in 0.1 M sodium cacodylate buffer (see Appendix) and fixed at 4° C for two days. Samples were then transferred to buffer rinse (see Appendix) and stored at 4 °C. Samples were then transferred to 1% (w/v) osmium tetroxide in 0.1 M sodium cacodylate buffer (see Appendix) for 2 h. They were then dehydrated through an ethanol series (30% for 30 min, 60% for 30 min, 90% for 30 min

and 100% twice for 30 min each) before critical point drying in a Bal-Tec 030 critical point dryer. Samples were mounted on specimen stubs using double-faced tape and gold sputter-coated for 1.5 min at 40 mA to coat to a thickness of *c.* 2 -3 nm (Edwards sputter coater, S150B, BOC Edwards, Wilmington, MA, US). Images were collected with a Scanning Electron Microscope (SEM; JEOL JSM6460LV; Jeol, Welwyn Garden City, UK). Images were taken at between 5 - 10 kV and a working distance of 10 mm.

6.2.2.2   Visualisation and analysis

Micrographs of a minimum of 5 randomly selected fields per fish on the epithelium of the yolk-sac were taken from a minimum of 5 fish in each experimental group at a magnification of x 1300. Each field corresponded to 7,137 μm^{-2}. Fields were randomly chosen from the yolk-sac epithelium that showed no fixation artifacts such as debris or cracks. Apical crypts were determined as either mucous cells or MRCs, dependant on external structure of apical opening *i.e.* displaying presence of globular material, and the number of each type in each field were counted and expressed as density (# crypt mm^{-2}) and percentage relative abundance of MRC (% of total number of MRCs) for each treatment at each time point. The surface area of MRC apical openings or apical exposure area was measured using ImageJ (version 1.44) (National Institutes of Health, US). Surface area measurements of MRC apical crypts were also expressed as size-frequency distribution of apical openings for each treatment at each time point.

6.2.2.3   3-Dimensional imaging

Images were collected with a scanning Electron Microscope (JEOL JSM6460LV) as described above (Section 6.2.2.2.) using a stage tilt between 0.5 - 1° for low topography

e.g. individual crypts and 6° for high topography *e.g.* gills. Stereo images were created using Scandium software.

6.2.3 Transmission electron microscopy with immunogold labelling of anti-Na$^+$/K$^+$-ATPase and CFTR

Freshwater larvae were sampled at time of transfer (3 dph) and at 24 and 48 h post-transfer to elevated salinities (*i.e.*12.5 and 20 ppt). Between three to five larvae were sampled for each treatment at each time point and controls *i.e.* larvae remaining in freshwater were also sampled. Transmission electron microscopy in combination with immunogold labelling was used to examine localisation of anti-Na$^+$/K$^+$-ATPase and anti-CFTR within active MRCs.

6.2.3.1 Whole-mount immunohistochemistry

A mouse monoclonal antibody raised against the α-subunit of chicken Na$^+$/K$^+$-ATPase (mouse anti-chicken IgG α5, Takeyasu *et al*. 1988) was used to detect integumental MRCs in yolk-sac larvae using whole-mount immunohistochemistry. A mouse monoclonal antibody (24:1; R&D Systems, Boston, MA, US) against 104 amino acids at the carboxyl terminus of the human CFTR was also used to detect integumental MRCs. The carboxyl-terminus of CFTR is highly conserved among vertebrates,and this antibody has previously been shown to be specifically immunoreactive with CFTR from several vertebrates, including teleost fish (Marshall *et al.*, 2002).

Whole-mount larvae were fixed and labelled according to the following protocol:

(i) Fixed in a 4% (w/v) paraformaldehyde in 0.1 M phosphate buffer (PB; pH 7.4) (see Appendix) for 24 hours at 4 °C,

(ii) Preserved in 70% ethanol at 4 °C until use,

(iii) Rinsed twice for 20 minutes each time with phosphate buffered saline (PBS) at room temperature,

(iv) Tails were dissected off and incubated with monoclonal antibody against α5-subunit of chicken Na^+/K^+-ATPase diluted 1:200 and CFTR diluted to 1.6 µg ml^{-1} with phosphate buffered saline (PBS) (see Appendix) containing blocking agents; 10% normal goat serum (NGS) (Vector Labs. UK), 1% bovine serum albumin (BSA) (Sigma Aldrich, UK) and 0.02% keyhole limpet haemocyanin (Sigma Aldrich, UK) overnight at 4 °C,

(v) Rinsed twice for 20 minutes each time in PBS at room temperature,

(vi) Incubated with secondary antibody Fluoronanogold™ Alexa Fluor 488 (Nanoprobes, U.S.) comprising a 1.4 nm nanogold particle to which a specific antibody fragment (anti-mouse) and a fluorochrome had been conjugated (see Figure 6.1.) overnight at 4° C in PBS with 1% non-fat milk powder,

(vii) Rinsed twice for 20 min each time in PBS at room temperature,

(viii) Rinsed twice for 5 min each time with PBS and 1% BSA at room temperature and kept in the dark at 4 ℃ until observation.
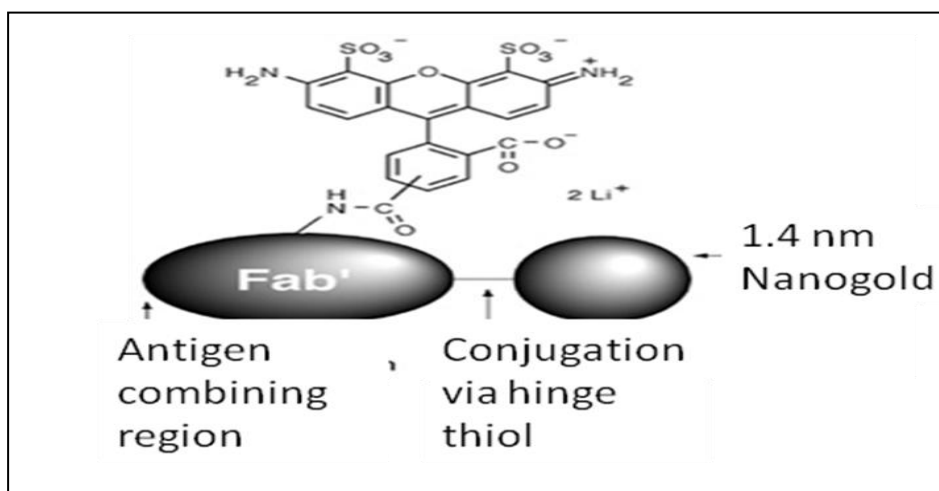
Figure 6. 1 Structure of Alexa Fluor® 488 and Nanogold® - Fab', showing covalent attachment of components.

(Source:http://www.nanoprobes.com/products/FluoroN.html#alexa488).

6.2.3.2 Immunogold labelling

Dissected tails that had been treated according to the protocol outlined above (Section 6.2.3.1.) until stage (viii) were then treated as follows:

(ix) Rinsed 2 x 5 min in distilled water (DW),
(x) Enhanced for approx. 10 min with GoldEnhance EM (Nanoprobes, U.S.) in order to increase the size of the 1.4 nm gold particle to c. 30 - 40 nm (see Figure 6.2.),

(xi) Rinsed quickly in DW,

(xii) Fixed in 2.5 ml of 2.5% (v/v) glutaraldehyde in 0.1 M sodium cacodylate buffer (pH 7.2) (see Appendix) at 4° C for 3 - 4 h,

(xiii) Transferred to c. 2.5 ml sodium cacodylate buffer rinse (see Appendix) and stored at 4° C until use,

(xiv) Dehydrated in 30 % ethanol with 2% urynl acetate for 1 h, 60% ethanol for 30 min, 90% ethanol for 30 min twice in 100% ethanol for 30 min and 45 min respectively,

(xv) Infiltrated in 50:50 LR White resin: 100 % ethanol for 60 min, infiltrated with LR White resin overnight and then sample place in mould, and heated in an oven at 60 ℃ for *c.* 24 h.
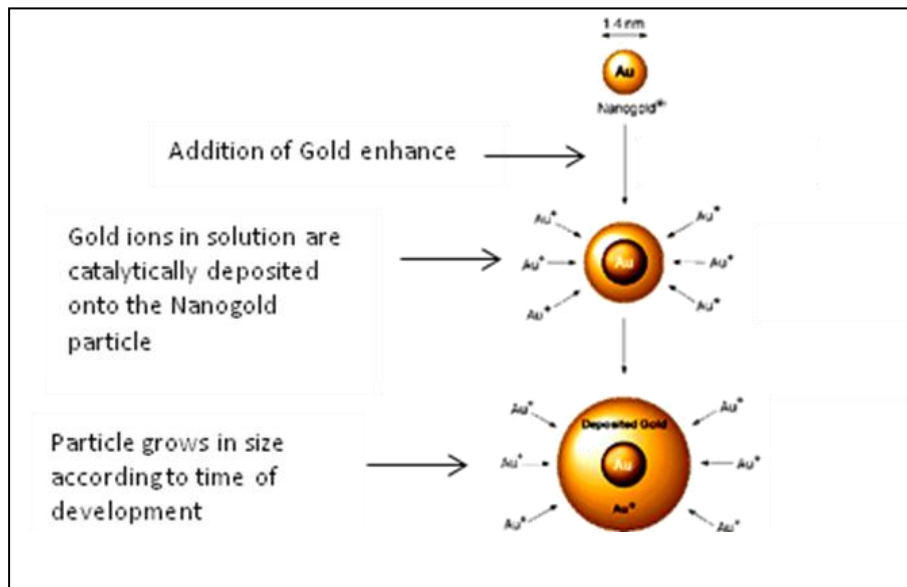
Figure 6. 2 Schematic representation of the action of GoldEnhance EM.

(Source: http://www.nanoprobes.com/products/GoldEnhance.html).

An ultrathin section (90 nm) were cut from each of the dissected tails and serial sections were made every 10 µm thereafter. Cut ultra-thin sections were placed on 200 mesh Formvar-coated copper grips, stained with a solution of 4% uranyl acetate in 50% alcohol and Reynold's lead citrate (see Appendix) and observed using an FEI Technai Spirit G2 Bio Twin transmission electron microscope.

6.2.4　Statistical analyses

Statistical analyses were carried out with Minitab 16 software using a General Linear Model or One-way analysis of variance (ANOVA) with Tukey's post-hoc pair-wise comparisons. Homogeneity of variance was tested using Levene's test and normality was tested using the Anderson-Darling test. Where data failed these assumptions, they were transformed using an appropriate transformation *e.g.* square root. Significance was accepted when $p < 0.05$.

6.3 Results

6.3.1 Morphological variations in size of mitochondria-rich apical crypts

Apical crypts, *i.e.* cells in contact with the external environment via an apical opening, were seen to be located at the boundaries of ridged, pavement cells on the yolk-sac of Nile tilapia (Figure 6.3. and 6.4.). Apical crypts of mucous cells were discriminated from those of MRCs, based on the presence of globular extensions within the crypt (Figure 6.3.F.).

There was a significant overall effect of salinity, age post-transfer and their interaction and 'sub-type' on surface area of MRC apical crypts (General Linear Model; $p < 0.001$) which is summarised in Table 6.2. and Figure 6.5. The relative frequency (%) of MRC apical surface area following transfer to elevated salinities is shown in Figure 6.6.

Table 6. 2 Analysis of Variance for effect of salinity, age post-transfer and their interaction and MRC 'sub-type' on surface area of apical crypts (mm^{-2}).(General Linear Model; $p < 0.001$).

Source	*DF*	*F*	*P-value*
Surface area of apical crypts (μm^{-2}):			
Salinity	2	11.61	0.001
Age post-transfer	1	4.21	0.001
Salinity vs. age post-transfer	2	10.16	0.001
'sub-type'	3	184.27	0.001
Error	466		
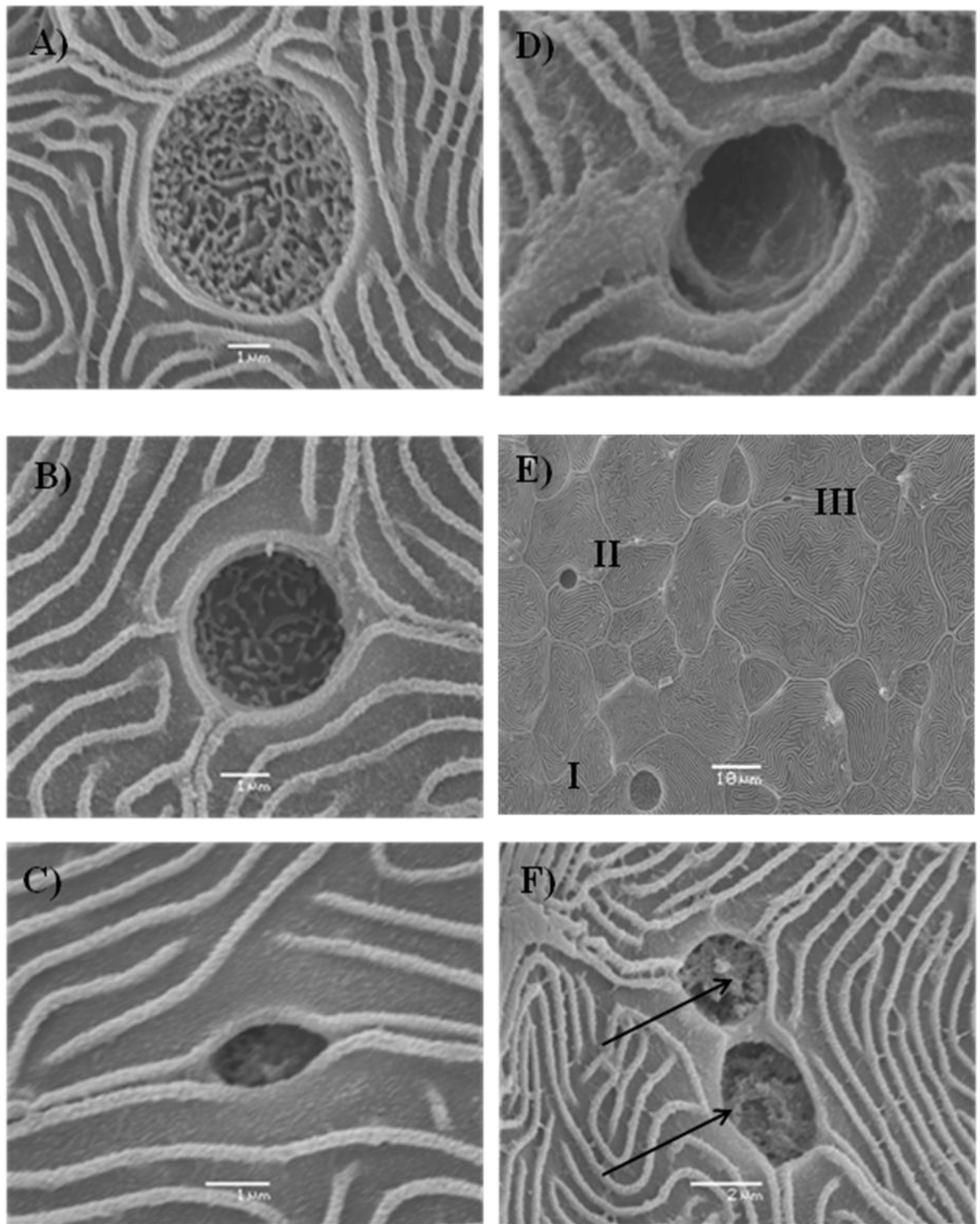
Figure 6. 3 Scanning electron micrographs. **A) – E)** Different 'sub-types' of MRCs based on their apical morphological appearance **A)** Type I [Bar = 1 μm], **B)** Type II [Bar = 1 μm], **C)** Type III [Bar = 1 μm], **D)** Type IV [Bar = 1 μm], **E)** 3 distinct MRC 'sub-types' I, II and III [Bar = 10 μm] and **F)** Apical openings mucous cell, *note* presence of globular extensions within crypts (arrows) [Bar = 2 μm].
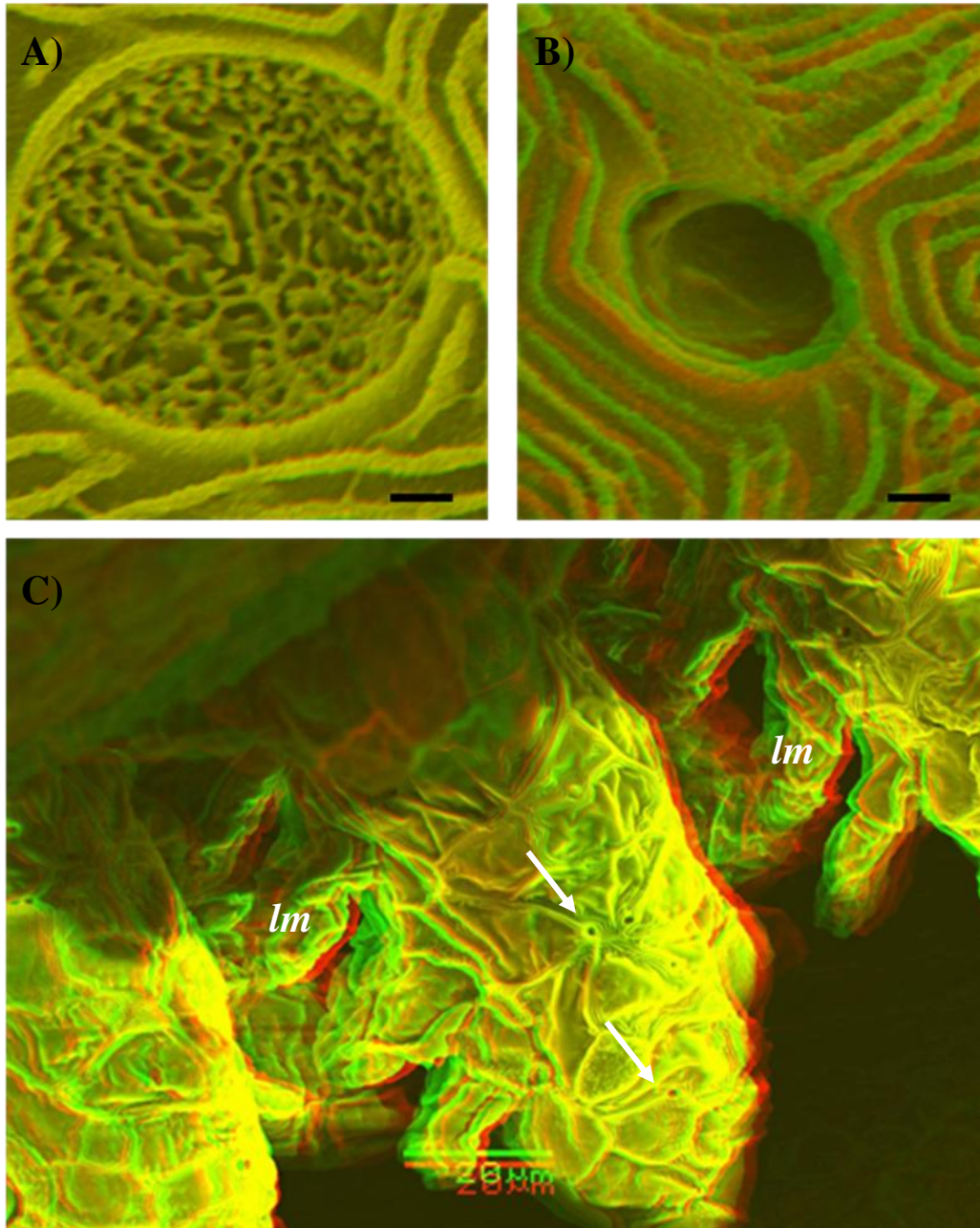
Figure 6. 4 3-D scanning electron micrographs of MRCs on Nile tilapia yolk-sac larvae. **A)** Type I apical opening of MRC on epithelium of yolk-sac of freshwater larvae at 3 days post-hatch [Bar = 1 µm], **B)** Type IV apical opening of MRC on epithelium of yolk-sac acclimated to 20 ppt at 48 hours post-transfer [Bar = 1 µm] and **C)** Gills showing filaments and secondary lamellae (lm) of yolk-sac larvae of Nile tilapia acclimated to 20 ppt at 48 h post-transfer, arrows point to Type IV apical crypts [Bar = 20 µm].
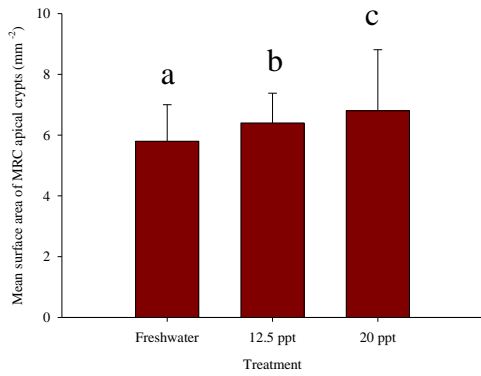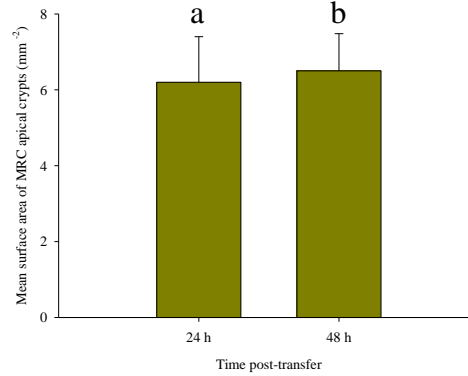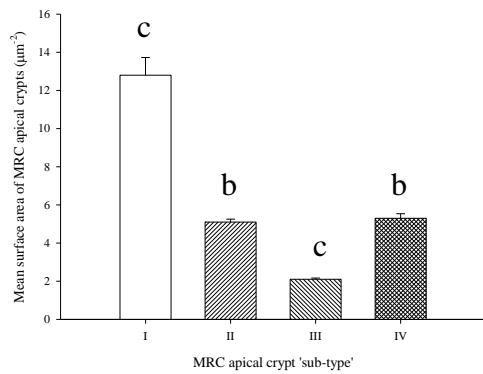
Figure 6. 5 Overall effects on surface area of MRC apical crypts of **A)** Salinity, **B)** Time post-transfer and **C)** MRC apical crypt 'sub-type' i.e Type I, II, III and IV. Mean ± S.E. Different letters indicate significant differences between bars (General Linear Model with Tukey's post-hoc pairwise comparisons; $p < 0.001$).
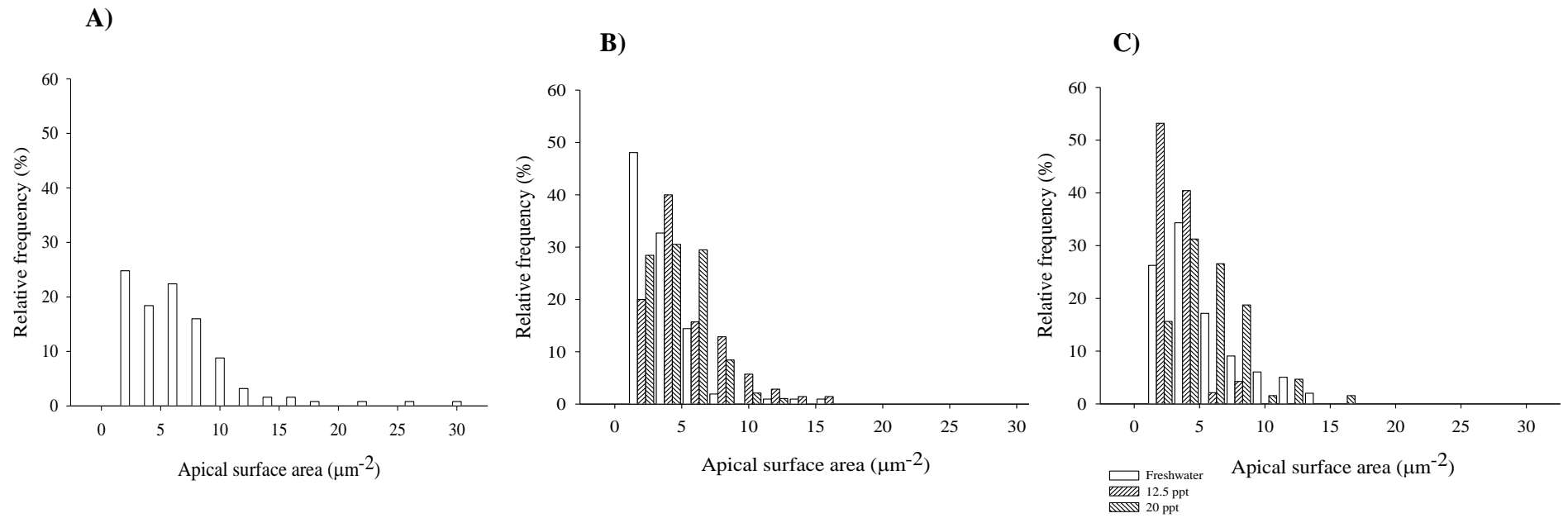
Figure 6. 6 Changes in percentage relative frequency of all apical surface area (μm^2) of MRCs on yolk-sac epithelium of Nile tilapia following transfer from freshwater to 12.5 and 20 ppt **A)** 0 h, **B)** 24 h post-transfer and **C)** 48 h post-transfer.

It was apparent that variations existed amongst apical crypts and, based on these differences in size and the observed morphology of the apical openings, a distinction could be made between apical crypts of mucous cells and MRCs, which could, in turn, be re-classified into four distinct groups or 'sub-types':

- *Type I*

This type displayed large, circular apical surfaces with flat or slightly exposed surface area with a mesh-like network of cellular extensions (Figure 6.3.A and E; Figure 6.4.A.). Type I was significantly larger than all other 'sub-types' (range $5.2 - 19.6 \ \mu m^{-2}$) (One-way ANOVA; $p < 0.05$) (Figure 6.5.C.; Table 6.3.).

- *Type II*

This type displayed smaller, circular or ovoid shaped apical surfaces with a shallower exposed area with microvilli (Figure 6.3.B and E). Type II was significantly larger than Type III but not Type IV (range $1.1 - 15.7 \ \mu m^{-2}$) (One-way ANOVA; $p < 0.05$) (Figure 6.5.C.; Table 6.3.).

- *Type III*

This type displayed circular or slightly ovoid and not so deeply invaginated apical crypts with some globular material (Figure 6.3.C and E). Type III was significantly smaller than other 'sub-types' (range $0.08 - 4.6 \ \mu m^{-2}$) (One-way ANOVA; $p < 0.05$) (Figure 6.5.C.; Table 6.3.).

- *Type IV*

This type displayed apical surfaces similar to Type II but were larger more circular with a deeply invaginated pit containing no apparent material (Figure 6.3.D; Figure 6.4.B

235

and C.). Type IV was significantly smaller than Type I and significantly larger than Type III (range 4.1 – 11.7 μm^{-2}) (One-way ANOVA; $p < 0.05$) (Figure 6.5.C.; Table 6.3.).

- *Mucous cells*

These displayed apical surfaces similar to Type II *i.e.* circular or slightly ovoid and shallower but containing globular material. Displayed a similar range in size to Type II (range 1.9 – 14.7 μm^{-2}) (One-way ANOVA; $p < 0.05$) (Figure 6.3.F.; Table 6.3.).

Table 6. 3 Morphometric measurements of apical crypts in the yolk-sac epithelium of Nile tilapia following transfer from freshwater to elevated salinities as determined by scanning electron microscopy. Data are mean ± S.E. plus range in brackets. Data within columns with different superscript letters are statistically different (One-way ANOVA with Tukey's post-hoc pair-wise comparison; $p < 0.05$).

Treatment	Freshwater			12.5 ppt		20 ppt	
Time (hours post-transfer)	0	24	48	24	48	24	48
Mean surface area (µm $^{-2}$) and (range):							
Type I	11.2 ± 1.18 [a]	13.2 ± 1.52 [a]	10.8 ± 1.01 [a]	14.1 ± 0.14 [a]	none	none	none
(range)	(5.2 - 19.6)	(10.5 - 13.5)	(8.8 - 11.9)	(13.9 – 14.3)			
Type II	5.4 ± 0.25 [b]	3.5 ± 0.19 [b]	5.1 ± 0.35 [b]	5.8 ± 0.40 [b]	4.6 ± 0.72 [a]	5.4 ± 0.38 [a]	8.6 ± 1.13 [a]
(range)	(1.7 - 10)	(1.4 - 6.9)	(1.1 - 15.7)	(2.2 - 10.4)	(2.7 - 7.8)	(2.6 - 11.09)	(5.51 - 11.7)
Type III	1.7 ± 0.16 [c]	1.3 ± 0.09 [c]	2.2 ± 0.30 [c]	2.3 ± 0.16 [c]	1.87 ± 0.14 [b]	2.14 ± 0.12 [b]	2.4 ± 0.07 [b]
(range)	(0.08 - 3.6)	(0.32 - 2.9)	(0.43 - 2.8)	(0.78 - 3.9)	(0.58 - 3.9)	(0.73 - 3.7)	(0.78 - 4.6)
Type IV	none	none	none	none	none	5.3 ± 0.25 [a]	6.1 ± 0.35 [c]
(range)						(4.1 - 8.3)	(4.1 - 11.7)
Mucous cells	4.4 ± 0.29 [b]	4.4 ± 0.06 [b]	4.1 ± 0.05 [b]	4.9 ± 0.47 [b]	3.9 ± 0.15 [a]	3.7 ± 0.48 [a]	7.3 ± 0.23 [a]
(range)	(1.9 – 10.9)	(3.6 - 6.6)	(1.5 - 14.7)	(2.6 – 11.6)	(3.1 – 5.6)	(2.2 – 9.6)	(6.1 - 12.9)

6.3.2 MRC apical crypt density

There was a significant overall effect of salinity and 'sub-type' on total density of MRC apical crypts (General Linear Model; $p < 0.001$) but not of age post-transfer or the interaction between salinity and age post-transfer ($p > 0.05$) which is summarised in Table 6.4. and Figure 6.7. Only data following transfer after 24 and 48 h was used for GLM analysis.

Table 6. 4 Analysis of Variance for effect of salinity, age post-transfer and their interaction and MRC 'subtype' on total density of apical crypts (# crypts mm^{-2}) (General Linear Model; $p < 0.001$).

Source	DF	F	P-value
Total density of MRC apical crypts mm^{-2}:			
Salinity	2	5.59	0.001
Age post-transfer	1	0.01	0.913
Salinity vs. age post-transfer	2	1.32	0.269
'sub-type'	3	2.03	0.001
Error	245		
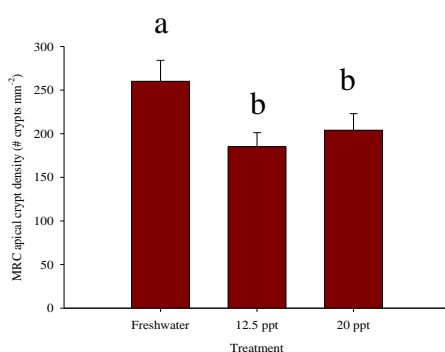
Figure 6. 7 Overall effect of salinity on total density of MRC apical crypts (# crypts mm^{-2}). Mean ± S.E. Different letters indicate significant differences between treatments (General Linear Model with Tukey's post-hoc pairwise comparisons; $p < 0.05$).

Further quantitative analysis showed that the density and the frequency *i.e.* percentage relative abundance of either MRC 'sub-types' or mucous cells of the total number of crypts varied according to experimental salinity and to time after transfer (Table 6.5; Figure 6.8.). In freshwater adapted larvae, there was always a lower percentage relative abundance and density (One-way ANOVA; $p < 0.05$) of Type I apical crypts, than either Type II or Type III. Occurrences of Type II and Type III were similar (One-way ANOVA; $p > 0.05$), regardless of time. Type IV crypts were not present in freshwater. Occurrence of mucous cells remained constant in freshwater (One-way ANOVA; $p > 0.05$).

Following transfer to 12.5 ppt, Type I crypts disappeared after 48 h, with numbers of Type II crypts declining to 5 % percentage relative abundance and Type III crypts increasing to 85 % abundance by 48 h post-transfer. Following transfer to 20 ppt, no Type I crypts were observed. Type II crypts disappeared by 48 h post-transfer and appeared to be replaced with Type IV crypts, which showed a relative abundance of 44 % by 48 h post-transfer (Table 6.5.; Figure 6.8.). The occurrence of mucous cells remained constant throughout with density not differing statistically at any time point (One-way ANOVA; $p > 0.05$).

Type I cells were present in freshwater-adapted larvae at all time points with no significant difference in overall density (One-way ANOVA; $p > 0.05$), however relative abundance declined to 3 %, following 24 h transfer to 12.5 ppt, disappearing completely by 48 h post-transfer. Correspondingly, in the group transferred to 20 ppt, Type I cells disappeared completely by 24 h post-transfer onwards. The density of Type II cells

remained constant throughout in freshwater-adapted larvae but declined significantly (One-way ANOVA; $p < 0.05$) following transfer to either 12.5 or 20 ppt and disappeared completely by 48 h post-transfer to 20 ppt. This pattern is also reflected in the decline in percentage relative abundance following transfer. The density of Type III cells also remained fairly constant throughout, displaying no significant differences in density amongst treatments and regardless of time (One-way ANOVA; $p < 0.05$). Type IV cells only appeared in 20 ppt adapted larvae from 24 h post-transfer onwards and density increased significantly after 48 h post-transfer (One-way ANOVA; $p < 0.05$). Relative abundance of Type IV cells was higher at 44 % at 48 h post-transfer compared with 19 % at 24 h post-transfer. (Table 6.5.; Figure 6.8.).

Table 6. 5 Percentage relative abundance (%) and density of apical crypts in the yolk-sac epithelium of Nile tilapia following transfer from freshwater to elevated salinities as determined by scanning electron microscopy. Data are mean ± S.E. (n = 5). Data within columns with different superscript letters are significantly different; data within rows with different numerals are statistically different (One-way ANOVA with Tukey's post-hoc pair-wise comparison; $p < 0.05$).

Treatment	Freshwater			12.5 ppt		20 ppt	
Time	0	24	48	24	48	24	48
Percentage relative abundance (% of total number):							
Type I	22	3	3	3	0	0	0
Type II	35	33	46	36	5	13	0
Type III	33	52	36	54	85	56	47
Type IV	0	0	0	0	0	19	44
Mucous cells	10	12	15	7	10	12	9
Density of apical crypts (crypts /mm^{-2}):							
Type I	$214.3 \pm 24.4^{b}_{1}$	$140.1 \pm 0.00^{a}_{1}$	$140.1 \pm 0.00^{a}_{1}$	$140.1 \pm 0.00^{b}_{1}$	none	none	none
Type II	$235.9 \pm 25.3^{a}_{12}$	$157.2 \pm 26.43^{b}_{12}$	$256.3 \pm 46.32^{b}_{1}$	$150.5 \pm 28.8^{b}_{2}$	$63.5 \pm 23.3^{a}_{2}$	$56.9 \pm 30.2^{a}_{2}$	none
Type III	$266.9 \pm 38.6^{a}_{1}$	$322.9 \pm 31.10^{c}_{1}$	$265.5 \pm 44.58^{b}_{1}$	$272.8 \pm 31.2^{c}_{1}$	$239.3 \pm 25.9^{b}_{1}$	$265.2 \pm 30.1^{b}_{1}$	$212.1 \pm 33.6^{b}_{1}$
Type IV	none	none	none	none	none	$148.4 \pm 8.2^{b}_{1}$	$247.9 \pm 31.2^{b}_{2}$
Mucous cells	$100.6 \pm 22.6^{c}_{1}$	$123.0 \pm 14.80^{a}_{1}$	$126.0 \pm 36.83^{a}_{1}$	$119.4 \pm 18.9^{a}_{1}$	$101.2 \pm 33.5^{a}_{1}$	$136.3 \pm 9.4^{b}_{1}$	$120.0 \pm 70.6^{a}_{1}$

A)

Type I
Type II
Type III
Type IV
Mucous cells
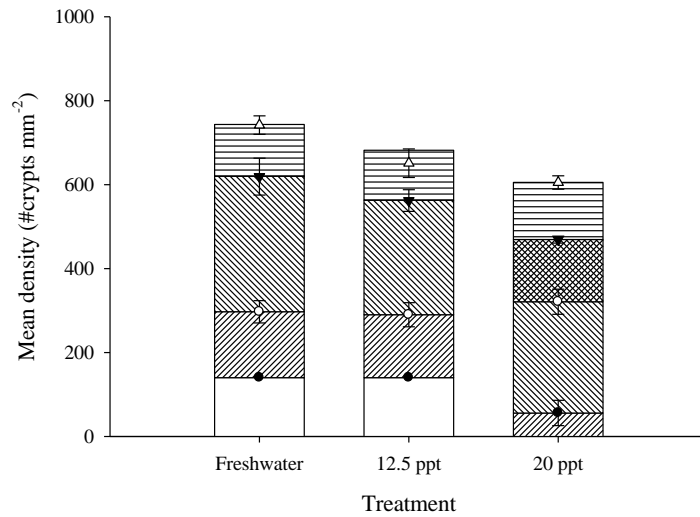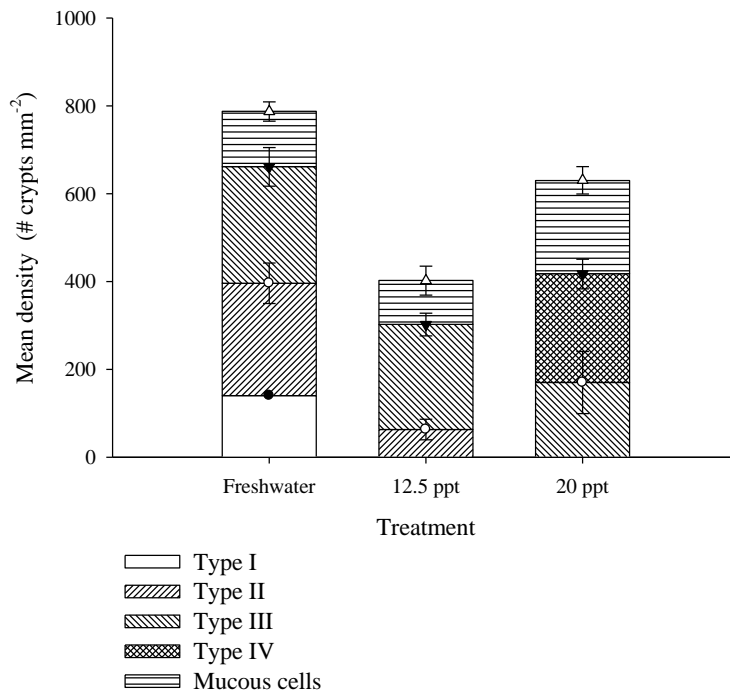
B)

Figure 6. 8 Effects of transfer from freshwater to 12.5 and 20 ppt on densities of different 'sub-types' of apical openings of MRCs on the epithelium of the yolk-sac of Nile tilapia transferred from freshwater to 12.5 and 20 ppt after **A)** 24 hours post-transfer and **B)** 48 hours post-transfer. Mean ± S.E. Statistical differences (One-way ANOVA with Tukey's post-hoc pair-wise comparison; $p < 0.05$) are presented in Table 6.4., rather than in graph, for clarity of presentation.

6.3.3 TEM observations of ultrastructure of active MRCs using immunogold labeling

6.3.3.1 anti-Na$^+$/K$^+$-ATPase

MRCs were identified on the basis of their distinct ultrastructural features and immunogold labelling of anti-Na$^+$/K$^+$-ATPase (Figures 6.10. − 6.13.). Nanogold particles were within the size range of 35 − 55 nm (Figure 6.15.B.). Variation in size was due to variation in enhancement time with GoldEnhance. Control samples *i.e.* those without primary antibody showed no binding of immunogold labelling supporting the specificity of the primary antibody used (Figure 6.9.). However, in tissue sections incubated with the primary antibody, no immunogold labelling is noted outside the MRC and associated structures, further supporting the specificity of the primary antibody (Figures 6.10 − 6.13).
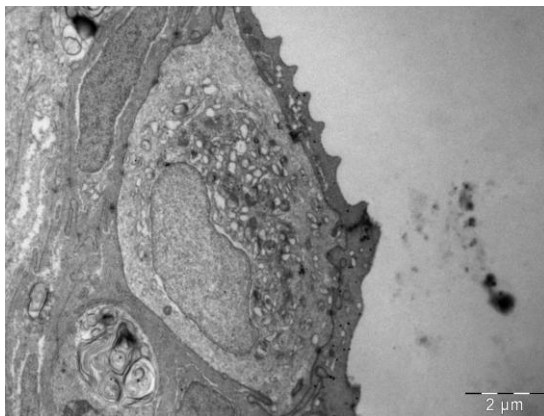
Figure 6. 9 Transmission electron micrographs of MRC in tail of yolk-sac Nile tilapia larvae. Control *i.e.* without anti-Na$^+$/K$^+$-ATPase illustrating lack of immunogold particles [Bar = 2 μm].

Four distinct types of active MRCs *i.e.* those in contact with the external environment were identified, based on apical appearances and immunogold localisation *i.e.* Type I, Type II, Type III and Type IV. In addition, mucous cells could be identified on the basis

of their ultrastructure and immuno-negative staining pattern.

- *Type I*

Type I MRCs displayed a shallower, lighter staining with a wide, flat apical opening with microvilli. The cell showed signs of degeneration *i.e.* distension of tubular system and disintegration of mitochondria, with no basolateral invaginations (Figure 6.10. A and B).

- *Type II*

Type II displayed high levels of Na^+/K^+-ATPase binding in the tubular system extending up the 'neck' of the MRC, with a narrower apical opening (Figure 6.11. A and B).

- *Type III*

Type III displayed a narrow apical opening with a dense basolateral tubular network and a clear apical band showing no mitochondria and less developed tubular system (Figure 6.12. A and B).

- *Type IV*

Type IV displayed a deep crypt with a larger opening, with mitochondria and tubular system extending to 'neck'. Tight junctions between MRC and pavement cell were also observed (Figure 6.13. A and B).

- *Mucous cells*

Mucous cells were observed in the uppermost layers of the epithelium, and were oval or round in shape and contained a large amount of lightly staining secretory vessicles (Figure 6.14.A and B).
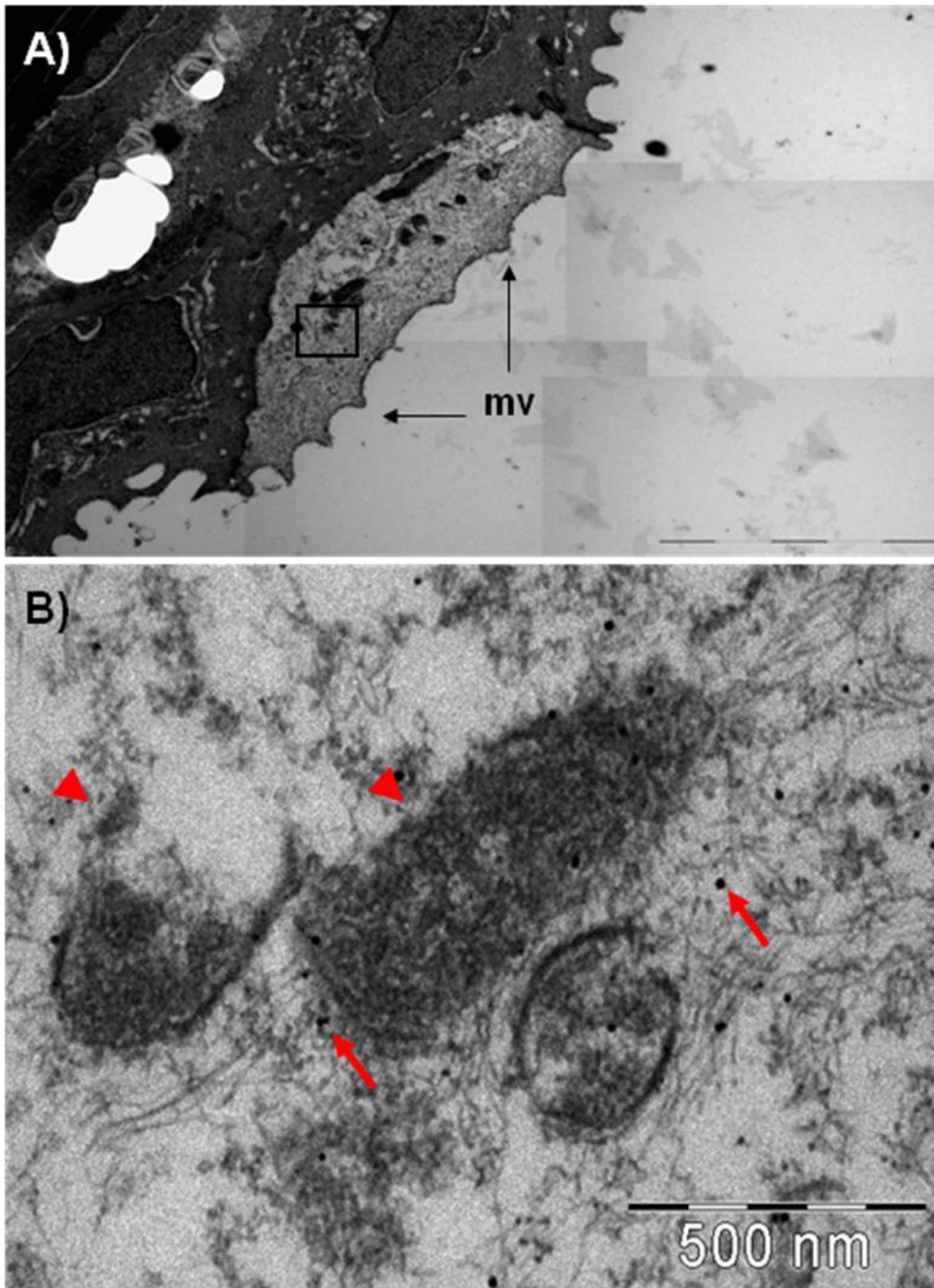
Figure 6. 10 Transmission electron micrographs of immunogold labelled anti-Na$^+$/K$^+$-ATPase Type I MRC in the tail of freshwater-adapted Nile tilapia larvae at 3 dph. **A)** Shallow, light-staining MRC with weak tubular system (mv; microvillious apical projections) [Bar = 5 μm] and **B]** Higher magnification of MRC cytoplasm within boxed area from A) showing disruption of organelle membrane (arrowhead) and disintegration of the tubular system with sparse anti-Na$^+$/K$^+$-ATPase immunogold labelling (arrows) [Bar = 500 nm].
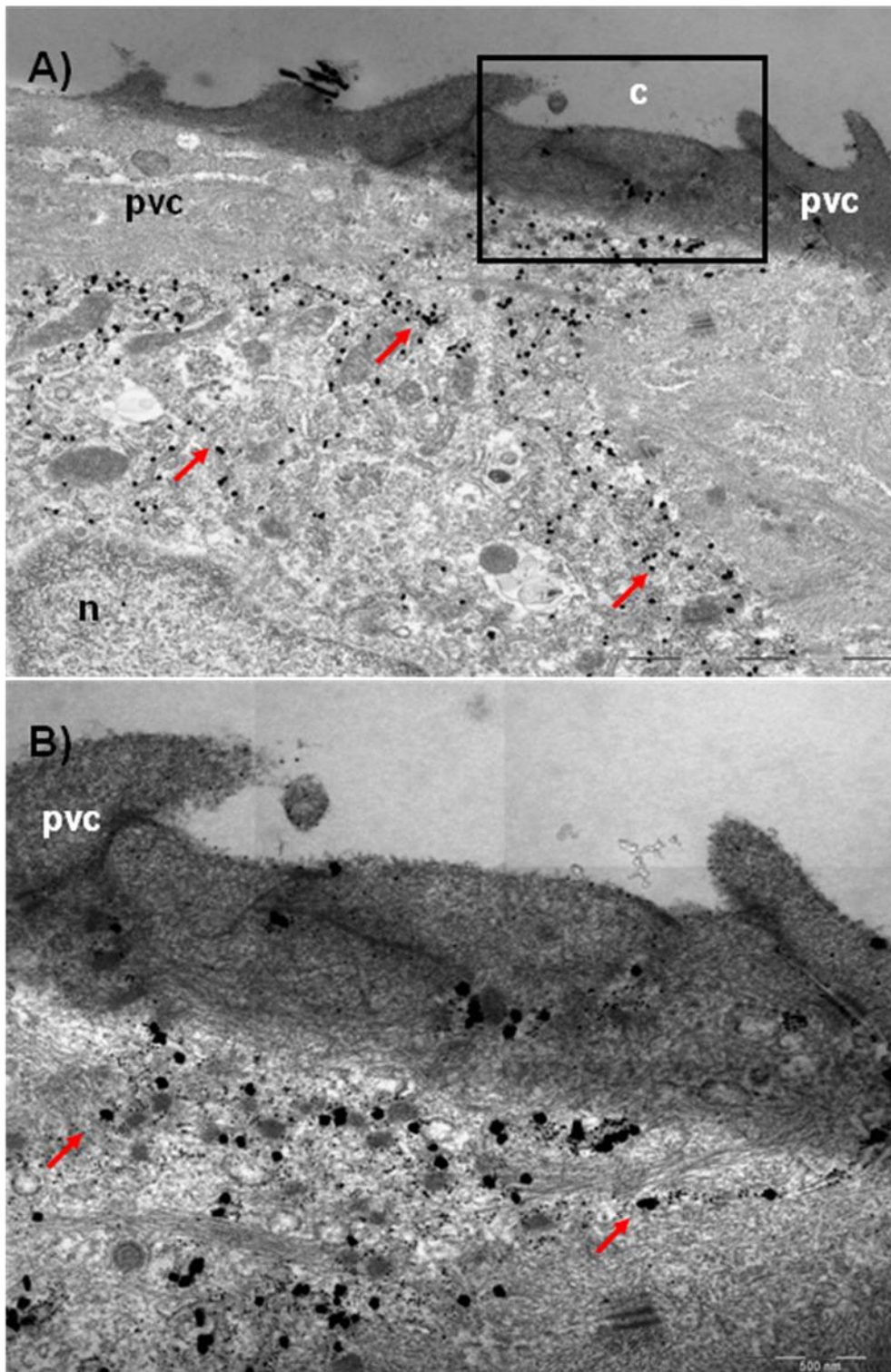
Figure 6. 11 Transmission electron micrographs of immunogold labelled anti-Na$^+$/K$^+$-ATPase Type II MRC in the tail of freshwater-adapted Nile tilapia larvae at 3 dph. **A)** MRC with immunolocalised Na$^+$/K$^+$-ATPase (arrows) extending throughout the cytoplasm (n; nucleus, pvc; pavement cell, c; apical crypt) [Bar = 2 μm] and **B)** Higher magnification of boxed area of apical crypt region from A) [Bar = 500 μm].
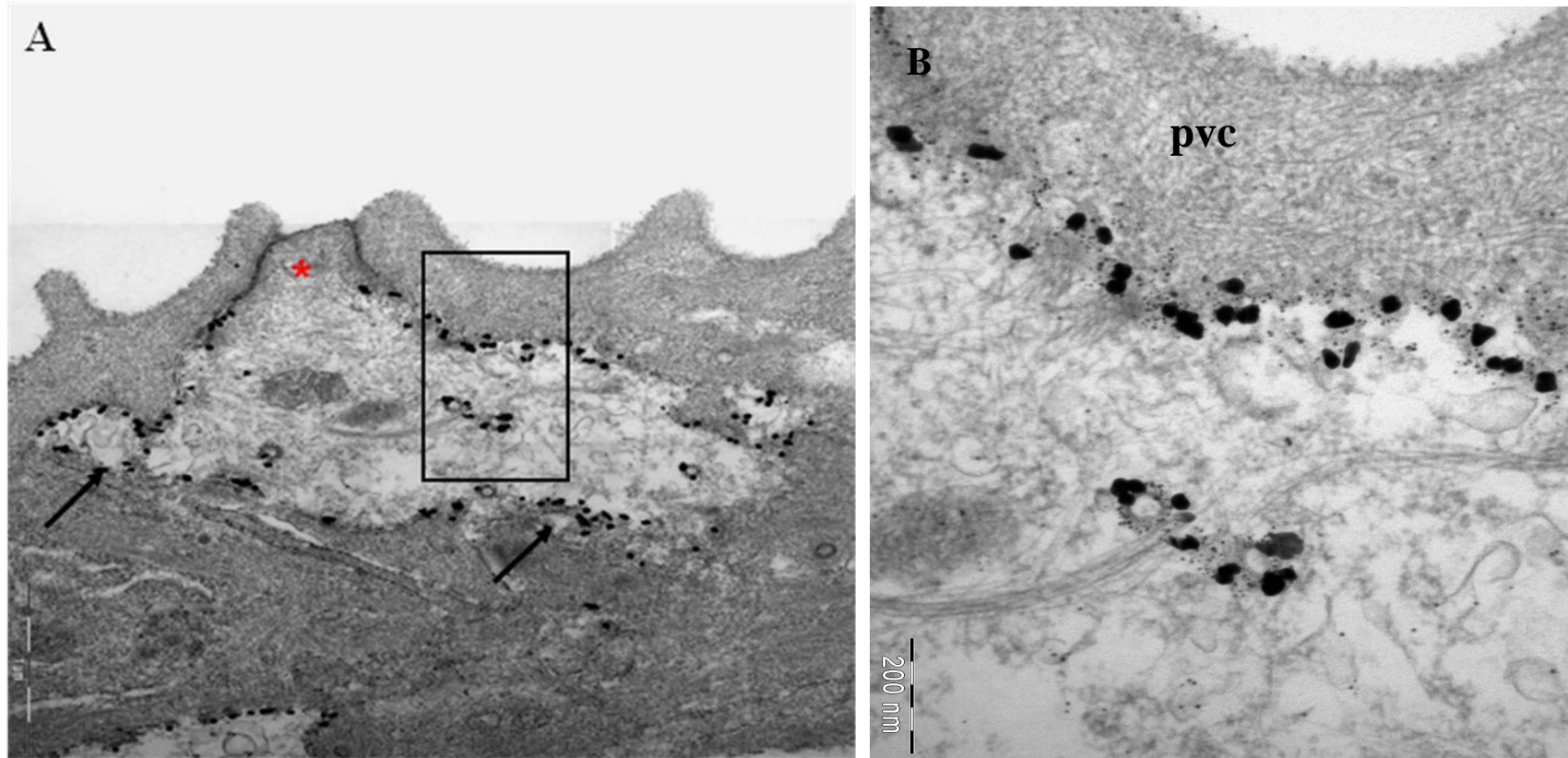
Figure 6. 12 Transmission electron micrographs of immunogold labelled anti-Na$^+$/K$^+$-ATPase Type III MRC in the tail of Nile tilapia larvae at 48 h post-transfer to 20 ppt. **A)** MRC with immunolocalised Na$^+$/K$^+$-ATPase (arrows). *Note* mitochondria and tubule poor sub-apical region (asterisk) [Bar = 1 μm] and **B)** Higher magnification of boxed area from A) showing relationship between immunolocalisation of Na$^+$/K$^+$-ATPase (arrow) and pavement cell (pvc) [Bar = 200 nm].
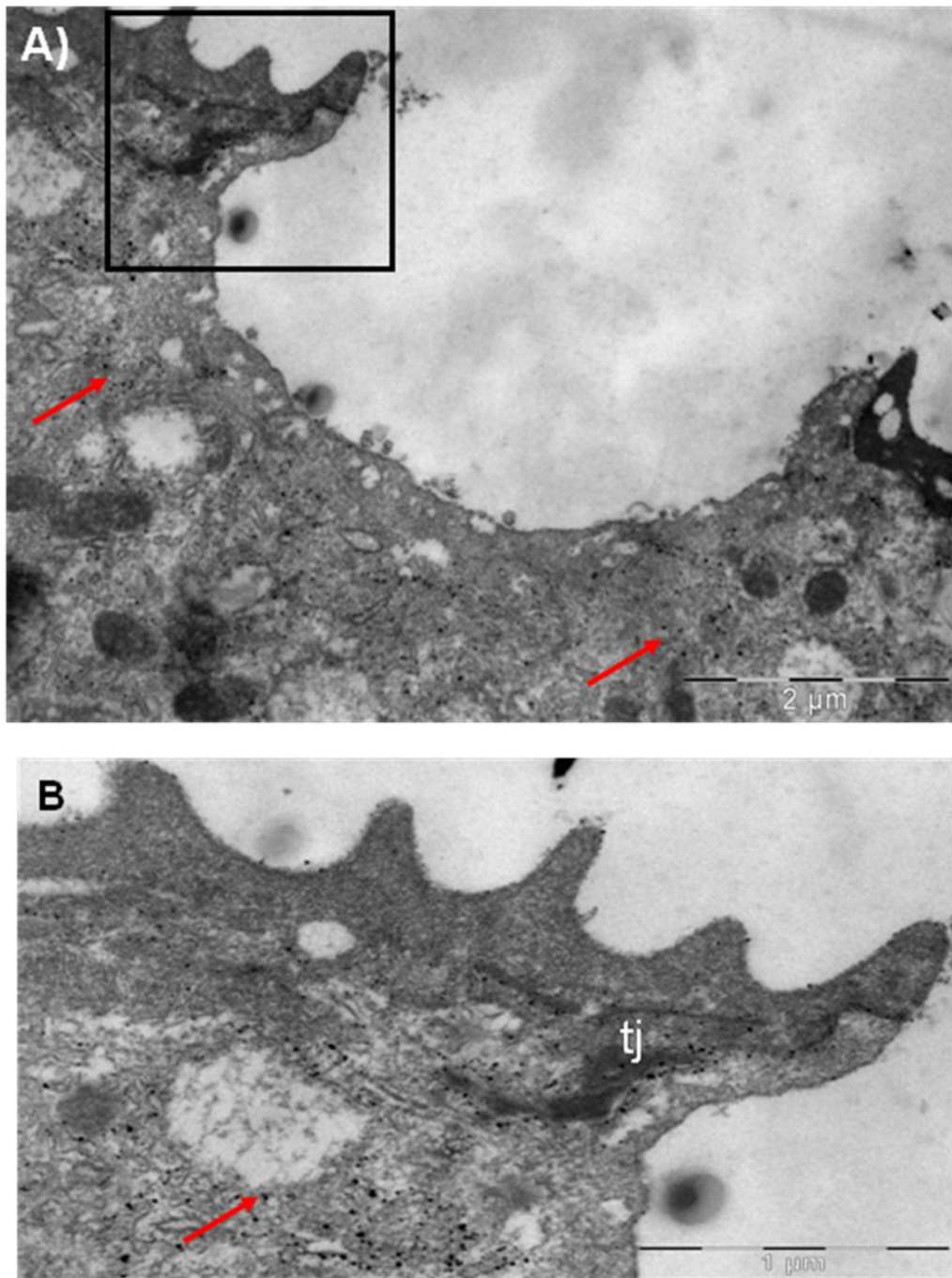
Figure 6. 13 Transmission electron micrographs of immunogold labelled anti-Na$^+$/K$^+$-ATPase Type IV MRC in the tail of Nile tilapia larvae at 48 h following transfer to 20 ppt. **A)** Apical region of MRC with crypt [Bar = 2 μm] and **B)** Higher magnification of boxed area located at the epithelium surface showing tight junction (tj) between MRC and neighbouring PVC. Arrows indicate immunogold labelling [Bar = 1 μm].
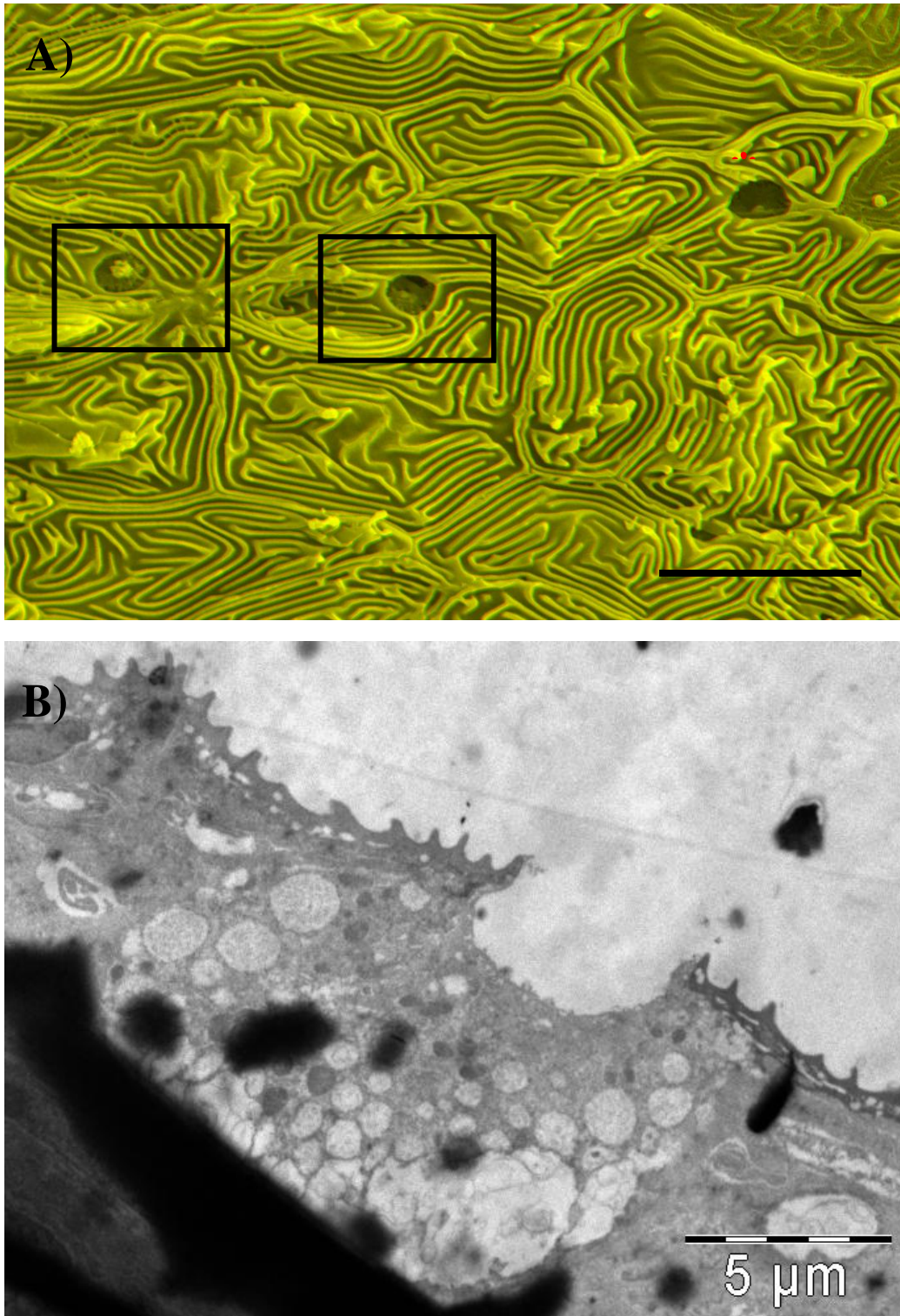
Figure 6. 14 Apical openings of mucous cells in the tail of Nile tilapia larvae at 48 h following transfer to 20 ppt. **A)** 3-D SEM micrograph showing a MRC Type II crypt (asterisk) and mucous cells (boxed areas) [Bar = 10µm] and **B)** TEM micrograph of mucous cell, anti-Na$^+$/K$^+$-ATPase negative [Bar = 5 µm].

6.3.3.2   anti-CFTR

Anti-CFTR immunogold labelling was only present on yolk-sac larvae transferred to 20 ppt at 48 h post-transfer. Immunolabelling was confined to the apical portion of the MRC (Figure 6.14.).
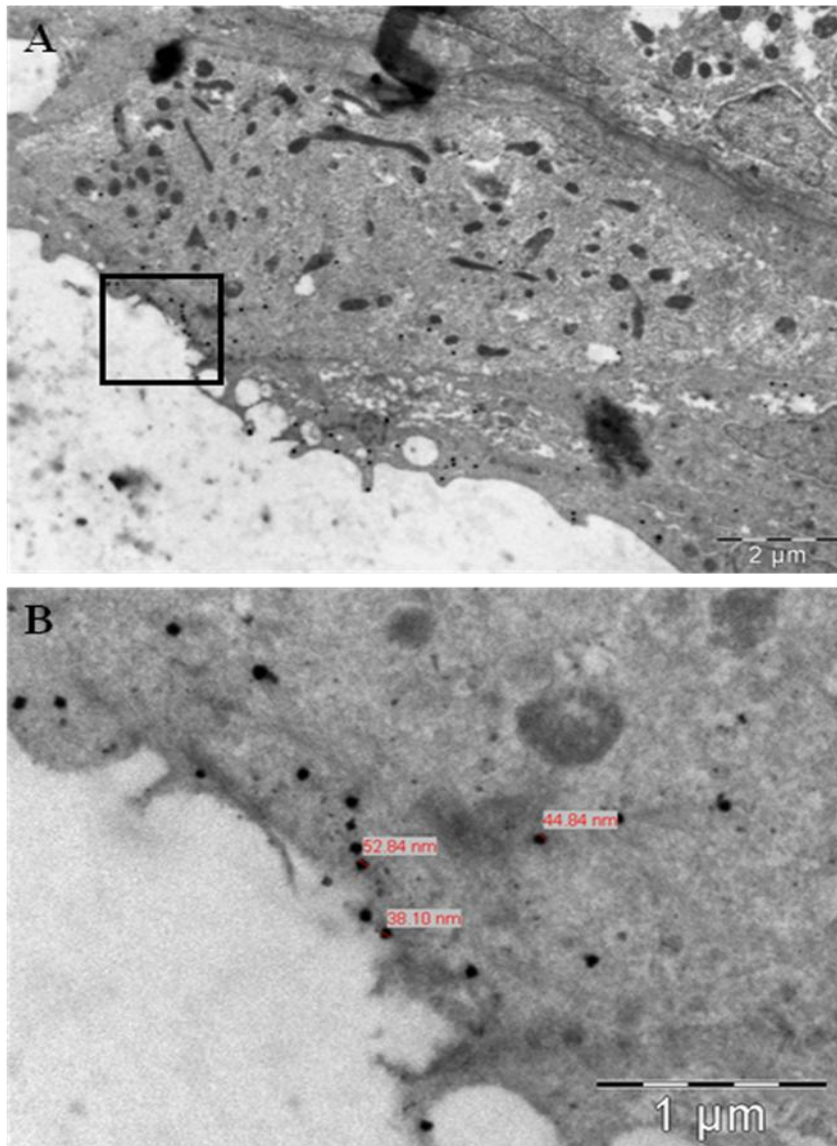
Figure 6. 15 Transmission electron micrographs of MRCs on tail of yolk-sac Nile tilapia larvae 48 h post-transfer to 20 ppt showing immunogold detection of anti-CFTR. **A)** Anti-CFTR labelling localised to apical region of cell [Bar = 2 μm] and **B)** Higher magnification of boxed area from A) showing apical region (measurements of immunogold particles in red) [Bar = 1 μm].

6.3.4 Functional classification of MRC apical crypt 'sub-types' using SEM quantification and TEM ultrastructural observations

Based on the observed variations both within and between varying environmental conditions in density, morphological differences *i.e.* size of apical openings combined with diversity in localisation patterns of anti-Na^+/K^+-ATPase at an ultrastructural level, it was possible to clarify the structure-function relationship and attempt to re-classify different 'sub-types' of MRC apical openings. Results are summarised below in Table 6.6.

Table 6.6 Reclassification of MRC types based on observations by scanning electron microscopy (SEM) and immunogold labeling transmission electron microscopy (TEM).

	New classification	SEM observations	TEM immunogold observations
Type I	Type I or degenerating form of a freshwater or absorptive MRC	This type displayed large, circular apical surfaces with flat or slightly exposed surface area with a mesh-like network of cellular extensions (Figure 6.3.A and E; Figure 6.4.A.). Type I was significantly larger than all other 'sub-types' (range 5.2 – 19.6 μm^{-2}) (One-way ANOVA; $p < 0.05$) (Figure 6.5.C.; Table 6.3.).	Type I MRCs displayed a shallower, lighter staining with a wide, flat apical opening with microvilli. The cell showed signs of degeneration *i.e.* distension of tubular system and disintegration of mitochondria, with no basolateral invaginations (Figure 6.10. A and B).
Type II	Type II or mature active absorptive MRC	This type displayed smaller, circular or ovoid shaped apical surfaces with a shallower exposed area with microvilli (Figure 6.3.B and E). Type II was significantly larger than Type III but not Type IV (range 1.1 – 15.7 μm^{-2}) (One-way ANOVA; $p < 0.05$) (Figure 6.5.C.; Table 6.3.).	Type II displayed high levels of Na^+/K^+-ATPase binding in the tubular system extending up the 'neck' of the MRC, with a narrower apical opening (Figure 6.11. A and B).
Type III	Type III or differentiating or active weakly functioning MRC	This type displayed circular or slightly ovoid and not so deeply invaginated apical crypts with some globular material (Figure 6.3.C and E). Type III was significantly smaller than other 'sub-types' (range 0.08 – 4.6 μm^{-2}) (One-way ANOVA; $p < 0.05$) (Figure 6.5.C.; Table 6.3.).	Type III displayed a narrow apical opening with a dense basolateral tubular network and a clear apical band showing no mitochondria and less developed tubular system (Figure 6.12. A and B).
Type IV	Type IV or mature active secreting form	This type displayed apical surfaces similar to Type II but were larger more circular with a deeply invaginated pit containing no apparent material (Figure 6.3.D; Figure 6.4.B and C.). Type IV was significantly smaller than Type I and significantly larger than Type III (range 4.1 – 11.7 μm^{-2}) (One-way ANOVA; $p < 0.05$) (Figure 6.5.C.; Table 6.3.).	Type IV displayed a deep crypt with a larger opening, with mitochondria and tubular system extending to 'neck'. Tight junctions between MRC and pavement cell were also observed (Figure 6.13. A and B).

6.4 Discussion

In the present study, morphological alterations in the apical openings of active MRCs were investigated in the epithelium of the yolk-sac of Nile tilapia following transfer from freshwater to brackish water environments. This is the first time that an integrated approach has been used to classify MRC apical crypts into 'sub-types' using a combination of SEM quantitative and qualitative analysis and complementary TEM immunogold labelling of Na^+/K^+-ATPase. Prior studies had recognised the existence of more than one type of MRC, based on apical morphology, in euryhaline teleosts as a response to variations in tonicity of the water *e.g.* killifish (*Fundulus heteroclitus*) (Hossler *et al*.,1985), Mozambique tilapia (*O. mossambicus)* (Hwang, 1988a; Wendelaar Bonga and van der Meij,1989; Pisam *et al.*, 1995; Kultz *et al.*, 1995), the hybrid tilapia (*O. mossambicus* x *O. niloticus*) (Cioni *et al.*, 1991), the Lake Magadi tilapia (*Oreochromis alcalicus grahami*) (Maina, 1990) and the striped bass (*Morone saxatilis*) (King and Hossler, 1991).

Lee *et al.* (1996) were the first to classify active MRCs in adult branchial tissue of the Mozambique tilapia into distinct sub-populations or 'sub-types' based on their morphological appearance and to correlate these morphological alterations to changes in the ionic composition of the environment to which they had been acclimated. Transfers of fish back and forth within media let to the important observation that the configuration of the apical membrane of MRCs may 'transform interchangeably' following transfer in order to ensure the survival of the fish (Lee *et al.,* 1996; p. 519). Indeed, the fact that MRCs possess the plasticity to allow alteration of their ion-

transporting function from ion absorption to ion secretion is well established (Hiroi *et al.,* 1999). Investigating variations in function and morphology of MRC sub-populations in varied hypotonic milieus *i.e.* local freshwater (*i.e.* Ca^+ 0.20 mM, Na^+ 0.2 mM, Cl^- 0.18 mM), hard freshwater (*i.e.* Ca^+ 2.00 mM, Na^+ 0.83 mM, Cl^- 0.85 mM) and dilute brackish water (5 ppt) (*i.e.* Ca^+ 0.70 mM, Na^+ 67.2 mM, Cl^- 85.46 mM), Lee *et al.* (1996) identified MRCs, based on their apical morphology, into the following three subtypes; sub-type 1 or wavy-convex characterised by a wide apical crypt (> 6 μm diameter) and a rough appearance of microvilli which were dominant in hard freshwater, sub-type II or shallow-basin, ovoid in shape and measuring 4 – 6 μm in diameter, occasionally with short microvilli, which predominated in local freshwater and sub-type III or deep-hole with narrow deep to oval pores (*c.* 2 μm diameter) with little or no internal structure visible which predominated in brackish water. Further work by Lee *et al.* (2000) elucidated the positive correlation between 'deep-hole' MRCs and adaptation to higher salinities (up to 30 ppt) in the Mozambique tilapia. The same authors subsequently defined these findings with composite studies using TEM, SEM and CSLM with anti-Na^+/K^+-ATPase combined with Con-A labelling of apical pits (Lee *et al.,* 2003).

This grouping has been widely accepted since then in tilapia (see Table 6.1.) but, more recently, combined studies on the selective immunolocalisation of ion pumps, transporters and channels *e.g.* Na^+/K^+-ATPase, Na^+/K^+/$2Cl^-$ co-transporter (NKCC), cystic fibrosis transmembrane conductance regulator (CFTR) or Cl^- channel, NCC and NHE_3 in tilapia embryonic skin (Hiroi *et al.,* 2005, 2008; Inokuchi *et al*., 2009) have attempted to define MRC types based on their different distribution patterns of ion transporters following transfer to varying environmental salinities, thus allowing a more

integrated approach to the study of structure of apical crypts and related function. Variations in immunolocalisation of ion transporting systems, correlative observations of apical openings of immunostained cells using differential interference contrast (DIC) images and quantification of time-course changes in MRC number and size in relation to the salinity of the external media, allowed a classification of active MRCs into four distinct types, which will be discussed below in the context of the findings of the current study.

In the present work, MRC Type I or degenerating form was only reported in freshwater-adapted tilapia and is considered to be equivalent to the large 'wavy-convex' type of Lee *et al.* (1996). In this study, Type I cells, whose relative abundance ranged between 3 – 22 % and whose apical surface area ranged between 5.2 – 19.6 μm^{-2}, is in agreement with Shiraishi *et al.* (1997) who reported a small proportion of apical openings, as observed by SEM in the yolk-sac membrane of freshwater adapted larval Mozambique tilapia, to possess relatively large apical openings, exceeding 10 μm^{-2}, with villous cytoplasmic projections. Both the presence of this large sized Type I cell in freshwater, and its disappearance following transfer to elevated salinities, as described in this study, has also been previously reported in the Mozambique tilapia (*O. mossambicus*) (Inokuchi *et al.*, 2009; Wang *et al.,* 2009; Lee *et al.*, 2003; Chang *et al.,* 2001, 2003; Shieh *et al.,* 2003; Lin and Hwang, 2001).

Perry *et al.* (1992) suggested that the size of apical openings may, to some extent, reflect ion transporting activity. Indeed, subsequent work concluded that the larger size and surface area and the resulting contact with the external environment of 'wavy-

convex' cells provided a greater capability for Cl^- uptake (Chang *et al*., 2001, 2003; Lin and Hwang, 2001; Wang *et al.,* 2009; Inokuchi *et al.,* 2009). However, in this study, the low proportion of MRCs displaying this type of apical opening in freshwater-adapted larvae could lead to a questioning of the importance of its functional role in ion absorption. TEM studies revealed a MRC with a wide but shallow apical opening in contact with the external environment with microvillous-like projections (Figure 6.10.A.) that most likely corresponds to 'sub-type' I, as defined by SEM (Figure 6.3.A.; Figure 6.4.A.). Immunogold labelling displayed weak Na^+/K^+-ATPase activity, as revealed by the low staining intensity of the immunogold particles, as well as degradation of organelles that is suggestive of cell death (Figure 6.10. A. and B.). A lower density of immunogold anti-Na^+/K^+-ATPase particles was similarly reported by Dang *et al.* (2000 a) in degenerating or apoptotic branchial MRCs of *O. mossambicus* exposed to copper. It is suggested, therefore, that this cell type, most likely, does not contribute significantly to ion absorption in larval stages of the Nile tilapia.

Apoptosis of MRCs in teleosts has been previously described under both pathogenic conditions *i.e.* toxicants in the rainbow trout (*O. mykiss*) (Daoust *et al.,* 1984; Mallat, 1985) and under physiological conditions in newly hatched rainbow trout (*O. mykiss*) (Rojo and Gonzalez, 1999), newly hatched brown trout (*S. trutta*) (Rojo *et al.,* 1997), the adult Mozambique tilapia (*O. mossambicus*) (Wendelaar Bonga and van der Meij, 1989; Wendelaar Bonga *et al.,* 1990) and the hybrid *O. mossambicus* x *Oreochromis urolepis hornorum* (Sardella *et al.,* 2004). These authors all report the ultrastructure of ageing MRCs as showing nuclear and cytoplasmic condensation and enlargement of the mitochondria surrounded by a distended tubular system. However only Rojo and Gonzalez (1999) in rainbow trout alevins (*O. mykiss*) and Wendelaar Bonga and van der

Meij (1989) in the adult *O. mossambicus* report ultrastructural evidence of a final engulfment of apoptotic MRCs by phagocytic cells. The failure to report incidences of phagocytosis in other studies and also in the present study cannot rule out the fact that this process is indeed taking place. The suggestion that a staging of degeneration of apoptotic MRCs exists *i.e.* that the removal of apoptotic MRCs includes an initial, an intermediate and a final stage, may explain the failure to report evidence of phagocytosis due to the fact that cut ultrathin sections in the current study, as viewed by TEM, did not happen to include MRCs in this final stage.

Interestingly, Hiroi *et al. (*2005) describe a proportion (approx. < 5%) of their Type II MRCs or active freshwater ion-absorptive type which displayed a basolateral Na^+/K^+-ATPase and apical NKCC distribution, as having a wide apical opening and rough apical surface when visualised by differential interference contrast microscopy. However they did not attempt to compare apical sizing within their Type II cells with staining intensity of co-transporters, which may have shed some further light on their role in active ion absorption.

It is established that apical surfaces of MRCs are flush with or slightly raised above adjoining pavements cells in most freshwater fishes (review Perry and Laurent, 1993). However recessed apical crypts have been reported in freshwater-adapted Tilapiine species *e.g.* the Mozambique tilapia (*Oreochromis mossambicus)* (Lee *et al.,* 1996, van der Heijden *et al.,* 1997; Uchida *et al.,* 2000; Inokuchi *et al*., 2008) and the Nile tilapia (*Oreochromis niloticus*) (Pisam *et al.,* 1993) which is in agreement with the slightly recessed MRC Type II apical openings that are evident in this study (Figure 6.3. B).

Absorptive epithelial cells, *i.e.* enterocytes of intestines and intercalated cells of renal collecting ducts, often possess a microvillus-rich apical membrane which is thought to provide an enlarged surface area for effective transport of ions (Lin and Hwang, 2001). Therefore, in the present study, the proliferation of this sub-type in freshwater, that is seen to decrease significantly upon transfer to elevated salinities, would suggest that it plays an active role in ion absorption, with microvilli increasing functional surface area for ion absorption, corresponding to the 'shallow-basin' type of MRC classified by Lee *et al.* (1996) based on apical morphology. In the current study, TEM reveals Na^+/K^+-ATPase immunogold labelling in the tubular system which extends throughout the cytoplasm of the cell up until the apical opening (Figure 6.11.) suggesting an active role in ion absorption. This would suggest that it is similar to the active absorptive Type II cell reported by Hiroi *et al.,* (2005) that displays Na^+/K^+-ATPase immunoreactivity extending throughout the cell, except for the nucleus.

The presence of mucous cells in teleost epithelium is well established. The observations of Vigliano *et al.* (2006) on the ultrastructural characteristics of the gills in juveniles of the Argentinian silverside (*Odontesthes bonariensis*) using both TEM and SEM, noted the presence of mucous cells, characterised by their ultrastructure *i.e.* round, flattened basally located nucleus and large amount of secretory vesicles and their apical appearance *i.e.* secreted mucins observed covering the apical surface of the cell, which is in agreement with the current study (Figure 6.3.F.; 6.14.). However the similarity of the apical crypts of mucous cells to those of MRCS has often caused confusion, possibly leading to an overestimation in quantification of MRC numbers. Klutz *et al.* (1995) describe the elaborate apical appearance of mucous cells on branchial epithelia of adult Mozambique tilapia, as observed by SEM, as possessing an apical opening with

visible mucous droplets with size of crypts varying widely according to the stage of the secretion process. However, they made no attempt to quantify or distinguish between them and active or functional MRC apical crypts, which was the focus of their study. Similarly, in the study of the effects of elevated salinity in the *O. mossambicus* x *O. urolepis hornorum* hybrid, some pores of mucous cells with developed globular extensions were observed by SEM on the surface of filamental epithelia but, as before, no attempt was made to differentiate between them and pores of functional MRCs (Sardella *et al.*, 2004). In addition, it was pointed out by van der Heijden *et al.* (1997) in their SEM study on MRC apical morphology in the adult Mozambique tilapia (*O. mossambicus*) that it was not possible, in all cases, to discriminate between a mucous cell and a MRC, based solely on morphology of the external appearance of apical surface. They commented that the globular structure observed in or on MRC crypts in freshwater fish (which corresponded to the 'shallow-basin' of Lee *at al.* (1996)) resembled the apical pores of mucocytes with mucosomes. The current study is, therefore, the first to report the quantification of mucous cells based on their apical appearance as identified by the presence of globular material within the crypt of the cell as a result of salinity challenge.

The presence of Type III MRCs in both freshwater and following transfer to elevated salinites is interesting. The smaller size of the exposed surface area of their crypt (apical surface area range $0.08 - 4.6 \ \mu m^{-2}$) is not entirely suggestive of a meaningful ion-absorptive role and, in addition, TEM studies reveal a mitochondrion and tubule poor sub-apical region at an ultrastructural level with weak immunogold staining for anti-Na^+/K^+-ATPase (Figure 6.12.). Hiroi *et al*. (2005) describes a 'dormant' Type III cell in freshwater displaying a basolateral staining of Na^+/K^+-ATPase and NKCC but with no

apical CFTR staining that decreases in density upon transfer to seawater. They propose that their disappearance following transfer to seawater suggests that these cells actively differentiate and synthesise CFTR *de novo* moving it to the apical membrane in order to become active secretory cells or Type IV cells which replace Type III cells upon transfer. Indeed, when transferred from seawater to freshwater, these changes in density of Type III and IV cells were shown in reverse. However they did not rule out the possibility that these cells had more than a 'dormant' role in freshwater and suggested a possible involvement in active ion absorption in hypo-osmotic conditions, due to the presence of an unquantified proportion of these cells displaying a weak NKCC apical staining suggestive of ion absorptive Type II cells.

This could offer an explanation for the observations made in this study. It is suggested that they are not 'dormant' as their high relative abundance (85 %) at 48 h post-transfer to 12.5 ppt and the concomitant lack of Type IV secretory MRCs would indicate that they indeed have an active, ionoregulatory role. It is suggested that Type III cells (Figure 6.3.C. and E.) are newly formed cells that have just reached the surface and include both MRCs undergoing active differentiation according to the external media and their corresponding osmotic requirements *i.e.* those synthesising NKCC *de novo* and placing it in the apical membrane, and actively absorptive MRCs whose small crypt size with a lack of visible material allowed them to be grouped accordingly.

Kultz *et al.* (1995) describe apical crypts in gill epithelia of *O. mossambicus* exposed to hyperosmotic media (60 ppt) as 'well-developed'. As has already been seen, it was Lee *et al.* (1996) who classified this type of MRC opening in gill epithelium of brackish-

water adapted *O. mossambicus* as 'deep-hole', characterised by a deeply invaginated pore, and subsequently reported this type to increase in density in the same species when transferred to elevated salinities (Lee *et al*., 2000, 2003). Similar results have been reported in the Mozambique tilapia by van der Heijden *et al.* (1997) Uchida *et al.* (2000); Hiroi *et al.* (2005). Therefore it is suggested that the Type IV or active secretory type in this study corresponds to the 'deep-hole' type previously described. It is well established that 'deep-hole' type crypts are actively involved in Cl⁻ secretion (Chang *et al.*, 2001, 2003; Lin and Hwang, 2001). It is suggested that, when the environmental Cl⁻ levels are raised, the apical membrane and exchangers are internalised in order to reduce the surface area which is vital for modulation of Cl⁻ uptake activities (Lin and Hwang, 2001). This would explain the appearance of Type IV MRCs, with a deeply recessed crypt, following transfer to 20 ppt that is seen in this study (Figure 6.3.D.; Figure 6.4.B. and C.; Figure 6.13.A.). The observed apical localisation of immunogold particles of anti-CFTR at 48 h post-transfer to 20 ppt and the corresponding CSLM immunolocalisation, revealing a ring-like fluorescence (Figure 6.15.A. − D.), is in agreement with the apical immuno-reactivity for CFTR described by Hiroi *et al.* (2005) for their Type IV or secretory seawater-type.

However, as has been seen above, two MRC 'sub-types' are reported to be present following transfer to elevated salinities *e.g.* Type III with a circular or slightly ovoid appearance occasionally with internal visible material that replaced Type I and II cells by 48 h post-transfer to 12.5 and 20 ppt, and Type IV with a larger, more circular appearance than Type III and a deeply invaginated pit that contained no apparent material that replaced Type I and II cells by 48 h post-transfer to 20 ppt. It, therefore, should be assumed that both Type III and IV are actively involved in ion secretion in

hyperosmotic environments. van der Heijden *et al.* (1997) reports that their seawater Type III crypts (equivalent to 'deep-hole') sometimes contained 'material of undefined origin' (p. 59) inside the pits but no attempt was made to quantify the differences between these varying types. However, recently, both 'shallow-basin' and 'deep-hole' sub-types were reported in gill epithelium of adult *O. mossambicus* following transfer to brackish water (20 ppt) from 3 h post-transfer until 96 h post-transfer, suggesting that both types play a significant role in ion secretion (Wang *et al.*, 2009). They report that, at 48 h post-transfer, a higher proportion of 'deep-hole' than 'shallow-basin' crypts were observed, which is in contrast to the present study, where an equal relative abundance of 47/44 % of Type III to Type IV cells was observed at 48 h post-transfer to 20 ppt respectively. This may be due to the fact that Wang *et al.* (2009) made no quantitative measurements of MRC apical opening diameter or surface area and 'sub-types' were grouped solely based on their appearance which may have led to an over estimation of deep-hole or those with a recessed appearance, which in the current study were classified as Type III due to their smaller size.

To conclude, while immunohistochemical studies have recognised the presence of a 'dormant' or differentiating type of MRC, previous SEM observations have not. This study, therefore, offers a reclassification of MRC sub-types based on the morphology of their apical appearance in combination with ultrastructural observations and Na^+/K^+-ATPase and CFTR localisation in an attempt to redefine structure function relationship of active MRC. In addition, the apical openings of mucous cells have been catagorised and quantified for the first time, based on the presence of globules of material, suggestive of secreted mucins, within the apical crypt, preventing an overestimation of counts of MRC apical crypt numbers.

7 Chapter 7 Morphological and ultrastructural changes to mitochondria-rich cells in the Nile tilapia following salinity challenge.

7.1 Introduction

7.1.1 Background

Adjustments to mitochondria-rich cell (MRC) morphology, as a response to environmental changes, are vital in conserving physiological function in the teleost. Laurent's (1984; p.75) comment that MRCs in freshwater and seawater-adapted teleosts 'display significant differences in relation to the milieu where the fish live' suggests that a MRC's ability to change form and function depends on the external environmental conditions and the required osmoregulatory role. It is this plasticity or adaptive response that contributes to euryhaline fishes' ability to inhabit both diverse and fluctuating environments.

7.1.2 Effects of salinity on functional differentiation of MRCs

Morphological changes to adult MRCs and modifications to their ion transporting function are interrelated. The implication that MRCs of euryhaline fishes possess the plasticity that allows alteration of their ion-transporting functions by modification in the localization of ion transport proteins on the apical and basolateral membranes suggests two opposite ion movements that are clearly dependant on their environment; the absorption of ions in freshwater and the secretion of ions in seawater. This change in

direction of ion transport as a result of changes in external ionic composition or salinity has been described by Marshall (2002) as 'diametrically different'. Mitochondria-rich cells in early life stages of teleost fishes similarly possess an adaptive capacity that allows them to change morphologically and biochemically to varying osmoregulatory conditions. The studies of Hwang and Hirano (1985) on the morphology of early stage MRCs in the ayu *(Plecoglossus altivelis)*, carp *(Cyprinus carpio)* and flounder *(Kareius bicoloratus)* showed that intercellular organisation and junctional structure of seawater adapted teleost species were notably different to those of freshwater adapted fishes; MRCs in seawater adapted fishes interdigitated with neighbouring cells and were linked with leaky junctions, whereas no such interdigitations or junctions were found in freshwater fishes. They concluded that this ability to modify structure and function was critical to their ability to adapt to varying environmental conditions, in this case salinity.

7.1.3   Immunodetection of MRCs in teleosts

The use of antibodies as a tool for localising molecules of interest in microscopy was first demonstrated in the 1940's (Coons *et al*., 1941) but immunohistochemical techniques came into wider use in the 1970's (Taylor and Burns, 1974; Taylor and Mason 1974). The first report of the use of an immunological approach used in the study of the fish gill was by Rahim *et al.* (1988) in the study of trout carbonic anhydrase. Present research relies mainly on the use of mammalian antibodies due to their species cross-reactivity and wide availability. The most widely used antibody in the study of osmoregulation and ionic transport in fish are the pan-specific antibodies for the α-subunit of Na^+/K^+-ATPase, due to the fact that the epitopes of these antibodies are conserved in most vertebrates and invertebrates (see Section 1.2.3.). Consequently they have been widely applied in the   study of MRC dynamics.

264

7.1.4 Background and general observations on MRC ultrastructure

Transmission electron microscopy has been extensively used to observe ultrastructural variations in MRCs, either as a response to changes in external environment or simply between existing variations or 'sub-types' in the same milieu. The general ultrastructure of the MRC appears relatively well conserved amongst species, as compared to surface morphology (Perry, 1997). From the earliest electron microscopy studies, it was accepted that MRCs contained cytoplasm that displayed a highly-developed membranous system comprising of anastomosed tubules that formed polygonal meshes, creating a network that encloses abundant mitochondria. Karnovsky (1971) was the first to use the reduced osmium staining technique to demonstrate that the tubular system of MRCs consisted, more specifically, of two distinct membranous systems; a faintly stained endoplasmic reticulum and a more densely stained tubular system that showed continuity with the laterobasal plasma membrane (Figure 7.1.).
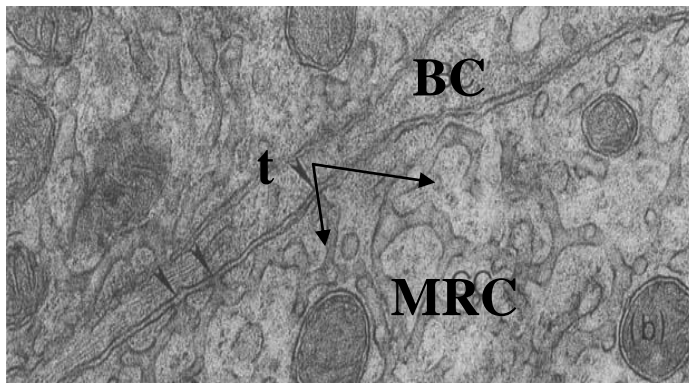
Figure 7. 1 Ultrastructure of mitochondria-rich cell (MRC) in freshwater-adapted *Oreochromis niloticus* showing detail of the tubular system. The membranes of tubules (t) are continuous with the plasma membrane (arrowheads) and join with the basement cell (BC). Reduced osmium staining; x 42 000. (From Cioni *et al.,* 1991).

Further studies suggested that the tubular system extended throughout the whole cytoplasm except for a narrow band located just below the apical surface. (Rambourg and Clermont, 1990). The vesiculo-tubular system was specifically identified in MRCs of fish gills by Pisam (1981) using the reduced osmium staining technique, although vesicles in the apical cytoplasm of MRCs had been reported prior to this *e.g*. Doyle and Gorecki (1961), Straus and Doyle (1961), Threadgold and Houston (1961, 1964), Shirai and Utida (1970) and Kikuchi (1977). The abundance of mitochondria is another conspicuous feature of MRCs. Described first by Karnaky *et al.* (1976), these rod-shaped organelles are closely associated with the tubular system and are, therefore, found dispersed evenly throughout the cytoplasm, except the apical zone (Pisam and Rambourg, 1991) and the Golgi region, which itself forms a supranuclear, continuous ribbon-like structure (Rambourg and Clermont, 1990). Endoplasmic reticulum, a continuous organelle that is found to be distributed homogeneously throughout the cytoplasm of the cell, has been reported to inter-cross the tubular system and consists of flattened cisternae interconnected by membranous tubules (Pisam and Rambourg, 1991).

Singer (1959) was the first to develop an iron-containing protein ferritin as an electron-dense marker for electron microscopy, and it was followed by the introduction of gold probes as immunolabels (Faulk and Taylor, 1971; Romano *et al.*, 1974; Romano and Romano, 1977; Roth and Binder, 1978). Previous immune-electron microscopy studies in teleosts, using a post-fixation staining technique to provide a visualisation of the localisation of specific transporters on the tubular system of MRCs, have revealed Na^+/K^+-ATPase labelling on the tubular system in MRCs in the sea bass (*Dicentrachus labrax*) (Varsamos *et al*., 2002), the Mozambique tilapia (*Oreochromis mossambicus*)

(Dang *et al*., 2000 a and b) and the Coho salmon (*Onchorynchus kisutch*) (Wilson *et al*., 2002 b).

7.1.5   Aims of the Chapter

It has been demonstrated that mitochondria-rich cells (MRCs) undergo structural differentiation due to their developmental stage (Chapter 5) or as a functional response, as evidenced by changes in apical morphology, to variations in the ionic composition of the external media (Chapter 6). Therefore the hypothesis that changes in density, abundance, size and appearance of MRC as a response to changes in ionic composition of the external media do in fact reflect cellular differentiation, either as an expression of their developmental stage or as a modulation of their function, will be investigated in this chapter.

In order to explore the hypothesis, the following aspects were addressed:

- The use of quantitative 3-D image analysis of confocal scanning electron microscopy in order to examine morphological responses and structural changes of MRCs following osmotic challenge during early life stages of the Nile tilapia.

- The development of a method that allows differentiation of active MRCs *i.e.* those in contact with external environment and non-active *i.e.* those not in contact or lying in a sub-cellular location.

- The development a reliable, pre-fixation immunogold technique that allows the study of the localisation of co-transporters and ion channel *i.e.* Na^+/K^+-ATPase

and CFTR at transmission electron microscope level (TEM) and complementary visualisation .

- The use of correlative transmission electron microscopy to examine ultrastructural features underlying the processes observed in confocal microscopy.

7.2 Materials and methods

7.2.1 Egg supply, artificial incubation systems and transfer regime

Broodstock were maintained as outlined in Section 2.1 and eggs were obtained by the manual stripping method as outlined in Section 2.1.2. Batches of eggs from several females were combined to provide a heterogeneous sample and eggs and yolk-sac larvae were reared as outlined in Section 2.3. At 3 days post-hatch yolk-sac larvae were transferred immediately from freshwater to the experimental salinities (*i.e.* 12.5 and 20 ppt) which were prepared as outlined in Section 2.2., and yolk-sac larvae were sampled after 24 and 48 hours.

7.2.2 Whole-mount immunohistochemistry with simultaneous labelling of pavement cells and nuclei

7.2.2.1 Antibodies

To quantify morphological changes to MRCs occurring as a result of transfer from freshwater to elevated salinities, larvae were sampled at time of transfer (3 dph) and at 24 and 48 h post-transfer to elevated salinities (*i.e*. 12.5 and 20 ppt). Controls *i.e*. larvae remaining in freshwater, were also sampled at the same time-points. A mouse monoclonal antibody, raised against the α-subunit of chicken Na^+/K^+-ATPase (mouse anti-chicken IgG α5, Takeyasu *et al*. 1988) was used to detect integumental MRCs.

Whole-mount larvae were fixed and labelled according to the whole-mount

immunohistochemistry protocol outlined in the previous chapter (Section 6.2.3.1.). Control samples were prepared without the primary antibody to determine the auto-fluorescence of the sample and the extent of non-specific binding.

7.2.2.2 Phalloidin staining

Following Stage (viii) (Section 6.2.3.1. Whole-mount immunohistochemistry), samples were further incubated for 2 h at room temperature with the actin label Alexa Fluor (594) phalloidin (Molecular Probes, Invitrogen) (4 µl of 0.2 U µl^{-1} phalloidin in 200 µl PBS) to allow visualisation of the pavement cells.

7.2.2.3 DAPI staining

DAPI (4',6-Diamidino-2-phenylindole) (Molecular Probes, Invitrogen) staining was used for nuclear staining. DAPI (Molecular Probes, Invitrogen). A few drops of 300 nM DAPI in de-ionised water were added to the tubes immediately prior to observation.

7.2.3 Image capture

Control and labelled samples were kept in the dark immediately prior to use. They were mounted in glycerin on a 35 mm glass base dish (Iwaki, Scitech Div., Japan) and observed using a Leica TCS SP2 AOBS confocal scanning laser microscope (CSLM) (Leica Microsystems, Milton Keynes, U.K.) coupled to a DM TRE2 inverted miscroscope (Leica Microsystems, Milton Keynes, U.K.) employing a x 63 oil/glycerol immersion objective.

Images were captured using grey, red, green and blue channels using appropriate excitation and emission wavelengths for the different fluorescent dyes (Table 7.1.). To avoid cross-talk, a sequential scanning configuration was used, with images collected successively rather than simultaneously in three separate scans. For standardisation of a reference point on the larvae, horizontal sectional images were taken in a plane parallel to the surface of the epithelium, as identified by the actin stain phalloidin. Images were always taken in the region of the tail somite lying immediately dorsal to the anus (Figure 7.2.).
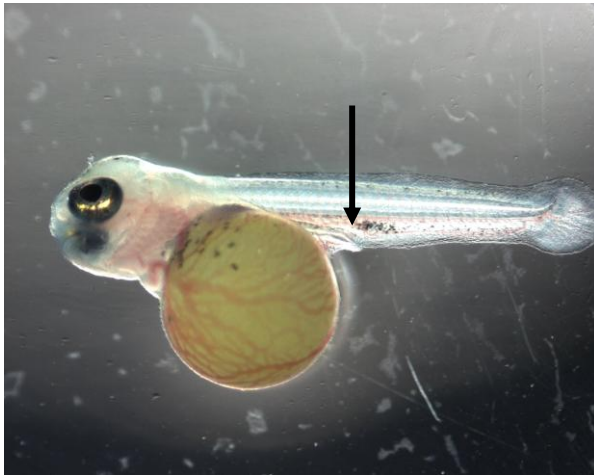
Figure 7. 2 Area of confocal microscopy measurement on tail of yolk-sac Nile tilapia larvae used for confocal scanning laser microscopy (arrow).

Table 7. 1 Properties of fluorescent dyes used to identify mitochondria-rich cells in integument of Nile tilapia larvae.

Target label	Probe	Channel	Excitation maximum (nm)	Emission maximum (nm)	Laser Line
Na^+/K^+-ATPase	Alexa Fluor – Fluoronanogold	Green	488	498	488
Nuclei	DAPI	Blue	405	411	405
Actin	Phalloidin – Texas Red	Red	594	600	594

For morphometric analysis of 3-D images, a z-stack comprising of 35 serial images was taken for each sample. This stack consisted of 35 x 2-D images, each lying in the plane of the epithelium with the deepest captured first and the shallowest last. All images were taken by scanning a frame area 1024 x 1024 pixels in the *x, y* plane. The size of an optical section was 150 μm x 150 μm x 1 μm (*x-y-z*) and confocal images were taken at 1 μm intervals to generate *z*-stacks. At least 5 fish per treatment group and 2 areas of observation per fish were scanned. CSLM sampling time per stack was approximately 5 min. A minimum of 10 immunoreactive cells were analysed for each fish.

7.2.4   Image analysis

For the image analysis, ImageJ (version 1.44) (National Institutes of Health, U.S.) with a 3-D Object Counter plug-in (3D-OC; Cordelières, F.P., 2010) was used, allowing quantification of a number of densitometric and morphometric features of immunolocalised target fields *i.e.* MRCs. A fixed threshold value was set according to initial visual inspection of a range of samples and this was used subsequently to ensure consistency and repeatability of the analysis. The output contained measurement data

for each cell as well as processed images for subsequent visual inspection. Where data was given in voxels, actual measurements were calculated, based on given size of a voxel *i.e.* 1 voxel = 0.14645 x 0.14645 x 1.03 μm.

Output data included:

- Volume of immunoreactive area (μm^{-3})

- Immunoreactive surface area (μm^{-2})

- Mean signal intensity of all the object's voxels

- Measurements relating to bounding box *e.g.* box encompassing each individual object (*i.e.* immunopositive MRC) – including the *x-y-z* coordinates of upper left hand corner of bounding box, and the width, height and depth of bounding box.

7.2.4.1 Determination of active vs. non-active MRCs

Scanned confocal images were taken from within the tissue moving towards the surface of the epithelium in order to reduce photo-bleaching of the fluorescent signal. Therefore, the output data *i.e.* the *z* coordinate of the top left hand corner of the bounding box, equalled the distance from the basolateral side of an immunopositive cell to the first scanned section *i.e.* 35 μm into the tissue. In order to calculate the distance of the top of an immunopositive cell from the surface of the epithelium, the *z* coordinate was added to the depth of the bounding box and then subtracted from the total depth of the scanned stacks *i.e.* 35 μm, which gave the distance of the apical side of the immunopositive cell from the surface of the epithelium.

Due to the unevenness of the epithelium of the tail of the yolk-sac larvae, as observed through the phalloidin staining of actin-containing pavement cells, it was determined that those immunopositive cells whose apical surface lay within 4 μm or less from the surface could be considered active and those immunopositive cells that lay more than 4 μm from the epithelial surface would be considered non-active. This allowed morphometric measurements *e.g.* volume, staining intensity and shape factor to be separately analysed based on functional-state. Figure 7.3. shows a graphical representation of the final positioning of MRCs based on the output data from ImageJ; the relative positioning of the MRCs in relation to the epithelium is demonstrated using a 3-D reconstruction of coordinates of the bounding box of each cell.
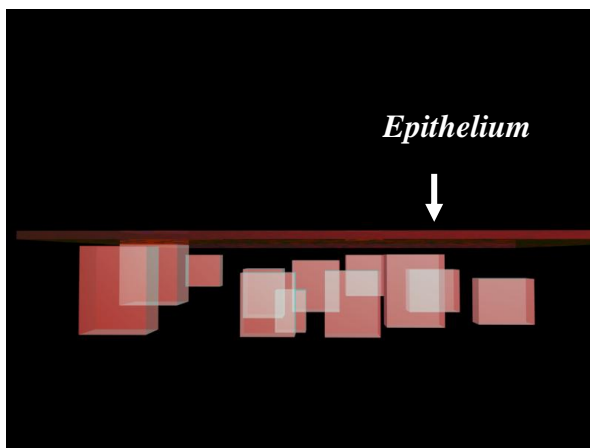
Figure 7. 3 3-D graphical representation of output data from ImageJ with 3-D Object Counter plug-in to demonstrate how distance from surface was calculated.

7.2.4.2 Density

Total density of immunoreactive cells were calculated for each area and expressed as # immunoreactive cells per mm^{-2} of epithelium. Densities of both active and non-active MRCs were quantified and the ratio of active MRCs to non-active MRC was calculated

as follows:

Percentage active MRC = (active MRCs per micrograph/total # MRCs per micrograph)* 100

Percentage non-active MRCs = (non-active MRCs per micrograph/total # MRCs per micrograph)* 100

7.2.4.3 Shape factor or sphericity

In order to determine whether the shape of the immunoreactive area of MRCs was affected by salinity or functional state shape factor or sphericity was calculated. Sphericity or the measure of how spherical an object is, is based on the ratio of surface area of a sphere with the same volume as the given shape to the surface area of the given shape. The sphericity of a sphere is 1 and values < 1 have a low sphericity and indicate a more elongate shape.

Sphericity (Ψ) was determined for each immunoreactive cell using the formula:

$$\Psi = \frac{\Pi^{1/3} (6 \times \text{volume of immunoreactive area})^{2/3}}{\text{immunoreactive surface area}}$$

7.2.4.4 Ratio of depth of bounding box: mean width of bounding box

The ratio of the depth of the 3-D bounding box to the mean of the width and height of the bounding box *i.e.* mean of the x and y coordinates for each immunopositive object, was calculated in order to give an indication of the shape of the immunopositive cell. If a cube has a ratio of 1:1, a ratio of $< 1:1$ would indicate a squatter or flatter shape and a ratio of $>1:1$ would indicate a more elongated shape.

Ratio was determined for each immunoreactive cell using the formula:

Ratio = Depth or z coordinate of bounding box/mean of width and height or x and y of bounding box.

7.2.5 Immunogold labelling

Transmission electron microscopy was used for examination of immunolocalisation of anti-Na$^+$/K$^+$-ATPase. Larvae were sampled at time of transfer from freshwater (3 dph) and at 24 and 48 h post-transfer to elevated salinities. Controls *i.e.* larvae remaining in freshwater were also sampled at the same time points. Dissected tails of three fish per treatment were fixed and labelled according to the protocol described in Section 6.2.3.1. and immunogold labelling was carried out according to the protocol outline in Section 6.2.3.2. An ultrathin section (90 nm) was cut from each of the dissected tails and serial sections were made every 10 μm thereafter. Cut ultra-thin sections were placed on 200 mesh Formvar-coated copper grips, stained with a solution of 4% uranyl acetate in 50% alcohol and Reynold's lead citrate (see Appendix) and observed using an FEI Technai Spirit G2 Bio Twin transmission electron microscope.

7.2.6 Statistical analyses

Statistical analyses were carried out with Minitab 16 software using a General Linear Model or One-way analysis of variance (ANOVA) with Tukey's post-hoc pair-wise comparisons. Homogeneity of variance was tested using Levene's test and normality was tested using the Anderson-Darling test. Where data failed these assumptions, they were transformed using an appropriate transformation *i.e.* square root. Significance was accepted when $p < 0.05$.

7.3 Results

7.3.1 Anti- Na$^+$/K$^+$-ATPase immunohistochemistry with confocal scanning laser microscopy

7.3.1.1 Observations

Immunoreactive cells lying beneath actin stained pavement cells were detected on the tail of Nile tilapia Na$^+$/K$^+$-ATPase in freshwater and 12.5 and 20 ppt (Figure 7.5.A.). Immunofluorescence was observed throughout the cell except for the nucleus (Figure 7.5.B.) and a clear apical opening or crypt could be observed in mature MRCs (Figure 7.5. C. and D.). No other cell types were distinctly stained above background levels and the antibody controls (*i.e.* without primary antibody) showed no staining (Figure 7.4.). MRCs were observed to possess immunopositive ramifying tubular extensions that appeared to emanate from the basolateral portion of the cell (Figure 7.6.A. and B.).
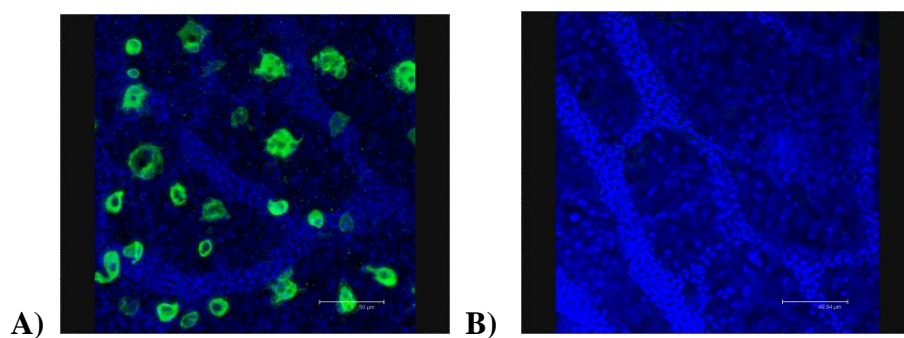
Figure 7. 4 Confocal laser scanning micrographs of yolk-sac epithelium of Nile tilapia at 3 dph. **A)** Immunopositive MRCs (anti-Na$^+$/K$^+$-ATPase, green) and nuclei (DAPI, blue) [Bar = 50 μm] and **B)** Control showing positive staining of nuclei (DAPI, blue) without anti- Na$^+$/K$^+$-ATPase [Bar = 49.84 μm].
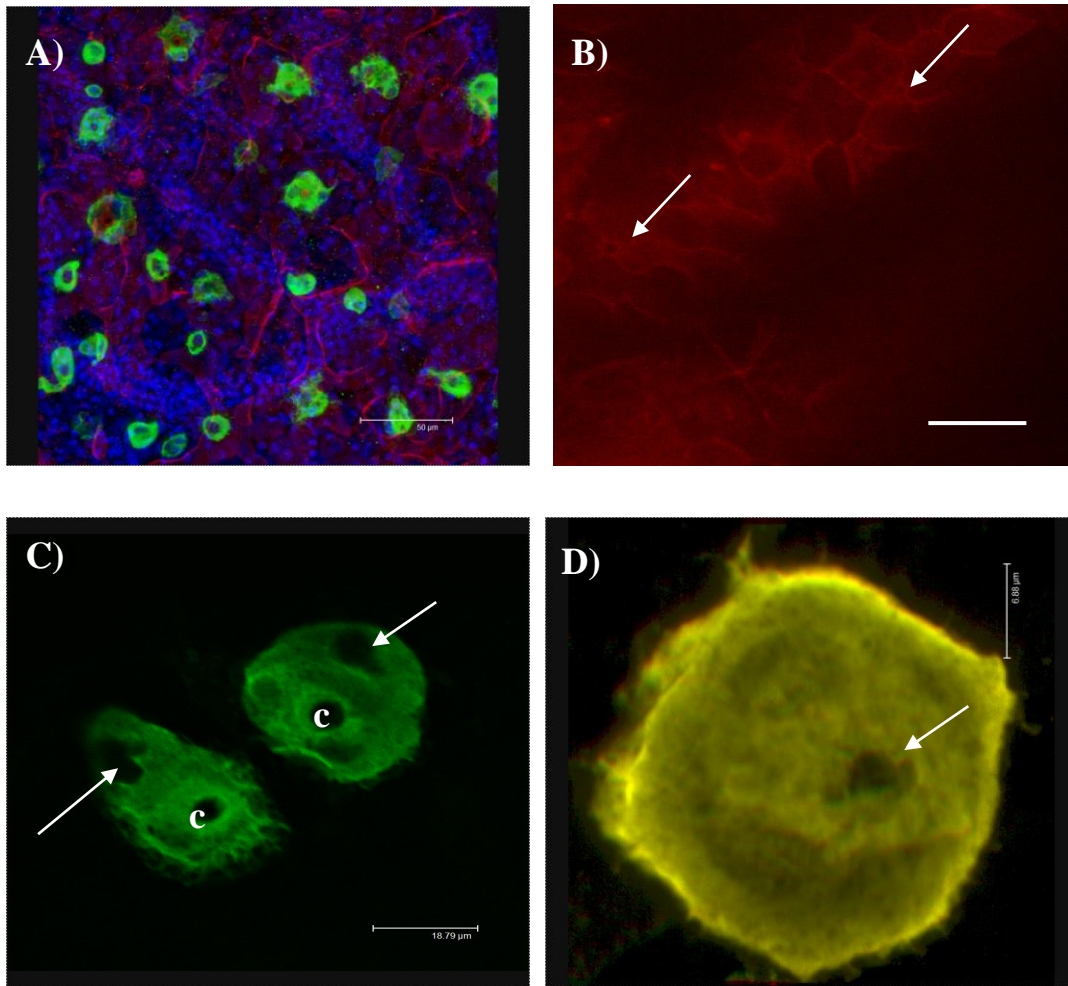
Figure 7. 5 Confocal laser scanning micrographs of MRCs on tail of freshwater adapted larvae at 3 dph. **A)** Triple staining of epithelium showing immunopositive MRCs (anti-Na$^+$/K$^+$-ATPase, green), pavement cells (Phalloidin, red) and nuclei (DAPI, blue) [Bar = 30 μm], **B)** Epithelium labelled with Phalloidin showing actin rings around MRC apical crypts (arrows) [Bar = 30 μm], **C)** Mature immunopositive anti-Na$^+$/K$^+$-ATPase MRCs (green) showing apical crypt (c) and shadows of unstained nuclei (arrows) [Bar = 18.79 μm] and **D)** 3-D confocal scanning laser micrograph of immunopositive single MRC showing apical crypt (arrow) [Bar = 6.88 μm].
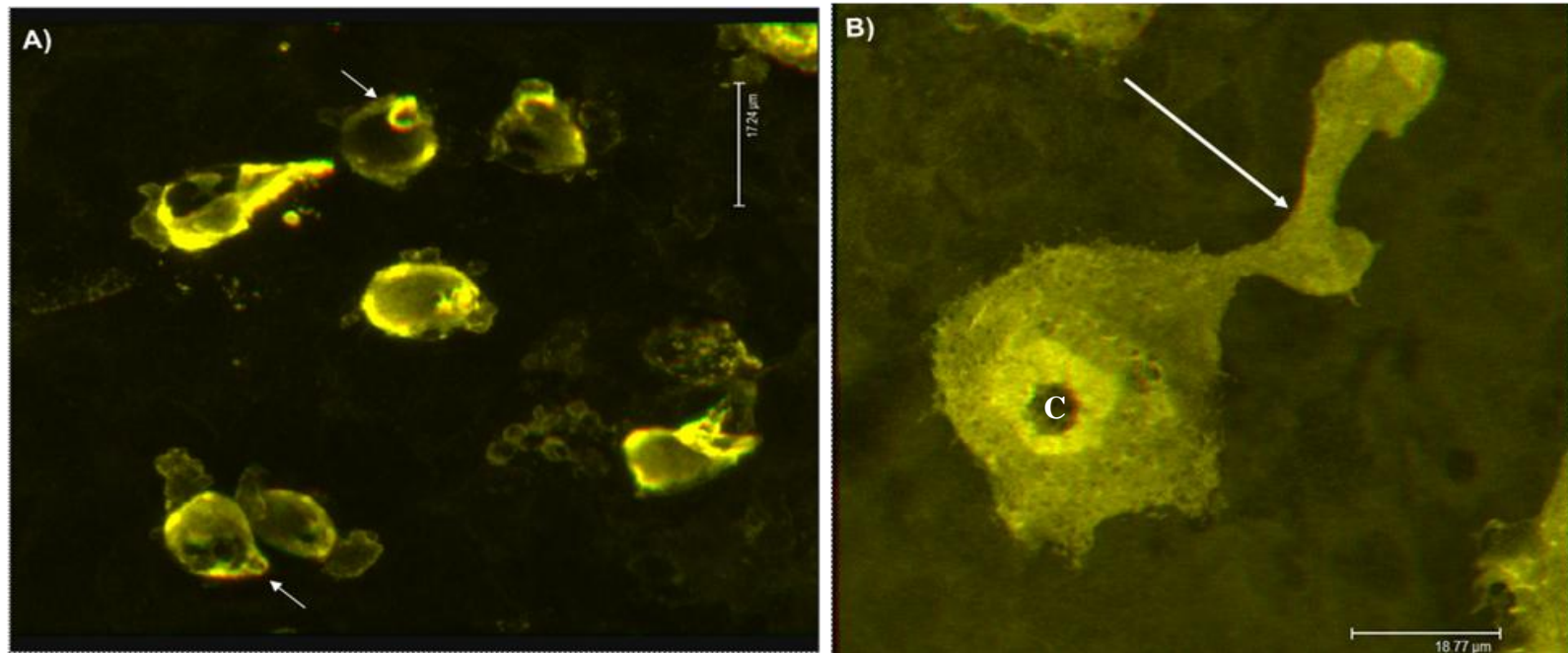
Figure 7. 6 3–D fluorescent confocal laser scanning micrographs of MRCs labelled with anti-Na$^+$/K$^+$-ATPase on tail of freshwater adapted larvae at 3 dph. **A)** Multiple MRCs with narrow necks extending to apical surface (arrows) showing fluorescent outcrops [Bar = 17.24 μm] and **B)** Single MRC showing apical crypt (c) and basolateral ramifying tubular extension (arrow) [Bar = 18.77 μm].

7.3.1.2   Determination of active and non-active MRCs

3-D image analysis of confocal stacks allowed visualisation of MRCs in relation to their spatial location which permitted assessment and classification of active and non-active MRCs based on the distance of the top of the immunopositive cell from the epithelial surface. There was a significant overall effect of functional-state *i.e.* activity or non-activity of MRCs on cell volume (μm^{-3}) and mean staining intensity. Results are summarised in Table 7.2. and Figure 7.7.

Table 7. 2 Analysis of Variance for effect of functional state on mean cell volume (μm^{-3}) and mean staining intensity (General Linear Model; $p < 0.001$).

Source	*DF*	*F*	*P-value*
MRC volume:			
Active vs. non-active MRCs	1	29.53	0.001
Error	228		
Mean staining intensity:			
Active vs. non-active MRCs	1	21.77	0.001
Error	228		

A)   **B)**
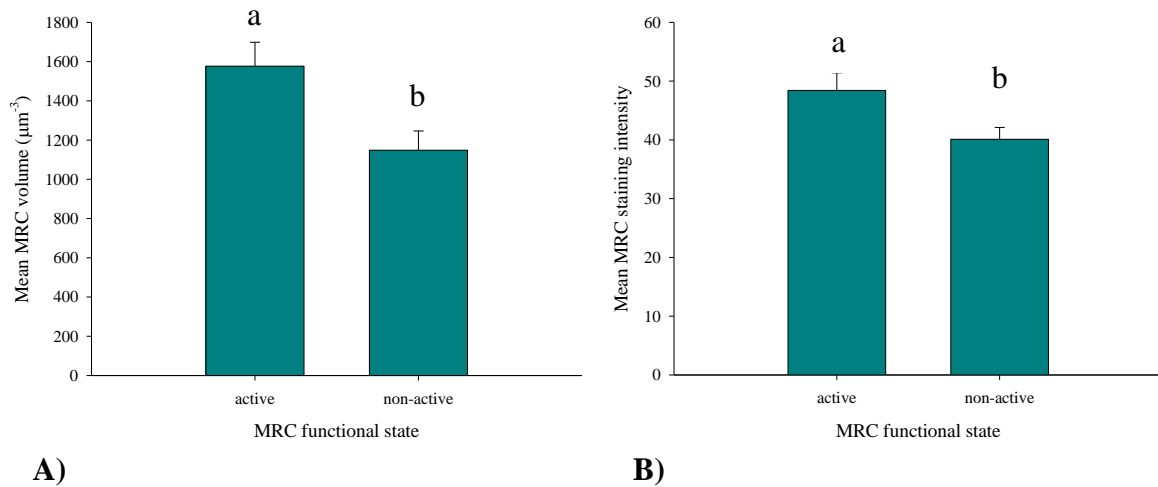
Figure 7. 7 Overall effect of functional state on **A)** MRC volume (μm^{-3}) and **B)** Mean staining intensity Mean ± S.E. Different letters indicate significant differences between bars (GLM; $p < 0.001$).

7.3.1.3   MRC density

There was a significant overall effect of salinity, time post-transfer and their interaction on total MRC density which is summarised in Table 7.3. and Figure 7.8.

Table 7. 3 Analysis of Variance for effect of salinity, time post-transfer and their interaction on total MRC density (# MRCs mm^{-2}) (General Linear Model; $p < 0.001$).

Source	DF	F	P-value
Total density of MRCs:			
Salinity	2	12.86	0.001
Time post-transfer	2	5.26	0.008
Salinity vs. age post-transfer	4	4.19	0.021
Error	51		

A)

B)
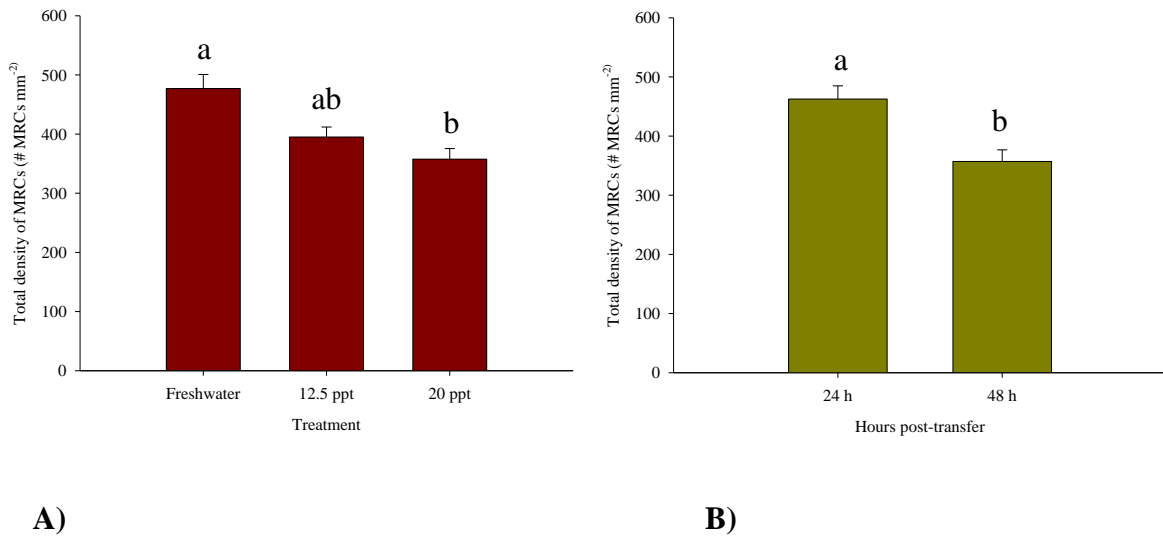
Figure 7. 8 Overall effect of **A)** Salinity and **B)** Time post-transfer on total MRC density (# MRCs mm^{-2}). Mean ± S.E. Different letters indicate significant differences between bars (GLM with Tukey's post-hoc pairwise comparisons; $p < 0.05$).

Total density of MRCs decreased following transfer to both 12.5 and 20 ppt from 24 h post-transfer. However, a significant decrease in total density of MRCs is also seen in larvae remaining in freshwater at 48 h post-transfer (Table 7.4.). Further quantitative analysis of active and non-active MRCs revealed that at both 24 and 48 h post-transfer to 20 ppt, the percentage of non-active MRCs was significantly higher than active MRCs, whereas following transfer to 12.5 ppt at both 24 and 48 h post-transfer the percentage of active MRCs was higher than that of non-active MRCs (Table 7.4. and Figure 7.9.).

Table 7. 4   Density of MRCs in tail epithelium of freshwater and brackish water adapted Nile tilapia as determined by immunohistochemistry and confocal scanning laser microscopy. Total density data are mean ± S.E. Percentage data is mean ± S.E. of active or non-active cells of total number of cells. Data within rows with different superscript letters are statistically different. (One-way ANOVA with Tukey's post-hoc pairwise comparisons; $p < 0.05$).

Treatment	Freshwater			12.5 ppt		20 ppt	
Time (hours post-transfer)	0	24	48	24	48	24	48
Total density of MRCs (# MRCs/mm^{-2})	478.9 ± 27.44 [ab]	607.3 ± 53.41 [a]	367.6 ± 26.18 [b]	425.3 ± 40.97 [ab]	333.3 ± 32.52 [b]	407.3 ± 45.05 [b]	375.3 ± 34.03 [b]
Density of active MRCs (% of total cells)	56.8 ± 6.75 [ab]	49.0 ± 5.44 [b]	66.8 ± 10.28 [a]	63.3 ± 9.51 [a]	59.44 ± 5.8 [ab]	44.4 ± 10.76 [b]	43.9 ± 8.49 [b]
Density of non-active MRCs (% of total cells)	43.2 ± 6.75 [ab]	50.1 ± 5.44 [a]	33.2 ± 10.28 [b]	36.7 ± 9.51 [b]	40.55 ± 5.8 [b]	55.6 ± 10.76 [a]	56.1 ± 8.49 [a]
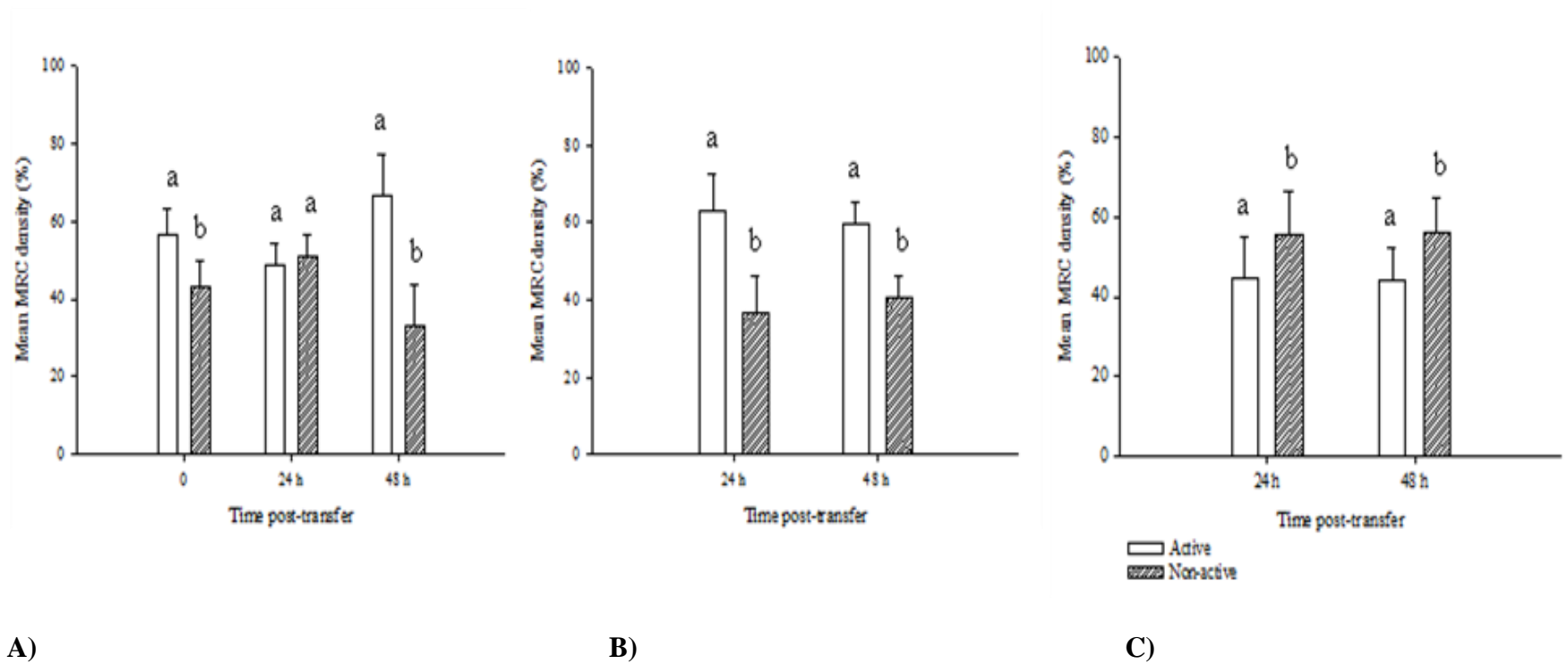
Figure 7. 9 Variations in MRC density (% of total MRCs) between active and non-active MRCs in tail of Nile tilapia following transfer from freshwater to elevated salinities as determined by immunohistochemistry and confocal scanning laser microscopy. **A)** Freshwater, **B)** 12.5 ppt and **C)** 20 ppt. Data are mean ± S.E. (n = 5). Different letters indicate significant differences between bars (One-way ANOVA with Tukey's post-hoc pair-wise comparison; $p < 0.05$).

7.3.1.4   MRC morphometrics

There was a significant overall effect of salinity, time post-transfer and their interaction on cell volume (μm^{-3}). There was also a significant overall effect of salinity, the interaction between salinity and age post-transfer but not of salinity on mean staining intensity. Results are summarised in Table 7.5.and Figure 7.10.

Table 7. 5 Analysis of Variance for effect of salinity, time post-transfer and their interaction on cell volumes and mean staining intensity (General Linear Model; p < 0.001).

Source	DF	F	P-value
MRC volume:			
Salinity	2	6.91	0.001
Time post-transfer	2	33.58	0.001
Salinity vs. age post-transfer	4	4.63	0.001
Error	219		
MRC mean staining intensity:			
Salinity	2	1.95	0.144
Time post-transfer	2	92.33	0.001
Salinity vs. age post-transfer	4	8.29	0.001
Error	219		
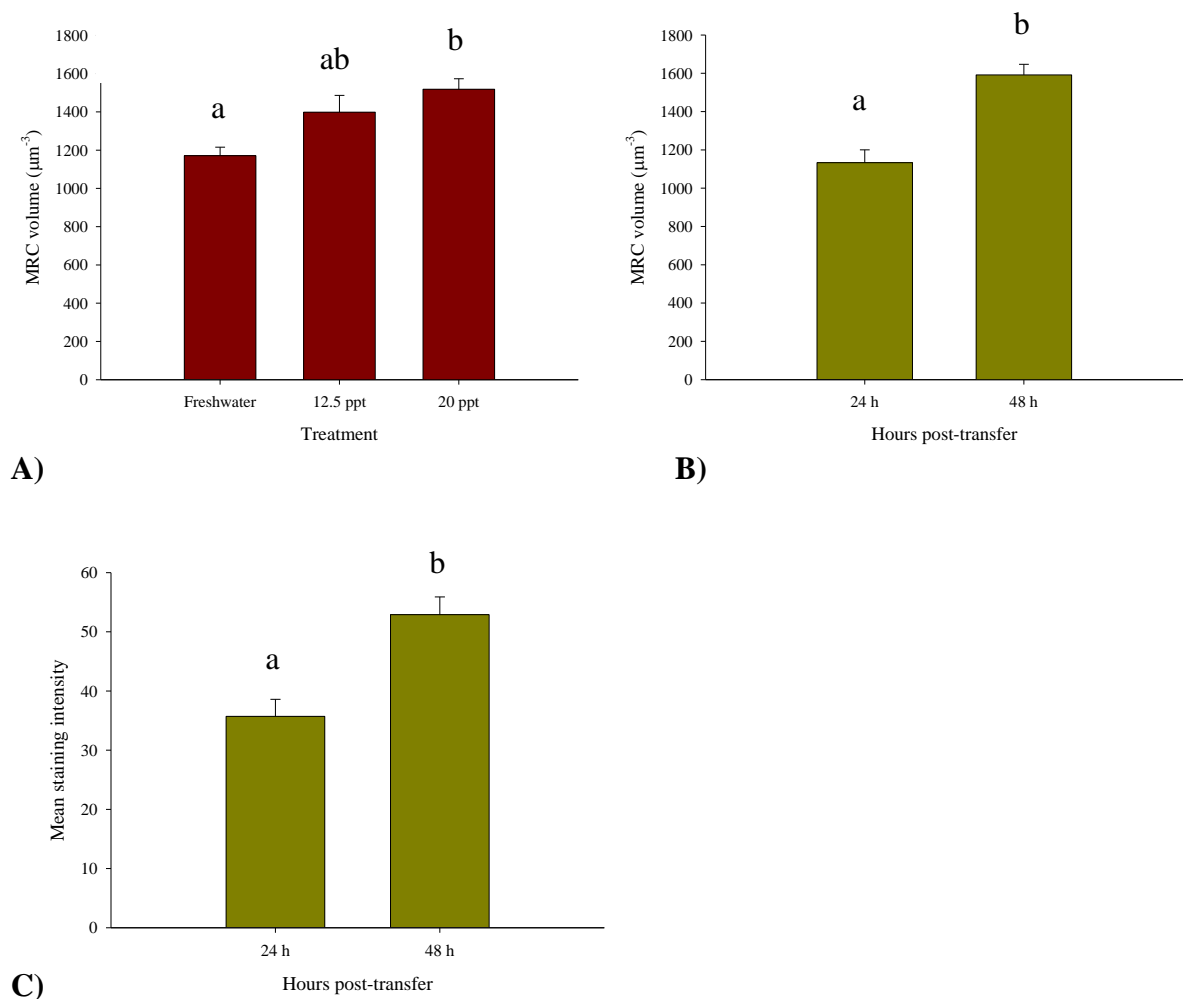
Figure 7. 10 Overall effect of **A)** Salinity and **B)** Time post-transfer on MRC cell volume and **C)** Overall effect of time post-transfer on MRC cell staining intensity. Mean ± S.E. Different letters indicate significant differences between bars (GLM with Tukey's post-hoc pairwise comparisons; $p < 0.001$).

Further quantitative morphometric analyses of active and non-active MRCs revealed that the volume of both active and non-active MRCs significantly increased from the freshwater values following transfer to elevated salinities by 48 h post-transfer (Table 7.6. and Figure 7.11.). Active MRCs always displayed a greater volume than their non-active counterparts (Table 7.6 and Figure 7.11.). Similarly, mean staining intensity of non-active MRCs was always significantly lower than that of active MRCs (Table 7.6

and Figure 7.12.).
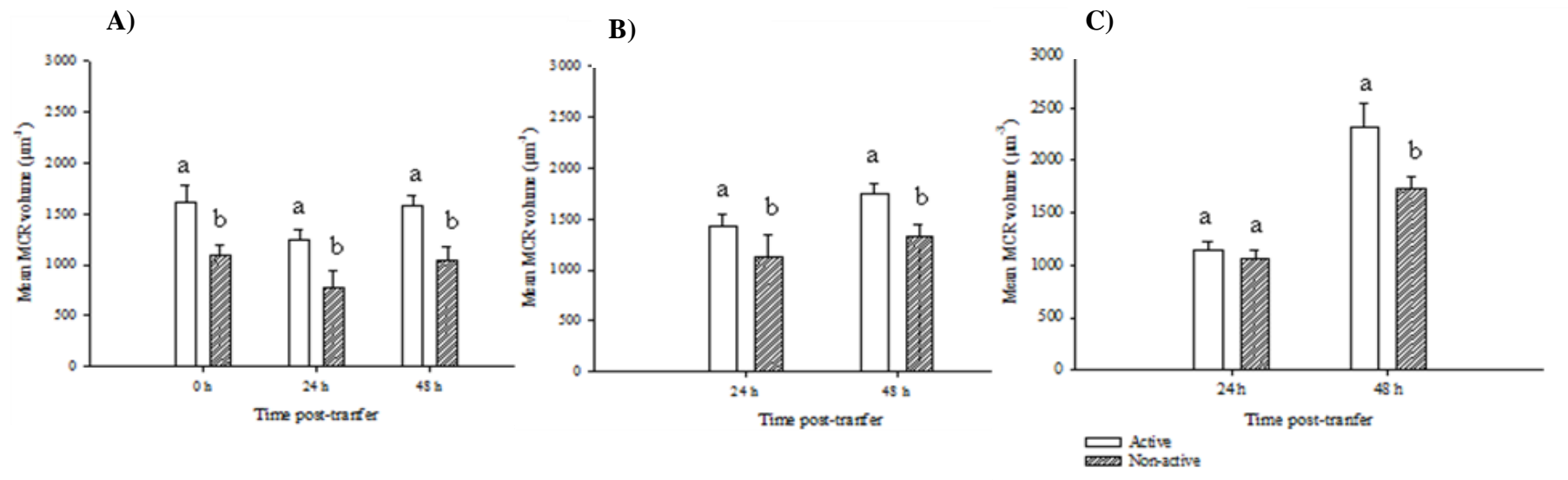
Figure 7. 11 Variations in immunoreactive cell volume between active and non-active MRCs in tail of Nile tilapia following transfer from freshwater to elevated salinities as determined by immunohistochemistry and confocal laser scanning microscopy. **A)** Freshwater, **B)** 12.5 ppt and **C)** 20 ppt. Data are mean ± S.E. (n = 5). Different letters indicate significant differences between bars (One-way ANOVA with Tukey's post-hoc pair-wise comparison; $p < 0.05$).
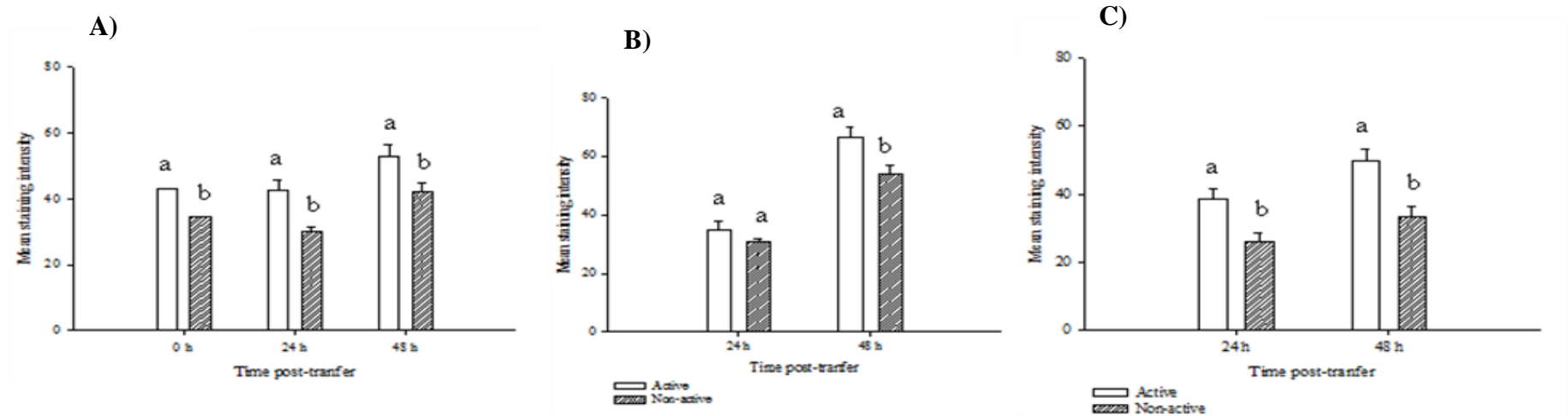
Figure 7. 12 Variations in mean staining intensity between active and non-active MRCs in tail of Nile tilapia following transfer from freshwater to elevated salinities as determined by immunohistochemistry and confocal laser scanning microscopy. **A)** Freshwater, **B)** 12.5 ppt and **C)** 20 ppt. Data are mean ± S.E. (n = 5). Different letters indicate significant differences between bars (One-way ANOVA with Tukey's post-hoc pair-wise comparison; $p < 0.05$).

Table 7. 6 MRC volume (μm^{-3}) and mean staining intensity in tail of Nile tilapia following transfer from freshwater to elevated salinities as determined by immunohistochemistry and confocal scanning laser microscopy. Data are mean ± S.E. (n = 5). Data within rows with different subscript letters are statistically different (One-way ANOVA with Tukey's post-hoc pair-wise comparison; p < 0.05).

Treatment	Freshwater			12.5 ppt		20 ppt	
Time (hours post-transfer)	0	24	48	24	48	24	48
Cell volume (μm^{-3})							
MRC functional state:							
Active	1618.9 ± 158.0 [b]	1253.6 ± 94.05 [a]	1574.2 ± 101.15 [b]	1422.7 ± 129.74 [b]	1740.1 ± 112.65 [bc]	1151.8 ± 72.91 [a]	2323.7 ± 218.43 [c]
Non-active	1087.9 ± 116.80 [b]	780.7 ± 161.87 [a]	1052.2 ± 122.61 [b]	1128.9 ± 218.25 [b]	1335.2 ± 119.21 [bc]	1064.1 ± 76.01 [b]	1728.0 ± 112.77 [c]
Mean staining intensity:							
MRC functional state:							
Active	43.2 ± 2.33 [ab]	42.7 ± 2.28 [ab]	52.7 ± 2.65 [b]	35.1 ± 1.95 [a]	66.3 ± 3.69 [c]	38.6 ± 2.94 [a]	49.7 ± 2.75 [b]
Non-active	34.46 ± 2.60 [a]	30.21 ± 3.19 [a]	42.06 ± 3.31 [b]	30.97 ± 2.60 [a]	53.93 ± 3.87 [b]	26.00 ± 3.02 [a]	33.44 ± 2.26 [a]

7.3.1.5 Sphericity

There was a significant overall effect of time post-transfer but not of salinity or functional state on sphericity. Results are summarised in Table 7.7.and Figure 7.13.

Table 7. 7 Analysis of Variance for effects of salinity, time post-transfer and their interaction and functional state on sphericity (General Linear Model; $p < 0.001$).

Source	DF	F	P-value
Sphericity:			
Salinity	2	1.49	0.137
Time post-transfer	2	24.58	0.001
Active vs. non-active	1	0.421	0.517
Error	284		
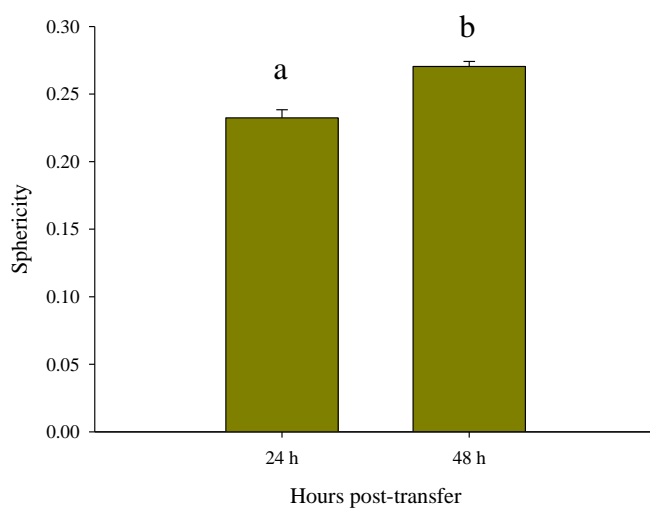
Figure 7. 13 Overall effect of time post-transfer on MRC sphericity, where 1.0 represents a perfectly spherical object. Mean ± S.E. Different letters indicate significant differences between bars (GLM; $p < 0.05$).

7.3.1.6 Ratio depth: mean width

There was a significant overall effect of salinity, the interaction between salinity and time post-transfer and functional state on the ratio of bounding box but not of time post-transfer. Results are summarised in Table 7.8.and Figure 7.14.

Table 7. 8 Analysis of Variance for effects of salinity, time post-transfer and their interaction and functional state on ratio of bounding box (General Linear Model; p < 0.001).

Source	DF	F	P-value
Ratio:			
Salinity	2	11.00	0.001
Time post-transfer	2	1.67	1.89
Salinity vs. time post-transfer	4	3.56	0.030
Active vs. non-active	1	31.63	0.001
Error	284		

A)   B)
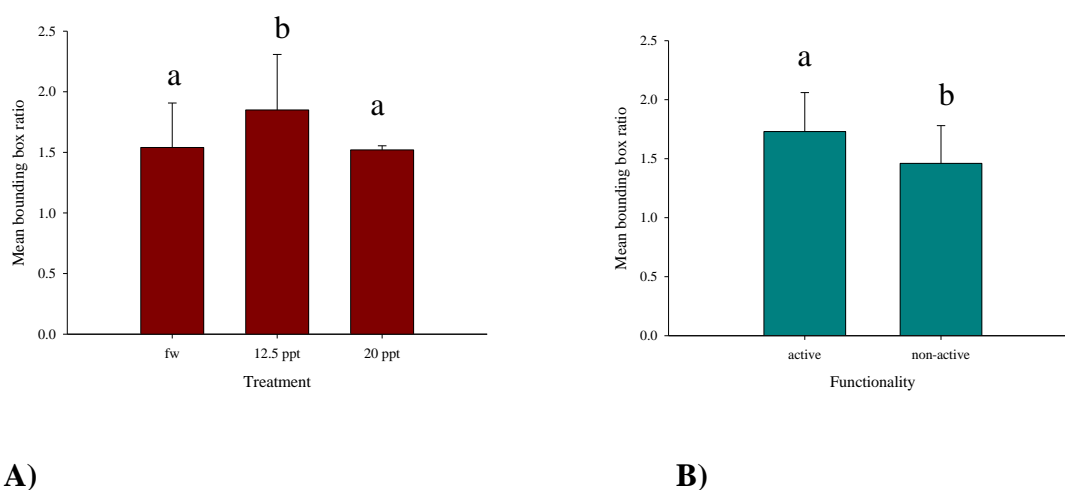
Figure 7. 14 Overall effect of **A)** Salinity and **B)** Functional state on the ratio of bounding box. Mean ± S.E. Different letters indicate significant differences between bars (GLM with Tukey's post-hoc pairwise comparisons; p < 0.05).

Further quantitative morphometric analyses of active and non-active MRCs revealed that the ratio of bounding boxes of non-active MRCs were always significantly higher *i.e.* box encompassing the immunoreactive object was squatter or less elongated than those of bounding boxes of active MRCs (Table 7.9. and Figure 7.15.). At 48 h post-transfer to elevated salinities, MRCs became more elongated than their freshwater counterparts, significantly in the case of those adapted to 12.5 ppt (Table 7.9. and Figure 7.15.).

Table 7. 9 Ratio of bounding boxes of MRCs of Nile tilapia following transfer from freshwater to elevated salinities as determined by immunohistochemistry and confocal scanning laser microscopy. Data are means (n = 5). Data within rows with different subscript letters are statistically different (One-way ANOVA with Tukey's post-hoc pair-wise comparison; p < 0.05).

Treatment	Freshwater			12.5 ppt		20 ppt	
Time (hours post-transfer)	0	24	48	24	48	24	48
Ratio mean width of bounding box: depth of bounding box:							
MRC functional state:							
Active	1.6 ± 0.07 [a]	1.8 ± 0.10 [ab]	1.6 ± 0.08 [a]	1.9 ± 0.07 [a]	2.1 ± 0.08 [b]	1.6 ± 0.05 [a]	1.7 ± 0.06 [a]
Non-active	1.3 ± 0.05 [a]	1.5 ± 0.07 [ab]	1.3 ± 0.13 [a]	1.6 ± 0.09 [ab]	1.7 ± 0.09 [b]	1.5 ± 0.07 [ab]	1.4 ± 0.06 [ab]
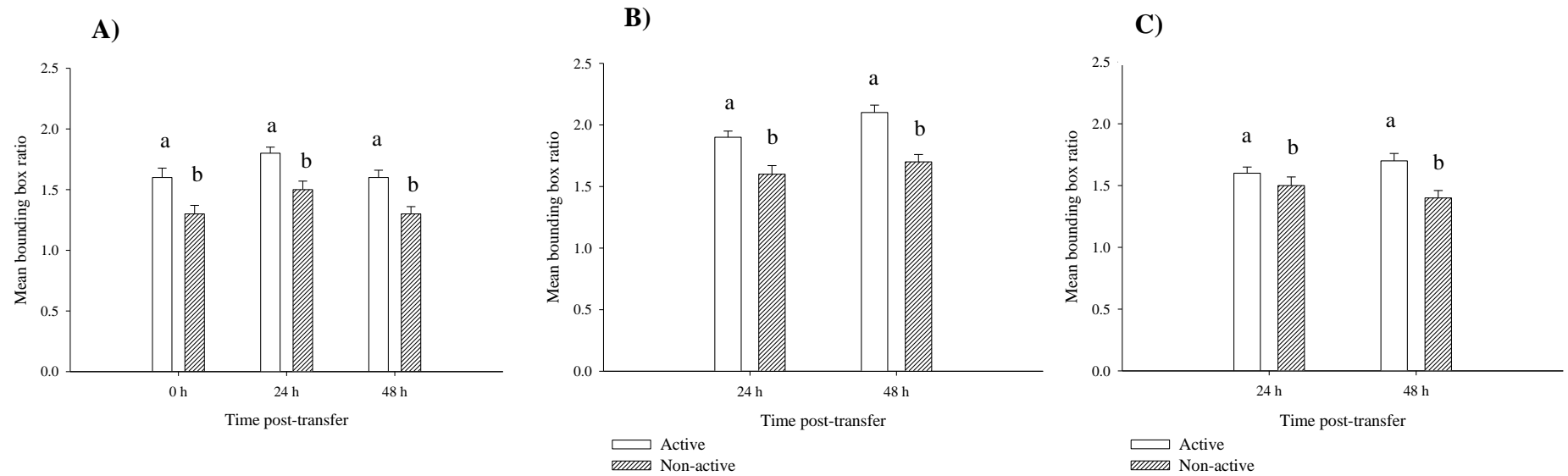
Figure 7. 15 Variations in ratio of bounding boxes of active and non-active MRCs in tail of Nile tilapia following transfer from freshwater to elevated salinities as determined by immunohistochemistry and confocal scanning laser microscopy. **A)** Freshwater, **B**) 12.5 ppt and **C)** 20 ppt. Data are mean ± S.E. Different letters indicate significant differences between bars (One-way ANOVA with Tukey's post-hoc pair-wise comparison; $p < 0.05$).

7.3.2   Observations on general MRC ultrastructure and immunogold localisation of anti-Na$^+$/K$^+$-ATPase using transmission electron microscopy

Mitichondria-rich cells were found as individual cells and no multi-cellular complexes were observed in this study. Na$^+$/K$^+$-ATPase immunoreactivity, as defined by immunogold labelling, was essentially restricted to MRCs. Mitichondria-rich cells were identified by the presence of characteristic morphological features and Na$^+$/K$^+$-ATPase immunoreactivity, as defined by immunogold labelling, was essentially restricted to MRCs. Control samples prepared without the primary antibody showed a lack of immunogold particles (see previous Chapter 6; Figure 6.9.)

7.3.2.1   Tubular system and immunogold labelling of anti-Na$^+$/K$^+$-ATPase

MRCs contained an extensive system of smooth-walled, tubules that formed a anastomosing network. Immunogold labelling clearly localised Na$^+$/K$^+$-ATPase on the tubular system (Figure 7.16.B.; Figure 7.17.C.; Figure 7.18.). Lower boxed area in Figure 7.17.A. shows immunogold-labelled areas that appeared to be connected with MRC and were found in both freshwater and brackish water adapted larvae, which may correspond to the immunopositive fluorescent outcrops seen by confocal scanning laser microscopy.

7.3.2.2   Golgi

Golgi apparatus, a continuous ribbon-like structure, appears as a series of independant stacks of saccules within the cytoplasm (Figure 7.18.B.)

7.3.2.3   Mitochondria

Rod-shaped mitochondria, closely associated with the tubular system, were found scattered in the cytoplasm of MRCs (Figure 7.16.B. and C. and Figure 7.18.).

7.3.3   Changes in ultrastructure associated with transfer to elevated salinities

The transfer of Nile tilapia from freshwater to elevated salinities induced changes in MRC ultrastructure. The density of immunogold particles appeared to increase following adaptation to 12.5 and 20 ppt at 48 hrs post transfer (Figure 7.18.). Similarly, the tubular system appeared denser in elevated salinities *i.e.* 12.5 and 20 ppt following transfer than in freshwater adapted larvae (Figure 7.18.), however the diameter of tubules in active MRCs did not appear to change according to salinity (Figure 7.17.C. and Figure 7.18.C.) remaining at approx. 40 – 60 nm diameter. Size and abundance of mitochondria did not appear to vary according to salinity.

7.3.4   Developmental stages of MRCs

In all treatments, circular shaped, sub-surface MRCs *i.e.* without an apical opening, were identified by their levels of mitochondria and anti-Na^+/K^+-ATPase positive immunogold labelling and appeared to resemble different developmental stages in the lifecycle of the MRC (Figure 7.19. to Figure 7.21.). Sub-surface or immature MRC were located within the epidermis. Early, immature MRCs lay close to the basement membrane and showed low numbers of mitochondria, a poorly developed tubular system with low numbers of immunogold localisation (Figure 7.19.). MRCs within the epidermis showed developing network of tubular system with a higher abundance of

immunogold localisation and mitochondria (Figure 7.20.). Mature MRCs lying close to the epidermal surface, displayed an intricate anastomosing network of tubules with abundance of immunolocalisation (Figure 7.21.).
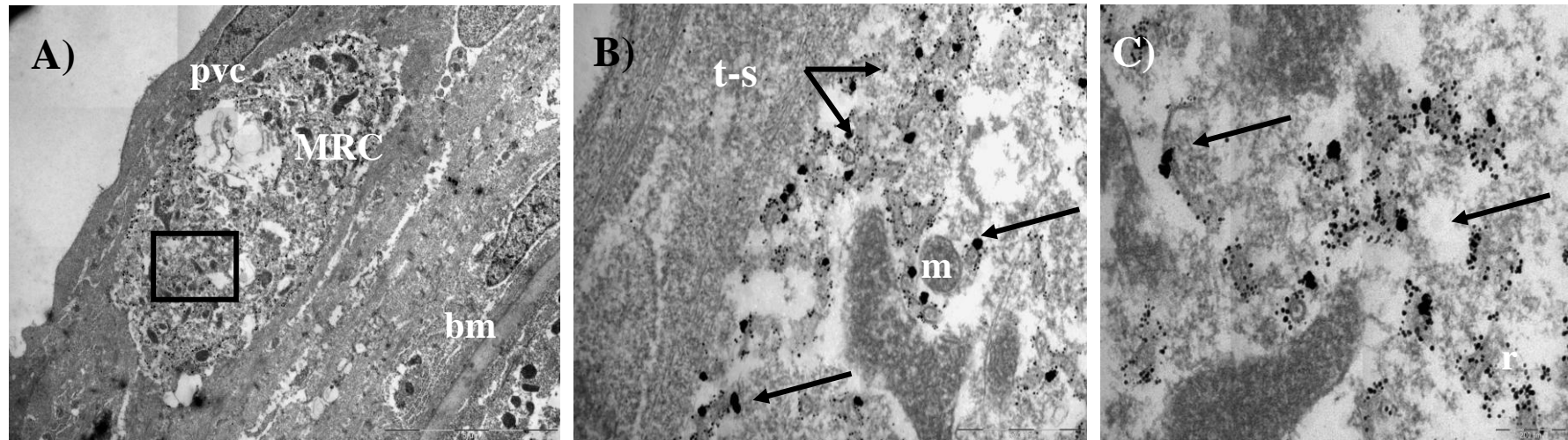
Figure 7. 16 Transmission electron micrograph of MRCs in Nile tilapia larvae adapted to 20 ppt at 5 dph. **A)** Mature MRC lying beneath pavement cells (pvc) (bm; basement membrane) [Bar = 2 μm], **B)** High magnification of boxed area from A) showing tubular system (t-s) and immunogold labelling (arrows) associated with the MRC cell periphery (m; mitochondria) [Bar = 200 nm] and **C)** High magnification of MRC tubular system showing immunogold labelling (arrows) (r; ribosomes) [Bar = 200 nm].
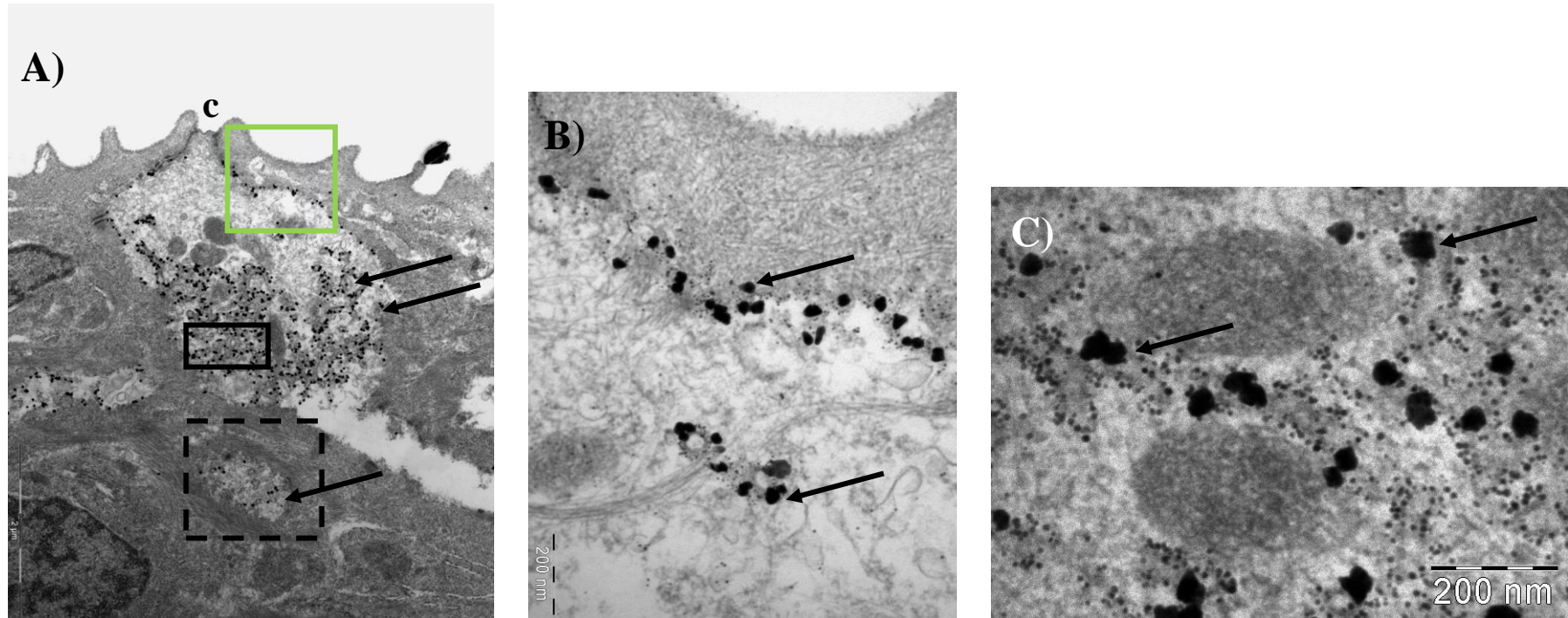
Figure 7. 17 Transmission electron micrograph of MRCs in freshwater-adapted Nile tilapia larvae at 5 dph. **A)** Mature MRC showing apical crypt (c) and immunogold labelling (arrows). Dashed box highlighting immunogold positive area associated with ramifying tubules as seen in CSLM (Figure 7.6.) [Bar = 2 μm], **B)** High magnification of immunogold labelling lining cell periphery (green boxed area from A) [Bar = 200 nm] and **C)** High magnification of black boxed area from A) showing immunogold labelling within tubular system. Tubules approx. 40 – 60 nm diameter [Bar = 200 nm].

301
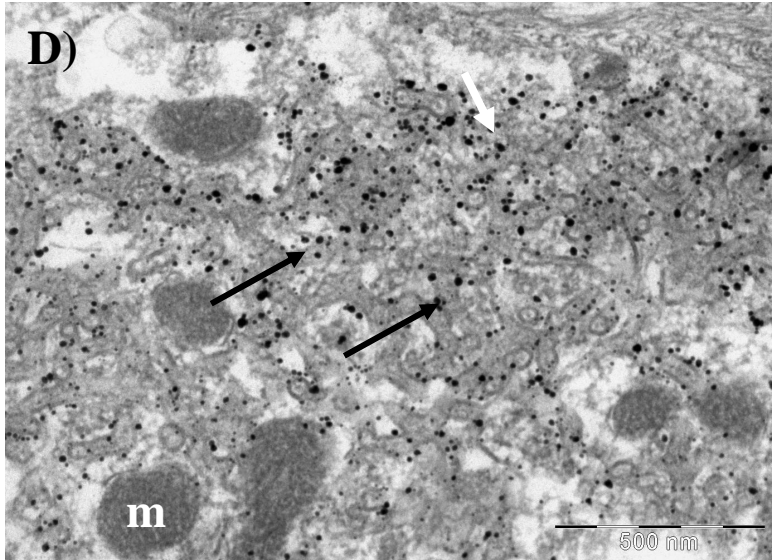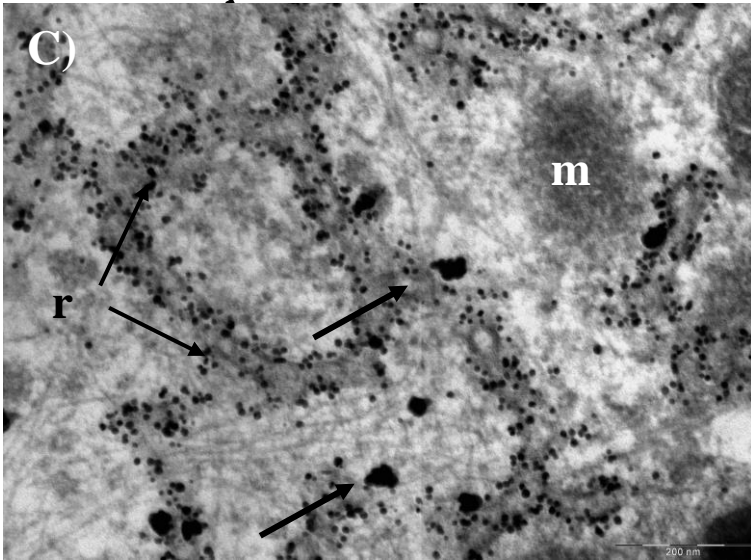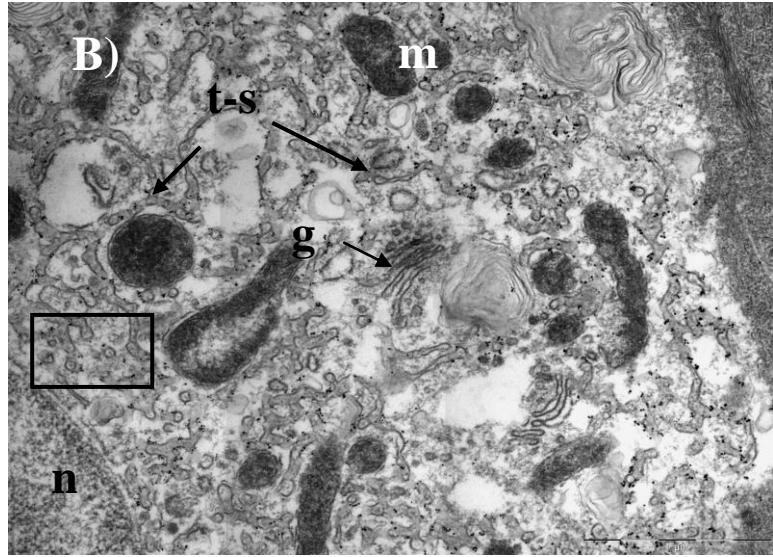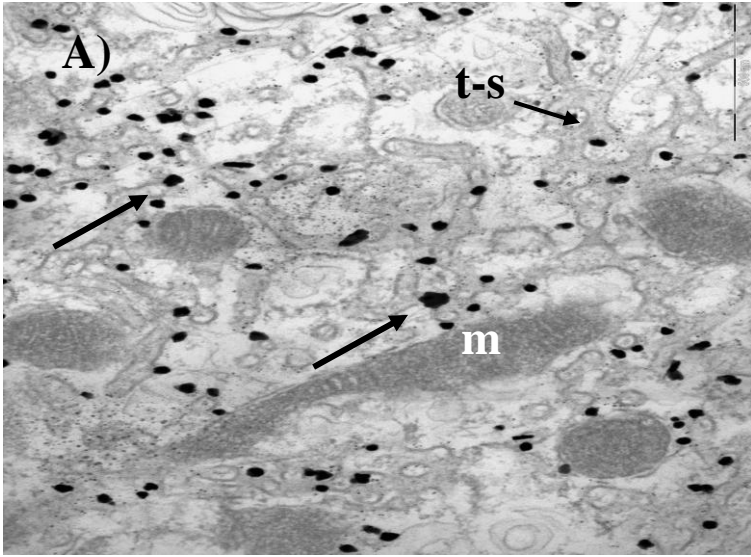
Figure 7. 18 Transmission electron micrographs showing distribution of Na^+/K^+-ATPase immunogold labelling (arrows) associated with the tubular membrane system of mature *i.e.* active MRCs in tail of yolk-sac Nile tilapia larvae. **A)** Loosely arranged tubular system (ts) in MRC of 3 dph freshwater larvae with immunogold staining (arrows) (m; mitochondria) [Bar = 500 nm], **B)** More developed tubular system in MRC of larvae at 24 h post-transfer to 12.5 ppt with immunogold staining (arrows) (m; mitochondria, n; nucleus, t-s; tubular system, Golgi apparatus g) [Bar = 1 μm], **C)** Higher magnification of boxed area from B) detailing anastomosing tubular system with immunogold staining (arrows) and ribosomes (r) (m; mitochondria) [Bar = 200 nm] tubules approx. 40 - 60 nm in diameter and **D)** MRC showing intricate tubular system and abundant immunogold staining (arrows) in larvae at 48 hrs post-transfer to 20 ppt (m; mitochondria) [Bar = 500 nm].
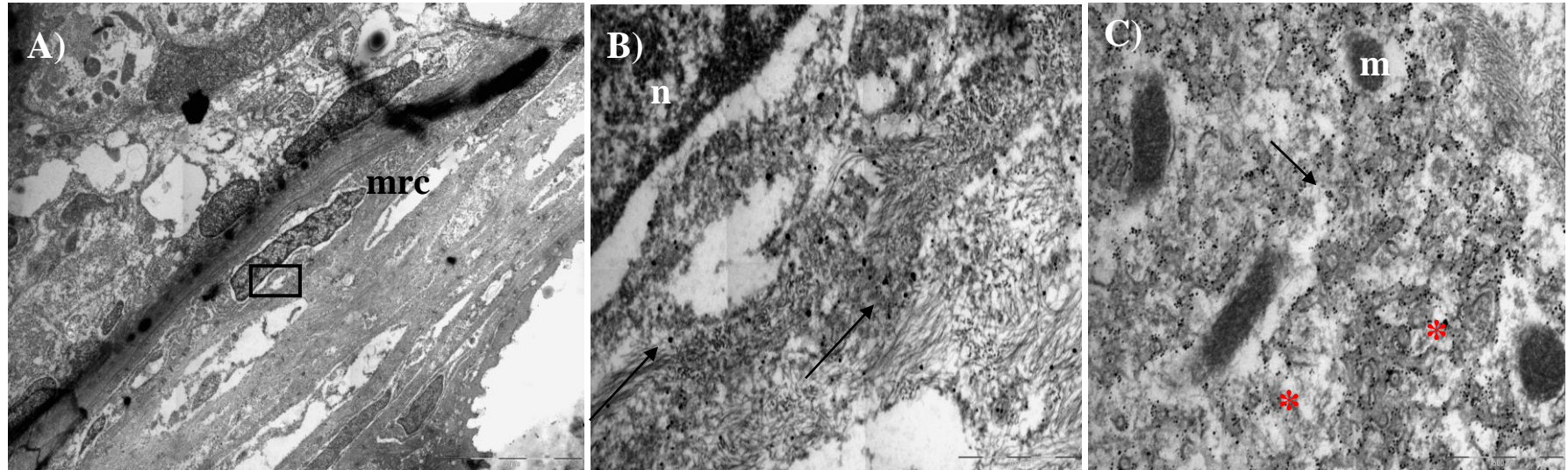
Figure 7. 19 Transmission electron micrographs of early, immature MRCs in tail of larvae 24 h post-transfer to 12.5 ppt. **A)** MRC located at basolateral region of epidermis [Bar = 5 μm], **B)** Higher magnification of boxed area from A) of cytoplasm of early immature MRC with poorly developed tubular system with immunogold localisation (arrows) (n; nucleus of MRC) [Bar = 500 nm] and **C)** Close up of tubular system and mitochondria of MRC from A) showing low density of immunogold labelling associated with Na^+/K^+-ATPase (arrow) and weakly defined anastomosing tubules (asterisks) (m; mitochondria) [Bar = 500 nm].
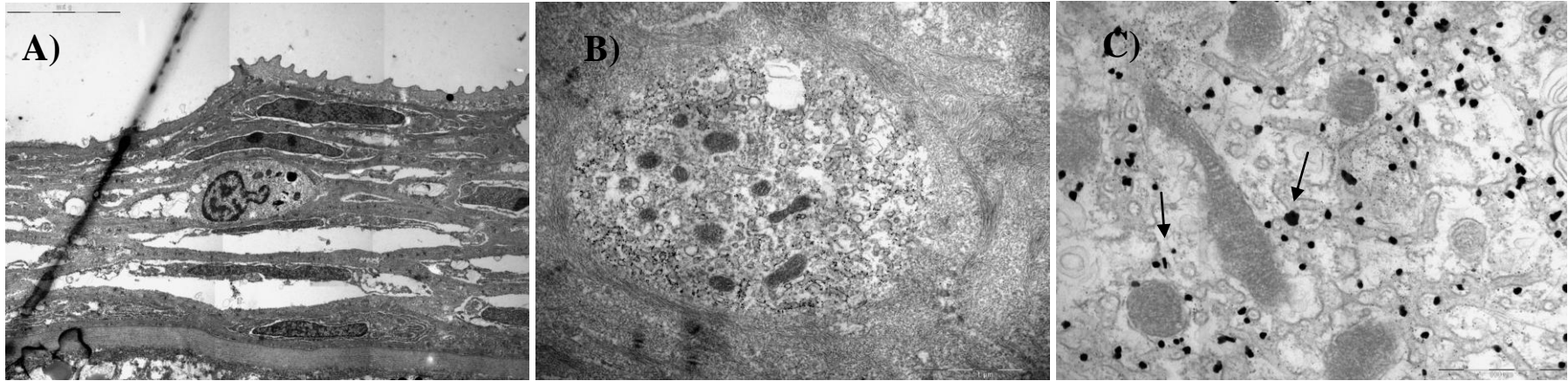
Figure 7. 20 Transmission electron micrographs of immature, sub-surface MRCs in tail of larvae 24 h post-transfer to 12.5 ppt. **A)** Sub-surface MRC showing a more circular shape [Bar = 5 μm], **B** Sub-surface MRC with characteristic abundance of mitochondria [Bar = 1 μm) and **C)** Higher magnification of tubular system showing developing network of tubular system with immunogold localisation (arrows) [Bar = 500 nm].
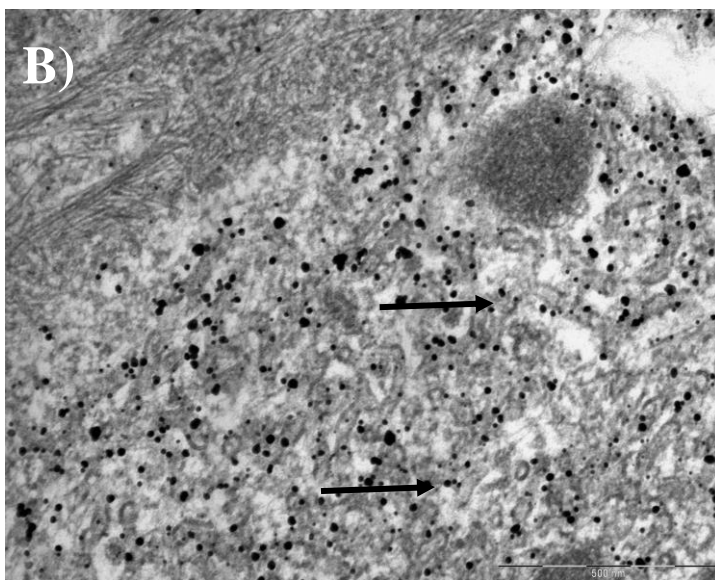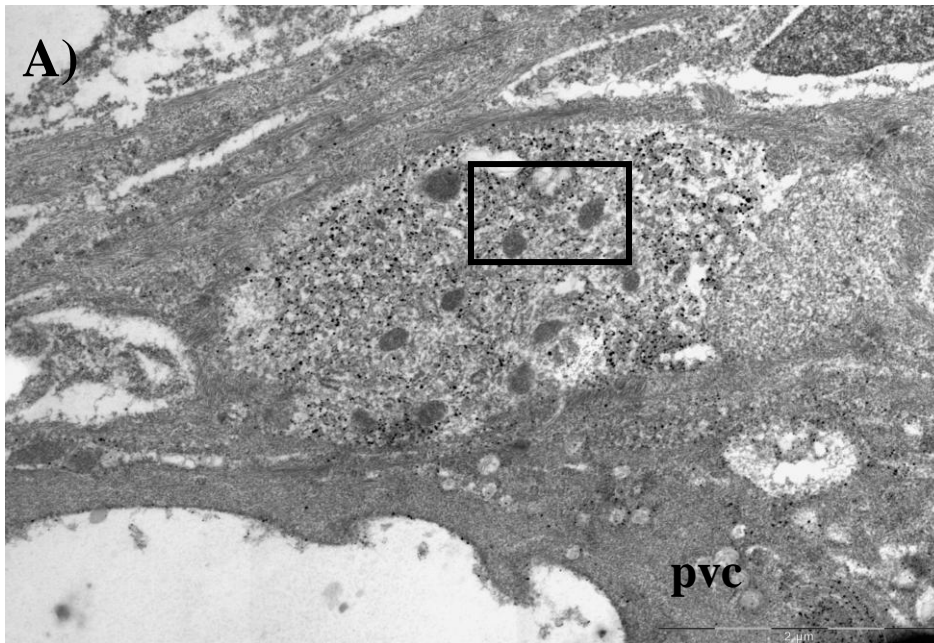
Figure 7. 21 Transmission electron micrographs of mature MRC in tail of larvae 24 h post-transfer to 12.5 ppt. **A)** Mature MRC located at surface of epidermis (pvc; pavement cell) [Bar = 2 μm] and **B)** Higher magnification of boxed area from A) showing intricate anastomosing network of tubules with abundance of immunolocalisation of Na^+/K^+-ATPase (arrows)[Bar = 500 nm].

7.4 Discussion

The classical model of MRC function holds that only 'mature' cells, *i.e.* those in contact with the external environment via an apical pit or crypt, are involved in ion transport (Wendelaar Bonga and van der Meij, 1989; Wendelaar Bonga *et al.,* 1990). Conventional quantification methods using fluorescent probes of mitochondria *e.g.* DASPEI and its analogue DASPMEI or anti-Na^+/K^+-ATPase do not give an accurate estimation of the dynamics of MRC function and distribution following transfer as they do not differentiate between developmental stages of MRCs, labelling all MRCs within the target tissue regardless of functional state, leading to an overestimation in density of functional ion-transporting cells. Therefore a method that allows an accurate assessment of both those MRCs that are actively involved in ionoregulation and sub-cellularly located MRCs, which are not nominally actively involved in ionoregulation, is obviously a valuable tool when studying MRC dynamics following salinity challenge.

It is generally accepted that computer-based image analysis offers an operator-independent method producing consistent and rapidly generated quantifications of cellular changes that prevents selection of subjective elements, common in manual microscopy-associated quantifications (Plasier *et al*., 1999). In the present study, a new method for discriminating between active and non-active MRCs is described, allowing an accurate and repeatable quantitative assessment of both density and various MRC morphometric traits in the

epithelia of yolk-sac Nile tilapia. Pre-captured confocal scanning laser generated stacks of triple-labelled MRCs are used in conjunction with an image analysis programme (ImageJ with 3-D Object Counter plug-in) in order to determine functional state, based on the distance of the MRC from the epithelial surface of the integument in yolk-sac larvae as labelled by the actin stain phalloidin.

In the current study, integumental MRCs were examined by both confocal scanning laser microscopy (CSLM) and transmission electron (TEM) on the dissected tail of the larvae in the region of the tail somite lying immediately dorsal to the anus (see Figure 7.2.). This section of the larvae was chosen because the tissue could easily be scanned using CSLM as it lay flat on the glass base dish and, also, provided an area of measurement that could be standardised easily. Similarly for TEM, the tail section proved easier to cut into ultrathin sections as previous attempts to cut through the thicker yolk-sac had resulted in poor sectioning with the epithelium lifting away from the yolk mass. As has previously been established in Chapter 5, integumental MRCs were present on the tail of yolk-sac larvae at 3 dph and showed no significant difference in density at 5 dph (Table 5.5.) therefore the tail area of yolk-sac larvae was regarded as representative of integumental MRCs.

Existing literature records prior attempts to classify MRCs on the basis of their functional state following salinity challenge. Fluorochrome conjugated lectins that label the exposed apical surfaces of MRCs, such as Concanavalin-A (Con-A), which binds specifically to α-

glucopyranosyl glycoprotein residues that are concentrated in the apical pits of MRCs (Goldstein *et al.*, 1969; Zadunaisky, 1984) or peanut agglutinin (PNA) which binds to terminal β-galactose residues (Goss *et al.*, 2001), have simultaneously been identified with either the mitochondrial staining DASPEI or DASPMEI or an Na^+/K^+-ATPase marker in order to identify the population of MRCs that have contact with the external environment and are assumed to have an active ionoregulatory role. Li *et al.* (1995) were the first to report this co-labelling method to identify mature or functional MRCs in the gills of juvenile Mozambique tilapia, but no quantification of active *vs.* non-active cells was attempted. Quantification of changes in density of active and non-active MRCs has, however, subsequently been reported in gills of adult Mozambique tilapia (van der Heijden *et al.*, 1996) and in Mozambique tilapia yolk-sac larvae (Lin and Hwang, 2004). However this method of differentiating between active and non-active MRCs has its drawbacks. van der Heijden *et al.* (1997) reported the presence of Con-A labelling on pavements cells, remarking that a lack of knowledge about the extent to which the glycoprotein composition and content within the apical pit of the MRC may affect the degree of Con-A binding could suggest limitations of the validity of the method.

However the methods developed and employed in the current study offer the advantage of allowing, for the first time, the classification of active and non-active MRCs based on their exact localisation within the target tissue. In addition, this technique offers the potential for further informative and quantitative studies on MRC density and morphology, based on MRC functional state. Interestingly, the significant decrease in percentage of active MRCs

308

in larvae transferred from freshwater to 20 ppt from 24 h post-transfer onwards reported in the present study is in agreement with prior studies, whose quantitative measurements of density were also based on active and non-active MRCs using the colabelling method described above. van der Heijden *et al.* (1997) found a decrease in density of both total and active MRCs following seawater adaptation in gills of adult Mozambique tilapia, and, Lin and Hwang (2004) reported a decrease in active MRCs on the yolk-sac membrane of Mozambique tilapia following transfer from freshwater to a hypertonic (high Cl^- environment).

The significant decrease in overall MRC density following transfer to elevated salinities reported here is in agreement with results previously reported in Chapter 5 of the current study; a significantly lower overall density of MRCs was recorded in 15 ppt compared to freshwater and further quantitative analysis reveals that this pattern existed regardless of location of MRCs *i.e.* yolk-sac membrane, tail, outer operculum and inner operculum (Table 5.5.). These results are in concordance with previous studies which reported a decrease in density of total MRCs following seawater adaptation in gills of the adult Mozambique tilapia (van der Heijden *et al.*, 1997; Lin and Hwang, 2004). However, conflicting results exist in the literature concerning the overall density of MRCs in hypotonic and hypertonic environments. No change in density of MRCs following transfer to elevated salinities was reported in the yolk-sac epithelia of embryonic and larval Mozambique tilapia (*O. mossambicus)* (Ayson *et al*., 1994; Hiroi *et al.*, 1999; Shiraishi *et al*., 1997) and in the adult goby (*Gillichthys mirabilis*) (Yoshikawa *et al.*, 1993). In

contrast, an increase in MRC density had been reported in the gills of adult teleost fishes following transfer to seawater; the goby (*Stenogobius hawaiiensis*) (McCormick *et al.*, 2003), the sea bass (*D. labrax*) (Varsamos *et al*., 2002 b), the Black-chinned tilapia (*S. melanotheron)* (Ouattara *et al*., 2009) and the Mozambique tilapia (*O. mossambicus*) (Lee *et al.*, 2000). The significant decrease in total density of MRCs remaining in freshwater from 24 h post transfer to 48 h post-transfer seen in this study can be explained by the clear ontogenic shift in MRC distribution as ionoregulatory function moves from integumental to branchial, as previously discussed in Chapter 5.

In the current work, correlative TEM studies demonstrated the simultaneous presence of both active and non-active MRCs, depending on their location within the epithelia of the larvae. However a caveat should be noted here when interpreting TEM sections – whilst the presence of an apical opening can be thought to provide direct evidence of functional state, a MRC with close proximity to a surface PVC but displaying no evident crypt should not be presumed to be a non-active cell. It is clear from Figure 7.22. that it depends where in the tissue the section is cut and a MRC that is in fact active may only show the areas underlying the PVCs. Sequential serial sectioning at a distance of 1 μm to form a complete picture of a MRC apart would overcome this problem.
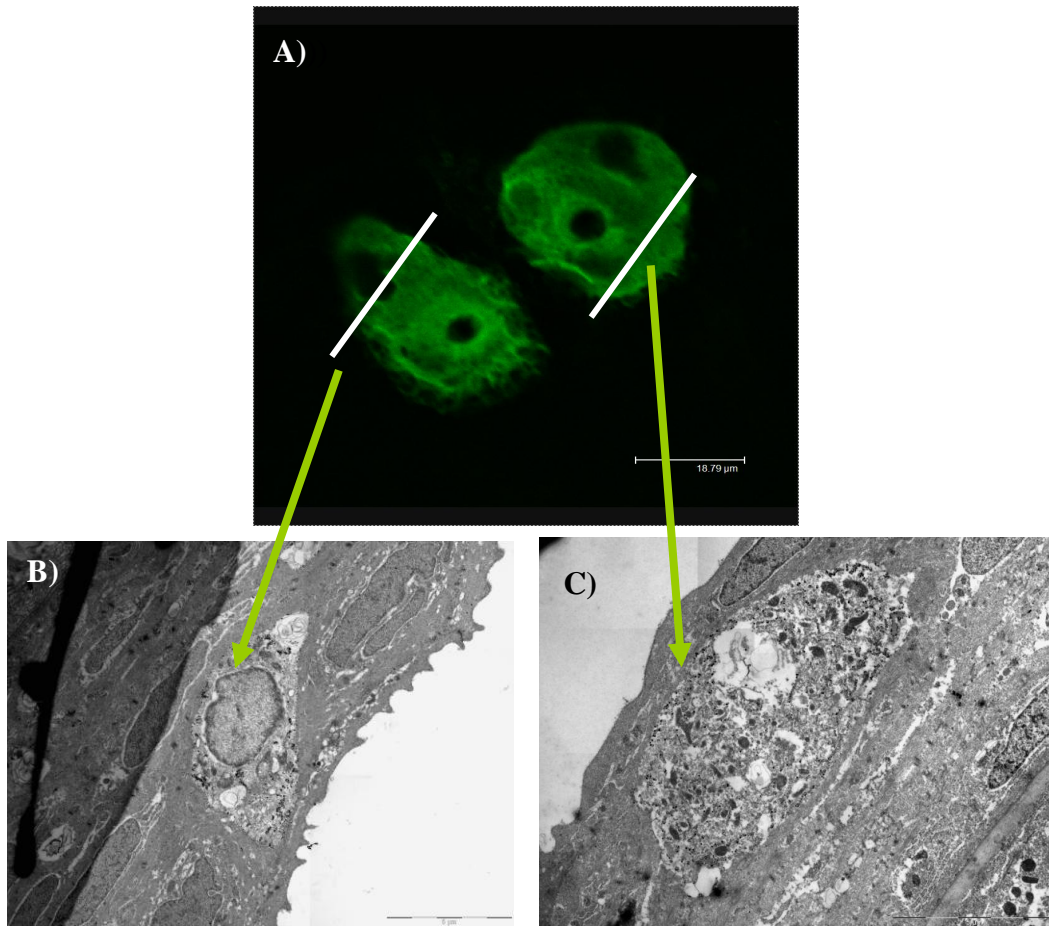
Figure 7. 22 A) Fluorescent confocal laser scanning microscope images of MRCs labelled with anti-Na$^+$/K$^+$-ATPase on tail of freshwater adapted yolk-sac Nile tilapia larvae [Bar = 18.79 um]. **(B-C)** Transmission electron micrographs of a MRC on tail of yolk-sac Nile tilapia larvae. **B)** Freshwater [Bar = 5 um] and **C)** 20 ppt 24 hrs post-transfer [Bar = 5 um].

In the current study MRCs *i.e.* showing immunogold labelling associated with the tubular system that had a sub-surface location in the tissue were presumed to be non-active MRCs. These non-active MRCs displayed ultrastructural features common to active MRCs *i.e.* numerous mitochondria, a tubular system and a positive immunogold staining for Na$^+$/K$^+$-

ATPase but differed in the intricacy of their tubular system and the density of their immunogold labelling (Figure 7.19.). Indeed, it is widely accepted that immature MRCs contain less Na^+/K^+-ATPase than mature active MRCs (Wendelaar Bonga *et al.*,1990; Perry and Laurent, 1993, Witters *et al.,* 1996). It has previously been suggested by Chretien and Pisam (1986) in their study on cell renewal and differentiation using autoradiography in combination with light and electron microscopy in gill epithelia of freshwater or seawater-adapted guppies, that MRCs, in both freshwater and seawater adapted fishes, originated from undifferentiated cells at the basal layer of the epithelium. In the present study, the movement of MRCs towards the external surface of the epithelium was seen to be characterised by an increase in volume and development of the tubular system, and in turn, abundance of Na^+/K^+-ATPase (Figure 7.20; Figure 7.21.). These results were in agreement with previous observations by Conte and Lin (1967) and Shirai and Utida (1970). Therefore the immunogold labelling technique that has been developed in the current study allows, for the first time, the positive identification of non-active MRCs that appear to originate at the basolateral regions of the epidermis and migrate upwards until they reach the surface, and form an apical crypt in contact with the external environment, at which time they can be deemed functionally active.

The actual presence of the transport protein Na^+/K^+-ATPase in sub-surface or non-active MRCs, *i.e.* cells that are non-functional, is interesting. Its role in ion transport, either directly through the movement of Na^+ and K^+ across the plasma membrane or indirectly

through generation of ionic and electrical gradients, is well established (see Section 1.2.3.), yet is still found in high levels, as seen in the current study, in non-functional cells.

Endocrine factors such as prolactin, growth hormone and cortisol, the most widely studied to date, have biochemical and morphological effects on fish osmoregulatory organs. Cortisol has been shown to stimulate gill Na^+/K^+-ATPase activity in killifish (*Fundulus heteroclitus*) (Pickford *et al*., 1970), American eel (*Anguilla rostrata*) (Epstein *et al.* 1971), Coho salmon (*Oncorhynchus kisutch*) (Richman and Zaugg, 1987; *Bjornsson et al.,* 1987), the Mozambique tilapia (*Oreochromis mossambicus*) (Dange, 1986), sea trout (*Salmo trutta*) (Madsen, 1990) and Atlantic salmon (*Salmo salar*) (Bisbal and Specker, 1991). Hypophysectomy reduces gill Na^+/K^+-ATPase activity in teleosts which was partially restored by cortisol treatment (Pickford *et al*., 1970; Butler and Carmichael, 1972; Bjornsson *et al*., 1987; Richman and Zaugg, 1987) due to removal of pituitary ACTH (a cortisol secretagogue). In addition, in vitro treatment of gill and opercular membrane by cortisol resulted in stimulation of Na^+/K^+-ATPase in Coho salmon (*O. kisutch*) (McCormick and Bern, 1989) and the Mozambique tilapia (*O. mossambicus*) McCormick, 1990) indicating its direct effect on these tissues. It is suggested that if osmoregulatory capacity is under endocrine control, then it is these endocrine factors that trigger the proliferation of Na^+/K^+-ATPase within undifferentiated cells at the basal layer of the epithelium as described above. This could explain the presence of Na^+/K^+-ATPase in non-functional MRCs, albeit in a lower abundance than in functional MRCs that are in contact with the external environment via apical openings.

In the present study, both salinity and time post-transfer had a significant overall effect on MRC volume (μm^{-3}) (GLM; $p < 0.05$) with MRC increasing in size following transfer to both 12.5 and 20 ppt. These results are also in concordance with results presented in Chapter 5 of this study , where mean 2-D Na^+/K^+-ATPase immunoreactive cell area (μm^{-2}) of integumental MRCs were always larger in brackish water larvae than freshwater from 1 dph until yolk-sac absorption. Changes in size of MRCs when transferred from freshwater to seawater were first reported in the opercular epithelium of the adult Mozambique tilapia (*O. mossambicus*) (Foskett *et al*., 1981) and subsequent and numerous studies have confirmed that MRCs become larger when fish were transferred from freshwater to seawater both in adult teleosts *e.g.* the Black-chinned tilapia (*S. melanotheron)* (Ouattara *et al*., 2009), Mozambique tilapia (*O. mossambicus)* (Uchida *et al.,* 2000; Kultz *et al*., 1995; van der Heijden *et al.,* 1997), Nile tilapia (*Oreochromis niloticus*) (Guner *et el*., 2005), Atlantic salmon (*Salmo salar*) (Langdon and Thorpe, 1985; Pelis *et al.,* 2001), Coho salmon (*Oncorhynchus kisutch*) (Richman and Zaugg, 1987), chum salmon (*Oncorhynchus keta)* (Uchida *et al*., 1996), guppy (*L. reticulatus*) (Pisam *et al.,* 1987) and killifish *(F. heteroclitus)* (Katoh *et al*., 2001, 2003) and in teleost embryos and larvae *e.g.* Mozambique tilapia (*O. mossambicus)* van der Heijden *et al*., 1999; Ayson *et al.,* 1994; Shiraishi *et al*., 1997; Hiroi *et al.,* 1999, 2005) and the ayu (*P. altivelis*) (Hwang, 1990).

However, measurements of MRC size, as described in Chapter 5 and in the literature, commonly report a cross-sectional area (μm^2) of the *x-y* projection of MRCs. The image analysis of confocal stacks using ImageJ with a 3-D Object Counter plug-in used in this

study has allowed, for the first time, the measurement of actual volume of anti-Na^+/K^+-ATPase immunoreactivity (μm^3). The measurement of MRC volume responses to changes in external salinity has only been reported previously using planimetry in the epithelial lining of killifish (*F. heteroclitus*) mounted in an Ussing chamber using inverted light microscopy fitted with differential interference optics (Zadunaisky, 1996). In contrast to the present study, cell volume was seen to decrease when facing hypertonicity or seawater. It should be noted that, in the current study, confocal images of anti-Na^+/K^+-ATPase immunoreactivity revealed ramifying outcrops of tubular extensions of MRCs (Figure 7.6.) that would certainly influence a cross sectional area measurement leading to a potential misrepresentation and overestimation of volume. The method described here however gives a truer representation of quantitative immunoreactive area.

Increased size of MRCs coincides with an increase in both expression and activity of Na^+/K^+-ATPase, that is directly correlated with enhanced salinity (Cutler *et al.,* 1995; D'Cotta *et al*., 2000; Feng *et al*., 2002; Wilson and Laurent, 2002), and a concomitant expansion of the tubular network for the incorporation of Na^+/K^+-ATPase (Uchida *et al.,* 2000; Lee *et al*., 2003). The significantly larger volume of active MRCs as compared to non-active MRCs following transfer to elevated salinities reported in the present study further confirms this, as it can be assumed that only active MRCs would respond to ionoregulatory challenges by increasing Na^+/K^+-ATPase expression and activity.

To strengthen this assumption, the significantly lower mean staining intensity of non-active MRCs as compared to active MRCs reported in this study further suggests that lower quantities and hence activity of Na^+/K^+-ATPase is present in non-active MRCs. It should be considered here, however, that a decrease in signal with tissue depth due to a decrease in antibody penetration could have played a role in the reported decrease in staining intensity of sub-cellular or non-active MRCs. However, in order to counteract effects of photo-bleaching of weaker stained cells, scanning was started within the tissue and moved towards the skin surface (see Section 7.2.3.). In addition, TEM ultrastructural studies confirm the increase in density of the tubular system and abundance of immunogold staining of Na^+/K^+-ATPase within active MRCs, *i.e.* those with an apical crypt, following transfer from freshwater to 12.5 and 20 ppt (Figure 7.18.). A similar increase in immunogold particle density was observed in the tubular system of branchial MRCs of *O. mossambicus* following cortisol treatment (Dang *et al.*, 2002b).

In the present study, neither functional state nor salinity was found to affect the 3-D sphericity of MRCs. Sphericity, as an indicator of cellular changes in MRCs, has been reported previously in the morphometrics measurement of MRCs in gills of the Atlantic salmon (*S. salar*) (Pelis and McCormick, 2001) and the goby (*S. hawaiiensis*) (McCormick *et al.*, 2003). Shape of branchial MRCs was not found to be affected by transfer from freshwater to 20 and 30 ppt in the goby (*S. hawaiiensis*) (McCormick *et al.*, 2003). However, these studies used the cross-sectional area and perimeter of immunopositive regions to calculate 2-D shape factor. The current study uses the volume and surface area

316

measurements of each immunoreactive object and uses a 3-D shape factor or sphericity. However, it should be noted that limitations exist in both these method. The ramifying outcrops emanating from MRCs, as revealed by both CSLM and TEM (Figure 7.6.A. and B; Figure 7.17.A.) which were described above as potentially affecting cross sectional area measurements, in turn could affect shape factor or sphericity as volume measurements include the immunoreactive tubular outcrops. However, the ratio of depth of MRCs to width did reveal a significant effect of both salinity and functional state on shape. The elongation of MRCs as they adapt to elevated salinities could also be a reflection of the previously reported increase in volume and staining intensity. Immature MRCs, lying within the epidermis, appeared to be rounder in shape as compared to active MRCs, with a lesser depth to width ratio. This is consistent with the circular appearance of sub-surface or immature MRCs, as revealed by TEM in the current study (Figure 7.20.). Active MRCs appear to make contact with the external environment via a neck-like extension ending in a apical crypt (Figure 7.6.A. and B.) which would explain the more elongated shape of active MRCs.

Immuno-electron microscopy has been reported in recent years to provide a visualisation of the localisation of specific transporters on the tubular system of MRCs at the electron microscope level, using a post-fixation immunohistchemical staining technique *i.e.* Na^+/K^+-ATPase to MRCs in the sea bass (*D. labrax*) (Varsamos *et al.*, 2002 b), Mozambique tilapia (*O. mossambicus*) (Dang *et al.,* 2000 a and b), Coho salmon (*O. kisutch*) (Wilson *et al.,* 2000 b) and V-ATPase to pavement cells and MRCs of Rainbow trout (*O. mykiss)*

(Sullivan *et al.,* 1995; Tresguerres *et al.,* 2006), mudskipper (*Periophthalmodon schlosseri*) (Wilson *et al*., 2000 b) and killifish (*F. heteroclitus*) (Katoh *et al*., 2003). The technique described here reports, for the first time, the use of a pre-fixation immunogold labelling technique using Fluoronanogold™ with a 1.4 nm nanogold particle in the study of MRC dynamics following salinity challenge in a teleost. It has been established that there is an inverse relationship between the size of colloidal gold particles and the subsequent density of immunolabelling (Takizawa and Robinson, 1994) therefore the ultra-small gold particle, used in this study, allowed better penetration than larger colloidial gold particles previously reported in anti-Na^+/K^+-ATPase post-fixation labelling of MRCs *i.e.* 10 nm (Dang *et al*., 2000a, 2000b; Varsamos *et al.*, 2002 b). The technique of enhancement of gold particle size was initially developed once colloidial gold labelling had been applied to light microscopy (Holgate *et al.,* 1983) and has subsequently been widely applied (review Lackie, 1996) and is reported here to allow improve visualisation at an ultrastructural level.

The previously unreported presence of tubular outcrops originating from active MRCs in both freshwater and brackish water adapted yolk-sac larvae in this study is interesting. The origin of accessory cells (ACs) has long been the subject of debate; whether they are less developed, young MRCs (Sardet *et al.,* 1979; Hootman and Philpott, 1980, Wendelaar Bonga *et al.,* 1990) or whether they are, in fact, a specific cell type typical for seawater fish (Dunel and Laurent, 1980, Laurent and Dunel, 1980). However the presence of ACs has been reported in a number of teleosts in freshwater killifish (*F. heteroclitus*) (Karnaky *et al.,* 1976), ayu (*Plecoglossus altivelis*) (Hwang, 1988), brown trout (*Salmo trutta*) (Pisam *et*

318

al., 1989) and the Mozambique tilapia (*O. mossambicus*) (Hwang, 1987, 1988; Wendelaar Bonga and van der Meij, 1989, 1990; Cioni *et al.,* 1991; Hiroi *et al*., 1999) which suggests the interpretation of these cells as young stages of MRCs rather than a specific cell type.

Chretien and Pisam (1986) studied cell renewal and differentiation using autoradiography in combination with light and electron microscopy in gill epithelia of freshwater and seawater-adapted guppies and suggested that MRCs and ACs had different origins and modes of differentiation. They suggested that ACs originated from undifferentiated cells located in the intermediate layers of the primary epithelium in contact with mature MRCs, maintaining contact with the apical portion of the MRC but never reaching the basement membrane. They reported that the first appearance of the rudimentary tubular system arose from lateral surface adjacent to MRC and later developed apical processes which interdigitated with the cytoplasm of the adjacent MRCs. It is suggested here that the fluorescent outcrops that were visualised by CSLM that appeared to be emanating from the basolateral portion of the MRCs in both freshwater and salinities are, in fact, forming ACs (Figure 7.6.). These ramifications may bud off from the MRC and rise up to make contact with the apical surface to form a multicellular complex (MCC). In addition, in the present study, TEM revealed immunopositive areas lying adjacent to active MRCs in a sub-surface location (Figure 7.17.A.) which may correspond to the ramifications as visualised by CSLM (Figure 7.6.). Serial sectioning to track the location and possible connection with the corresponding MRC could identify the suggested relationship between these cells. In addition, further quantification using this correlative approach as to the effects of salinity

on the appearance of these outcrops could give an indication of whether they were more prevalent in higher salinities, as ACs are usually associated with seawater adaptation.

Therefore to conclude, the present study reports a novel method for discriminating between and non-active MRCs based on their location within the epithelium of the larvae and allows a repeatable and accurate quantitative assessment of MRC dynamics using CSLM following salinity challenge in the Nile tilapia during early life stages. In addition, image analysis using ImageJ with a 3D Object Counter plugin has allowed, for the first time, a measurement of actual volume of Na^+/K^+-ATPase immunoreactivity, rather than a 2-D cross-sectional area, which gives a more representative quantitative measurement of immunoreactive area of MRCs. The post-fixation immunogold staining technique, which is reported here for the first time in the study of MRCs, has allowed a clear and specific visualisation of the cellular location of Na^+/K^+-ATPase within the target cells. This integrated approach, combined with CSLM, offers valuable insight into the cellular localisation of Na^+/K^+-ATPase, MRC morphology and dynamics as a response to osmoregulatory challenge that is reflected in the fish's ability to alter osmoregulatory strategies following salinity challenge.

8 Chapter 8 General Discussion

It has become increasingly clear in recent years that, given our finite resources, long-term sustainability of aquaculture must be based on an efficient use of natural resources. Improved farming practices, scope and efficiency of culture systems and knowledge of the adaptability of fish species must keep pace with growing world aquaculture consumption without compromising the overall integrity of our ecosystems. As the earth's climate warms and large-scale atmospheric circulation patterns change, a physical impact in fresh water and marine environments is expected, bringing with it a network of ecological changes and challenges. The existing ground water characteristics will alter due to infiltration of saline waters, and the resulting salination of lands will put pressure on available agricultural land and fresh water resources. These biotope changes may have profound effects upon fish stocks in both capture fisheries and culture, and it is likely that the greatest impact will be on the most sensitive, early stages of fish biology. Considering, in nature, fish population recruitment occurs during the larval and juvenile stages, variations in environmental quality that affect survival and ultimate size of spawning population and resulting reproductive potential will have a major determining effect of long term dynamics of fish populations (Rose *et al.,* 1993). From an aquaculture perspective, economic considerations are at the forefront when considering optimal environmental conditions for productions of stock.

The early phase of the life cycle is usually thought of as the most crucial period due to the poorly developed regulatory system *i.e.* gills and kidneys and the rapidly occurring developmental changes *i.e.* actively growing organs have shown increased sensitivity to xenobiotics (Ozoh, 1979). Indeed, a variety of studies have shown that the egg, embryo, yolk-sac larvae and early feeding stages are more sensitive to variations in environmental quality than juveniles and adult stages using criteria such as survival, hatchability, developmental abnormalities, growth and bioenergetics *e.g.* contaminants (Smit *et al.* 1998; Lin and Hwang, 1998), pH (McCormick and Jensen, 1989) and temperature (Rose *et al.*, 1993; Staggs and Otis, 1996). The Nile tilapia (*Oreochromis niloticus*, Linnaeus 1758), whose distribution has now extended well beyond its natural range, dominates tilapia aquaculture because of its adaptability and fast growth rate. Although not considered to be amongst the most salt-tolerant of the cultured tilapia species, the Nile tilapia still offers considerable potential for culture in low-salinity water. Data regarding the ontogeny of osmoregulation and adaptive strategies of this commercially important teleost fish provides valuable tools for predicting timing of occurrence of adaptive ability and improving larval rearing techniques. Additionally, an increase in knowledge of the limits and basis of salinity tolerance of Nile tilapia during the particularly sensitive early life stages and the ability to predict responses of critical life-history stages to environmental change could prove invaluable, extending the scope of this globally important fish species. The overall aim of this thesis was, therefore, to explore the scope of tolerance and the physiological adaptability of early life stages of the Nile tilapia when faced with osmoregulatory challenge. The nature of the related mechanisms that provide osmoregulatory capacity

322

during the early life stages of the Nile tilapia were also investigated, with special reference to the role of the mitochondria-rich cell or MRC.

It is well established that measurement of osmolality provides a valid route for the evaluation of the osmoregulatory status of fishes (Alderdice, 1988), therefore the first part of this work (Chapter 3) aimed to explore the responses and physiological effects of osmotic challenge (range 0 – 32 ppt) during ontogeny in the Nile tilapia through the measurement of embryo and larval osmolality and resulting osmoregulatory capacity. In addition, it assessed the short-term responses of yolk-sac larvae to abrupt transfer from freshwater to a range of salinities (range 7.5 – 25 ppt) in terms of osmoregulatory capacity, survival and the related incidence of deformity. It was clear from the results that ontogenic changes in the osmoregulatory capability of eggs and yolk-sac larvae of the euryhaline Nile tilapia occurred; osmolality of embryos immediately post-transfer to elevated salinities (7.5 – 20 ppt) appeared to be proportional to and directly related to the osmolality of the external media, but then to drop to a more steady state during embryogenesis and the yolk-sac period, suggesting that an ontogenic regulatory control is evident which is, in turn, reflected in larval ability to withstand transfer to elevated salinities. This observed increase in osmoregulatory control, *i.e.* the ability to maintain homeostasis in the face of hyper-osmotic conditions, is mirrored in the concurrently improved survival and decrease in observed incidence of deformity and is schematically illustrated in Figure 8.1.
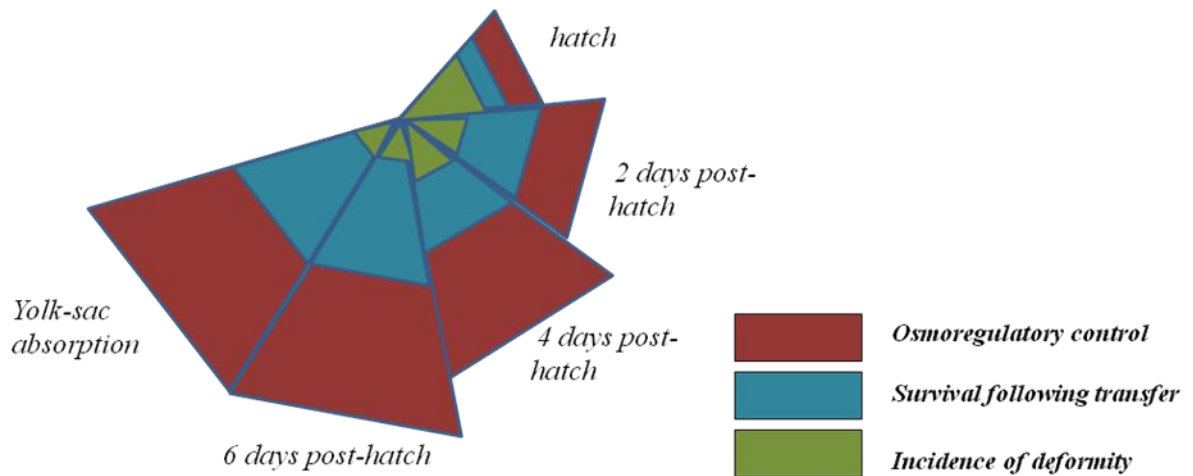
Figure 8. 1 Schematic representation of the ontogeny of osmoregulatory status during the yolk-sac absorption period.

Whilst the existence of a relationship between tolerance to osmotic stress and the capacity to osmoregulate has been well established in adult fish (Alderdice, 1988), it has only been shown in teleost larvae in only a few species to date (Varsamos *et al.*, 2005). These studies have been mainly confined to marine teleost species, in an attempt to explain species and developmental stage-specific distribution. This is the first study to give a complete picture of the ontogeny of osmoregulatory capacity over a range of salinities during successive early life stages of the euryhaline Nile tilapia and served to form the basis for subsequent chapters in this thesis by providing valuable insights into ontogenic variations in the capacity of this species to hyper- and hypo-regulate over a range of salinities.

The succeeding chapter (Chapter 4) aimed to refine these fundamental findings, and studies were designed to investigate whether developmental stage, in combination with timing of transfer, influenced both embryonic and yolk-sac larval ability to withstand osmotic challenge through the assessment of the effects of varying low salinities (0 - 32 ppt) on hatchability, survival, growth and energetic parameters. In the 1980s, the advantages of early salinity exposure during the early hatchery phase on subsequent culture performance in the Nile tilapia (Watanabe *et al*., 1985 b) had been established, but since that time it would seem that little work has been carried out that focused on this commercially important species. Recently, interest has been shown by the commercial aquaculture sector specifically in Egypt to expand its culture in sea and brackish water and the research by El-Sayed *et al*. (2003) on the effects of varying dietary protein levels and water salinity on spawning performance of Nile tilapia broodstock and subsequent growth of their larvae reported that, whilst spawning performance and larval growth were better in freshwater than at 7 and 14 ppt, especially at the higher broodstock dietary protein levels (40%), it was still viable to produce seed and on-grow larvae at those salinities. This study was expected to provide both practical and applied research into viable aquacultural practices that could minimise freshwater requirements during the early life stages of the Nile tilapia.

It was demonstrated that embryos were able to tolerate transfer to varying rearing salinities (0 – 25 ppt). Results also showed that optimum timing of transfer of eggs from freshwater to elevated salinities was 3 - 4 h post-fertilisation, following manual stripping and fertilisation of eggs and, although there was a significant inverse effect of salinity on

hatching and developmental rates (GLM; $p < 0.05$), hatching rates of above 60% were obtained within this range. These findings have a direct practical application in tilapia hatcheries where, in general, spawning occurs naturally in freshwater and eggs are removed from the buccal cavity of the females and are then transferred to elevated salinities several days after spawning has occurred. The reported pattern of survival from hatch until yolk-sac absorption, with mortalities in elevated salinities occurring primarily during early yolk-sac development and stabilising from 5 dph onwards, are in agreement with results from the preceding chapter which had recognised that early life stages of the Nile tilapia possess an ability to osmoregulate that varies ontogenically and, once hatching occurs, osmolality levels begin to move towards a more constant range until yolk-sac absorption, suggesting a gradual improvement in the ability to osmoregulate as the larvae develop. Survival at yolk-sac absorption was seen to vary amongst trials but overall viable survival rates were still observed, with no statistical differences observed between freshwater and 7.5 ppt. The observed results of the present study have implications for both the development of hatchery production methods and for the future potential for aquaculture of this species in brackish water. Early low salinity exposure would not only minimise freshwater hatchery requirements but also may confer a pre-adaptation before transfer to higher salinities for on-growing (Watanabe *et al.*, 1985 b).

It has therefore been established that Nile tilapia embryos and larvae are able to live in media whose osmolality differs from their own blood osmolality. This tolerance is due to the presence of numerous integumental or cutaneous mitochondria-rich cells (MRCs)

commonly observed on the yolk-sac membrane and other body surfaces of fish embryos and larvae which appear to play a definitive role in osmoregulation during early development. An ontogenic transfer of regulative, osmoregulatory function from the integumental system to the developing branchial epithelial sites, culminating in the fully-functioning, branchial MRCs has also been widely reported. While much of the published work concerning the effects of salinity on the integumental MRCs has been carried out in the Mozambique tilapia (*Oreochromis mossambicus*), because of its strong euryhalinity, the only study found to date on the Nile tilapia is Fishelson and Bresler's (2002) comparative study on early life stages of various Tilapiine *spp.*, despite the fact that this species dominates global tilapia aquaculture. The work presented in Chapter 5 aimed to offer a more comprehensive study of the ontogenetic development of osmoregulatory system of this lesser studied but commercially important species.

A clearly defined temporal staging of the appearance of MRCs, conferring ability to cope with varying environmental conditions during early development, was evident throughout the yolk-sac period. The ontogenic pattern of MRC distribution was seen to change in both freshwater and brackish water with cell density decreasing significantly on the body from hatch to 7 days post-hatch, but appearing on the inner opercular area at 3 days post-hatch and increasing thereafter. An overview of results from Chapters 3, 4 and 5 in the form of a schematic representation of the ontogenic profile of the Nile tilapia during early life stages is shown in Figure 8.2. Integumental MRCs reflect the declining pattern observed on the measured body skin areas from hatch until yolk-sac absorption and branchial development

refers to the observed development of the gills and related morphological development of the branchial system *i.e.* mouth opening, opercular covering etc. including the observed increase in density of immunopositive MRCs in the inner opercular area from 5 days post-hatch onwards that was reported in Chapter 5 of this study. The increasing trend in larval survival indicated in this diagram parallels the observed pattern following transfer of embryos at $3 - 4$ h post-fertilisation following hatch until yolk-sac absorption as observed in Chapter 4 of this study, and the increase in osmoregulatory capacity mirrors the reported pattern in capability to maintain homeostasis in the face of hyper-osmotic environments, as seen in Chapter 3. It is apparent, therefore, that an integrated series of events seems to be occurring during the early development of the Nile tilapia; cellular changes, such as the differentiation of MRCs, and anatomical modifications, such as development of branchial epithelia, are reflected in the physiological outcome or ability to osmoregulate. This diagram illustrates that early life stages of Nile tilapia appear to face the greatest osmoregulatory challenge immediately after hatching, yet show an increasing capacity to maintain ionic and osmotic balance that is conferred ontogenically through the yolk-sac period.
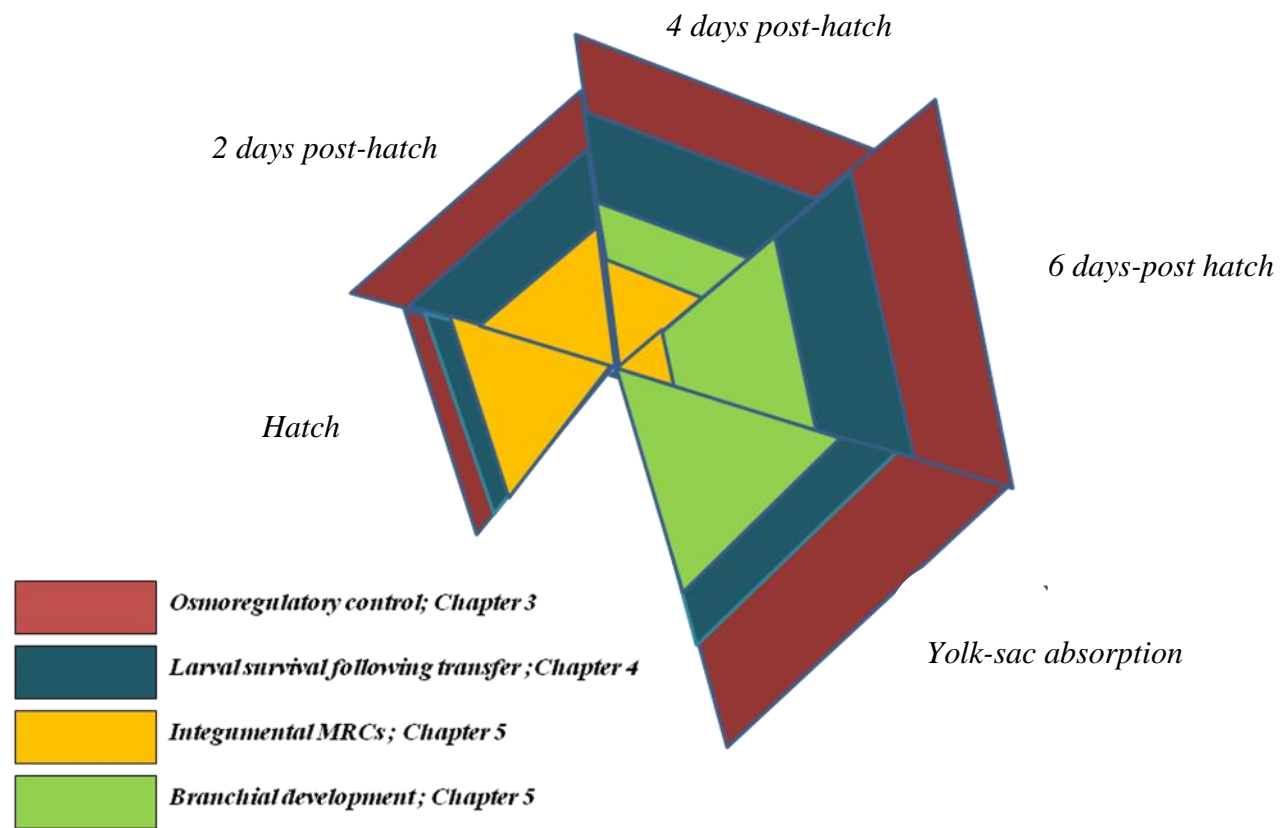
Figure 8. 2 Schematic representation of the ontogenic profile of the Nile tilapia during early life stages.

The central message of Chapter 5 was therefore the importance and role of integumental MRCs in the osmoregulatory ability of early life stages of the Nile tilapia. Adjustments to MRC morphology, as a response to environmental changes, are vital in conserving physiological function in the teleost, as it is this adaptive response that contributes to euryhaline fishes' ability to inhabit both diverse and fluctuating environments (Marshall, 2002). Further studies therefore aimed to examine the plasticity of the integumental MRCs during early life stages following osmotic challenge in order to gain insight into the relationship between structure and function during this adaptation process. It was apparent from existing literature that attempts to classify MRCs, based on their external or apical morphological appearance, had resulted in arbitrary and conflicting classifications. Therefore, in this study, a combination of quantitative and qualitative methods were used, including both scanning electron microscopy and transmission electron microscopy combined for the first time with a newly developed pre-fixation immunolabelling technique, in order to allow a reappraisal and reclassification of MRC 'sub-types' based on their apical appearance, underlying ultrastructure and immunolocalisation of key ion-transporters and channels *i.e.* Type I or absorptive, degenerating form, Type II or active absorptive form, Type III or differentiating form and Type IV or active secreting form. In addition, it catagorised and quantified for the first time the apical openings of mucous cells, which appear similar in size and morphology to MRC apical openings, and whose inclusion in previous quantitative studied have often led to an overestimation in MRC numbers. This advancement in knowledge contributes to the understanding of MRC apical crypt morphology during adaptation following salinity challenge.

The key message of Chapter 6 was that morphological changes to apical openings of MRCs and modifications to their ion transporting function in relation to external environment were interrelated. Further studies aimed to explore the hypothesis that changes in density, abundance, size and appearance of MRC as a response to changes in ionic composition of the external media do in fact reflect cellular differentiation, either as an expression of their developmental stage or as a modulation of their function. Chapter 5 had already established the use of immunohistochemical techniques in the detection of MRCs in integument of Nile tilapia. In general, progress in immunohistochemisty and immunocytochemistry has been dependant on the development and optimisation of reporter systems for the visualisation of antibody-binding to cell and tissue antigens and advancements in multimodal, correlative microscopic techniques, *i.e.* the combination of fluorescent and electron microscopy, offer valuable insight into cellular and sub-cellular structure/function relationships (Robinson and Vandré, 1997). Immunohistochemistry on whole-mount larvae using Fluoronanogold™ (Nanoprobes, U.S.) as a secondary immunoprobe has allowed fluorescent labelling with the high resolution of confocal scanning laser miscroscopy combined with the detection of immunolabelled target molecules at an ultrastructural level, using transmission electron microscopy. Although the microscopic techniques used in the current study cannot strictly be described as correlative, as the exact same cell is not examined by both imaging techniques, this integrated approach offers advantages over a single imaging procedure and can allow visualisation of the specific localisation of target molecules, both in a 3-D setting and at an ultrastructural level, providing important insights into MRC form and function.

If the classical model of MRC function holds that only 'mature' cells, *i.e.* those in contact with the external environment via an apical pit or crypt, are involved in ion transport (Wendelaar Bonga and van der Meij, 1989; Wendelaar Bonga *et al.,* 1990), then a method that allows an accurate assessment of both those MRCs that are actively involved in ionoregulation and sub-cellularly located MRCs, which are not nominally actively involved in ionoregulation, is obviously a valuable tool when studying MRC dynamics following salinity challenge. In the present study, a new method for discriminating between active and non-active MRCs is described, allowing, for the first time, an accurate and repeatable quantitative assessment of both density and various MRC morphometric and densitometric traits in the epithelia of yolk-sac Nile tilapia. In addition, this technique offers the potential for further informative and quantitative studies on MRC density and morphology, based on MRC functional state. It is clear that limitations exist in the 2-dimensional measurements commonly used in analysis of MRCs both described in the present study (Chapter 5) and in the literature which commonly report a cross-sectional area (μm^2) of the *x-y* projection of MRCs. In the current study confocal images of anti-Na^+/K^+-ATPase immunoreactivity revealed ramifying outcrops of tubular extensions of MRCs (Figure 7.6.) that would certainly influence a cross sectional area measurement leading to a potential misrepresentation and overestimation of surface area. However, the image analysis of confocal stacks using ImageJ with a 3-D Object Counter plug-in used in this study has allowed, for the first time, the measurement of actual volume of anti-Na^+/K^+-ATPase immunoreactivity (μm^3) and gives a more representative measurement of quantitative immunoreactive area.

The technique of immunogold labelling has not been extensively applied in the study of structure/function relationships of the MRC in teleosts. This may be due to the limitations that exist in the post-fixation technique immunogold labelling methods that have been used. Post-fixation of ultrathin sections is laborious and background staining is also an intrinsic problem (pers. observations). In addition, in order to preserve the antigenicity of the epitopes, the use of a 'soft' fixation technique results in poor preservation of the cellular membraneous structures of the tissue, such as the tubular system (Tresguerres *et al.,* 2006) giving poor results in terms of ultrastructural integrity and accurate staining patterns. The technique that has been developed in the current study reports, for the first time, a reliable and repeatable pre-fixation immunogold labelling technique to allow visualisation of both Na^+/K^+-ATPAse and CFTR within MRCs and offers the potential for further studies on quantification of immunobinding and measurement of functionally active tubular systems in both active and non-active MRCs.

Future work on the ontogeny of osmoregulation will rely on the application of new techniques (Varsamos, 2005). Whilst conventional imunohistochemistry techniques provide information on spatial patterns of protein distribution, they do not allow the underlying changes in mRNA levels to be studied (Davies, 1993). Therefore whole mount *in situ* hybridization of mRNA encoding proteins specific to the ion transporter proteins would give a valuable insight into both spatial and temporal localization gene expression and mechanisms of gene expression and regulation.

This thesis has targeted the most vulnerable ontogenetic stages in order to examine the ability of the euryhaline Nile tilapia to osmoregulate and has investigated both the the scope of tolerance and the nature of this physiological adaptability. The results of this study confirms the euryhaline nature of the early life stages of the Nile tilapia, showing that, during incubation, salinities up to 20 ppt are tolerable, although reduced hatching rates at 15 ppt and above suggest that these salinities may be less than optimal. Survival at yolk-sac absorption displayed a significant ($p < 0.05$) inverse relationship with increasing salinity and mortality was particularly heavy in the higher salinities of 15, 20 and 25 ppt and mortalities occurring primarily during early yolk-sac development, yet stabilised from 5 dph onwards. Knowledge of osmoregulatory capacity is vital to the improvement of hatchery management practices and could extend the scope of this species into brackish water environments. In addition, insights have been made into basic iono-regulatory processes that are fundamental to the understanding of osmoregulatory mechanisms during early life stages of teleosts.

References

Agarwal, S. and John, P. A. (1988). Studies on the development of the kidney of the guppy, *Lebistes reticulatus*. Part 1. The development of the pronephros. *J. Animal Morphol. Physiol.* **35** (17-24).

Akiyama, D.M. and Anggawati, A.M. (1999). Polyculture of shrimp and tilapia in East Java. *American Soybean Association (ASA) Technical Bulletin* AQ **47** 7 pp.

Al-Ahmad, T. A., Ridha, M. and Al-Ahmed, A.A, (1988). Production and feed ration of the tilapia *Oreochromis spilurus* in seawater. *Aquaculture* **73** (111-118).

Al-Amoudi, M, M. (1987). Acclimation of commercially cultured *Oreochromis* species to seawater – an experimental study. *Aquaculture* **65** (333-343).

Alderdice, D. F., Rosenthal, H. and Velsen, F. P. J. (1979). Influence of salinity and cadmium on capsule strength in Pacific herring eggs. *Helgol. wiss. Meeresunters* **32** (49-162).

Alderdice, D.F. (1988). Osmotic and ionic regulation in teleost eggs and larvae. In: *Fish Physiology: vol. XIA* (W.S. Hoar and D.J. Randall, eds), pp. 163-251. Academic Press, New York.

Andreasen, E. A., Spitsbergen, J. M., Tanguay, R. L., Stegeman, J. J., Heideman, W. and Peterson, R. E. (2002). Tissue-specific expression of AHR2, ARNT2, and CYP1A in zebrafish embryos and larvae: Effects of developmental stage and 2,3,7,8-tetrachlorodibenzo-p-dioxin exposure. *Toxicol. Sci.* **68** (403-419).

Anger, K. (2003). Salinity as a key parameter in the larval biology of decapod crustaceans. *Invertebr. Reprod. Dev.* **43** (29–45).

Avella, M., Berhaut, J. and Bornancin, M. (1993). Salinity tolerance of two tropical fishes, *Oreochromis aureus*, and *O. niloticus*, 1. Biochemical and morphological changes in the gill epithelium. *J. Fish Biol.* **42** (243–254).

Avella, M. and Bornancin, M. (1989). A new analysis of ammonia and sodium transport through the gills of the freshwater rainbow trout (*Salmo gairdneri*). *J. Exp. Biol.* **142** (155–175).

Ayson, F.G., Kaneko, T., Hasegawa, S. and Hirano, T. (1994). Development of mitochondria-rich cells in the yolk-sac membrane of embryos and larvae of tilapia, *Oreochromis mossambicus*, in fresh water and seawater. *J. Exp. Zool.* **270** (129-135).

Bailly, Y., Dunel-Erb, S. and Laurent, P. (1992). The neuroepithelial cells of the fish gill filaments: indolamine-immunocytochemistry and innervation. *Anat. Rec.* **233** (143-161).

Balarin, J.D. and Hatton, J.P. (1979). Tilapia: a guide to their biology and culture in Africa. University of Stirling, Scotland.

Balarin, J.D. and Haller, R.D. (1982). The intensive culture of tilapia in tanks, raceways and cages. In: *Recent Advances in Aquaculture.* (J.F. Muir and R.J. Roberts, eds.), pp. 266–355. Croom Helm, London.

Banks, M.A., Holt, G.J. and Wakeman, J.M. (1991). Age-linked changes in salinity tolerance of larval spotted seatrout (*Cynoscion nebulosus*, Cuvier). *J. Fish. Biol.* **39** (505-514).

Bardach, J.E., Ryther, J. H. and McLarney, W.D. (1972). Aquaculture: the farming and husbandry of freshwater and marine organisms. In: *The Farming and Husbandry of Freshwater and Marine Organisms*, p. 868. Wiley-Interscience, New York.

Bayoumi, A.R. (1969). Notes on the occurrence of *Tilapia zillii* (Pisces) in Suez Bay. *Mar. Biol.* **4** (255–256).

Behrends, R.G., Nelson, R.O., Smitherman, S. and Stone, H.M. (1982). Breeding and culture of the red-gold color phase of tilapia. *J. World Maricult. Soc.* **13** (210–220).

Bennett, A. F., Dawson W. R. and Putnam, R. W. (1981). Thermal environment and tolerance of embryonic Western Gulls. *Physiol. Zool.* **54** (146–154).

Birrell, L., Cramb, G. and Hazon, N. (2000). Osmoregulation during the development of glass eels and elvers. *J. Fish Biol.* **56** (1450–1459).

Bisbal, G. A. and Specker, J. L. (1991). Cortisol stimulates hypoosmoregulatory ability in Atlantic salmon, *Salmo salar L. J. Fish Biol.* **39** (421–432).

Björnsson, T., Yamauchi, K., Nishioka, R.S., Deftos, L.J. and Bern, H.A. (1987). Effects of hypophysectomized and subsequent hormonal replacement therapy on hormone and osmolality status of coho salmon, *Oncorhynchus kisutch. Gen. Comp. Endocrinol.* **68** (421–430).

Bodinier, C., Sucré, E., Lecurieux-Belfond, L., Blondeau-Bidet, E. and Charmantier, G. (2010). Ontogeny of osmoregulation and salinity tolerance in the gilthead sea bream *Sparus aurata. Comp. Biochem. Physiol. Part A.* **57** (220-228).

Boeuf, G. and Payan, P. (2001). How should salinity influence fish growth? *Comp. Biochem. Physiol. Part C.* **130** (411–423).

Bolla, S. and Ottesen, O.H. (1998). The influence of salinity on the morphological development of yolk-sac larvae of Atlantic halibut, *Hippoglossus hippoglossus* (L.). *Aquaculture Research* **29** (203-209).

Bowen, H. (1982). Feeding, digestion and growth — quantitative considerations. In: *The Biology and Culture of Tilapias* (R.S.V. Pullin and R.H. Lowe-McConnel, eds.) pp. 141–156. *ICLARM Conference Proceedings No. 7*, Manila, Philippines.

Brown, J.A. and Tytler, P. (1993). Hypoosmoregulation of larvae of the turbot, *Scophthalmus maximus*, drinking and gut function in relation to environmental salinity. *Fish Physiol. Biochem.* **10** (475– 483).

Brown, P. (1992). Gill chloride cell surface-area is greater in freshwater-adapted adult sea trout (*Salmo trutta*, L.) than those adapted to sea water. *J. Fish Biol.* **40** (481-484).

Bruton, M.N. and Boltt, R.E. (1975). Aspects of the biology of *Tilapia mossambica* Peters (Pisces: Cichlidae) in a natural freshwater lake (Lake Sibaya, South Africa). *J. Fish. Biol.* **7** (423-445).

Bullock, A.M. and Roberts, R.J. (1975). The dermatology of marine teleost fish: 1. The normal integument. *Oceanography and Marine Biology: an Annual Review* **13** (383-411).

Butler, D. G. and Carmichael, F. J. (1972). Na^+-K^+-ATPase activity in eel *(Anguilla rostrata)* gills in relation to changes in environmental salinity: role of adrenocortical steroids. *Gen. Comp. Endocrinol.* **19** (42 1-427).

Carmelo, A. (2002). Commercial culture of *Oreochromis spilurus* in open seawater cages and onshore tanks. *The Israeli Journal of Aquaculture* **54** (27-33).

Carroll, R. L. (1988)**.** Vertebrate Paleontology and Evolution. W. H. Freeman and Co., New York.

Cech, J.J. (1990). Respirometry. In. *Methods for Fish Biology*. (C.B.Schreck and P.B. Moyle. eds.), pp. 335-365. American Fisheries Society, Bethseda, Maryland, USA.

Chang I.C., Lee, T.H., Yang, C.H., Wei,Y.Y., Chou, F.I. and Hwang, P.P. (2001). Morphology and function of gill mitochondria-rich cells in fish acclimated to different environments. *Physiol. Biochem. Zool.* **74** (111–119).

Chang I.C., Wei, Y.Y., Chou,v F.I. and Hwang, P.P. (2003). Stimulation of Cl^- uptake and morphological changes in gill mitochondria-rich cells in freshwater tilapia (*Oreochromis mossambicus*). *Physiol. Biochem. Zool*. **76** (544–552).

Chervinski, J. (1982). Environmental physiology of tilapias. In: *The biology and culture of tilapias.* (R.S.V.Pullin R.H. Lowe-McConnell eds.), pp. 119-128. *ICLARM Conference Proceedings No. 7*, Manila, Philippines.

Chervinski, J. and Zorn, M. (1974). Notes on the growth of *Tilapia aurea* (Steindachner) and *Tilapia zillii* (Gervais) in seawater ponds. *Aquacuture* **2** (23-29).

Chimits, P. (1955). Tilapia and its culture. A preliminary bibliography. *FAO Fish. Bull.* **8** (1–33).

Chretien, M. and Pisam, M. (1986). Cell renewal and differentiation in the gill epithelium of fresh or salt water adapted euryhaline fish as revealed by (3^H) thymidine radioautography. *Biol. Cell* **56** (137-150).

Cioni, C., Demerich, P., Cataldi, E. and Cataudella, S. (1991). Fine structure of chloride cells in freshwater and seawater adapted *O. niloticus* (L.) and *O. mossambicus* (Peters). *J. Fish Biol.* **39** (197-210).

Collins, L.A. and Nelson, S. G. (1993). Effects of temperature on oxygen consumption, growth and development of embryos and yolk-sac larvae of *Siganus randalli* (Pisces: Siganidae). *Marine Biology* **117** (195-204).

Conte, F. P. and D. Y. Lin. (1967). Kinetics of cellular morphogenesis in gill epithelium during sea water adaptation of *Oncorhynchus mykiss* (Walbaum). *Comp. Biochem. Physiol. Part A.* **23** (945–957).

Coons, A.H., Creech, H.J. and Jones, R.N. (1941). Immunological properties of an antibody containing a fluorescent group. *Proc. Soc. Exp. Biol. Med.* **47** (200–202).

Copeland, D.E. (1948). The cytological basis of chloride transfer in the gills of *Fundulus heteroclitus. J. Morphol.* **82** (201-227).

Coughlan, D.J. and Gloss, S.P. (1984). Early morphological development of gills in smallmouth bass (*Micropterus dolomieu*). *Can. J. Zool.* **62** (951–958).

Coward, K. and Bromage, N.R. (1999). Spawning periodicity, fecundity and egg size in laboratory-held stocks of a substrate-spawning tilapiine, *Tilapia zillii* (Gervais). *Aquaculture* **171** (251–267).

Craik, J.C.A. and Harvey, S.M. (1987). A biochemical method for distinguishing between wild and farmed salmonid fishes by their carotenoid pigmentation. *J. Forensic Sci. Soc.* **27** (47-55).

Crocker, P.A., Arnold, C.R., DeBoer, J.A. and Holt, G.J. (1983). Blood osmolality shift in juvenile red drum *Sciaenops ocellatus* L. exposed to fresh water. *J. Fish Biol.* **23** (315-319).

Curtis, B.J. and Wood, C.M. (1991). The function of the urinary bladder *in vivo* in the freshwater rainbow trout. *J. Exp. Biol.* **155** (567–583).

Cutler, C.P. and Cramb, G. (2002). Branchial expression of an aquaporin 3 (AQP-3) homologue is downregulated in the European eel (*Anguilla anguilla*) following seawater acclimation. *J. Exp. Biol.* **205** (2643–2651).

Cutler, C.P., Sanders, I.L., Hazon, N. and Cramb, G. (1995). Primary sequence, tissue specificity and expression of the Na^+/K^+-ATPase $\beta1$ subunit in the European eel *Anguilla anguilla. Fish Physiol. Biochem.* **14** (423-429).

Cutler, C.P., Brezillon, S., Bekir, S., Sanders, I.L., Hazon, N. and Cramb, G. (2000). Expression of a duplicate Na^+/K^+-ATPase $\beta1$-isoform in the European eel (*Anguilla anguilla*). *Am. J. Physiol. - Regulatory, Integrative and Comparative Physiology* **279** (222–229).

Daborn, K., Cozzi, R.R.F. and Marshall W.S. (2001). Dynamics of pavement cell-chloride cell interactions during abrupt salinity change in *Fundulus heteroclitus*, *J. Exp. Biol.* **204** (1889–1899).

Dang, Z.C., Lock, R.A.C., Flik, G. and Wendelaar Bonga, S.E. (2000 a). Na^+/K^+-ATPase immunoreactivity in branchial chloride cells of *Oreochromis mossambicus* exposed to copper. *J. Exp. Biol.* **203** (379–387).

Dang, Z., Balm, P., Flik, G., Wendelaar-Bonga, S. and Lock, R. (2000 b). Cortisol increases Na^+/K^+-ATPase density in plasma membranes of gill chloride cells in the freshwater tilapia *Oreochromis mossambicus. J. Exp. Biol.* **203** (349–355).

Dangé, A. D. (1986). Branchial Na^+, K^+-ATPase activity in freshwater or seawater acclimated tilapia, *Oreochromis (Sarotherodon) mossambicus*: effects of cortisol and thyroxine. *Gen. Comp. Endocrinol*. **62** (341-343).

Daoust, P. Y., Wobeser, G. and Newstead, J. D. (1984). Acute pathological effects of inorganic mercury and copper in gills of rainbow trout. *Vet. Pathol*. **21** (93–101).

Davenport, J. and Lonning, S. (1980). Oxygen uptake in developing eggs and larvae of the cod (*Gadus morhua* L.). *J. Fish Biol*. **16** (249-256).

Davenport, J*.,* Lønning, S. and Kjørsvik, E. (1981*).* Osmotic and structural changes during early development of eggs and larvae of the cod, *Gadus morhua* L. *J. Fish Biol*. **19** (317–331).

Davies, J.T. (1993). *In situ* hybridization. In: *Immunocytochemistry: A practical approach* (J.E.Beesley ed.). Oxford University Press, UK.

D'Cotta, H., Valotaire, C., le Gac, F. and Prunet, P. (2000). Synthesis of gill Na^+/K^+-ATPase in Atlantic salmon smolts: differences in α-mRNA and α-protein levels. *Am. J. Physiol. - Regulatory, Integrative and Comparative Physiology* **278** (101-110).

Degnan, K.J. and Zadunaisky, J.A. (1980). Passive sodium movements across the opercular epithelium: the paracellular shunt pathway and ionic conductance. *J. Membr. Biol*. **55** (175-185).

Degnan, K.J., Karnaky, K.J. Jr. and Zadunaisky, J.A. (1977). Active chloride transport in the *in vitro* opercular skin of a teleost (*Fundulus heteroclitus*), a gill-like epithelium rich in chloride cells. *J. Physiol. (London)*. **271** (155-191).

Depeche, J. (1973). Infrastructure superficielle de la vesicule vitelline et dusac pericardique de l'embryon de *Poecilia reticulata* (Poisson Teleosteen). *Z. Zellforsch*. **141** (235–253).

De Rengis, G. and Bornancin, M. (1984). Ion transport and gill ATPases. In: *Fish Physiology Vol X*. (W.S.Hoar and D.J. Randall eds.), pp 65-104. Academic Press, London.

De Silva, C.D., Premawansa, S. and Keembiyahetty, C.N. (1986). Oxygen consumption in *Oreochromis niloticus* (L.) in relation to development, salinity, temperature and time of day. *J. Fish Biol*. **29** (267-277).

Doroshev, S.I. and Aronovich, T.M. (1974). The effects of salinity on embryonic and larval development of *Eleginus navaga* (Pallas), *Boreogadus saida* (Lepechin) and *Liopsettaglacialis* (Pallas). *Aquaculture* **4** (353–362).

Doyle, W. L. and Gorecki, D. (1961). The so-called chloride cell of the fish gill. *Physiol. Zool*. **34** (81-85).

Drummond, I.A., Majumbar, A., Hentschel, H., Elger, M., Solnica-Krezel, L., Schier, A.F., Neuhauss, C.F., Stemple, D.L., Zwartkruis, F., Rangini,Z., Driever, W. and Fishman, M. (1998). Early development of the zebrafish pronephros and analysis of mutations affecting pronephric function. *Development* **125** (4655–4667).

Dunel, S, and Laurent, P. (1980). Ultrastructure of marine teleost gill epithelia: SEM and TEM study of the chloride cell apical membrane. *J. Morphol.* **16** (175–186).

Dunel-Erb, S., Bailly, Y. and Laurent, P. (1982). Neuroepithelial cells in fish gill primary lamellae. *J. Appl Physiol.* **53** (1342-1353).

Eckstein, B. and Spira. M. (1965). Effect of sex hormones on gonadal differentiation in a cichlid, *Tilapia aurea*. *Biological Bulletin* **129** (482–489).

Elger, M. and Hentschel, H. (1981). The glomerulus of a stenohaline fresh-water teleost, *Carassius auratus*, adapted to saline water. *Cell Tiss. Res.* **220** (73–85).

El-Sayed, A.M. (2006). Tilapia culture in salt water: Environmental requirements, nutritional implications and economic potentials. 8th Symposium on Advances in Nutritional Aquaculture. November 15–17, Nuevo Leon, Mexico.

El-Sayed, A.M., Mansour, C.R., and Ezzat, A.A. (2003). Effect of dietary protein level on spawning performance of Nile tilapia broodstock reared at different water salinities *Oreochromis niloticus*. *Aquaculture* **220** (619–632).

Epstein, F. H., Cynamon, M. and McKay, W. (1971). Endocrine control of Na-K-ATPase and seawater adaptation in *Anguilla rostrata*. *Gen. Comp. Endocrinol.* **16** (323–328).

Ernst, D.H. (1989). Design and operation of a hatchery for seawater productin of tilapia in the Caribbean. In: *Proc. Gulf Carib. Fish. Inst*. (G.T. Waugh and M.H. Goodwin, eds.), pp. 420-434.

Ernst, D.H., Watanabe, W.O., Ellington, L.J., Wicklund, R.I. and Olla, B.L. (1991). Commercial scale production of Florida red tilapia seed in low- and brackish-salinity tanks. *J. World Aquaculture Society* **32** (36-44).

Estudillo, C. B., Duray, M.N., Marasigan, E.T. and Emata, A.C. (2000). Salinity tolerance of larvae of the mangrove red snapper (*Lutjanus argentimaculatus*) during ontogeny. *Aquaculture* **190** (155-167).

Evans, D.H. (1999). Ionic transport in the fish gill epithelium. *J. Exp. Zool.* **283** (641–652).

Evans, D.H., Claiborne, J.B., Farmer, L., Mallery, C.H., and Krasny, E.J., Jr. (1982). Fish gill ionic transport: methods and models. *Biol. Bull.* **163** (108-130).

Evans, D. H., Piermarini, P. M. and Potts, W. T. W. (1999). Ionic transport in the fish gill epithelium. *J. Exp. Zool.* **286** (641–652).

Evans, D.H., Piermarini, P.M. and Choe, K.P. (2005). The multifunctional fish gill: dominant site of gas exchange, osmoregulation, acid-base regulation and excretion of nitrogenous waste. *Physiological Review* **85** (97-117).

FAO (2004) Committee for Inland Fisheries of Africa, Entebbbe, Uganda. Current economic opportunities in sub-Saharan Africa. FAO (CIFA/XIII/2004/8).

FAO (2005) FishStat Plus 2005. Aquaculture production statistics 1997-2004. Food and Agricultural Organisation of the United Nations, Fisheries and Aqauculture Department, Rome, Italy.

FAO (2010) FishStat Plus 2010. Aquaculture production statistics 1997-2008. Food and Agricultural Organisation of the United Nations, Fisheries and Aqauculture Department, Rome, Italy.

Farmer G.L. and Beamish F.H.W. (1969). Oxygen consumption of *Tilapia nilotica* in relation to swimming speed and salinity. *J. Fish Res. Bd. Can*. **26** (2807-2821).

Faulk, W.P. and Taylor, G.M. (1971). An immunocolloidal method for the electron microscope. *Immunochemistry* **8** (1081-1089).

Febry, R. and Lutz, P. (1987). Energy partitioning in fish: the activity related cost of osmoregulation in an euryhaline cichlid. *J. Exp. Biol.* **128** (63-85).

Feng, S.H., Leu, J.H., Yang, C.H., Fang, M.J., Huang, C.J. and Hwang, P.P. (2002). Gene expression of Na^+/K^+-ATPase $\alpha1$ and $\alpha3$ subunits in gills of the teleost *Oreochromis mossambicus*, adapted to different environmental salinities. *Marine Biotechnology* **4** (379–391).

Fenwick, J. C., Wendelaar Bonga, S. E. and Flik, G. (1999). *In vivo* bafilomycin-sensitive Na^+ uptake in young freshwater fish. *J. Exp. Biol.* **202** (3659-3666).

Field, M., Karnaky, K. J., Smith, P. L., Bolton, J. E. and Kinter, W. B. (1978). Ion transport across the isolated intestinal mucosa of the winter flounder *Peudopleuronectes americanus*. I. Functional and structural properties of cellular and paracellular pathways for Na and Cl. *J. Membr. Biol.* **41** (265–293).

Fineman-Kalio, A.S. (2008). Preliminary observations on the effect of salinity on the reproduction and growth of freshwater Nile tilapia, *Oreochromis niloticus* (L.), cultured in brackishwater ponds. *Aquaculture Research* **19** (313-320).

Finn, R.N., Fyhn, H.J. and Evjen, M.S. (1991). Respiration and nitrogen metabolism of Atlantic halibut eggs (*Hippoglossus hippoglosus*). *Marine Biology* **108** (11-19).

Fitzgerald, W.J. (1979). The red orange tilapia — a hybrid that could become a world favourite. *Fish Farming Int.* **6** (26–27).

Fitzsimmons, K. (2000). Tilapia: The most important aquaculture species in the 21st Century. In: *Tilapia Aquaculture in the 21st century* (K. Fitzsimmons and C. Carvalho, eds.), pp. 3-8. Proceedings from the Fifth International Symposium on Tilapia in Aquaculture. Rio de Janeiro, Brazil.

Fitzsimmons, K. (2001). Polyculture of tilapia and penaeid shrimp. *Global Aquaculture Advocate* **4** (43-44).

Fitzsimmons, K. (2006). In: *Tilapia: Biology, Culture, and Nutrition.* (C. Lim and C. D.Webster, eds.), pp. 607-618. Hawthorn Press, New York.

Fishelson, L. (1990). Scanning and transmission electron microscopy of the squamose gill-filament epithelium from fresh- and seawater-adapted tilapia. *Environ. Biol. Fish* **5** (161-165).

Fishelson, L. (1995). Ontogenesis of cytological structures around the yolk-sac during embryological and early larval development of some cichlid fishes. *J. Fish. Biol.* **47** (479-491).

Fishelson, L. and Popper, D. (1968). Experiments on rearing fish in saltwater near the Dead Sea, Israel. *FAO Fish Rep.* **44** (244–245).

Fishelson, L. and Bresler, V. (2002). Comparative studies of the development and differentiation of chloride cells in tilapiine fish with different reproductive styles. *J. Morph.* **253** (118–131).

Flegel T.W. and Alday-Sanz, V. (1998). The crisis in Asian shrimp aquaculture: current status and future needs, *J. Appl. Ichthy.* **14** (269–273).

Foskett, J.K., Logsdon, C.D., Turner, T., Machen, T.E. and Bern, H.A. (1981). Differentiation of the chloride extrusion mechanisms during seawater adaptation of a teleost fish, the cichlid *Sarotherodon mossambicus*. *J. Exp. Biol*. **93** (209-224).

Forstner, H. and Gnaiger, E. (1983). Calculation of equilibrium oxygen concentration. In: Polarographic Oxygen Sensors: Aquatic and Physiological Applications. (E. Gnaiger and H. Forstner, eds.), pp. 321-333. Springer, Berlin.

Foskett, J.K. and Scheffey, C. (1982). The chloride cell: definitive identification as the salt-secretory cell in teleosts. *Science* **8** (164-166).

Franklin, G. E. (1990). Surface ultrastructure changes in the gills of sockeye salmon (Teleostei: *Oncorhynchus nerka*) during seawater transfer: comparison of successful and unsuccessful seawater adaptation. *J. Morph*. **20** (13–23).

Frick, J.H. and Sauer, J.R. (1973). Examination of a biological cryostat/nanoliterosmometer for use in determining the freezing point of insect hemolymph. *Ann. Entomol. Soc. Am*. **66** (781– 783).

Frizzell, R. A., Halm, D. R., Musch, M. W., Stewart, C. P. and Field, M. (1984). Potassium transport by flounder intestinal mucosa. *Am. J. Physiol.* **246** (946–951).

Fryer, G. H. and Iles, T. D. (1972). The cichlid fishes of the Great Lakes of Africa: Their biology and evolution. TFH Publications, New Jersey, USA.

Fujimura, K. and Okada, N. (2007). Development of the embryo, larva and early juvenile of Nile tilapia *Oreochromis niloticus* (Pisces: Cichlidae); Developmental staging system. *Development, Growth & Differentiation* **49** (301–324).

Franklin, C.E. and W. Davidson, W. (1989). S.E.M. observations of morphologically different chloride cells in freshwater-adapted sockeye salmon, *Oncorhynchus nerka*. *J. Fish Biol.* **34** (803–804).

Galman, O.R. and Avtalion, R.R. (1983). A preliminary investigation of the characteristics of red tilapia from the Philippines and Taiwan. In: *International Symposium on Tilapia in Aquaculture* (L. Fishelson and Z. Yaron eds.), pp 291-301. Tel Aviv University Press, Israel.

Gallis, J.L. and Bourdichon, M. (1976). Changes of (Na^+–K^+) dependent ATPase activity in gills and kidneys of two mullets *Chelon labrosus* (Risso) and *Liza ramada* (Risso) during fresh water adaptation. *Biochimie* **58** (625– 627).

García-Ayala, A., García Hernández, M.P., Quesada, J.A. and Agulleiro, B. (1997). Immunocytochemical and ultrastructural characterization of prolactin, growth hormone and somatolactin cells from the Mediterranean yellowtail (*Seriola dumerilii*, Risso 1810). *Anat Rec*. **247** (395–404).

Garcia-Perez, A., Alston, D. and Cortes-Maldonado, R. (2000). Growth, survival, yield and size distribution of freshwater prawn, *Macrobrachium rosenbergii*, and tilapia, O*reochromis niloticus*, in polyculture and monoculture systems in Puerto Rico. *J. World Aquac. Soci.* **31** (446-451).

Giese A.C. (1957). Cell Physiology. W.B. Saunders Co., Philadelphia, pp. 534.

Gilbert, W., deSouza, S. J. and. Long, M. Y. (1997). Origin of genes. *Proc. Natl. Acad. Sci. USA* **94** (7698–7703).

Goldstein, I. J., So, L. L., Yang, Y. and Callies, Q. C. (1969). The interaction of concanavalin a with IgM and the glycoprotein phytohemagglutinins of the waxbean and the soybean. *J. Immunol*. **103** (695-698).

Gonzalez, M. E., Blanquez, M. J. and Rojo, C. (1996). Early gill development in the rainbow trout, *Oncorhynchus mykiss. J. Morphol*. **229** (201–217).

Goss, G.G. and Perry, S.F. (1994). Different mechanisms of acidbase regulation in rainbow trout (*Oncorhynchus mykiss*) andAmerican eel (*Anguilla rostrata*) during NaHCO$_3$ infusion. *Physiol. Zool*. **67** (381–406).

Goss, G., Perry, S. and Laurent, P. (1995). Ultrastructural and morphometric studies on ion and acid-base transport processes in freshwater fish. In. *Fish Physiology; vol 14: Cellular and molecular approaches to fish ionic regulation* (C.M. Wood and T.J. Shuttleworth, eds.), pp. 257-284. Academic Press, London.

Goss, G.G., Adamia, S. and Galvex, F. (2001). Peanut lectin binds to a subpopulation of mitochondria-rich cells in the rainbow trout epithelium. *Am. J. Physiol.* **281** (1718–1725).

Greenwell, M., Sherrill, J. and Clayton, L. (2003). Osmoregulation in fish. Mechanisms and clinical implications. *Vet. Clin. Exot. Am*. **6** (169– 189).

Griffiths, R.W. (1974). Environment and salinity tolerance in the genus *Fundulus. Copeia* (319-331).

Gross, W.J. (1954). Osmotic responses in the sipunculid worm *Dendrostomum zostericolum. J. Exp. Biol.* **31** (402-423).

Guggino, W.B. (1980 a). Water balance in embryos of *Fundulus heteroclitus* and *F. bermudae* in seawater. *Am. J. Physiol.* **238** (36–41).

Guggino, W.B. (1980 b). Salt balance in embryos of *Fundulus heteroclitus* and *F. bermudae* adapted to seawater. *Am. J. Physiol.* **238** (42–49).

Guner, Y., Zden, O., Auirgan, H., Altunok, M. and Kizak, V. (2005). Effects of salinity on the osmoregulatory functions of the gills in Nile tilapia (*Oreochromis niloticus*). *Turkish Journal of Veterinary and Animal Science* **29** (1259-1266).

Hahnenkamp, L, Senstad, K. and Fyhn, H.J. (1993). Osmotic and ionic regulation of yolksac larvae of Atlantic halibut (*Hippoglossus hippoglossus*). In.

Physiological and biochemical aspects of fish development. (B.T. Walter and H.J. Fyhn, eds.), pp. 259-262.University of Bergen, Norway.

Handy, R.D. (1989). The ionic composition of rainbow trout body mucus. *Comp. Biochem. Physiol. Part A.* **93** (571-575).

Hart, P.R. and Purser, G.J. (1995). Effects of salinity and emperature on eggs and yolk sac larvae of the greenback flounder (Rhombosolea tapirina Gunther, 1982). *Aquaculture* **136** (221-230).

Head, W.D., Zerbi, A. and Watanabe, W.O. (1996). Economic evaluation of commercial scale, salt-water pond production of Florida red tilapia in Puerto Rico. *J. World Aqua. Soc.* **27** (275-289).

Hickling, C.F. (1963). The cultivation of tilapia. *Scientific American* **5** (143-153).

Hickman, C.P. and Trump, B.F. (1969). The kidney. In: *Fish Physiology, vol. 1.* (W.S. Hoar, W.S. and D.J. Randall, eds.), pp. 91– 239. Academic Press, NewYork.

Hill, A., Howard, C. V., Strahle, U. and Cossins, A. (2003). Neurodevelopmental defects in zebrafish (*Danio rerio*) at environmentally relevant dioxin (TCDD) concentrations. *Toxicol. Sci.* **76** (392-399).

Hirano, T. and Mayer-Gostan, N. (1976). Eel esophagus as an osmoregulatory organ. *Proc. Natl. Acad. Sci. USA.* **73** (1348– 1350).

Hirano, T., Morisawa, M. and Suzuki, K. (1978). Changes in plasma and ceolomic fluid composition of the mature salmon (*Oncorhynchus keta*) during freshwater adaptation. *J. Comp. Biochem. Physiol. Part A* **61** (5-8).

Hiroi, J., Kaneko, T., Seikai, T. and Tanaka, M. (1998). Developmental sequence of chloride cells in the body skin and gills of Japanese flounder (*Paralichthys olivaceus*) larvae. *Zool. Sci.* **15** (455–460).

Hiroi, J., Kaneko, T. and Tanaka, M. (1999). *In vivo* sequential changes in chloride cell morphology in the yolk-sac membrane of Mozambique Tilapia (*Oreochromis mossambicus*) embryos and larvae during seawater adaptation. *J. Exp. Biol.* **202** (3485–3495).

Hiroi, J., McCormick, S.D., Ohtani-Kaneko, R. and Kaneko, T. (2005). Functional classification of mitochondrion-rich cells in euryhaline Mozambique tilapia (*Oreochromis mossambicus*) embryos, by means of triple immunofluorescence staining for Na^+/K^+-ATPase, $Na^+/K^+/2Cl^-$ cotransporter and CFTR anion channel. *J. Exp. Biol.* **208** (2023–2036).

Hiroi, J., Yasumasu, S., McCormick, S.D., Hwang, P.P. and Kaneko, T. (2008). Evidence for an apical Na-Cl co-transporter involved in ion uptake in a teleost fish. *J. Exp. Biol.* **211** (2584-2599).

Hirose, S., Kaneko, T., Naito, N. and Takei, Y. (2003). Molecular biology of major components of chloride cells. *Comp. Biochem. Physiol. Part B* **136** (593-620).

Holgate, C.S., Jackson, P.I., Cowen, P.N. and Bird, C.C. (1983). Immunogold–silver staining: new method of immunostaining with enhanced sensitivity. *J. Histochem. Cytochem.* **31** (938–944).

Holland, N. D. and Chen, J.-Y. (2001). Origin and early evolution of the vertebrates: new insights from advances in molecular biology, anatomy, and palaeontology. *BioEssays* **23** (142–151).

Holliday, F. G. T. (1965). Osmoregulation in marine teleost eggs and larvae. *Calif. Coop. Oceanic Fish. Invest. Rep.***10** (89-95).

Holliday, F.G.T. (1969). The effects of salinity on the eggs and larvae of teleosts. In *Fish Physiology: Excretion, Ionic Regulation and Metabolism: vol. I* (W.S.Hoar and D.J. Randall, eds.), pp. 239–309. Academic Press, London.

Holliday, F.G.T. and Blaxter, J.H.S. (1960 a). Oxygen uptake of developing eggs and larvae of the herring (*Clupea harengus*). *J. Mar. Biol. Assoc*. **44 (**711-723).

Holliday, F. G. T., Blaxter, J. H. S. (1960 b). The effects of salinity on the developing eggs and larvae of the herring (*Clupea harengus*). *J. Mar. Biol. Assoc*. **39** (591-603).

Holliday, F. G. T. and P. M. Jones. (1965). Osmotic regulation in the embryo of the herring (*Clupea harengus*). *J. Mar. Biol. Assoc.* **45** (305-311).

Holliday, F, G. T. and Jones, M. P. (1967). Some effects of salinity on the developing eggs and larvae of the plaice (*Pleuronectes platessa*). *J. Mar. Biol. Assoc.* **47** (39-48).

Holstvoogd, C. (1957). The postembryonic development of the pronephros in *Clupea harengus* L. *Arch. Neerl*. (455–466).

Hootman, S. R. and Philpott, C.W. (1980). Accessory cells in teleost branchial epithelium. *Am. J. Physiol.* **238** (185-198).

Hopkins, K.D. (1983). Tilapia culture in arid lands. ICLARM Newsletter **6** (8-9).

Hopkins, K.D., Ridha, M., Leclercq, D., Al-Meeri, D. and Alahmad, T. (1989). Screening tilapia for culture in sea water in Kuwait. *Aquaculture Research* **20** (389-397).

Hossler F.E., J.R. Ruby, and T.D. McIlwain. (1979). The gill arch of the mullet, *Mugil cephalus*. I. Surface ultrastructure. *J. Exp. Zool.* **208** (379–398).

Hossler F.E., Musil, G., Karnaky, K.J. Jr., and Epstein, F.H. (1985). Surface ultrastructure of the gill arch of the killifish, *Fundulus heteroclitus*, from seawater and freshwater, with special reference to the morphology of apical crypts of chloride cells. *J. Morphol.* **185** (377–386).

House, C. R. and Green, K**.** (1965). Ion and water transport in the isolated intestine of the marine telost *Cottus scorpius*. *J. Exp. Biol.* **42** (177–189).

Hu, F. and Liao, I.C. (1979). The effect of salinity on the eggs and larvae of grey mullet, *Mugil cephalus*. ICES/ELF Symp./RA:**6**.

Hughes, G.M. (1979). Scanning electron microscopy of the respiratory surface of trout gills. *Jour. Zool. London* **187** (443-453).

Hughes, G. M. (1984). General anatomy of the gills. In: *Fish physiology, vol. X(A):* (W.S. Hoar and J.Randall, eds.). Academic Press, London.

Hulet, W.H. (1978). Structure and functional development of the eel leptocephalus *Ariosoma balearicum* (De La Roche 1809). *Phil. Trans. Roy. Soc. London Ser. B* **282** (107-138).

Hwang, P.P. (1987). Tolerance and ultrastructural responses of branchial chloride cells to salinity challenge in the euryhaline teleost *Oreochromis mossambicus*. *Marine Biology* **94** (643-649).

Hwang, P.P. (1988). Multicellular complex of chloride cells in the gills of freshwater teleosts. *J. Morphol.* **196** (15–22).

Hwang, P.P. (1989). Distribution of chloride cells in teleost larvae. *J. Morph.* **200** (1–8).

Hwang, P.P. (1990). Salinity effects on development of chloride cells in the larvae of ayu (*Plecoglossus altivelis*). *Mar. Biol.* **107** (1–7).

Hwang, P.P. and. Hirano, R. (1985). Effects of environmental salinity on intercellular organization and junctional structure of chloride cells in early stages of teleost development. *J. Exp. Zool.* **236** (115–126).

Hwang, P.P. and Sun, C.M. (1989). Putative role of adenohypophysis in the osmoregulation of Tilapia larvae (*Oreochromis mossambicus*, teleostei): an ultrastructural study. *Gen. Comp. Endocrinol.* **73** (335– 341).

Hwang, P.P. and Wu, S.M. (1988). Salinity effects on cytometrical parameters of the kidney in the euryhaline teleost *Oreochromis mossambicus* Peters. *J. Fish Biol.* **33** (89–95).

Hwang, P. and Wu, S. (1993). Role of cortisol in hypoosmoregulation in larvae of the tilapia (*Oreochromis mossambicus*). *Gen. Comp. Endocrin.* **92** (318-324).

Hwang, P.P., Sun, C.M. and Wu, S.M. (1988). Characterization of gill Na^+/K^+ activated adenosinetriphosphatase from tilapia *Oreochromis mossambicus*. *Bulletin of the Institute of Zoology, Zoological Academia Sinica* **27** (49-56).

Hwang, P.P., Sun, C.M. and Wu, S.M. (1989). Changes of plasma osmolality, chloride concentration and gill Na^+/K^+ ATPase activity in tilapia *Oreochromis mosssambicus* during seawater acclimation. *Mar. Biol.* **100** (295-299).

Hwang, P.P., Tsai,Y.N. and Tung, Y.C. (1994). Calcium balance in embryos and larvae of the freshwater-adapted teleost *Oreochromis mossambicus*. *Fish. Physiol. Biochem.* **13** (325–333).

Hwang, P.P., Fang, M.J., Tsai, J.C., Huang, C.J. and Chen, S.T. (1998). Expression of mRNA and protein of Na^+/K^+-ATPase α subunit in gills of tilapia (*Oreochromis mossambicus*). *Fish Physiol. Biochem.* **18** (363–373).

Inokuchi, M., Hiroi, J., Watanabe, S., .Lee, K.M. and Kaneko, T. (2008). Gene expression and morphological localisation of NHE3, NCC and NKCC1a in branchial mitochondria-rich cells of Mozambique tilapia (*Oreochromis mossambicus*) acclimated to a wide range of salinities. *Comp. Biochem. Physiol. Part A* **151** (151-158).

Inokuchi, M., Hiroi, J., Watanabe, S., Hwang, P.P. and Kaneko, T. (2009). Morphological and functional classification of ion-absorbing mitochondria-rich cells in the gills of Mozambique tilapia. *J. Exp. Biol.* **212** (1003–1010).

Iwai, T. (1969). On the chloride cells in the skin of larval puffer, *Fugu niphobles* (Jordan and Snyder). *La Mer* **72** (6–31).

Iwama G.K., Takemura, A. and Takano K. (1997). Oxygen consumption rates of tilapia in fresh water, sea water and hypersaline sea water. *J. Fish Biol*. **51** (886-894).

Jalabert, B., Moeau, J., Planquette, P. and Billard, R. (1974). Determinisme du sexe chez *Tilapia macrochir* et *Tilapia nilotica*: Action de la methyltestosterone dans l'alimentation des alevins sur la differenciation sexuell; Proportion des sexes dans la descendance des males "inverses". *Annals de Biologie de Animal Biochimie and Biophysique* **14** (720–739).

Job, S. V. (1969 a). The respiratory metabolism of *Tilapia mossambica* (Teleostei). I. The effect of size, temperature and salinity. *Mar. Biol.* **2** (121-126).

Job, S. V. (1969 b). The respiratory metabolism of *Tilapia mossambica* (Teleostei) 11. The effect of size, temperature and salinity and partial pressure of oxygen. *Mar. Biol.* **3** (222-226).

Jonassen, T.M., Pittman, K. and Imsland, A.K. (1997). Seawater acclimation of tilapia, *Oreochromis spilurus spilurus* Gunter, fry and fingerlings. *Aquaculture Research* **28** (205-214).

Kabir Chowdhury, M.A., Yang,Y., Lin, C.K. and El-Haroun, E.R. (2006). Effect of salinity on carrying capacity of adult Nile tilapia *Oreochromis niloticus* L. in recirculating systems. *Aquaculture Research* **37** (1627-1635).

Kalber, F.A. and Costlow Jr., J.D. (1966). The ontogeny of osmoregulation and its neurosecretory control in the decapod crustacean (*Rhithropanopeus harrisii*) (Gould). *Am. Zool.* **6** (221–229).

Kamal, A.H.M.M. and Mair, G.C. (2005). Salinity tolerance in superior genotypes of tilapia, *Oreochromis niloticus Oreochromis mossambicus* and their hybrids. *Aquaculture* **247** (189–201).

Kamiya, M. (1972). Sodium-potassium-activated adenosinetriphosphatase in isolated chloride cells from eel gills. *Comp. Biochem. Physiol. Part B* **43** (611-617).

Kamler, E. (1992). Ontogeny of yolk-feeding fish: an ecological perspective. *Rev. Fish. Biol. Fish*. **12** (79-103).

Kaneko, T., Hasegawa, S., Takagi, Y., Tagawa, M., and Hirano, T. (1995). Hypoosmoregulatory ability of eyed-stage embryos of chum salmon. *Marine Biology* **122** (165– 170).

Kaneko, T. and Shiraishi, K. (2001). Evidence for chloride secretion from chloride cells in the yolk-sac membrane of Mozambique tilapia larvae adapted to seawater. *Fisheries Science* **67** (541-543).

Kao, C.Y. and Chambers, R. (1954). Internal hydrostatic pressure of the *Fundulus* egg. I. The activated egg. *J. Exp. Biol*. **31** (139-149).

347

Karnaky, K.J., Kinter, L.B., and Stirling, C.E. (1976). Teleost chloride cell. II. Autoradiographic localization of gill Na$^+$/K+ ATPase in killifish *Fundulus heteroclitus* adapted to low and high salinity environments. *J. Cell Biol.* **70** (157-177).

Karnaky, K. J. (1986). Structure and function of the chloride cell of *Fundulus heteroclitus* and other teleosts. *American Zoologist* **26** (209-224).

Karnovsky, M.J. (1971). Use of ferrocyanide-reduced osmium tetroxide in electron microscopy. *Proc. 14th Ann. Meet. Am. Soc. Cell Biol.*, **146**.

Katoh, F., Shimizu, A., Uchida, K. and Kaneko, T. (2000). Shift of chloride cell distribution during early life stages in seawater-adapted killifish (*Fundulus heteroclitus*). *Zool. Sci.* **17** (11–18).

Katoh, F., Hasegawa, S., Kita, J., Takagi, Y., and Kaneko, T. (2001). Distinct seawater and freshwater types of chloride cells in killifish, *Fundulus heteroclitus*. *Can. J. Zool.* **79** (822–829).

Katoh, F., Hyodo, S. and Kaneko, T. (2003). Vacuolar-type proton pump in the basolateral plasma membrane energizes ion uptake in branchial mitochondria-rich cells of killifish *Fundulus heteroclitus*, adapted to a low ionenvironment. *J. Exp. Biol.* **206** (793–803).

Kaushik, S.J., Dabrowski, K. and Luque, P. (1982). Patterns of nitrogen excretion and oxygen consumption during ontognenesis of common carp (*Cyprinus carpio*) *Can. J. Fish. Aquatic Sciences* **39** (1095-1105).

Kerstetter, T.H.L., Kirschner, L.B. and Rafuse, D.D. (1970). On the mechanism of sodium ion transport by the irrigated gills of rainbow trout *(Salmo gairdneri). J. Gen. Physiol.* **56** (342-350).

Keys, A. B. and Willmer, E. N. (1932). Chloride secreting cells in the gills of fishes with special reference to the common eel. *J. Physiol. (Lond.)* **76** (368 -378).

Kikuchi, S. (1977). Mitochondria-rich (chloride) cells in the gill epithelium from four species of stenohaline freshwater teleosts. *Cell Tissue Res.* **18** (87-98).

King, J.A.C. and Hossler, F.E. (1991). The gill arch of the striped bass (*Morone saxatilis*). IV. Alterations in the ultrastructure of chloride cell apical crypts and chloride efflux following exposure to seawater. *J. Morphol.* **209** (165–176).

King, J. A. C., Abel, D. C. and DiBona, D. R. (1989). Effects of salinity on chloride cells in the euryhaline cyprinodontid fish *Rivulus marmoratus*. *Cell Tissue Res.* **257** (367 -377).

Kinne, O. (1964). The effects of temperature and salinity on marine and brackish water animals. II. Salinity and temperature salinity combinations. *Oceanographic and Marine Biology* **2** (281-339).

Kirk, R.G. (1972). A review of the recent development in tilapia culture with special reference to fish farming in the heated effluents of power stations. *Aquaculture* **1** (45-60).

Kirschner, L.B. (2004). The mechanism of sodium chloride uptake in hyperregulating aquatic animals. *J. Exp. Biol*. **207** (1439–1452).

Kjorsvik, E., Davenport, J. and Lonning, S. (1984). Osmotic changes during the development of eggs and larvae of the lumpsucker *Cydopterus lumpus* L. *J. Fish Biol*. **24** (311-321).

Kristiansen. H. R. and Rankin, J. C**.** (2001). Discrimination between endogenous and exogenous water sources in juvenile rainbow trout fed extruded dry feed. *Aquat. Living Resour.* **14** (359 -366).

Krogh, A**.** (1939). Osmotic Regulation in Aquatic Animals. Cambridge University Press, UK.

Kultz, D., Jurss, K. and Jonas, L. (1995). Cellular and epithelial adjustments to altered salinity in the gill and opercular epithelium of a cichlid fish (*Oreochromis mossambicus*). *Cell Tissue Res.* **279** (65–73).

Kuo, H. and Tsay, T.T. (1984). Study on the genetic improvement of red tilapia cross breeding and its growth. *Bull. Taiwanese Fish. Res. Inst.* **36** (69–92).

Lackie, P.M. (1996). Immunogold silver staining for light microscopy. *Histochem. Cell Biol.* **106** (9–17).

Langdon, J.S. and Thorpe, J.E. (1985). The ontogeny of smoltification: developmental patterns of gill Na^+/K^+-ATPase, SDH and chloride cells in juvenile Atlantic salmon, *Salmo salar* L. *Aquaculture* **45** (83–95).

Lasker, R. and Theilacker, G.H. (1962). Oxygen consumption and osmoregulation by single Pacific sardine eggs and larvae (*Sardinops caerulea* Griard). *J. Cons. Perm. int. Explor. Mer*. **27** (25-33).

Lasker, R. and Threadgold, L.T. (1968). Chloride cells in the skin of the larval sardine. *Exp. Cell Res*. **52** (582– 590).

Lasserre, P. (1971). Increase of (Na^+K^+) -dependent ATPase activity in gills and kidneys of two euryhaline marine teleosts, *Crenimugil labrosus* (Risso, 1826) and *Dicentrarchus labrax* (Linnaeus, 1758), during adaptation to fresh water. *Life Sci*. **10** (113– 119).

Laurence, G.C. (1969). The energy expenditure of largemouth bass larvae, *Micropterus salmoides*, during yolk absorption. *Trans. Am. Fish. Soc*. **98** (398-405).

Laurent, P. (1984). Gill internal morphology. In: *Fish Physiology, Vol. X* (W.S. Hoar and D.J. Randall, eds), pp. 73–183. Academic Press, New York.

Laurent, P. (1985). A survey of the morpho-functional relationships between epithelia, vasculature and innervation within the fish gills. In: *Morphology in Vertebrates* (H. R. Duncker and G. Fleischer, eds.), pp.339-351. Gustav Fischer, Stuttgart, New York.

Laurent, P. and Dunel, S. (1980). Morphology of gill epithelia in fish. *Am. J. Physiol.* **238** (147–159).

Laurent, P. and Perry, S. (1991). The effects of cortisol on gill chloride cell morphology and ionic uptake in the freshwater trout *Salmo gairdneri. Cell tissue Res*. **259** (429–442).

Lee, C. S. and Menu, B. (1981). Effects of salinity on egg development and hatching in grey mullet *Mugil cephalus* L. *J. Fish Biol*. **19** (179-188).

Lee, C.S., Hu, F. and Hirano, R. (1981). Salinity tolerance of fertilized eggs and larval survival in the fish *Sillago sihama. Mar. Ecol. Prog. Ser.* **4** (169–174).

Lee, T.H., Hwang, P.P., Lin, H.C. and Huang, F.L. (1996). Mitochondria- rich cells in the branchial epithelium of the teleost, *Oreochromis mossambicus*, acclimated to various hypotonic environments. *Fish Physiol. Biochem*. **15 (**513-523).

Lee, T.H., Tsai, J.C., Fang, M.J., Yu, M.J. and Hwang, P.P. (1998). Isoform expression of Na^+/K^+-ATPase α-subunit in gills of the teleost *Oreochromis mossambicus. Am. Jour. Physiol*. **275** (926–932).

Lee, T.H., Hwang, P.P., Shieh, Y.E. and Lin, C. H. (2000). The relationship between 'deep-hole' mitochondria-rich cells and salinity adaptation in the euryhaline teleost, *Oreochromis mossambicus. Fish Physiol. Biochem.* **23** (133-140).

Lee, T.H., Feng, S.H., Lin, C.H., Hwang, Y.H., Huang, C.L. and Hwang, P.P. (2003). Ambient salinity modulates the expression of sodium pumps in branchial mitochondria-rich cells of Mozambique tilapia, *Oreochromis mossambicus. Zool. Sci.* **20** (29–36).

Lemarie, G., Dosdat, A., Coves, D., Dutto, G., Gasset, E. and Person, L.R.J. (2004). Effect of chronic ammonia exposure on growth of European sea bass (*Dicentrarchus labrax*) juveniles. *Aquaculture* **229** (479-491).

Li, J., Eygensteyn, J., Lock, R.A.C., Verbost, P.M., van der Heijden, A.J.H., Wendelaar Bonga, S.E. and Flik, G. (1995). Branchial chloride cells in larvae and juveniles of freshwater tilapia *Oreochromis mossambicus. J. Exp. Biol.* **198** (2177–2184).

Li, J., Quabius, E.S., Wendellar Bonga, S.E. and Lock, R.A.C. (1998). Effects of waterborne copper on branchial Na+-transpost in Mozambique tilapia (*Oreochromis mossambicus*). *Aquat. Toxicol*. **43** (1-11).

Liao, I.C. and Chen, S.L. (1983). Studies on the feasibility of red tilapia culture in saline water. In. *Proceeding of the International Symposium of Tilapia in Aquaculture.* (L. Fishelson and Z. Yaron eds.), pp. 524-533. Israel Tel Aviv University, Israel.

Likongwe, J.S., Stecko, T.D., Stauffer J.R. and Carline, R.F. (1996). Combined effects of water temperature and salinity on growth and feed utilization of juvenile Nile tilapia *Oreochromis niloticus* (Linneaus). *Aquaculture* **146** (37-46).

Lin, H. and Randall, D.J. (1995). Proton pumps in fish gills. In: *Cellular and Molecular Approaches to Fish Ionic Regulation, Fish. Physiol., Vol. 14.* (C.M. Wood and T.J. Shuttleworth, eds.), pp. 229– 255. Academic Press, London.

Lin, H.C. and Hwang, P.P. (1998). Acute and chronic effects of gallium chloride on tilapia (*Oreochromis mossambicus*) larvae. *Bull. Environ. Contam. Toxicol*. **60** (931-935).

Lin, L.Y., and Hwang, P.P. (2001). Modification of morphology and function of integument mitochondria-rich cells in tilapia larvae (*Oreochromis mossambicus*) acclimated to ambient chloride levels. *Physiol. Biochem. Zool*. **74** (469-476).

Lin, L. Y. and Hwang, P.P. (2004). Activation and inactivation of mitochondria-rich cells in tilapia larvae acclimated to ambient chloride changes. *J. Exp. Biol.* **207** (1335-1344).

Lin, L.Y., Weng, C.F. and Hwang, P.P. (1999). Effects of cortisol on ion regulation in developing tilapia (*Oreochromis mossambicus*). *Physiol. Biochem. Zool*. **72** (397– 404).

Lin, L.Y., Chiang, C.C., Gong, H.Y., Cheng, C.Y., Hwang, P.P. and Weng, C.F. (2003). Cellular distributions of creatine kinase in branchia of euryhaline tilapia (*Oreochromis mossambicus*). *Am. J. Physiol. Cell Physiol*. **284** (233-241).

Lonning, S. and Davenport, J. (1980). The swelling egg of the long rough dab, *Hippoglossoides platessoides limandoides* (Bloch). *J. Fish Biol*. **17** (359-378).

Lotan, R. (1960). Adaptability of *Tilapia nilotica* to various saline conditions. *Bamidgeh* **12** (96–100).

Lowe-McConnell, R..H. (1982). Tilapias in fish communities. In: *The Biology and Culture of Tilapias, ICLARM Conference Proceedings No. 7*. (R.S.V. Pullin and R.H. Lowe-McConnell, eds.), pp. 83–113. International Center for Living Aquatic Resources Management, Manila, Philippines.

Loya, Y. and Fishelson, L. (1969). Ecology of fish breeding in brackish water ponds near the Dead Sea (Israel). *J. Fish Biol.* **1** (261-278).

MacIntosh, D.J. and Little, D.C. (1995). Nile tilapia *(Oreochromis niloticus)*. In: *Broodstock Management and Egg and Larval Quality, Chapter 12*. (N.R. Bromage and R.J. Roberts eds.), pp. 277-320. Blackwell Scientific Ltd., Cambridge, Massachusetts, USA.

Mallat, J. (1985). Fish gill structural changes induced by toxicants and other irritants: a statistical review. *Can. J. Fish. Aquat. Sci.* **42** (630–648).

McAndrew, B. J. (2000). Evolution, phylogenetic relationships and biogeography. In: *Tilapias: Biology and Exploitation, Fish and Fisheries Series 25*. (M.C.M. Beveridge, and B. J. McAndrew, eds.), pp. 1-32. Kluwer Academic Publishers, USA.

McCormick, S.D. (1990). Cortisol directly stimulates differentiation of chloride cells in tilapia opercular membrane. *Am. J. Physiol.* **259** (857–863).

McCormick, S. D. (1995). Hormonal control of gill Na^+,K^+-ATPase and chloride cell function. In: *Fish Physiology: Cellular and Molecular Approaches to Fish Ionic Regulation, Vol. 14,* pp. 285–315. (C. M. Wood, and T. J. Shuttleworth, eds), Academic Press, London.

McCormick, J.H. and Jensen, K.M. (1989). Chronic effects of low pH and elevated aluminium on survival, maturation, spawning and embryo-larval development of the fathead minnow in soft water. *Water, Air and Soil Pollution* **43** (293-307).

McCormick, S.D. and Bern, H.A. (1990). In vitro stimulation of Na^+/K^+-ATPase activity and ouabain binding by cortisol in coho salmon gill, *Am. J. Physiol.* **256** (707–715).

McCormick, S. D., Sundell, K., Bjornsson, B. T., Brown, C. L. and Hiroi, J. (2003). Influence of salinity on the localization of Na^+/K^+-ATPase, $Na^+/K^+/2Cl^-$ cotransporter (NKCC) and CFTR anion channel in chloride cells of the Hawaiian goby (*Stenogobius hawaiiensis*). *J. Exp. Biol.* **206** (4575-4583).

McDonald, D. G. and Wood, C. M. (1981). Branchial and renal acid and ion fluxes in the rainbow trout, *Salmo gairdneri*, at low environmental pH. *J. Exp. Biol.* **91** (101-118).

McGeachin, R.B., Wicklund, R..I., Olla, B.L. and Winton, J.R. (1987). Growth of *Tilapia aurea* in seawater cages. *J. World Aquaculture Society* **18** (31-34).

Mc Kim, J.M. 1977. Evaluation of tests with early life stages of fish for predicting long term toxicity. *J. Fish. Res. Bd. Can.* **34** (1148 – 1154).

Madsen, S.S. (1990). The role of cortisol and growth hormone in seawater adaptation and development of hypoosmoregulatory mechanisms in sea trout parr (*Salmo trutta trutta*). *Gen. Comp. Endocrinol.* **79** (1–11).

Madsen, S.S., Jensen, M.K., Nøhr, J., and Kristiansen, K. (1995) Expression of Na^+-K^+-ATPase in the brown trout, *Salmo trutta*: *in vivo* modulation by hormones and seawater. *Am. J. Physiol.* **269** (1339-1345).

Maina, J. N. (1990). A study of the morphology of the gills of an extreme alkalinity and hyperosmotic adapted teleost *Oreochromis alcalicus grahami* (Boulenger) with particular emphasison the ultrastructure of the chloride cells and their modifications with water dilution: a SEM and TEM study. *Anat. Embryol.* **181** (83-98).

Maina, J. N. (1991). A morphometric analysis of chloride cells in the gills of the teleosts *Oreochromis alcalicus* and *Oreochromis niloticus* and a description of presumptive urea excreting cells in *O. alcalicus. J. Anat.* **175** (131-145).

Marshall, W. S**.** (2002). Na^+, Cl^-, Ca^{2+} and Zn^{2+} transport by fish gills: retrospective review and prospective synthesis. *J. Exp. Zool.* **293** (264 -283).

Marshall, W. S., Bryson, S. E., Darling, P., Whitten, C., Patrick, M., Wilkie, M., Wood, C. M. and Buckland-Nicks, J. (1997). NaCl transport and ultrastructure of opercular epithelium from a freshwater-adapted euryhaline teleost, *Fundulus heteroclitus. J. Exp. Zool.* **277**2(13 -237).

Marshall, W.S., Lynch, E.and Cozzi, R. (2002). Redistribution of immunofluorescence of CFTR anion channel and NKCC cotransporter in chloride cells during adaptation of the killifish *Fundulus heteroclitus* to sea water. *J. Exp. Biol.* **205** (1265-1273).

Mangor-Jensen, A. (1987*).* Water balance in developing eggs of the cod *Gadus morhua* L*. Fish Physiol. Biochem.* **3** (17–24).

May, R.C. (1971). Effects of delayed initial feeding on larvae of grunion *Leuresthes tenuis* (Ayres). *Fish. Bull. U.S.* **69** (411–425).

May R.C. (1974) Effects of temperature and salinity on yolk utilisation on *Bairdiella icistia* (Jordan and Gilbert) (Pisces: Sciaenidae). *J. Exp. Mar. Biol. Ecol*. **16** (213-225).

Meriwether, F.H., Scura, E.D. and Okamura, W.Y. (1984). Cage culture of red tilapia in prawn and shrimp ponds. *J. World Mariculture Society* **15** (254-265).

Miyazaki, H., Kaneko, T., Hasegawa, S. and T. Hirano. (1998). Developmental changes in drinking rate and ion and water permeability during early life stages of euryhaline tilapia, *Oreochromis mossambicus*, reared in fresh water and seawater. *Fish Physiol. Biochem.* **18** (277-284).

Morgan, J.D. and Iwama, G.K. (1991). Effects of salinity on growth, metabolism and ion regulation in juvelnile rainbow and steelhead trout (*Onchorhynchus mykiss*) and fall Chinook salmon (*Onchorhynchus tshawytscha*). *Can. J. Fish. Aquat. Sci*. **48** (2083-2084).

Morgan J.D., Jensen, J.O. and Iwama, G.K. (1992). Effects of salinity on aerobic metabolism and development of eggs and alevins of steelhead trout (*Oncorhynchus mykiss*) and fall Chinook salmon (*Oncorhynchus tshawytscha).* *Can. J. Zool*. **70** (1341-1346).

Motais, R. and Garcia-Romeu, F. (1972). Transport mechanisms in the teleostean gill and amphibian skin. *Annu. Rev. Physiol.* **34** (141–176).

Musch, M.W., Orellana, S.A., Kimberg, L.S., Fiel, M., Halm, D.R., Kransky, E.J. and Fritzzel, R.A. (1982). Na–K–Cl cotransport in the intestine of a marine teleost. *Nature* **300** (351– 354).

Nagashima, K. and Ando, M. (1993). Characterization of esophageal desalination in the seawater eel *Anguilla japonica*. *J. Comp. Physiol. Part B* **164** (47– 54).

Nebel, C., Negre-Sadargues, G. and Charmantier, G. (2005). Morphofuntional ontogeny of the excretory system of the European sea-bass *Dicentrarchus labrax*. *Anat. Embryol*. **209** (193-206).

Nelson, N. and Harvey, W. R. (1999). Vacuolar and plasma membrane V-ATPases. *Physiol. Rev.* **79** (361 -385).

Nishimura, H. and Imai, M. (1982). Control of renal function in freshwater and marine teleosts. *Fed. Proc*. **41** (2355–2360).

Nishimura, H. and Fan, Z. (2003). Regulation of water movement across vertebrate renal tubules. *Comp. Biochem. Physiol. Part A* **136** (479– 484).

O'Connell, C.P. (1981). Development of organ systems in the northern anchovy *Engraulis mordax* and other teleosts. *Am. Zool*. **21** (429– 446).

Okamoto, T., Kurokawa, T., Gen, K., Murashita, K., Nomura, K., Shibahara, H., Kim, S.K.,Matsubara, H., Ohta, H. and Tanaka, H. (2009). Influence of salinity on morphological deformities in cultured larvae of Japanese eel, *Anguilla japonica*, at completion of yolk resorption. *Aquaculture* **293** (113−118).

Olson, K.R. (1996). Scanning electron microscopy of the fish gill. In: *Fish Morphology: horizons of new research* (H.M.Dutta and J.S.D. Mushi, eds.), pp.31–45. Science Publishers, Lebanon.

Olson, K.R. (2000). Respiratory system. Gross functional anatomy. In: *The Laboratory Fish* (G. K. Ostrander, ed.), pp.151–159. Academic Press, London.

Onken, H., Tresguerres, M. and. Luquet, C.M. (2003). Active NaCl absorption across posterior gills of hyperosmoregulating *Chasmagnathus granulatus*, *J. Exp. Biol.* **206** (1017–1023).

Østby, G.C., Finn, R.N., Norberg, B. and Fyhn, H.J. (1999). Osmotic aspects of final oocyte maturation in Atlantic halibut. In: *Proc. 6th Int. Symp. Reprod. Physiol. Fish.*, (B. Norberg, O.S. Kjesbu, G.L. Taranger, E. Anderson, and S.O. Stefansson, eds.). pp 289-291. Inst. Mar. Res. Univ., Bergen.

Otto, R.G. (1971). Effects of salinity on the survival and growth of pre-smolt coho salmon (*Oncorhynchus kisutch*). *J. Fish. Res. Board Can.* **28** (343–349).

Ouattara, N.G., Bodinier, C., Nègre-Sadargues, G., D'Cotta, H., Messad, S., Charmantier, G., Panfili, J. and Baroiller, J.F. (2009). Changes in gill ionocyte morphology and function following transfer from fresh water to hypersaline waters in the tilapia *Sarotherodon melanotheron*. *Aquaculture* **290** (155–164).

Ozoh, P.T.E. (1979). Malformations and inhibitory tendencies induced to *Brachydanio rerio* (Hamilton-Buchanan) eggs and larvae due to exposures in low concentration of lead and copper ions. *Bull. Environm. Contam. Toxicol.* **21** (668-675).

Parmalee, J.T. and Renfro, J.L. (1983). Esophageal desalinization of seawater in flounder. Role of active sodium transport. *Am. J. Physiol.* **245** (888–893).

Parry, G. (1966). Osmotic adaptation in fishes. *Biol. Rev.* **41** (392-444).

Payne, A.I. and Collinson, R.I. (1983). A comparison of the biological characteristics of *Sarotherodon niloticus* (L.) with those of *S. aureus* (Steindachner) and other tilapia of the delta and lower Nile. *Aquaculture* **30** (335-351).

Pelis, R.M. and McCormick, S.D. (2001). Effects of growth hormone and cortisol on Na$^+$-K$^+$-2Cl$^-$ cotransporter localization and abundance in the gills of Atlantic salmon. *Gen. Comp. Endocrinol.* **124** (134–143).

Perry, S. F. (1997). The chloride cell: structure and function in the gills of freshwater fishes. *Annu. Rev. Physiol.* **59** (325 -347).

Perry, W.G. and Avault, J.W. (1972). Comparisons of striped mullet and tilapia for added production in caged catfish studies. *Prog. Fish-Cult.* **34** (229–232).

Perry, S. F. and Laurent, P. (1989). Adaptational responses of rainbow trout to lowered external NaCl concentration: Contribution of the branchial chloride cell. *J. Exp. Biol.* **147** (147–168).

Perry, S. F. and Laurent, P. (1993). Environmental effects on fish gill structure and function. In: *Fish Ecophysiology.* (J.C. Rankin, and F.B. Jensen, eds.), pp. 231–264. Chapman and Hall, London.

Perry, S.F. and McDonald, G. (1993). In : *The Physiology of Fishes*. (D.H. Evans, ed.), pp. 251-278). CRC, Boca Raton, USA.

Perry, S.F., Goss, G.G. and Laurent, P. (1992). The interrelationships between gill chloride cell morphology and ionic uptake in four freshwater teleosts. *Can. J. Zool.* **70** (1775–1786).

Perschbacher, P.W. (1992). A review of seawater acclimation procedures for commercially important euryhaline tilapias. *Asian Fisheries Science* **5** (241-248).

Peterson, R.H. and Martin-Robichaud D.J. (1983). Embryo movements of Atlantic salmon (*Salmo salar*) as influenced by pH, temperature and stage of development. *Can. J. Fish. Aquat. Sci*. **40** (777-782).

Pfeiler, E. (1984). Effect of salinity on water and salt balance in metamorphosing bonefish (*Albula*) leptocephali. *J. Exp. Mar. Biol. Ecol.* **82** (183-190).

Philippart J.C. and Ruwet J.C. (1982). Ecology and distribution of tilapias. In: *The biology and culture of tilapias.* (R.S.V. Pullin and R.H. Lowe-McConnell, eds.), pp. 15-59. ICLARM, Manila, Philippines.

Phillips, T.A. and Summerfelt, R.C. (1999). Gill development of larval walleyes. *Am. Fish. Soc.* **128** (162– 168).

Philpott, C. W. (1966). The use of horseradish peroxidase to demonstrate functional continuity between the plasmalemma and the unique tubular system of the chloride cell. *J. Cell Biol.* **31** (86-91).

Philpott, C.W. (1980). Tubular system membranes of teleost chloride cells: osmotic response and transport sites. *Am. J. Physiol.* **238** (171-184).

Pickford, G.E., Pang, P.K.T., Weinstein, E., Torretti, J., Hendler, E. and Epstein, F.H. (1970). The response of the hypophysectomized cyprinodont, *Fundulus heteroclitus*, to replacement therapy with cortisol: Effects on blood serum and sodium-potassium activated adenosine triphosphatase in the gills, kidney, and intestinal mucosa. *Gen. Comp. Endocrinol*. **14** (524-434).

Piermarini, P.M. and Evans, D.H. (2000). Effects of environmental salinity on Na^+/K^+-ATPase in the gills and rectal gland of the euryhaline elasmobranch (*Dasyatis sabina*). *J. Exp.Biol.* **203** (2957-2966).

Pisam, M. (1981). Membranous systems in the chloride cell of teleostean fish gills, their modifications in response to the salinity of the environment. *Anat. Rec.* **200** (401–414).

Pisam, M. and Rambourg, A. (1991). Mitochondria-rich cells in the gill epithelium of teleost fishes: an ultrastructural approach. *Int. Rev. Cyt*.**130** (191– 232).

Pisam M., Caroff, A. and Rambourg, A. (1987). Two types of chloride cells in the gill epithelium of a freshwater-adapted euryhaline fish: *Lebistes reticulatus*; their modifications during adaptation to saltwater. *Am. J. Anat*. **179** (40–50).

Pisam, M., Prunet, P. and Rambourg, A. (1989). Accessory cells in the gill epithelium of the freshwater rainbow trout *Salmo gairdneri. Am. J. Anat*. **184** (311-320).

Pisam, M., Boeuf, G., Prunet, P. and Rambourg, A. (1990). Ultrastructural features of mitochondria-rich cells in stenohaline freshwater and seawater fishes. *Am. J. Anat*. **187** (21–31).

Pisam, M., Auperin, B., Prunet, P., Rentier-Delrue, F., Martial, J. and Rambourg, A. (1993). Effects of prolactin on alpha and beta chloride cells in the gill epithelium of the saltwater adapted tilapia *Oreochromis niloticus. Anat. Rec*. **235** (275–284).

Pisam, M. Aurperin, C., Prunet, P., and Rambourg, A. (1995). Apical structures of mitochondria-rich alpha and beta cells in euryhaline fish gill. *Anat. Rec*. **241** (13–24).

Plasier, B., Lloyd, D.R., Paul, G.C., Thomas, C.R. and Al-Rubeai M. (1999). Automatic image analysis for quantification of apoptosis in animal cell culture by annexin-V affinity assay. *J. Immunol. Methods* **229** (81-95).

Popper, D. and Lichatowich, T. (1975). Some practical methods for harvesting fish ponds and handling live fish. *Aquaculture* **6** (395–398).

Prager, D. J., and Bowman, R. L. (1963). Freezing-Point Depression: New Method for Measuring Ultramicro Quantities of Fluids. *Science* **142**, (237).

Prunet, P. and Bornancin, M. (1989). Physiology of salinity tolerance in tilapia: an uptake on basic and applied aspects. *Aquatic Living Resources* **2** (91-97).

Pullin, R.S.V. and Lowe-McConnell, R.H. (1982). The Biology and Culture ofTilapias. ICLARM Conference Proceeding 7. 423p.

Pullin, R.S.V., Palomares, M.L., Casal, C.V., Dey, M.M. and Pauly, D.. (1997). Environmental impacts of tilapias. In: *Tilapia aquaculture. Proceedings from the Fourth International Symposium on Tilapia in Aquaculture, Volume 2.* (K. Fitzsimmons, ed.), pp. 554-570. Northeast Regional Agriculture Engineering Service (NRAES) Cooperative Extension, Ithaca, New York.

Rahim, S. M., Delaunoy, J. P. and Laurent, P. (1988). Identification and immunocytochemical localization of two different carbonic anhydrase isoenzymes in teleostean fish erythrocytes and gill epithelia. *Histochemistry* **89** (451-459).

Rambourg, A., Clermont, Y. and Chretien, M. (1989). Tridimensional analysis of the formation of secretory vesicles in the Golgi apparatus of absorptive columnar cells of the mouse colon. *Biol. Cell*. **65** (247–256).

Rana, K.J. (1985). Influence of egg size on the growth, onset of feeding, point-of-no-return and survival of unfed *Oreochromis mossambicus* fry. *Aquaculture* **46** (119-131).

Rana, K.J. (1986). An evaluation of two types of containers for the artificial incubation of *Oreochromis* eggs. *Aquaculture and Fisheries Management* **17** (139-145).

Rana, K.J. (1988). Reproductive biology and the hatchery rearing of tilapia eggs and fry. In: *Recent Advances in Aquaculture, vol. 3.* (J.F. Muir and R.J. Roberts, eds.), pp. 343-406. Croom Helm, London, UK.

Randall, D.J. and Daxboeck, C. (1984). Oxygen and carbon dioxide transfer across fish gills. In: *Fish Physiology*, (W. S. Hoar and D. J. Randall, eds.), pp. 263-314. Academic Press, New York.

Rao, G. (1968). Oxygen consumption of rainbow trout in relation to activity and salinity. *Can. J. Zool.* **46 (**781-786).

Reid, S. D., Hawkings, G. S., Galvez, F. and Goss, G. G**.** (2003). Localization and characterization of phenamil-sensitive Na^+ influx inisolated rainbow trout gill epithelial cells. *J. Exp. Biol.* **206** (551-559).

Reitan, K.I., Rainuzzo, J.R., Øie, G. and Olsen, Y. (1993). Nutritional effects of algal addition in first-feeding of turbot (*Scophthalmus maximus* L.) larvae. *Aquaculture* **118** (257–275).

Rengmark, A.H., Slettan, A., Lee, W.J. Lie, O. and Lingaas, F. (2007). Identification and mapping of genes associated with salt tolerance in tilapia. *J. Fish Biol.* **71** (409-422).

Reynolds, E.S. (1963). The use of lead citrate at high pH as electron-opaque stain in electron microscopy. *J. Cell.* **17** (208-212).

Richman III, N.H. and Zaugg, W.S. (1987). Effects of cortisol and growth hormone on osmoregulation in pre- and de-smoltified Coho salmon (*Oncorhynchus kisutch). Gen. Comp. Endocrinol.* **65** (189-198).

Ridha M.T. (2006). Evaluation of growth performance of non improved and improved strains of the Nile tilapia *Oreochromis niloticus* (L.). *J. World Aquaculture Society* **37**(218-223).

Riegel, J.A. (1998). Analysis of fluid dynamics in perfused glomeruli of the hagfish *Eptatretus stouti* (Lockington). *J. Exp. Biol.* **201** (3097–3104).

Riestenpatt, S.*,* Onken, H. and Siebers, D. (1996)*.* Active absorption of Na^+ and Cl^- across the gill epithelium of the shore crab *Carcinus maenas*: Voltage-clamp and ion-flux studies. *J. Exp. Biol.* **199** (1545-1554*).*

Riis-Vestergaard, J. (1982).Water and salt balance of halibut eggs and larvae (*Hippoglossus hippoglossus*). *Mar. Biol.* **70** (135-139).

Roberts, R., Bell, M., and Young, H., (1973). Studies of the skin of plaice (*Pleuronectes platessa* L.): II. The development of larval plaice skin. *J. Fish Biol.* **5** (103–108).

Robinson, J.M. and Vandré, D.D. (1997). Efficient immunocytochemical labeling of leukocyte microtubules with FluoroNanogold: an important tool for correlative microscopy. *J. Histochem. Cytochem.* **45** (631–642).

Rojo, C. and González, E. (1999). Ontogeny and apoptosis of chloride cells in the gill epithelium of newly hatched rainbow trout. *Acta Zoologica* **80** (11–23).

Rojo, M.C., Blanquez, M.J. and Gonzalez, M.E. (1997). Ultrastructural evidence for apoptosis of pavement cells, chloride cells and hatching gland cells in the developing branchial area of the trout *Salmo trutta*. *J. Zool.* **243** (637-651).

Romana-Eguia, M.R.R. and Eguia, R.V. (1999). Growth of 5 Asian red tilapia strains in saline environments. *Aquaculture* **108** (1-12).

Romano, E.L., Stolinski, C. and Hughes-Jones, N.C. (1974). An antiglobulin reagent labeled with colloidal gold for use in electron microscopy. *Immunochemistry* **11** (521-525).

Romano, E.L. and Romano, M. (1977). Staphylococcal protein A bound to colloidal gold: a useful reagent to label antigen-antibody sites in electron microscopy. *Immunochemistry* **14** (711-713).

Rombough, P.J. (1999). The gill of fish larvae. Is it primarily a respiratory organ or an ionoregulatory structure? *J. Fish Biol.* **55** (186–204).

Rombough P. J. (2004). Gas exchange, ionoregulation and the functional development of the teleost gill. *Am. Fish. Soc. Symp.* **40** (47–83).

Ron, B. Shimoda, S.K., Iwama, G.K. and Grau, E.G. (1995). Relationships among ration, salinity, 17 α-methyltestosterone and growth in the euryhaline tilapia, *Oreochromis mossambicus*. *Aquaculture* **135** (185-193).

Rose, K.A., Cowan, J.H., Houde, E.D. and Coutant, C.C. (1993). Individual based modelling of environmental quality effects on early life stages of fishes: A case study using striped bass. *American Fisheries Society Symposium*. **14** (125-145).

Roth, J. and Binder, M. (1978). Colloidal gold, ferritin and peroxidase for electron microscopic double labeling lectin technique. *J. Histochem. Cytochem.* **26** (163-169).

Sardella, B., Matey, V., Cooper, J., Gonzalez, R. and Brauner, C. (2004). Physiological, biochemical and morphological indicators of osmoregulatory stress in 'California' Mozambique tilapia (*Oreochromis mossambicus* × *O. urolepis hornorum*) exposed to hyper saline water. *J. Exp. Biol.* **207** (1399–1413).

Sardet, C., Pisam, M. and Maetz, J. (1979). The surface epithelium of teleostean fish gills. Cellular and junctional adaptations of the chloride cell in relation to salt adaptation. *J. Cell Biol.* **80** (96 -117).

Sasai, S., Kaneko, T., Hasegawa, S. and Tsukamoto, K. (1998). Morphological alteration in two types of gill chloride cells in Japanese eel (*Anguilla japonica*) during catadromous migration. *Can. J. Zool.* **76** (1480–1487).

Satchell, G. H. (1991). *Physiology and Form of Fish Circulation*. Cambridge University Press, Cambridge, UK.

Scheiner-Bobis, G. (2002), The sodium pump. *European J. Biochem.* **269** (2424–2433).

Schofield, P.J., Todd Slack, W. Peterson, M.S. and Gregoire, D.R. (2007). Assessment and control of an invasive aquaculture species: an update on Nile tilapia in Coastal Mississippi after Hurricane Katrina. *Southeastern Fishes Council Proceedings* **49** (9-15).

Schreiber, A.M. (2001). Metamorphosis and early larval development of theflatfishes (Pleuronectiformes): an osmoregulatory perspective. *Comp. Physiol. Part B* **129** (587– 595).

Schreiber, A.M. and Specker, J.L. (1998). Metamorphosis in the summer flounder (*Paralichthys dentatus*): influence of stage-specific thyroidal status on larval development and growth. *Gen. Comp. Endocrinol.* **111** (156–166).

Scott, G.R., Rogers, J.T., Richards, J.G., Wood, C.A. and Schulte, P.M. (2004). Intraspecific divergence of ionoregulatory physiology in the euryhaline teleost *Fundulus heteroclitus*: possible mechanisms of freshwater adaptation. *J. Exp. Biol.* **207** (3399–3410).

Segner, H., Storch, V., Reinecke, M. and Kloas, W. (1994). The development of functional digestive and metabolic organs in turbot (*Scophthalmus maximus*). *Mar. Biol.* **11** (471– 486).

Shanklin, D.R. (1959). Studies on the *Fundulus* chorion. *J. Cell. Comp. Physiol*. **43** (1-11).

Shelbourne, J.E. (1957). Site of chloride regulation in marine fish larvae. *Nature* **180** (920–922).

Shelton, W.L. (2002). Tilapia culture in the 21st century. In: *Proceedings of the International Forum on Tilapia farming in the 21st Century*. (Guerrero, R.D. III and M.R. Guerrero-del Castillo, eds.), pp. 1-20. Philippine Fisheries Association Inc., Los, Banos, Laguna, Philippines.

Shelton, W.L. and Popma, T. J. (2006). In: *Tilapia: biology culture and nutrition.* (C. Lim and C.D. Webster, eds.), pp. 1-27. Haworth Press, London.

Shelton, W.L., Hopkins, K.D. and Jensen, G.L. (1978). Use of hormones to produce monosex tilapia. In: *Culture of Exotic Fishes Symposium Proceedings. Fish Culture Section,* (R.O. Smitherman, W. L. Shelton and J. L. Grover, eds.), pp. 10–33. American Fisheries Society, Auburn, USA.

Shi Z., Huang, X., Fu, R., Wang, H. Luo H., Chen, B. Liu M. and Zhang, D. (2008). Salinity stress on embryos and early larval stages of the pomfret *Pampus punctatissimus. Aquaculture* **275** (306-310).

Shieh, Y.E. Tsai, R.S. and Hwang, P.P. (2003). Morphological Modification of Mitochondria-Rich Cells of the Opercular Epithelium of Freshwater Tilapia, *Oreochromis mossambicus*, Acclimated to Low Chloride Levels. *Zool. Studies* **42** (522-528).

Shikano, T. and Fujio, Y. (1998 a). Immunolocalisation of Na$^+$/K$^+$-ATPase and morphological changes in two types of chloride cells in the gill epithelium during seawater and freshwater adaptation in a euryhaline teleost, *Poecilia reticulata. J. Exp. Zool.* **281** (80-89).

Shikano, T. and Fujio,Y. (1998 b). Relationships of salinity tolerance to immunolocalisation of Na$^+$/K$^+$-ATPase in the gill epithelium during seawater and freshwater adaptation of the guppy, *Poecilia reticulata*. *Zool. Sci*. **15** (35–41).

Shiraishi, K., Kaneko, T., Hasegawa, S. and Hirano, T. (1997). Development of multicellular complexes of chloride cells in the yolk-sac membrane of Tilapia (*Oreochromis mossambicus*) embryos and larvae in seawater. *Cell Tissue Res*. **288** (583–590).

Shirai, N. and Utida, S. (1970). Development and degenerative of the chloride cell during sea water and fresh water adaptation of the Japanese eel (*Anguilla japonica*). *Zeit. Zellforsch. Microsk. Anat*. **103** (247-264).

Silva, P., Solomon, R., Spokes, K. and Epstein, F. (1977). Ouabain inhibition of gill Na-K-ATPase: relationship to active chloride transport. *J. Exp. Zool*. **199** (419-426).

Singer, S. J. (1959). Preparation of an electron-dense antibody conjugate. *Nature* **183** (1523-1533).

Singer, T.D., Clements, K.M., Semple, J.W., Schulte, P.M., Bystriansky, J.S., Finstad, B., Fleming, I.A. and McKinley, R.S. (2002). Seawater tolerance and gene expression in two strains of Atlantic salmon smolts. *Can. J. Fish. Aquat. Sci*. **59** (125-135).

Skadhauge, E. (1969). The mechanism of salt and water absorption in the intestine of the eel (*Anguilla anguilla*) adapted to waters of various salinities. *J. Physiol*. **204** (135–158).

Smit, L., Du Preez, H.H. and Steyn, G.J. (1998). Influence of natural silt on the survival of *Oreochromis mossambicus* yolk-sac larvae. *Koedoe* **41** (57-62).

Smith, H. W. (1932). Water regulation and its evolution in the fishes. *Q. Rev. Biol*. **7** (1-26).

Sower, S.A. and Schreck, C.B. (1982). Steroid and thyroid hormones during sexual maturation of coho salmon (*Oncorhynchus kisutch*) in seawater or fresh water. *Gen. Comp. Endo*. **47** (42-53).

Specker, J.L., Schreiber, A.M., McArdle, M.E., Poholek, A.J., Henderson, J. and Bengtson, D.A. (1999). Metamorphosis in summer flounder: Effects of acclimation to low and high salinities. *Aquaculture* **176** (145-154).

Staggs, M.D. and Otis, K.J. (1996). Factors affecting first-year growth of fishes in Lake Winnebago, Wisconsin. *North American Journal of Fisheries Management* **16** (608-618).

Stickney, R.R. (1986). Tilapia tolerance in saline water: a review. *The Progressive Fish-Culturalist* **48** (161- 167).

Straus, L.P. and Doyle, W.L. (1961) Fine structure of the so called chloride cells of the gills of the guppy. *Amer. Zool*. **1** (392-401).

Subasinghe, R.P. and Sommerville, C. (1988). Possible cause of mortality of *Oreochromis mossambicus* eggs under artificial incubation. In: *Proceedings of the First Asian Fisheries Forum*, Manila, Philippines, pp. 337-340.

Sullivan, G.V., Fryer, J.N. and Perry, S.F. (1995). Immunolocalisation of proton pumps (H$^+$-ATPase) in pavement cells of rainbow trout gill. *J. Exp. Biol.* **198** (2619-2629).

Suresh A.V. and Lin C.K. (1992 a). Tilapia culture in saline water: a review. *Aquaculture* **106** (201-226).

Suresh A.V. and Lin C.K. (1992 b). Effect of stocking density on water quality and production of red tilapia in a recirculated system. *Aquaculture Engineering* **11** (1-22).

Swanson, C. (1996). Early development of milkfish: effects of salinity on embryonic and larval metabolism, yolk absorption and growth. *J. Fish Biol*. **48** (405-421).

Swanson, C. (1998). Interactive effects of salinity on metabolic rate, activity, growth and osmoregulation in the euryhaline milkfish (*Chanos chanos*) *J. Exp. Biol*. **201** (3355-3366).

Takahashi, K., Hatta, N., Sugawara, Y. and Sato, R. (1978). Organogenesis and functional revelation of alimentary tract and kidney of chum salmon. *Tohoku J. Agric. Res.* **29** (98– 109).

Takeyasu, K., Tamkun, M.M., Renaud, K.J. and Fambrough, D.M. (1988). Ouabain-sensitive (Na$^+$ / K$^+$)-ATPase activity expressed in mouse L cells by transfection with DNA encoding the α-subunit of an avian sodium pump. *J. Biol. Chem.* **263** (4347-4354).

Takizawa, T. and Robinson, J.M. (1994). Use of 1.4-nm immunogold particles for immunocytochemistry on ultra-thin cryosections. *J. Histochem. Cytochem.* **421** (615–1623).

Taylor, C. R., and Burns, J. (1974). The demonstration of plasma cells and other immunoglobulin-containing cells in formalin-fixed paraffin embedded tissues using peroxidase-labelled antibody. *J. Clin. Path.* **27** (14-20).

Taylor, C. R., and Mason, D. Y. (1974). The immunohistological detection of intracellular immunoglobulin in formalin-paraffin sections from multiple myeloma and related conditions usingthe immunoperoxidase technique. *Clin. Exp. Immunol*. **18** (417- 429).

Threadgold, L.T. and Houston, A.H. (1961). An electron study of the 'Chloride Secretory Cell' of *Salmo salar* L. with reference to plasma-electrolyte regulation. *Nature* **190** (612-614.).

Tipsmark, C.K., Madsen, S.S., Seidelin, M., Christensen, A.S., Cutler,C.P. and Cramb, G. (2002). Dynamics of Na$^+$/K$^+$/2Cl$^-$ cotransporter and Na$^+$/K$^+$-ATPase expression in the branchial epithelium of brown trout (*Salmo trutta*) and Atlantic salmon (*Salmo salar*). *J. Exp. Zool.* **293** (106-118).

Threadgold, L.T. and Houston, A.H. (1964). An electron microscope study of the chloride cell of *Salmo salar. Exp. Cell Res*. **34** (1-23).

Tresguerres, M., Katoh, F., Fenton, H., Jasinska, E. and Goss, G.G. (2005). Regulation of branchial V-H$^+$-ATPase, Na$^+$/K$^+$-ATPase and NHE$_2$ in response to acid and base infusions in the Pacific spiny dogfish (*Squalus acanthias*). *J. Exp. Biol*. **208** (345–354).

Tresguerres, M., Katoh, F., Orr, E., Parks, S.K. and Goss, G.G. (2006). Chloride uptake and base secretion in freshwater fish: a transepithelial ion-transport metabolon? *Physiol. Biochem. Zool*. **79** (981–996).

Trewavas, E. (1982). Generic groupings of Tilapiini used in aquaculture. *Aquaculture* **27** (79–81).

Trewavas, E. (1983). Tilapinne Fishes of the Genera *Sarotherodon*, *Oreochromis* and *Danakilia. London : British Museum (Natural History*) pp. 583.

Tsuzuki, M.Y., Strussmann, C.A. and Takashima, F. (2008). Effect of salinity on the oxygen consumption of larvae of the Silversides *Odontesthes hatcheri* and *O. bonariensis* (Osteichthyes, Atherinopsidae). *Brazilian archives of Biology and Technology* **51** (563-567).

Tytler, P. and Blaxter, J.H.S. (1988). The effects of external salinity on the drinking rates of the larvae of herring, plaice and cod. *J. Exp. Biol*. **138** (1 –15).

Tytler, P. and Ireland, J. (1995). The influence of temperature and salinity on the structure and function of mitochondria in chloride cells in the skin of the larvae of the turbot (*Scophthalmus maximus*). *Journal of Thermal Biology* **20** (1–14).

Tytler, P., Bell, M. V. and Robinson, J. (1993). The ontogeny of osmoregulation in marine fish: effects of changes in salinity and temperature. In. *Physiological and Biochemical Aspects of Fish Development,* (B.T. Walther and H.J. Fyhn, eds.), pp. 249– 258. University of Bergen, Norway.

Tytler, P., Ireland, J. and Fitches, E. (1996). A study of the structure and function of the pronephros in the larvae of the turbot (*Scophthalmus maximus*) and the herring (*Clupea harengus*). *Mar. Freshwater Behav. Physiol*. **28** (3 – 18).

Uchida, N. and King, J.E. (1962). Tank culture of tilapia. *U.S. Fish. Wildl. Serv., Fish Bull*. **62** (21–52.)

Uchida, K., Kaneko, T., Yamauchi, K. and Hirano, T. (1996). Morphometrical analysis of chloride cell activity in the gill filaments and lamellae and changes in Na$^+$/K$^+$-ATPase activity during seawater adaptation in chum salmon fry. *J. Exp. Zool*. **276** (193-201).

Uchida, K., Kaneko, T., Miyazaki, H., Hasegawa, H. and Hirano, T. (2000). Excellent salinity tolerance of Mozambique tilapia (*Oreochromis mossambicus*): elevated chloride cell activity in the branchial and opercular epithelia of the fish adapted to concentrated seawater. *Zool. Sci*. **17** (149–160).

Unuma, T., Kondo, S., Tanaka, H., Kagawa, K., Nomura, K. and Ohta, H. (2005). Relationship between egg specific gravity and egg quality in the Japanese eel, *Anguilla japonica. Aquaculture* **246** (493–500).

van der Heijden, A.J.H., Verbost, P.M. Eygensteyn, J., Li, J., Wendelaar Bonga, S.E. and Flik, G. (1997). Mitochondria-rich cells in gills of tilapia (*Oreochromis*

mossambicus) adapted to fresh water or sea water: quantification by confocal scanning laser microscopy. *J. Exp. Biol*. **200** (55-64).

van der Heijden, A.J.H., van der Meij, J.C.A., Flik, G. and Bonga, S.E.W. (1999). Ultrastructure and distribution dynamics of chloride cells in tilapia larvae in fresh water and sea water. *Cell Tiss. Res.* **297** (119–130).

Varsamos, S., Connes, R., Diaz, J.P., Barnabé, G. and Charmantier, G. (2001). Ontogeny of osmoregulation in the European sea bass *Dicentrarchus labrax* L. *Mar. Biol*. **138** (909–915).

Varsamos, S., Diaz, J.P., Charmantier, G., Blasco, C., Connes, R. & Flik, G. (2002 a). Location and morphology of chloride cells during the post-embryonic development of the European sea bass, *Dicentrarchus labrax. Anat. Embryol.* **205** (203–213).

Varsamos, S., Diaz, J.P., Charmantier, G., Flik, G., Blasco, C. and Connes, R. (2002 b). Branchial chloride cells in sea bass (*Dicentrarchus labrax*) adapted to freshwater, seawater and doubly-concentrated seawater. *J. Exp. Zool.* **293** (12-26).

Varsamos, S., Nebel, C. and Charmantier, G. (2005). Ontogeny of osmoregulation in postembryonic fish: A review. *Comp. Biochem. Physiol. Part A* **141** (401-429).

Venturini, G., Cataldi, E., Marino, G., Pucci, P., Garibaldi, L., Bronzi, P. and Cataudella, S. (1992). Serum ions concentration and ATPase activity in gills, kidney and oesophagus of European sea bass (*Dicentrarchus labrax*, Pisces, Perciformes) during acclimation trials to fresh water. *Comp. Biochem. Physiol. Part A.* **103** (451– 454).

Vigliano F. A, Aleman N, Quiroga M. I, and Nieto J. M, (2006) Ultrastructural Characterization of gills in Juveniles of the Argentinian Silverside. *Anat. Histol. Embryol.* **35** (76–83).

Villalobos S.A. (1996). Developmental toxicity studies in embryos of the teleost medaka (*Oryzias latipes*) exposed to selected environmental contaminants. PhD thesis. University of Californian, Davis, CA, USA.

Villegas, C.T. (1990). Growth and survival of *Oreochromis niloticus, O. mossambicus* and their F$_1$ hybrids at various salinities. In: *The second Asian Fisheries Forum* (R. Hirano and I. Hanya, eds.), pp. 507-510. Asian Fisheries Society, Manila, Philippines.

Vine, P.J. (1980). Cultivation of fishes of the family Cichlidae in the Red Sea. In: *Proceedings of Symposium on the Coastal and Marine Environment of the Red Sea, Gulf of Aden and Tropical Western Indian Ocean. Vol. 2.*, pp. 389-399. The Red Sea and Gulf of Aden Environmental Programme, Khartoum, Sudan.

von Westernhagen, H., Dethlefsen, V., Cameron, P., Berg, J. and Fürstenberg, G. (1988) Developmental defects in pelagic fish embryos from the western Baltic. *Helgoländer Meeresunters*. **42** (13-36).

Vize, P.D., Seufert, D.W., Carroll, T.J. and Wallingford, J.B. (1997). Model systems for the study of kidney development: use of the pronephros in the analysis of organ induction and patterning. *Dev. Biol*. **188** (189– 204).

Wales, B. (1997). Ultrastructural study of chloride cells in the trunk epithelium of larval herring, *Clupea harengus*. *Tissue and Cell* **29** (439–447).

Walsh, W.A. and Lund Jr., W.A. (1989). Oxygen consumption by eggs of the grubby, *Myoxocephalus aenaeus*, and the longhorn sculpin, *Myoxocephalus octodecemspinosus*. *Can. J. Zool.* **67** (1613-1619).

Wales, B. and Tytler, P. (1996). Changes in chloride cell distribution during early larval stages of *Clupea harengus*. *J. Fish Biol.* **49** (801– 814).

Walsh W.A., Swanson, C. and Lee C.S. (1991 a). Combined effects of temperature and salinity on embryonic development and hatching of striped mullet, *Mugil cephalus*. *Aquaculture* **97** (281-289).

Walsh, W. A., Swanson, C. and Lee, C.S. (1991 b). Effects of development, temperature,and salinity on metabolism in eggs and yolk-sac larvae of milkfish, *Chanos chanos* (Forskål). *J. Fish Biol.* **39 (**115–125).

Wang, J., Liu, L., Zhang, Q. B., Zhang, Z. S., Qi, H. M., and Li, P. C. (2009). Synthesized over-sulphated, acetylated and benzoylated derivatives of fucoidan extracted from *Laminaria japonica* and their potential antioxidant activity *in vitro*. *Food Chem.* **114** (1285-1290).

Wang, P-J., Lin, C-H., Hwang, L-Y., Tsung, H-L . and Hwang, P-P. (2009). Differential responses in gills of euryhaline tilapia *Oreochromis mossambicus* to various hyperosmotic shocks. *Comp. Biochem. Physiol. Part A.* **152** (544-551).

Watanabe, S., Kaneko, T. and Watanabe, Y. (1999). Immunocytochemical detection of mitochondria-rich cells in the brood pouch epithelium of the pipefish, *Syngnathus schlegeli*: structural comparison with mitochondria-rich cells in the gills and larval epidermis. *Cell Tissue Res*. **295** (141– 149).

Watanabe, S., Kaneko, T. and Aida, K. (2005). Aquaporin-3 expressed in the basolateral membrane of gill chloride cells in Mozambique tilapia *Oreochromis mossambicus* adapted to freshwater and seawater. *J. Exp.Biol*. **208** (2673–2682).

Watanabe, W.O. (1991). Saltwater culture of tilapia in the Caribbean. *World Aquaculture* **22** (49-54).

Watanabe W.O. and Kuo C.M. (1985). Observations on the reproductive performance of Nile tilapia (*Oreochromis niloticus*) in laboratory aquaria at various salinities. *Aquaculture* **49** (315-323).

Watanabe, W.O., Kuo, C-M. and M-C. Huang, M-C. (1984). Experimental rearing of Nile tilapia fry (*Oreochromis niloticus*) for saltwater culture. In: *ICLARM Tech. Rep. 14*, p. 28. International Center for Living Aquatic Resources Management, Manila, Philippines.

Watanabe W.O., Kuo, C.M. and Huang, M.C. (1985 a). The ontogeny of salinity tolerance in the tilapias *Oreochromis aureus*, *O. niloticus* and an *O. mossambicus* x *O. niloticus* hybrid, spawned and reared in freshwater. *Aquaculture* **47** (353-367).

Watanabe W.O., Kuo, C.M. and Huang, M.C. (1985 b). Salinity tolerance of Nile tilapia fry (*Oreochromis niloticus*) spawned and hatched at various salinities. *Aquaculture* **48** (159-176).

Watanabe, W.O., Ellingson, L.J., Wicklund, R.I. and Olla, B.L. (1988). The effects of salinity on growth, food consumption and conversion in juvenile monosex male Florida red tilapia. In: *The Second International Symposium on Tilapia in Aquaculture, ICLARM Conference Proceedings 15 (*R.S.V. Pullin, T. Bhukaswan, K. Tonguthai and J.L. Maclean eds.), pp. 515–523. ICLARM, Manila, Philippines.

Watanabe, W.O., Burnett, K.M., Olla, B.L. and Wicklund, R.I. (1989 a). The effects of salinity on reproductive performance of Florida red tilapia. *J. World Aquacult. Soc.* **20** (223–229).

Watanabe, W.O., French, K.E., Ernst, D.H., Olla, B.L. and Wicklund, R.I. (1989 b). Salinity during early development influences growth and survival of Florida red tilapia in brackish and seawater. *J. World Aquacult. Soc.* **20** (134–142).

Watanabe, W.O., Ellington, L.J., Olla, B.L., Ernst, D.H. and Wicklund, R.I. (1990). Salinity tolerance and seawater survival vary ontogenetically in Florida red tilapia. *Aquaculture* **87** (311-321).

Watanabe, W.O., Mueller, K.W., Head, W.D. and Ellis S.C. (1993). Sex reversal of Florida red tilapia in brackish water tanks under differenttreatment durations of 17 -ethyltestosterone administered in feed. *J. App. Aqua*. **2** (29–42).

Watanabe, W.O., B.L. Olla, R.L. Wicklund and W.D. Head. (1997). Saltwater culture of Florida red tilapia and other saline-tolerant tilapias: a review. In: *Tilapia in the Americas, Vol. 1* (B.A. Costa-Pierce and J.E. Rakocy, eds.), pp. 54-141.World Aquaculture Society, Baton Rouge, Lousiana, United States.

Watrin, A. and Mayer-Gostan, N. (1996). Simultaneous recognition of ionocytes and mucous cells in the gill epithelium of turbot and in the rat stomach. *J. Exp. Zool*. 276 (95–101).

Wendelaar Bonga, S.E. (1997). The stress response in fish. *Physiol. Rev*. **77** (591–625).

Wendelaar Bonga, S.E. and van der Meij, J.C.A. (1989). Degeneration and death by apoptosis and necrosis of the pavement and chloride cells in the gills of the teleost. *Cell Tissue Res*. **255** (235–243).

Wendelaar Bonga, S.E., Flik, G., Balm, P.H.M. and van der Meij, J.C.A. (1990). The ultrastructure of chloride cells in the gills of the teleost *Oreochromis mossambicus* during exposure to acidified water. *Cell Tissue Res*. **259** (575–585).

Weisbart, M. (1968). Osmotic and ionic regulation in embryos alevins and fry of the five species of Pacific salmon. *Can. J. Zool*. **4** (385-397).

Whitear, M. (1970). The skin surface of bony fishes. *J. Zool. (London)* **160** (437–454).

Wilson, J.M. and Laurent, P. (2002). Fish gill morphology: inside out. *J. Exp.Zool*. **293** (192–213).

Wilson, J.M., Laurent, P. and Tufts, B.L. (2000 a). NaCl uptake by the branchial epithelium in freshwater teleost fish: an immunological approach to ion-transport protein localization. *J. Exp. Biol.* **203** (2279–2296).

Wilson, J. M., Randall, D. J., Donowitz, M., Vogel, A. W. and Ip, Y. K. (2000 b). Immunolocalisation of ion-transport proteins to branchial epithelium mitochondria-rich cells in the mudskipper (*Periophthalmodon schlosseri*). *J. Exp. Biol.* **203** (2297 -2310).

Witters, H., Berckmans, P. and Vangenechten, C. (1996). Immunolocalization of Na$^+$,K$^+$-ATPase in the gill epithelium of rainbow trout, *Oncorhynchus mykiss*. *Cell Tissue Res*. **283** (461–468).

Wohlfarth, G.W. and Hulata, G. (1983). Applied genetics of tilapias (Second revised edition), p. 26. *ICLARM Studies and Reviews* **6**.

Wong, C.K.C. and Chan, D.K.O .(1999). Isolation of viable cell types from the gill epithelium of Japanese eel *Anguilla japonica*. *Am. J .Physiol.* **276** (363-373)

Woo, N.Y.S. and Kelly, S.P. (1995). Effects of salinity and nutritional status on growth and metabolism of *Sparus sarba* in a closed seawater system. *Aquaculture* **135** (229-238).

Wu, S.M., Jong, K.J. and Kuo, S. Y. (2003). Effects of copper sulphate on ion balance and growth in tilapia larvae (*Oreochromis mossambicus*). *Arch. Environ. Contam. Toxicol* **45** (357-363).

Yamamoto, T. (1944). On the excitation-conduction gradient in the unfertilized egg of the lamprey, *Lampetra planeri*. *Proc. imp. Acad. Japan* **20.**

Yanagie, R., Lee, K. M., Watanabe, S. and Kaneko, T. (2009). Ontogenic change in tissue osmolality and developmental sequence of mitochondria-rich cells in Mozambique tilapia developing in freshwater. *Comp. Biochem. Physiol. Part A*. **154** (263-26).

Yap, W. G. (2001). The lowdown on world shrimp culture II. *INFOFISH International* **3** (20-27).

Yi, Y. and Fitzsimmons, K. (2004). Tilapia-shrimp polyculture in Thailand. In: *New Dimensions in Farmed Tilapia. Proceedings of ISTA 6.* (R. Bolivar, G. Mair, and K. Fitzsimmons, eds). pp. 777-790. Bureau of Fisheries and Aquatic Resources, Manila, Philippines.

Yoshikawa, J.S.M., McCormick, S.D., Young, G. and Bern, H. (1993). Effects of salinity on chloride cells and Na$^+$, K$^+$-ATPase in the teleost *Gillichthys mirabilis*. *Comp. Biochem. Physiol. Part A* **105** (311–317).

Young, P.S. and Dueñas, C.E. (1993). Salinity tolerance of fertilized eggs and yolk-sac larvae the rabbitfish *Siganus guttatus* (Bloch). *Aquaculture* **112**, (363–377).

Zadunaisky, J. A. (1984). The chloride cell: the active transport of chloride and the paracellular pathways. In: *Fish Physiology*, *vol. 10 B* (W. S. Hoar and D. J. Randall, eds.), pp. 130-176. Academic Press, Orlando.

Zadunaisky, J. A. (1996). Chloride cells and osmoregulation. *Kidney International* **49** (1563-1567).

Zambonino Infante, J.L. and Cahu, C.L. (2001). Ontogeny of the gastrointestinal tract of marine fish larvae. *Comp. Biochem. Physiol. Part A.* **130** (477-487).

Zhang, G., Shai, G., Shi, Y., Zhu,Y., Jianzhong, L. and Zang, W. (2010). Effects of salinity on embryos and larvae of tawny puffer *Takifugu flavidus. Aquaculture* **302** (71-75).

Appendix

General buffers

Phosphate buffered saline, pH 7.4 (PBS)

Sodium Phosphate (NaH_2PO_4)	0.438 g
Sodium hydrogen phosphate ($Na2HPO_4$)	1.28 g
Sodium chloride (NaCl)	4.385 g

Dissolve in 400 ml distilled water, pH 7.4 make up to 500 ml.

0.1 M Phosphate buffer, pH 7.4 (PB)

Monosodium phosphate monohydrate ($NaH_2PO_4.H_2O$)	0.3116 g
Disodium phosphate heptahydrate (Na_2HPO_4 $7H_2O$)	2.074 g

Dissolve in 100 ml distilled water and mix, store in 'fridge.

Fixatives

4% (w/v) paraformaldehyde in 0.1 M phosphate buffer (PB)

Add 0.4 g paraformaldehyde to 100 ml phosphate buffer (PB) (pH 7.4)
Dissolve over heater stirrer in hood, allow to cool. Make fresh stock as required.

0.2 M Sodium cacodylate (w/v) buffer stock solution

Sodium cacodylate	10.7 g

Dissolve in 240 ml distilled water, in fume cupboard adjust to pH 7.2 – 7.4 with 0.1M
HCl, make up to 250 ml with distilled water. Store in 'fridge.

2.5% gluteraldehyde (v/v) in 0.1 M sodium cacodylate buffer

Glutaraldehyde is bought as a 25% stock solution (100ml) and stored in the fridge
For 2.5%, mix 10ml stock with 90ml 0.1 M sodium cacodylate buffer in a measuring cylinder, dispense in 3ml aliquots in glass vials and store in freezer.

Sodium cacodylate buffer rinse

Dilute 0.2M sodium cacodylate buffer stock solution to 0.1M, add 0.1M sucrose and store in 'fridge.

Stains

4 % Uranyl acetate

4% uranyl acetate   0.2 g
50% ethanol

Dissolve uranyl acetate in 50% ethanol and store at 4ºC.

Reynold's Lead Citrate

Lead nitrate ($PbNO_3^{2-}$)   1.33 g
Sodium citrate ($Na_3C6H5O_7.2H_2O$)   1.76 g

Dissolve salts in 15 ml distilled water and mix, leave to stand for 30 min then add 8 ml fresh 1 M NaOH to dissolve. Make up to 50 ml with DW, store at 4 ºC, centrifuge before use.